

# Automatic extraction of constraints in manipulation tasks for autonomy and interaction

THÈSE N° 8059 (2018)

PRÉSENTÉE LE 8 JUIN 2018

À LA FACULTÉ DES SCIENCES ET TECHNIQUES DE L'INGÉNIEUR  
LABORATOIRE D'ALGORITHMES ET SYSTÈMES D'APPRENTISSAGE  
PROGRAMME DOCTORAL EN ROBOTIQUE, CONTRÔLE ET SYSTÈMES INTELLIGENTS

ÉCOLE POLYTECHNIQUE FÉDÉRALE DE LAUSANNE

POUR L'OBTENTION DU GRADE DE DOCTEUR ÈS SCIENCES

PAR

Ana-Lucia URECHE

acceptée sur proposition du jury:

Prof. A. Ijspeert, président du jury  
Prof. A. Billard, directrice de thèse  
Prof. B. Argall, rapporteuse  
Prof. B. Wrede, rapporteuse  
Prof. P. Dillenbourg, rapporteur



ÉCOLE POLYTECHNIQUE  
FÉDÉRALE DE LAUSANNE

Suisse  
2018



---

# ABSTRACT

TASKS routinely executed by humans involve sequences of actions performed with high dexterity and coordination. Fully specifying these actions such that a robot could replicate the task is often difficult. Furthermore the uncertainties introduced by the use of different tools or changing configurations demand the specification to be generic, while enhancing the important task aspects, i.e. the constraints. Therefore the first challenge of this thesis is inferring these constraints from repeated demonstrations. In addition humans explaining a task to another person rely on the persons ability to apprehend missing or implicit information. Therefore observations contain user-specific cues, alongside knowledge on performing the task. Thus our second challenge is correlating the task constraints with the user behavior for improving the robots performance. We address these challenges using a Programming by Demonstration framework.

In the first part of the thesis we describe an approach for decomposing demonstrations into actions and extracting task-space constraints as continuous features that apply throughout each action. The constraints consist of: (1) the reference frame for performing manipulation, (2) the variables of interest relative to this frame, allowing a decomposition in force and position control, and (3) a stiffness gain modulating the contribution of force and position. We then extend this approach to asymmetrical bimanual tasks by extracting features that enable arm coordination: the master-slave role that enables precedence, and the motion-motion or force-motion coordination that facilitates the physical interaction through an object. The set of constraints and the time-independent encodings of each action form a task prototype, used to execute the task.

In the second part of the thesis we focus on discovering additional features implicit in the demonstrations with respect to two aspects of the teaching interactions: (1) characterizing the user performance and (2) improving the user behavior. For the first goal we assess the skill of the user and implicitly the quality of the demonstrations by using objective task-specific metrics, related directly to the constraints. We further analyze ways of making the user aware of the robot's state during teaching by providing task-related feedback. The feedback has a direct influence on both the teaching efficiency and the user's perception of the interaction. We evaluated our approaches on robotic experiments that encompass daily activities using two 7 degrees of freedom Kuka LWR robotic arms, and a 53 degrees of freedom iCub humanoid robot.

**Keywords:** programming by demonstration, constraints extraction, bimanual tasks, coordination constraints, learning and adaptive systems, robot facial displays, interaction dynamics, interaction metrics, human factors



---

# RÉSUMÉ

La dextérité et la coordination sont critiques à l'exécution de tâches quotidiennes chez l'humain, cependant cette exécution est aussi sujette à une certaine incertitude résultante de la variété des outils utilisés ou des configurations possibles. Il est donc difficile de spécifier univoquement les actions qu'un robot doit répliquer afin d'accomplir une tâche sans limiter le pouvoir de généralisation de la solution produite. Le premier objectif de cette thèse est donc l'extraction de contraintes propres à une tâche depuis un ensemble de démonstrations. Au cours des démonstrations, les comportements humains sont indicatifs des dimensions importantes du mouvement. Il est donc important, comme deuxième objectif, de corrélérer les contraintes identifiées en premier lieu aux comportements observés lors des démonstrations. Cette corrélation permet à la fois d'évaluer l'intention de l'utilisateur et d'améliorer la performance du robot. Afin de répondre à nos objectifs, nous optons pour l'approche de programmation par démonstration.

La première partie de cette thèse consiste en la décomposition des démonstrations en actions et l'extraction de contraintes en tant que sets de variables de contrôle continues, applicables sur l'entière durée de l'exécution de la tâche observée. Les contraintes sont définies comme étant: (1) le cadre de référence, (2) les variables de contrôle qui permettent la décomposition en composante de force et de position au sein du cadre de référence, et finalement, (3) la rigidité en gain du système qui module les contributions de la force et de la position. L'approche est ensuite étendue aux tâches bimanuelles asymétriques grâce à l'extraction de caractéristiques qui facilitent la coordination; l'interaction maître-esclave établit la priorité, tandis que la coordination mouvement-mouvement ou force-mouvement facilite l'interaction avec un objet. Cet ensemble de contraintes, encodées indépendamment du temps, permet de spécifier un prototype d'exécution pour une tâche donnée.

En deuxième partie, l'intérêt est tourné vers la découverte de comportements complémentaires implicite à la démonstration. Ces caractéristiques sont déterminées afin d'évaluer deux aspects de l'interaction avec le robot: (1) la performance de l'utilisateur et (2) l'amélioration du comportement de l'utilisateur. Ayant extrait un prototype d'exécution basé sur des contraintes, il est possible d'évaluer la performance d'un utilisateur en fonction des comportements qui accompagnent la tâche. Nous pouvons ensuite étudier l'impact d'un retour visuel provenant de l'évaluation de la performance de l'utilisateur par le robot sur l'apprentissage de la tâche. Notre approche est évaluée à l'aide de deux plateformes robotiques: deux Kuka LWR ayant chacun sept degrés de liberté, et un robot humanoïde iCub en comptant cinquante-trois.

**Mots Cle:** programmation par démonstration, extraction de contraintes, tâches bimanuelles, systèmes d'apprentissage et d'adaptation, expressions faciales du robot, dynamique d'interaction, mesures d'interaction, facteurs humains



*To my husband Vlad and our son Ioan,  
who bring endless joy to my life*



---

# ACKNOWLEDGMENTS

I would like to thank my advisor Aude Billard for giving me the opportunity to pursue my Phd in such a wonderful environment – the LASA lab. I am thankful for all the patience and support throughout the thesis, the scientific discussions and personal advice which have made this experience possible and very enriching. I am also grateful for having the opportunity to work with different robots, to meet people from around the world, and to travel for presenting my work.

I also acknowledge my thesis examiners, Prof. Brenna Argall, Prof. Britta Wrede, and Prof. Pierre Dillenbourg for taking the time to review my thesis and for providing valuable comments that led to the improvement of the manuscript. I also thank Prof. Auke Ijspeert who served as president of the jury.

I am really thankful to my colleagues who have made this lab a great place to work. I thank Brenna Argall, Basilio Noris, Sahar El-Khoury, Felix Duvallet, Jose Medina, Mustafa Suphi Erden, Mohammad Khansari, and Daniel Grollman, postdocs during my stay in the lab, for all the scientific discussions and life lessons. I specifically thank Brenna Argall, for the time spent helping me improve my writing skills; Sahar El-Khoury and Basilio Noris for their positive attitude and always bringing a fresh perspective in all our discussions; and Felix Duvallet for all the advice on life outside the lab.

I also thank my fellow PhD colleagues: Seungsu Kim, Ashwini Shukla, Luka Lukic, Nadia Figueroa, Sina Mirrazavi, Guillaume de Chambrier, Ravin De Souza, Miao Li, Nicolas Sommer, Klas Kronander, Hang Yin, Mahdi Khoramshahi, and Iason Batzianoulis. I learned a lot by seeing you go through this process and I enjoyed sharing with you the breaks, lunches, pizzas, ski outings and all the good times we had. Special thanks to my office mates throughout the years: Mohammad Kansari, Miao Li, Neda Taymourtash, Nicolas Sommer and Joel Ray for keeping a joyful atmosphere.

My special thanks to Nadia Figueroa and Sina Mirrazavi for their technical skillfulness, but most of all for their constructive attitude, positiveness and confidence. Thank you for being close friends and always helping me in so many ways. I also thank Ashwini Shukla, Guillaume de Chambrier, and Miao Li for all the nice moments, jokes, and time spent in the gym. My thanks to Ravin de Souza, and Miao Li for giving me insight into their work using the glove and robotic hand.

I also acknowledge the newer people - Walid Amanhoud, Ilaria Lauzana, Andrew Sutcliffe, Leonardo Urbano, Kunpeng Yao, Michael Bombile. I didn't get the chance to know them so well, but they are continuing to make this lab great. I feel lucky to have got to know so many other people who were part of the lab only for a short period of time, but who enriched the atmosphere through cultural, culinary, and life-related debates: Silvia Magrelli, Joao Silverio, Prof. Kenji Tahara, Brahayam Ponton, Neda Taymourtash, AJung Moon, Yue Zhou, Kevin Gonyop Kim, Wissam Bejjani, Ajay Tanwani, Bidan Huang.

I am grateful to our lab's secretary Joanna Erfani, as well as Corinne Lebet and Sandra Roux from the doctoral school for their prompt support in all administrative matters. I acknowledge the EU projects that supported my research. Furthermore I would like to thank all the approximately 150 people who took part in my user studies. Thank you for your time, interest, and open mindedness.

Last but not least this thesis would have not been possible without the endless support, love and encouragement of my husband Vlad. I am grateful for all his efforts and commitment to our family, and most of all for sharing the joy of welcoming our son Ioan into this world, as he was born during the making of this thesis. Many thanks to my parents, my brother, and my parents-in-law for all their advice, support and the nice moments we spent together.

---

# TABLE OF CONTENTS

<b>1</b>	<b>Introduction . . . . .</b>	<b>3</b>
1.1	Motivation . . . . .	3
1.2	Goals of this thesis . . . . .	5
1.3	Context . . . . .	6
1.4	Approach . . . . .	12
1.5	Contributions . . . . .	15
1.6	Thesis Outline . . . . .	16
<b>2</b>	<b>Constraint–representation of unimanual tasks . . . . .</b>	<b>19</b>
2.1	Forward . . . . .	19
2.2	Introduction . . . . .	20
2.3	Related Work . . . . .	23
2.3.1	Automatic extraction of reference frames . . . . .	23
2.3.2	Automatic extraction of force information . . . . .	24
2.3.3	Task segmentation . . . . .	25
2.3.4	Constraint based motion planning . . . . .	27
2.4	Method . . . . .	27
2.4.1	Determining the Task Constraints . . . . .	29
2.4.2	Constraint–based Motion Learning . . . . .	32
2.4.3	Constraint–based Execution . . . . .	36
2.5	Validation . . . . .	36
2.5.1	Experiment I. Vegetable Grating Task . . . . .	37
2.5.2	Experiment II. Battery removal from charger . . . . .	42
2.6	Discussion . . . . .	45
2.6.1	Open Parameters . . . . .	45
2.6.2	Advantages . . . . .	47
2.6.3	Limitations . . . . .	49
2.7	Conclusions . . . . .	50
<b>3</b>	<b>Constraint–representation of coordinated behavior . . . . .</b>	<b>51</b>
3.1	Forward . . . . .	51
3.2	Introduction . . . . .	52
3.3	Related Work . . . . .	54
3.3.1	Coordination in bimanual tasks . . . . .	54
3.3.2	Coordination in physically collaborative tasks . . . . .	56
3.3.3	Task representations and execution . . . . .	56
3.3.4	Summary of the extraction of task constraints . . . . .	57
3.4	Method . . . . .	61
3.4.1	Master–slave coupling between the arms . . . . .	63
3.4.2	Encoding of the hand shape and grasping quality . . . . .	67
3.4.3	Transition conditions . . . . .	69
3.5	Validation . . . . .	71

3.5.1	Mellon Scooping . . . . .	71
3.5.2	Vegetable Peeling . . . . .	73
3.5.3	Bowl Mixing . . . . .	74
3.6	Discussion . . . . .	76
3.6.1	Advantages . . . . .	76
3.6.2	Limitations . . . . .	76
3.6.3	Stability considerations . . . . .	80
3.6.4	Future Work . . . . .	80
3.7	Conclusions . . . . .	81
<b>4</b>	<b>User skill assessment based on task constraints . . . . .</b>	<b>83</b>
4.1	Forward . . . . .	83
4.2	Introduction . . . . .	84
4.3	Related Work . . . . .	87
4.3.1	User assessment in teaching interactions . . . . .	87
4.3.2	User assessment during an interaction . . . . .	87
4.3.3	Particularities of bimanual behavior . . . . .	88
4.4	User performance assessment . . . . .	89
4.4.1	Study design . . . . .	89
4.4.2	Data analysis . . . . .	93
4.4.3	Results . . . . .	95
4.5	Possible causes of poor performance . . . . .	108
4.5.1	Motion strategy . . . . .	108
4.5.2	Tool use in relation to the task constraints . . . . .	109
4.5.3	Contact Localization . . . . .	110
4.5.4	Re-grasping . . . . .	112
4.5.5	Visual Feedback . . . . .	113
4.6	Robot performance during task execution . . . . .	114
4.7	Performance estimation based on hand state . . . . .	115
4.7.1	Classification with SVM . . . . .	116
4.7.2	Classification with feedforward neural network . . . . .	117
4.8	Discussion . . . . .	118
4.8.1	Advantages . . . . .	119
4.8.2	Limitations . . . . .	119
4.9	Conclusions . . . . .	121
<b>5</b>	<b>Interaction dynamics in PbD . . . . .</b>	<b>123</b>
5.1	Forward . . . . .	123
5.2	Introduction . . . . .	123
5.3	Related Work . . . . .	124
5.4	Experiment I. Facial displays validation . . . . .	126
5.4.1	iCub Facial Displays . . . . .	126
5.4.2	Study Design . . . . .	127
5.4.3	Results . . . . .	131
5.5	Experiment II. Robot feedback during teaching interactions . . . . .	135
5.5.1	Study Design . . . . .	137
5.5.2	Results . . . . .	140
5.6	Discussion . . . . .	147
5.6.1	Experiment I. Facial Expressions . . . . .	147
5.6.2	Experiment II. Robot feedback . . . . .	148
5.7	Conclusions . . . . .	150

<b>6</b>	<b>Conclusions</b>	<b>151</b>
6.1	Contributions	151
6.2	Limitations	152
6.3	Future Work	153
6.4	Final Words	154
<b>7</b>	<b>Appendix. Initial video rating for the user study in Chapter 4</b>	<b>157</b>
7.1	Video rating assessment	157
7.2	Video rating results	158
	<b>References</b>	<b>163</b>







# INTRODUCTION

---

## 1.1 Motivation

---

Humans perform daily activities, switching between actions with ease, manipulating multiple tools in a dexterous way, and coordinating their arms to exert desired effects on objects by inducing a relative motion or force. Actions are typically performed either individually or collaborating with another person. Additionally humans can effortlessly master new skills by simply watching other persons execute a task, by receiving instructions and by rehearsing until obtaining the desired goal. They are also able to transfer skills just as easily by directing the other person's attention to the important aspects of the task.

When faced with the challenge of learning a new task, humans often integrate various learning modalities: visual, verbal, auditory, kinesthetic. Combining sensory feedback such as visual and kinesthetic guidance provided manually by a coach for learning a bimanual rhythmic task is shown to lead to an improved performance (Zhu et al., 2017). However learners might prefer a certain modality. For example students perform best when assigned to their preferred learning style. This applies to both sports coaching Dunn (2009) as well as to teaching a technical skill, such as cardiac dissection where students preference was linked to their learning style (Allavena et al., 2017): using a simulator for kinesthetic learners versus video recordings of the task for visual learners. In other cases visual information alone might not be sufficient for transferring all the aspects of the task, and directly experiencing it might lead to better results.

Kinesthetic learning in particular is commonly used in tasks that require experiencing the body movement in areas such as crafts, sports, medical and rehabilitation. Since it makes use of muscle memory, the kinesthetic information of the skill can be reused in situations when visual information is limited. This is fundamental in precision tasks, such as surgeon training (Pinzon et al., 2016). Kinesthetic learning is also preferred in nursing (Stirling, 2017) and was shown to improve engagement of nursing students (Elissa, 2014).

Typically in sports this method is used in conjunction with other methods such as: feedback from a knowledgeable coach and observing peer performance in elite gymnastics Hars and Calmels (2007); the use of mental imagery in athletes regardless of the type sport they practice (Gregg et al., 2016), and also

for improving accuracy and performance in tennis [Guillot et al. \(2012\)](#).

In rehabilitation the sense of touch is often used to compensate for another missing or impaired sense, for example using haptic applications for training students with impaired vision ([Murphy and Darrah, 2015](#)). Robotic devices are often used for various cases of motor and neurorehabilitation: such as gait ([Morone et al., 2017](#)), or upper limb training in stroke subjects ([Taheri et al., 2016](#); [Milot et al., 2016](#)) or spinal cord injured subjects ([Kadivar et al., 2011](#)). Furthermore tactile feedback from a vibrotactile suit can improve accuracy when learning a new motor task ([Lieberman and Breazeal, 2007](#)).

In the case of fine manipulation, using a haptic assistive device was shown to improve writing of persons suffering from sensorimotor integration disorders ([Atashzar et al., 2013](#)); conversely the force exerted when writing (both the grip force and the force exerted by the pen on the writing surface) has been shown to be significant in characterizing impaired handwriting ([Schneider et al., 2010](#)).

In this thesis we focus on teaching robots how to perform common manipulation tasks. We take a programming by demonstration approach given the extent of kinesthetic learning in humans and the complexity of the information that the human teacher needs to transfer. Many daily life tasks, require specialized tools such as a knife or a peeler. For maneuvering these tools humans often employ both arms, such that one offers support (i.e. by holding, stabilizing, assisting) while the other is performing active manipulation (such as cutting, mixing, scooping etc. see [Fig. 1.1](#)). Since these actions typically demand precise motions or exerting forces, learning such tasks often requires kinesthetic practice, aside examples and instructions.

However robots are expected to learn and perform such routine tasks with just as much ease as humans and in a reliable way. This constitutes an important challenge as adaptation to new configurations, new tools and new scenarios should happen on the fly. Therefore the possibility to learn by observing the user and to integrate kinesthetic information about the task has the potential to speed up robot learning in domestic environments. Additionally the ability to reuse or refine skills ([Sauter et al., 2012](#)), as well as observing which aspects remain consistent in similar tasks improve the robot’s ability to apply the same skill in different contexts.

Furthermore the interaction with the user should be intuitive for non-technical persons and the robot’s state should be transparent ([Breazeal, 2009](#)). Therefore alongside the skill learning capability, robots are expected to display social behavior, and enable a safe interaction ([Ding et al., 2013](#)). Such aspects have an impact on the human perception of the interaction and acceptance of the robot. Consequently the second challenge, namely of providing optimal feedback for the user, tackled by this thesis relies on understanding and relating the robot’s performance with the important aspects of the task; understanding user behavior relative to the robot and the task; and deciding on which feedback modality would best emphasize the current robot state.



**Figure 1.1** Daily activities and corresponding setup for kinesthetically demonstrating them to a robot. Humans perform with ease activities that typically require manipulating tools, and changing the state of the objects by applying forces. Cutting or peeling a vegetable requires *force control*; slicing or chopping an onion requires *stiffness modulation*; *arm coordination* is used when rolling a dough with both hands moving in symmetry with each other, or when asymmetrically coordinating to mix the contents of a bowl, by holding it with one hand and mixing with the other. Finally a *precise use of the tools* is essential for achieving task goals.

## 1.2 Goals of this thesis

---

Therefore this thesis focuses on developing approaches for obtaining task representations and improving human-robot interaction, using a Programming by demonstration approach.

We aim to sequence the task into actions and represent each action through a set of soft constraints. This information can be directly used by the robot during execution by embedding it in the control law. The purpose is to allow robots to easily acquire new skills that extend their original set of capabilities by observing and interacting with human users.

This calls attention to three key issues which represent the goals of this thesis:

- (1) *bootstrapping knowledge for learning* by extracting important aspects of the task (i.e. constraints that remain invariant across multiple demonstrations) from observing the humans performing real life tasks. Our aim is to extract segmentation points coordination variables and to determine whether this is a position versus force control type of task.
- (2) *user performance assessment* by correlating the task constraints with the way the user manipulates the tools to obtain the desired effect.

- (3) *transparency for the user* by providing feedback aimed at improving the dynamics of the human-robot interaction during teaching and implicitly improving the quality of the demonstrations.

Our first goal relates to information that cannot be easily programmed into a robot, such as how to modulate the stiffness of the arm when performing a certain movement or how to apply a force. However a human has this knowledge empirically and can easily demonstrate the task. Thus the robot extracts information which is implicit in the demonstrated behavior, but constitutes aspects that are key to the task success and should be reproduced according to the given context. For example the force applied when grating different vegetables depends on how soft they are; pouring sauce depends on moving relative to the container in which it should be poured; successfully scooping requires adjusting the stiffness of both arms as one applies a force and the other is resisting the motion; mixing in a bowl or peeling a vegetable also require arm coordination and continuous adaptation.

While realising the first goal gives the robot autonomy in executing the task, realising our second goal gives the robot awareness about user behavior, namely assessing if the user is performing the task properly with respect to the constraints extracted previously. This has multiple implications that lead to a more responsive and initiative-taking robot. Firstly the robot can decide from which demonstrations or which users to learn the task in order to obtain better performance. Secondly the robot can enforce the constraints when executing the task collaboratively with the human, by adopting an assistive behavior.

Finally our last goal focuses on improving robot’s responsiveness by providing relevant feedback in a social manner. To reveal the robot’s state while performing a manipulation task, the feedback should be related directly to the task constraints. Moreover the feedback should be presented in a social manner, using facial cues, voice, gestures, to encourage human engagement in the interaction.

### 1.3 Context

---

The approaches proposed in this thesis make use of different types of interaction, aimed at improving both learning and human engagement. We study interaction during programming by demonstration as a modality of passing knowledge from the user to the robot. However the dynamics of the interaction is influenced by both the user’s behavior and the human perception of this behavior. We thus review the general context of social robotics, its applications to learning and its influence on the user to position our work.

Social robots are robots capable of interacting with humans in a social manner, making use of cues such as facial expressivity, speech and gestures. Therefore they can offer a rich interaction, making them suitable for domestic environments as in human-human interaction the quality of the communication determines engagement and responsiveness. For daily interaction with naive users robots are expected to be aware of their environment and to express their state in a given situation (Breazeal, 2009). Hegel et al. (2011) distinguish between two ways a robot can transmit information to the user: signals that resemble human communication (such as speech, hand gestures, etc) or artificial signals correlated with the user’s understanding of its behavior (LEDs, GUIs).

Interaction with social robots has proven effective in several areas: autism spectrum disorder (long term studies show improvements in the behavior of autistic children when using social robots such as Kaspar due to their simplified facial features (Iacono et al., 2011)), robots that resemble animals (Stanton et al., 2008) used for encouraging social interaction between the elderly or stimulate attention in children (Nakanishi et al., 2014), artistic expression (Levillain et al., 2017), therapy and education, stimulating creativity (Kahn et al., 2014), dementia care (Shibata, 2012; Hebesberger et al., 2016) promoting exercise and healthy living (Fasola and Matarić, 2013; Ros et al., 2016), interacting with children suffering from diabetes (Alotaibi and Choudhury, 2015; Coninx et al., 2016) or in general to intermediate interaction between children (Hirose et al., 2014; Yamazaki et al., 2013).

In our work we aim to enhance the interaction with the user during Programming by Demonstration with social feedback for two reasons. Firstly communicating the state of the robot relative to the important aspects of the task gives the human an understanding of how well the demonstration is performed. For example in a task in which it is crucial to apply proper forces, mapping force values to the intensity of facial expressions or a form of verbal feedback can help the human understand what the robot is perceiving and thus improve the human demonstrations. Secondly giving the feedback in a natural way, through social cues (unlike e.g. displaying numeric values on a screen) makes it very intuitive for the user, and in consequence the user might be more engaged in the interaction.

While a robot’s capabilities for human-like communication are limited and can vary depending on the robot’s embodiment, still expressive modalities such as speech and gaze keep a user engaged and focused in the interaction (Ivaldi et al., 2017; Kennedy et al., 2017). Additionally making use of these expressive modalities leads to perceiving the robot as ”friendly” or ”helpful” which increases and sustains user engagement (Corrigan et al., 2015). However deciding when and how to make use of the expressive behavior is mostly task

specific, typically being displayed when a particular event takes place. An emotion can also be displayed based on a more complex architecture incorporating personality models and mood (Han et al., 2013).

One significant downside of social robotics is that as they tend to be more human-like (i.e. (Ishiguro, 2008; Becker-Asano and Ishiguro, 2011)) people tend to perceive them as "uncanny". Mori (1970) explained this effect by the "uncanny valley" concept, stating that as the human likeliness of a robot increases (from industrial robots to toy robots), so does the human affinity. However there is a major drop in affinity as the likeliness increases, but fails to come close to the resemblance of a healthy person. The perception of a robot as being "uncanny" can be caused by the body appearance (Kanda et al., 2008) affecting the nonverbal behavior of the human, appearance of the face and facial expressions (Seyama and Nagayama, 2007); or lack of human-like skin in robotic hands which fail to display a soft tissue, or temperature properties similar to that of the humans (Cabibihan et al., 2006), placing a prosthetic hand in the valley.

The existence of the "uncanny valley" effect plays an important role in the interaction (Ho and MacDorman, 2017) and bridging the valley can be done in several ways: by focusing on the minimal design requirements, natural and diverse human-like motions (Ishiguro, 2008), response time taken needed by a robot during communication (Shiwa et al., 2009), displaying emotions during social interaction (Koschate et al., 2016). Dealing with these aspects can lead to humans accepting robots as interaction and collaboration partners, even from a small age (Park et al., 2015). In our work we aim to avoid the uncanny valley effect by providing basic facial expressions implemented using LEDs.

Social robotics focuses mostly on the use of verbal feedback as well as a set of non-verbal cues (facial display of emotions, gestures). Providing haptic feedback, in the form of touch and force when in physical contact, is a less prevalent form of interaction. However touch plays an important role as haptic feedback enables people to collaborate in a task that requires physical contact. Similarly, when collaborating with a robot for physically manipulating an object both the human and the robot adapt to the force transmitted through the object by the other partner.

Noohi and Zefran (2014) propose a set of metrics for characterizing performance in collaborative tasks by analyzing the forces applied with respect to cooperativeness, effectiveness and efficiency of the collaboration. Human exchange haptic cues as a communication method that complements gestures, gaze or verbal communication (Javaid et al., 2014) and such interaction patterns can be classified based on force-velocity patterns (Madan et al., 2015). Moreover haptic stimuli can carry additional information. A simple 1 DOF device can provide stimuli with affective nuances Bianchi et al. (2017) or can indicate changes in dominance between partners in haptic interaction (Groten et al., 2009).

In our work we focus on the importance of haptic interaction in collaborative tasks. For example a robot can predict the intention of the human to apply a

force and adapt by increasing its stiffness. This haptic cue can be a signal for the human that the robot is ready for the task. Conversely a human can signal its intention to start a manipulation task by the intensity of the tactile contacts when holding a tool.

---

#### LEARNING FROM HUMAN DEMONSTRATIONS

---

Teaching a robot through instructions and demonstrations is a natural method of task learning (Nicolescu and Mataric, 2003), similar to the way a human teaches another human (Peacock, 2001). It mainly consists of providing the demonstrations, generalization over multiple demonstrations using statistical methods and practice trials (Nicolescu and Mataric, 2003) while the users should be engaged in the interaction in each stage (Amershi et al., 2014). Practice trials are useful in tasks where replays of the demonstrations are required in order to record forces, or tactile information not influenced by the touch of the human (Sauser et al., 2012), while allowing the human to observe what the robot has learned and adjust the following demonstrations accordingly (Pais et al., 2013).

Demonstration modalities include (a) *observing a human* performing the task (based on visual data, or object tracking, and suitable for basic tasks, such as reaching); (b) directly driving the robotic arm(s) to experience the forces required by the task (*kinesthetic demonstrations* in which the robot records proprioceptive data consisting of position and force); (c) *active teaching* which combines observations while kinesthetic demonstrations are used for refining the motions (Calinon and Billard, 2007c). These approaches presume that the user demonstrates the full trajectories. Thus they are suitable for complex tasks that require well defined motions.

Active teaching can also be employed in the form of corrective feedback (Argall et al., 2011) or critique (Argall et al., 2007) coming from the human teacher which helps in iteratively learning and refining a task policy. These type of incremental learning approaches (Vijayakumar et al., 2005) enable natural human-robot interactions (Breazeal et al., 2004) and long-term learning (Grollman and Jenkins, 2007).

An alternative approach are key-frame demonstrations (Akgun and Thomaz, 2016) in which the user focuses on the desired final poses of the robot in each action. Keyframe demonstrations are useful when demonstrating the trajectory is irrelevant for the task, or when it is impractical (e.g. robot’s limbs are not backdrivable or are too large for the humans to move). However this loses the fluidity and dynamics of the motion.

Kinesthetic demonstrations in particular assume that a human user directly moves the robot arms for teaching the required actions. Thus they represent a particular case of human-robot physical interaction. Unlike observational learning in kinesthetic teaching the robot can experience the forces required for completing the task. The human touch can be mapped to different behaviors,

such as: teaching desired levels of stiffness for different joints by wiggling the robot (Kronander and Billard, 2014); pressing on robot’s fingertips for teaching it different configurations for holding an object and the corresponding tactile feedback (Sauser et al., 2012). Complementary to the proprioception information, the effect that an action has on an object or on the environment can bring important information about the task. Focusing on different parts of the scene can be done by specifying ”perceptual landmarks” (Huang and Cakmak, 2016).

One problem is that of providing good demonstrations or improving the human demonstrations in time. One such approach is ”teaching guidance” in the form of instructions provided to the demonstrator and derived from heuristics (Cakmak and Thomaz, 2014b). End-users can be trained into using a Programming by Demonstration interface, with video examples proven to be more efficient than written text (Cakmak and Takayama, 2014). Multiple demonstrations that showcase the same task performed in changing conditions are typically required for a good generalization however this can be tiring for the user and can result in low quality or non-exhaustive training sets. One approach to address this issue is crowdsourcing the cases in which the learned action would not be effective (Forbes et al., 2014).

Alternatively the robot can provide feedback relative to the learned behavior by adapting online its joint stiffness (Kronander and Billard, 2014); or iteratively through rounds of replay and refinement of the demonstrated gesture (Sauser et al., 2012). In our work we focus on correlating the tactile response on a robot’s fingertips with expressive modalities such as facial displays to inform the demonstrator in real-time of how suitable the current posture is. This leads to a decrease in the time necessary for demonstrating the task, and an increase in the user’s satisfaction with the robot’s behavior. Using a social partner can influence the outcome of a learning interaction (Cakmak et al., 2010).

Throughout the different chapters of this thesis we take a programming by demonstration approach in which we use kinesthetic teaching to allow the robot to record full trajectories and to experience the forces required by the task. Based on this information we sequence the task and extract the reference frame to be used in each action. We then determine the important variables to be used on each axis of the previously extracted frame, obtaining a decomposition for performing hybrid control in that frame. We also determine a stiffness modulation factor weighting the contribution of position and force on each axis.

We thus contribute to extracting task constraints from human demonstrations emphasising the force and stiffness aspects, whereas existing works focus mainly on kinematic constraints Calinon (2007). Alternatively in the keyframe approach (Akgun and Thomaz, 2016) the user is explicitly drawing the robot’s attention to the important aspects of the task, thus making them explicit rather than extracting them.

Additionally when demonstrating bimanual tasks we propose a custom setup in which a demonstrator can backdrive a robotic arm with one hand, and demon-

strate the task of the other hand dexterously wearing a dataglove that records the motion of the fingers. This allows us to record the motion of the fingers and the tactile activation as the user is maneuvering the tool, in conjunction with the state of the robot. From this information we extract coordination patterns between the two arms and generalize the task to be executed either autonomously or in physical collaboration with a human partner.

---

#### USER-PERCEIVED INTERACTION

---

Designing a social robot augmented with expressive capabilities is done with the aim of improving the user’s perception of these stimuli and interaction experience. Multiple human factors play a decisive role in the dynamics of the interaction. One such factor is the change in authority when humans have to share or delegate responsibility with robots (Hinds et al., 2004), which can lead to observing emerging models of interaction such as the master-servant case observed in Sung et al. (2007). In Programming by Demonstration the human user is in a position of power and authority as the person holding the task knowledge. This explains the need for a responsive robot that behaves as expected.

Complementary to the concept of *authority* is that of *trust* that contributes to maintaining the interaction. Yagoda and Gillan (2012) describe trust as a multi-dimensional concept, dependant of the task, the human-robot team and the context. In PbD tasks, trust of the robot is expected to increase if the robot showcases reliable behavior. Also trust can be maintained through appropriate feedback reflecting the robot’s state. For example a robot employing gestures to signal poor task performance was perceived by the user as trustworthy (van den Brule et al., 2016)

Social norms also apply to human-robot interaction (Huettenrauch et al., 2006), and can have a major role in teaching tasks. Firstly, spatial distance and orientation of the robot with respect to the human (Hall, 1966), as well as the robot’s approaching speed (Sardar et al., 2012) impact the interaction. When demonstrating a task to a robot it is easier to keep the robot fixed and let the user approach the robot at a convenient distance. Secondly, gestures can foster HRI along with other communication mechanisms. Nehaniv et al. (2005) identify five classes of gestures specific to HRI, however Otero et al. (2006) show that only two of them (interactional and manipulative gestures) occur naturally in demonstrating a household task to a robot.

Lastly, touch-based interaction affect the human perception of the robot. When touching a robot humans have different expectations on how this should respond in terms of moving the touched part, looking towards that part of the body or stiffening the concerned part of the body (Basoeki et al., 2015). On the other hand being touched by a robot can be encouraging for a human (Shiomi et al., 2017). However humans prefer particular touching behaviors. A user study aimed at analyzing the force and finger motion during a patting

gestures (Cabibihan et al., 2011) shows that human subjects prefer particular hand configurations, using mostly the wrist, palm and proximal phalanges rather than distal phalanges. However people respond positively to a touch initiated by a robotic nurse for either cleaning or comforting regardless of the presence of verbal communication (Chen et al., 2011).

In teaching interactions the knowledge that the user has about the task can influence the outcome of the learning as well as the perceived interaction. Therefore it is important for the robot to distinguish between a proficient and an unskilled user demonstrating the same task. Allowing the robot to passively characterize user performance while demonstrating a task can improve and direct the provided feedback. Alternatively roles can be inversed and a robot having a representation of a task can become assistive, helping an unskilled user improve its performance.

Human performance can be assessed based on various metrics most of them being time-based: reaction time, time to task completion etc. Other factors that are used in assessing human performance are fine and gross dexterity, reaction time and visual acuity and depth perception (Paperno et al., 2016). A user study with 89 participants performed by Paperno et al. (2016) showed that dexterity could be a good predictor of user performance in simple robotic tasks such as pick-and-place or find-and-fetch.

In our work we contribute to improving human perceived interaction by two means. Firstly we provide social feedback which proved to improve user engagement and satisfaction with the outcome of the teaching procedure. Secondly we propose a method for evaluating user performance using the extracted task constraints as benchmark. Based on this information the robot can adapt to the users intentions and can improve its own performance relative to the task goal. Thus this can lead to an improved interaction.

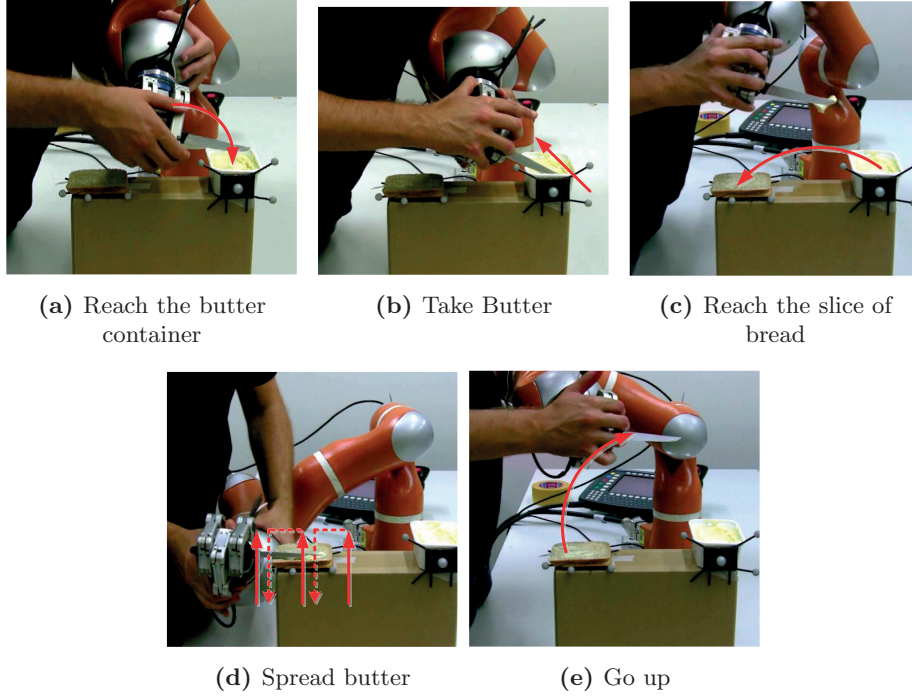
## 1.4 Approach

---

In this thesis we focus on tasks that presume successfully completing a sequence of actions. For example spreading butter on a slice of bread (as illustrated in Fig. 1.2) consists of reaching with the knife on top of the butter container, scraping butter with the knife, reaching the slice of bread, spreading butter, and finally taking the tool away.

Similarly pouring a glass of water consists of reaching for the bottle, identifying a glass and placing it in the proper position, reaching for the glass, pouring the desired amount of water and reaching for the table to put down the bottle. Completing each low-level action depends on properly understanding what information is important for that region of the task (e.g. forces, torques, tactile information, or the position of the end-effector).

This requires dealing with multiple aspects: a high dimensional input-space



**Figure 1.2** Sequence of logical steps in demonstrating the *Butter Spreading Task*

(as a demonstration typically consist of data from multiple sensors: proprioceptive position and force sensed by the robot, vision tracking for external objects, hand shape information if tracking the users hand), motion segmentation, determining the relative importance of each input dimension in each region of the task (extract the task constraints).

Current approaches address these problems separately, while this thesis explores the possibility of directly using the extracted constraints for generating robot control strategies.

The work described in the following chapters relies on two main tools:

- kinesthetic Programming by Demonstration (PbD) for acquiring data;
- Cartesian impedance control for executing the robot's motion

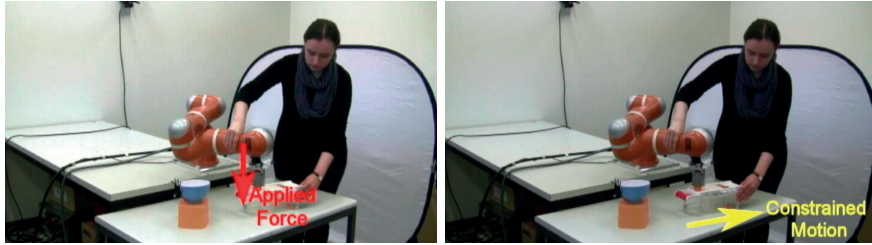
We use kinesthetic PbD to teach robots how to perform various tasks: such as grating or peeling vegetables, scooping etc (illustrated in Fig. 1.1). A human user is required to perform the same task in varying configurations of the objects, while backdriving a robotic arm (see Fig. 1.3).

Based on this information we extract task constraints as features that have remained consistent across demonstrations (in Fig. 1.4 we exemplify this for a grating task in which the motion is constrained horizontally along the main axis of the grater, while a vertical force is constantly applied).

They represent constraints guiding the motion of each arm as well as bimanual constraints ensuring arm coordination. Additionally we make the assump-



**Figure 1.3** Demonstrating the grating task from different starting positions



**Figure 1.4** Constraints in the grating task.

tion that the way the user holds the tool influences the forces applied in the task. Based on this information we extract embodiment constraints allowing a robot to anticipate and adapt to a human’s intention to apply a force when executing a task collaboratively.

We use the extracted constraints first to guide model learning (i.e. encoding profiles or motion, force and stiffness) and secondly for parameterizing a Cartesian impedance controller at runtime. We thus use a single controller for the whole task duration, switching the reference frame, adapting the stiffness of the arm, and where possible employing hybrid control by using a decomposition in force and position control along the axis of the desired reference frame.

Lastly we explore various modalities of giving feedback to the user during teaching interactions such as to maximize engagement and the robot’s performance as the teaching outcome. Understanding and adapting to user particularities, as well as acquiring task skills, allows optimal human-robot interaction. Our approaches are validated on common daily tasks and we assess aspects of human-robot interaction through user studies with naive subjects.

## 1.5 Contributions

---

### **Constraint-based task representation**

We propose an approach for learning task specifications automatically, by observing human demonstrations. Using this allows a robot to combine representations of individual actions to achieve a high-level goal. We hypothesize that task specifications consist of variables that present a pattern of change that is invariant across demonstrations.

We identify these specifications at different stages of task completion. Changes in task constraints allow us to identify transitions in the task description and to segment them into sub-tasks. We extract the following task-space constraints: (1) the reference frame in which to express the task variables, (2) the variable of interest at each time step, position or force at the end effector; and (3) a factor that can modulate the contribution of force and position in a hybrid impedance controller.

We then extend this approach to bimanual tasks by automatically determining the role of the arms as master or slave; the type of coupling as simple motion coordination, or force-motion coordination; and the pre-condition that enables the transition between actions.

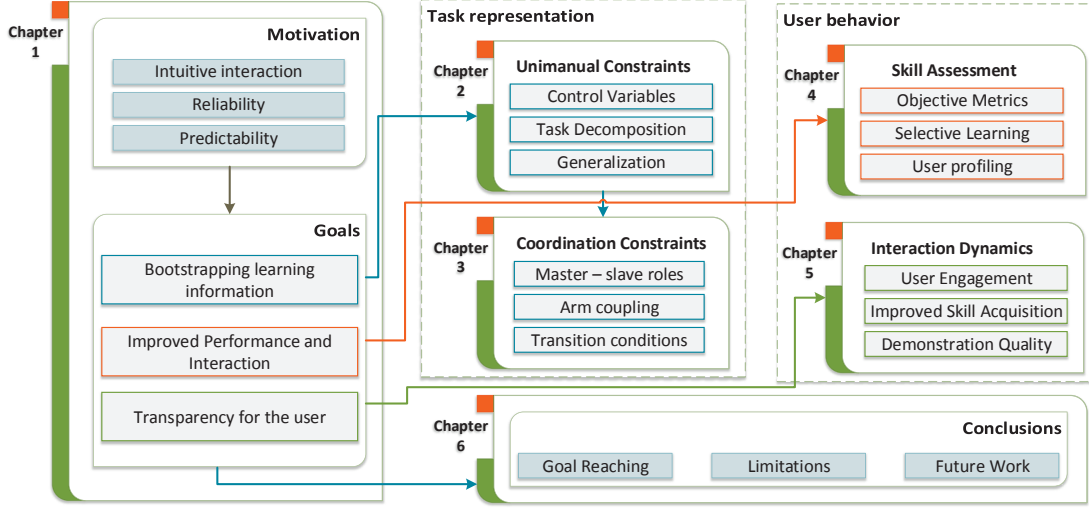
### **Context-aware execution**

We use the task representation obtained above to give the robot the ability to perform a task in two cases: (1) autonomous execution, in which a robot can execute a unimanual or bimanual task following the extracted constraints. (2) collaborative execution, in this case, alongside the task representation used previously we also assess the user's specific manner to use the tools when executing the task.

We analyze the grasping quality as an indication of whether the grasp is adapted for exerting forces and torques across directions of interest. These features allow the robot to anticipate and adapt to the user's actions, when performing the task collaboratively.

### **User performance assessment in force control tasks**

We propose an approach for automatically assessing the performance from demonstration data of multiple users. We develop objective task-specific metrics. These are related directly to the task constraints which we extract automatically. The determined skill is then used for selectively learning parts of the task from different users. We test the system performance on a daily task.



**Figure 1.5** Conceptual organization of the chapters.

## Sustained interaction dynamics through robot feedback

We evaluate an iterative teaching procedure, by correlating the user’s perceived satisfaction with the quality of the demonstration across both objective and subjective metrics. We show that robot provided feedback, in particular facial expressivity, significantly improves the user experience and perception of the whole interaction.

## 1.6 Thesis Outline

The results in this thesis have been either previously published or are currently under submission. Following the thesis structure we provide a brief summary of each chapter. The logical flow is illustrated in Fig. 1.5.

### Chapter 2. Constraint-based task representation

This chapter presents an approach for extracting unimanual task constraints from human demonstrations. They consist of the reference frame, the relevant variables and the stiffness modulation. A change in the constraints determines a switch to a new action, thus segmenting the data into meaningful parts. The constraints drive model learning and facilitate the control of the robot by parameterizing a cartesian impedance controller used throughout the task. This work has been published in [Ureche et al. \(2015\)](#).

**Chapter 3.** Constraint-representation of coordinated behavior

In this chapter we extend the approach introduced previously to bimanual tasks, and extract additional coordination features that are included in the task representation. We use this representation for both autonomous and collaborative execution. This chapter is based on a journal publication currently under review [Pais Ureche and Billard \(2017a\)](#).

**Chapter 4.** User skill assessment based on task constraints

In this chapter we use the previous proposed approach of constraints extraction to assess a user’s performance when demonstrating the task. This provides an objective assessment which is task-specific but performed automatically with respect to the constraints. We evaluated this approach through a user study where we show a correlation between the identified skill of the user when demonstrating the task and the performance of the robot when autonomously executing the same task from the models extracted from that user. This work is under review in [Pais Ureche and Billard \(2017b\)](#).

**Chapter 5.** Interaction dynamics in PbD

In this chapter we focus on improving teaching interactions through feedback provided by the robot. We conducted a user study on the iCub humanoid robot to explore various modalities of providing feedback that was correlated with the teaching quality. Facial expressivity, specific to humanoid robots, proved to be the most efficient way of communicating states that led to increased demonstration quality and user satisfaction. This work was presented in [Pais et al. \(2013\)](#).

**Chapter 6.** Conclusions

We conclude by an overall assessment of our contributions with respect to the goals identified in the introductory section. We discuss the limitations of our approaches and identify directions for future work.



# CONSTRAINT—REPRESENTATION OF UNIMANUAL TASKS

The work presented in this chapter has been published in:

*Pais Ureche A. L., Umezawa K, Nakamura Y, Billard A (2015) **Task parameterization using continuous constraints extracted from human demonstrations**, IEEE Transactions on Robotics, 31(6), 1458 – 1471, [TRO 2015]*

## 2.1 Forward

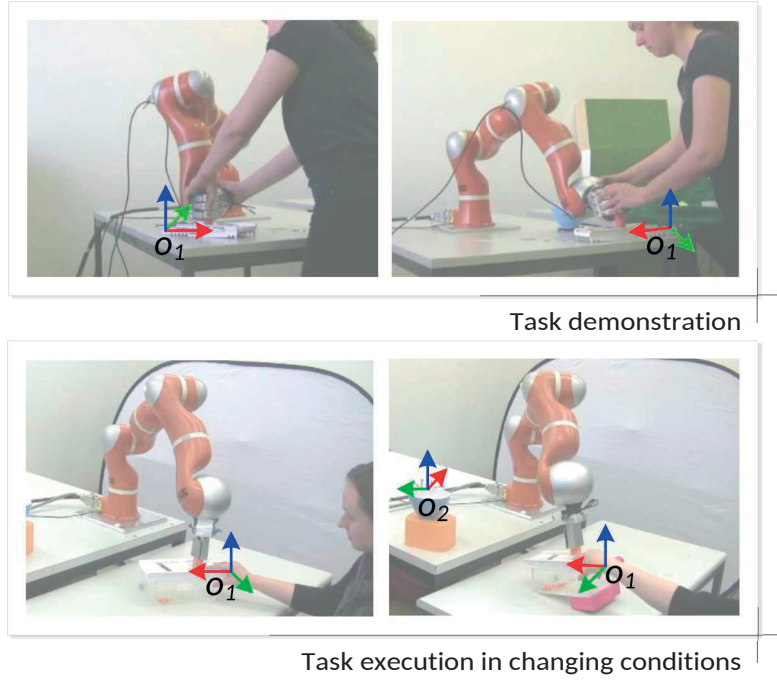
---

Under the general theme of this thesis of extracting and using task constraints, in this chapter we focus on unimanual constraints. We specifically target manipulation tasks, that consist of several actions requiring different specifications, such as a position-controlled reaching action, followed by a force-controlled manipulation action and an additional reaching movement. In this chapter we propose an approach for learning these task specifications automatically, by observing kinesthetic human demonstrations.

We hypothesize that task specifications consist of variables that present a pattern of change that is invariant across demonstrations. We identify these specifications at different stages of task completion. Changes in task constraints allow us to identify transitions in the task description and to segment them into sub-tasks. We extract the following task-space constraints: (1) the reference frame in which to express the task variables, (2) the variable of interest at each time step, position or force at the end effector; and (3) a factor that can modulate the contribution of force and position in a hybrid impedance controller.

The extracted constraints serve two purposes: first they guide model learning such that we encode the variables of interest across the corresponding relevant directions. Secondly they parameterize a Cartesian impedance controller used for the entire task duration which allows switching between the reference frames of each action, applying the corresponding force-motion profiles and adapting the stiffness of the arm.

We validate the approach on a 7 DOF Kuka arm, performing 2 different tasks: grating vegetables and extracting a battery from a charging stand. Using this constraint-representation allows the robot to combine specifications of individual actions to achieve a high-level goal.



**Figure 2.1** From recording human demonstrations (top row), we detect the relevant frame of reference and the direction in which to apply a hybrid force and position controller. In this figure the robot has correctly extracted that the frame of reference is attached to the grater and that force has to be applied along the vertical axis, whereas position control is needed along the horizontal plane of the grater. This allows the robot to reproduce the task even when the grater is moved to a different position and orientation (bottom row).

## 2.2 Introduction

Daily activities such as dish washing or preparing a meal often require completing multiple actions while interacting with different objects. When performing such tasks, humans are able to focus on the key aspects necessary for achieving the goal. For example when grating a vegetable they naturally push against the grater, and focus on maintaining a certain speed and contact force with the grating surface. Moreover, humans naturally introduce variability by repositioning objects or by using different paths between two objects.

Consequently, obtaining a feature-based representation for such high-level tasks requires:

1. relating these features to the objects in the task (extracting the local frame of reference).
2. accounting for the large variability between demonstrations and deciding what feature should be reproduced (extracting task constraints with respect to trajectories, force profiles and necessary stiffness modulation)

In this work we propose an approach for automatically extracting continuous

task constraints required for successfully completing a task. We consider the task presented in Fig. 2.1, consisting of grating a vegetable and disposing the remains. We use Programming by Demonstration (PbD) to record a set of kinesthetic demonstrations while varying the initial positions of the robot and the spatial configuration of the objects used.

We use the demonstration data to extract the object to be used in each part of the task (either  $o_1$  or  $o_2$ , see Fig. 2.1) and the way the task should be performed (i.e. alternating force and position control). More specifically we consider a hybrid impedance controller:

$$\tau = J^T(K(x - x_r) + F) \quad (2.1)$$

where  $\tau \in \mathbb{R}^n$  is the joint control input for an  $n$  degrees of freedom manipulator,  $J$  is the Jacobian. The following variables:  $x_r \in \mathbb{R}^D$ , the reference cartesian position,  $F \in \mathbb{R}^D$ , the desired force and  $K \in \mathbb{R}^{D \times D}$ , the stiffness matrix are extracted from the user demonstrations. In this case the number of dimensions is  $D = 3$ .

We aim to learn a parametrization of this control law applicable for the whole task duration. Our approach exploits the variability between demonstrations to learn a criterion for determining a notion of coherence in the demonstration.

First for each time step, we extract a reference frame  $R$  in which the variables are most consistent. In some cases this may represent a quasi-orthogonal decomposition of position and force control along the axes of the object, although we continuously use a Cartesian impedance controller.

Secondly we extract the variables of interest in the selected reference frame. Specifically, a task variable (such as the force perceived at the end effector) might have a large variability within a demonstration, thus indicating that it becomes important only in a given region of the task. Regions in which a variable changes very little throughout a set of sequential demonstrations prove coherency in that part of the task. Therefore we focus on extracting such behaviors as the task constraints that should be reproduced.

Third we extract the stiffness parameter  $K$  which allows us to modulate the contribution of position and force when there is no decomposition in hybrid control as well as to ensure safe interaction and proper task completion.

These task specifications change when switching from one action to another. Typically we record demonstrations of a full task, consisting of several such actions. Applying our method automatically segments the demonstration data. The grating task for example consists of 3 distinct phases: reaching for the grater, grating and reaching for the trash can. Two reference frames are used (Fig. 2.1): object  $o_1$  (the grater) for the first two segments and object  $o_2$  (the bowl) for the third part of the task.

Automatically obtaining this decomposition guides the learning phase of the PbD framework. A different model can be learnt for each atomic action

(using various machine learning techniques for motion encoding), in the local frame of reference, using the data between two changes of constraints. In our approach we learn from the demonstrations a time-invariant path profile for the directions along which position is the variable of interest ( $x_r$ ). For the directions along which force is important, we learn a dependency between the desired force profile and the desired trajectory. For the particular task of grating vegetables we obtain a decomposition of force and position control. This applies to the motion along the grater’s surface where force control is performed (thus  $F$  becomes a function of other variables, such as in Eq. 2.2,  $F = f(x_1)$ ), while position is controlled on the other two axes, leading to:

$$\tau = J^T R \begin{bmatrix} K_1(x_1 - x_{r_1}) \\ K_2(x_2 - x_{r_2}) \\ F \end{bmatrix} \quad (2.2)$$

Our approach is aimed at bootstrapping information for learning and has the following contributions:

1. it automatizes learning, by bootstrapping information about the task, and parameterizing the learned models. It performs automatic task segmentation and reduces the number of the variables encoded for each segment by extracting the important ones. This simplifies the learned model by focusing only on the variables of interest resulted from this decomposition (e.g. instead of learning a full encoding of 3D force vs. 3D position model, one simplifies the model by encoding just the force profile corresponding to the axis where this is applied).
2. it identifies task constraints directly from variables that can be used for control (end effector position, force and stiffness) and offers a clear decomposition of these. This enables a consistent encoding of all the subtasks for using a single controller and ensures a smooth execution by directly embedding the constraints. This is applied through a Cartesian impedance controller, by modulating the stiffness (e.g. having zero stiffness on one axis is equivalent to performing pure force control on that axis). Therefore we learn a stiffness modulation profile to be applied online during the execution.
3. the learned skill is generalizable to different locations or similar objects. This is achieved by learning the desired control with respect to the determined object frame (i.e. relating the action to the object on which this is performed). The system is robust to perturbations due to the time-invariant encoding.
4. it extracts task constraints without requiring any prior information about the goal of the task, actions in the task or models of the objects.

Next we review related work in Section 2.3 and describe the different stages of our task constraints extraction in Section 2.4. We contrast the extraction of constraints for two tasks differing in the duration and number of important variables in Section 2.5. We discuss the advantages and limitations of our approach in Section 2.6.

## 2.3 Related Work

---

In this work we focus on extracting artificial task constraints as described in Villani and De Schutter (2008); Howard et al. (2009), based on the variability observed in the demonstration data. The idea that invariants in motion determine important task features was first used by Bobick and Wilson (1997) for recognizing gestures from continuous data, and representing them as an enchainment of states. In our work we use the variance not only to segment data but also to determine the relative importance between various variables and the frame in which these are most consistent. We reconstruct the task from a sequence of states, parameterized with the extracted constraints. Therefore we review related work with respect to automatic extraction of constraints, task segmentation, and constraint-based motion planning.

### 2.3.1 AUTOMATIC EXTRACTION OF REFERENCE FRAMES

---

In our previous work (Calinon et al., 2007) we proposed extracting the reference frame in a manipulation task with respect to a proposed metric of imitation. Data recorded from demonstrations (arm joint angles, hand cartesian position relative to the objects and gripper status) is projected into a lower dimensionality latent space and further encoded in a time-dependent manner using a Gaussian Mixture Model (GMM). Gaussian Mixture Regression (GMR) is used to reproduce the motion. In an early attempt, temporal variations are encoded in an Hidden Markov Model (HMM) and implicit segmentation is performed through HMM states (Calinon et al., 2006). These implementations have the limitations of encoding the motion in a time-dependent manner. Additionally in our approach we focus only on the end effector state (actual position and force, observed in the demonstration), thus making the skill easily transferable to other robotic platforms. Moreover we increase the task complexity and the number of encoded constraints.

A different method of selecting a task-space is based on three criteria (Muhlig et al., 2009): a variance-based analysis of object trajectories, attention focus on objects in the task and an evaluation of the teacher’s discomfort during demonstration. While this method takes into account many factors, it is applied solely to vision-tracked human demonstrations. In our case the demonstrations are performed kinesthetically in order to allow the robot to experience forces

that should be applied on objects. Moreover analyzing if the human maintains an uncomfortable posture during demonstration might reveal that the particular action was important for the task (Muhlig et al., 2009). In our case a direct evaluation is done on robot’s proprioceptive data, while the user chooses an arbitrary position for demonstration.

The approaches mentioned above lack information about how the manipulation is performed that in some tasks may be key to successful execution. Therefore we build on these existing approaches by extracting constraints with respect to force profiles and robot stiffness in different regions of the task, and assess the effects this has on task completion.

Expressing the control variables in the local reference frame of the object on which manipulation is performed at a given time, allows the robot to properly execute the task when the positions of the objects change in the scene. Moreover this allows us to consider constraints not only as factors that limit the robot’s motion (Stilman, 2007), but that also add meaning to the motion (i.e. a grating motion, characterized by a given force and motion profile, is only meaningful when performed on a grater in the context of a grating scenario).

In some cases there might be multiple actions performed on the same object. The methods presented above extract one reference frame, but cannot disambiguate between the different positioning needed for each action. In our work we address this issue by also extracting an attractor frame (relative to the reference frame extracted above).

### 2.3.2 AUTOMATIC EXTRACTION OF FORCE INFORMATION

---

The ability to successfully perform complex tasks resides in making use of additional sensing. For example, assessing joint torque values can be an indicator of whether the motion of the end effector is constrained Sukhoy et al. (2012). Therefore the second aspect that we address is detecting axes in task space where force control applies and encoding these force profiles. Typically the decision of choosing an axis in task space on which to perform force control or position control is engineered in advance. In the proposed approach we were able to automatically determine an arbitrary reference frame with respect to the object of interest in which a decomposition of force and position control can be obtained and we selected the suitable type of control that applies to each axis. However, adding the force information, while of high importance for the task, can be challenging depending on the platform. Kinesthetic teaching for demonstrating the motion might need to be used in conjunction with a haptic device for demonstrating the required force profile (Kormushev et al., 2011).

Additionally the stiffness is an important parameter when executing a task, as varying the robot’s stiffness according to the task ensures safer interaction (Calinon et al., 2010). In our approach we determine the required stiffness mod-

ulation as a relative measure between the contribution of force and position on each axis of the object. This leads to learning hybrid control in an automatically determined frame.

### 2.3.3 TASK SEGMENTATION

---

The constraints extraction topic is complementary to performing task segmentation which on the long term offers the possibility to easily recognize, classify and reuse motions (Wang et al., 2003; Lin and Kulic, 2011; Shim and Thomaz, 2011).

Typically in robot learning from demonstration of a task that consists of several actions, each gesture is shown to the robot separately. The main reason is that task specifications change from action to action. In the proposed approach we are able to automatically determine when these task specifications need to change and the next set of specifications.

In our work we do not explicitly seek to segment the data, however segmentation occurs naturally when the task constraints change, resulting in meaningful segments that encode atomic actions. This allows a flexible representation of the task, exploiting the local behavior in each sub-task. A vast majority of recent works in segmentation focus solely on motion data represented by sets of joint positions or hand positions and orientation retrieved by motion capture systems in the case of human motion and by robots proprioception in the case of robotic motions. However very few works focus on segmenting task data that includes force information.

The existing approaches for motion segmentation (Wang et al., 2003) rely on either (1) classification based on existing motion primitives used for prior training (Mangin and Oudeyer, 2012; Tao et al., 2012; Kulic et al., 2012); (2) looking for changes in a variable, like zero-crossings (Takano and Nakamura, 2006); or (3) clustering similar motions by means of unsupervised learning (Kulic et al., 2008; Grollman and Jenkins, 2010). The downside of these approaches is the need of prior task knowledge, which may be poor and incomplete in real-life situations. Moreover they are sensitive to the variables encoded and have difficulties when applied to data such as force information where a large number of zero crossings may appear, making the encoding of motion primitives difficult.

The first approach for segmentation can ease robot control because of the existence of motion primitives. However while it is safe to assume that human motions are likely to follow a specific pattern in a known context, rather than being random (as shown in (Bennewitz et al., 2005)), a major drawback is the need to include prior knowledge. It also restricts the scope of segmentation by knowing what the task is about, such as segmenting motions used in robot assisted surgery (Tao et al., 2012).

The second segmentation involves searching for zero velocity crossings (ZVC)

(Takano and Nakamura, 2006) or other changes in a variable compared to a known state (Sukhoy et al., 2012). This approach is sensitive to the variables encoded while one needs to find a way that would ensure optimal segmentation across all task dimensions. Regions of low variance have been alternatively used to determine segmentation points Lee et al. (2011). Furthermore most of them rely on other techniques for human motion analysis which include (Wang et al., 2003): Dynamic Time Warping (DTW) used in the temporal alignment of recorded data; or HMM for analyzing data that varies in time (such as hand movements sign language (Matsuo et al., 2008)). Additionally when humans demonstrate a task to a robot, they may stop during the demonstration to rearrange an object or teach in a different manner. In these cases the above mentioned approaches over-segment the data.

The third approach encompasses a more complex view of human motion, such as learning and clustering motion primitives in an incremental manner, from observing humans (Kulic et al., 2008). The method in (Kulic et al., 2008) performs unsupervised segmentation based on motion encoded through an HMM. The obtained segments are clustered according to a measure of relative distance and organized in a tree structure. It encodes generic motions at the root, that gradually become more specialized close to the leaves. The algorithm allows to change the model according to known primitives (Kulic and Nakamura, 2008), and to use the same learned model not only for recognizing, but also for generating motions (Kulic et al., 2012). While being one of the most robust implementations to date, the approach lacks time independency in motion encoding.

These approaches, while efficient, have the shortcoming of being task specific and requiring a considerable amount of prior knowledge which may be poor and incomplete in real-life situations. Thus they achieve little generalization across a wide range of tasks. They also fail to model specific features of the motion, focusing mainly on changes in position. Moreover these algorithms focus on extracting motion primitives, as opposed to learning a parametrization of a control system that remains the same all along the task, as in our approach. This allows learning and reproducing a task in a seamless manner.

Our approach departs from the above-mentioned implementations by: (1) taking a broader view on the task and analyzing the motion also with respect to constraints that apply to forces and stiffness; (2) extracting task constraints from a low number of demonstrations, while removing the over-segmentation; (3) finding the relevant atomic actions in a task, without embedding any prior information about the goal of the task, nor models of the objects.

This makes the approach suitable for tasks that encompass switching between multiple atomic actions. Moreover we consider continuous constraints that may apply throughout or only on a subpart of the task. Finally, we use a single controller throughout the task execution, while the constraints identify values taken by the variables of the impedance controller as the task unfolds.

### 2.3.4 CONSTRAINT BASED MOTION PLANNING

---

Knowing the constraints that apply to each action that is to be performed can lead to a better task planning (Oriolo and Vendittelli, 2009; Ye and Alterovitz, 2011). A constraint-based representation of a complex task can be used by a high level planner (Beetz et al., 2010) for executing plans or for inferring motion grammars (Dantam and Stilman, 2013) for a high-level representation.

Common ways of encoding the task sequence use: Finite State Machines (FSM) (Schutter et al., 2007; Niekum et al., 2013), Petri nets, Markov Models (Lee et al., 2011; Arsenio, 2004), graph and tree representations (Jäkel et al., 2010; Konidaris et al., 2012).

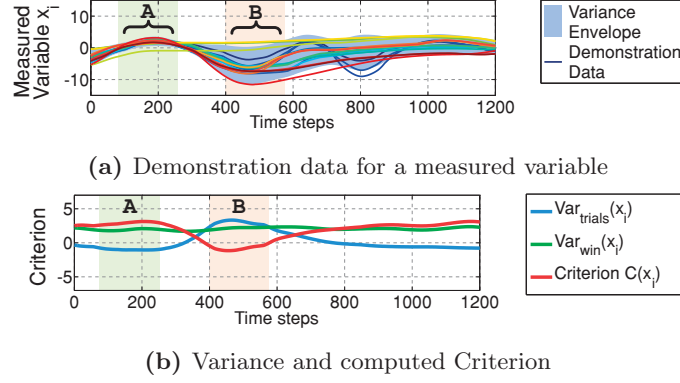
In our work we consider the sequence of atomic actions implicit in the demonstration. We therefore determine a Finite State Machine (FSM) to execute the task. The states are not known a priori but extracted. They correspond to the atomic actions identified previously and encode their corresponding constraints. Our implementation takes a low-level approach by encoding constraints, directly in the control variables. This guarantees the task success without knowing the conceptual goal, and allows isolating atomic actions for individual reuse. The task is executed using a single controller and embedding the constraints online, during the execution.

## 2.4 Method

---

We consider a set of  $N$  demonstrations of a task performed under changing conditions, using a number  $N_o$  of objects. The data set is a vector of  $L = 2$  components  $\xi_d^i = \{F_d^i, x_d^i\}$  consisting of end effector measurements of force and position. The upper indices correspond to representing the data in the reference frame of each object  $o_i$ ,  $i \in 1 \dots N_o$ , while the lower indices correspond to the dimensions considered  $d = 1 \dots D$ . The  $\xi^0$  corresponds to the original recorded data (in  $R_0$ ), the fixed referential in the base of the robot. The data was temporally aligned using Dynamic Time Warping (DTW), resulting in a set of length  $T$ . Each demonstration is composed of a series of  $T \cdot D \cdot L$  measurements, with  $t = 1 \dots T$  number of time steps,  $d = 1 \dots D$ , dimension of each of the  $l = 1 \dots L$  components.

We postulate that if a variable (a) changes value *significantly* within a single demonstration and (b) changes this value in a *systematic* way across demonstrations then this variable is *significant* for the task. It hence becomes a task constraint that should be reproduced. We thus propose a criterion, computed for all variables  $D \cdot L$  and all objects  $N_o$ , given by the difference between the variance over the time window and that over trials. This allows comparing the task variables in a relative manner, without setting any hard thresholds. At



**Figure 2.2** Example of recorded data and computed variance over trials ( $Var_{trial}$ ) and over a time window ( $Var_{win}$ ) for a measured variable  $x_i$ . Region **A** shows data with little variance across trials (i.e. a feature of that should be reproduced). Region **B** shows data with large variance over trials, and low variance over a time window (almost constant).

each time step the criterion is computed on each dimension as:

$$C(\xi_{d,l}^i) = Var_{win}(\xi_{d,l}^i) - Var_{trial}(\xi_{d,l}^i) \quad (2.3)$$

thus comparing the force and position measurements on each axis. The obtained value is normalized  $C(\xi_{d,l}^i) \in [-1, 1]$ . The variances  $Var_{trial}$  and  $Var_{win}$  are defined as:

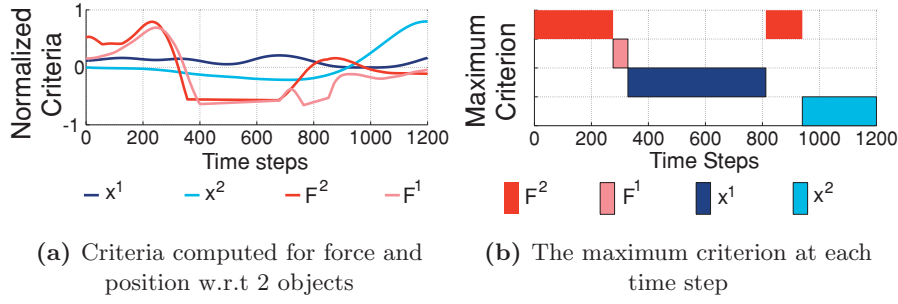
$$Var_{trial}(\xi_{d,l}^i) = \frac{1}{N} \sum_{i=1}^N (Var(\xi_{d,l}^i)) \quad (2.4)$$

$$Var_{win}(\xi_{d,l}^i(t:t+\omega)) = \frac{1}{N} \sum_{i=1}^N (Var(\xi_{d,l}^i(t:t+\omega))) \quad (2.5)$$

The values of the two variances are normalized such that  $Var_{trial}, Var_{win} \in [-1, 1]$ .

In a typical robotic task a minimum of  $D \cdot L$  variables have to be compared if using a 3D measurement of position and force (3 groups of 2 variables). The total number of criteria to be computed for a task is given by  $N_C = N_o \cdot L \cdot D$ . The size of the time window is an open parameter. In this case it is chosen arbitrarily as being the shortest time period in which we see noticeable changes in the task flow.

The proposed method for extracting the task constraints is illustrated below, on an uni-dimensional measurement ( $D = 1$ ) of two variables: force  $F \in \mathbb{R}$  and cartesian position  $x \in \mathbb{R}$  of the robot's end effector. For the purpose of this example we drop the lower index  $d$ . We also consider two objects  $o_1, o_2$ . The data set is composed of the pair of elements:  $\xi^i = \{F^i, x^i\}$  considered to be recorded over a number of  $N$  demonstrations of a task (see Fig. 2.2 (a)). This determines  $N_C = 4$  computed criteria, as shown in Fig. 2.3 (a).



**Figure 2.3** Comparison between the criteria computed for uni-dimensional measurements of force (F) and position (x) in 2 reference frames ( $RF_1$  and  $RF_2$ ).

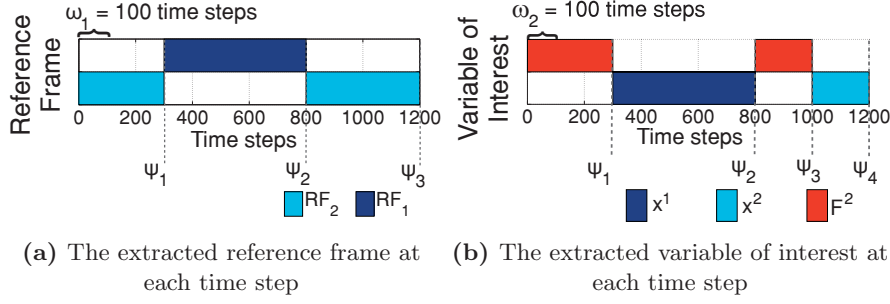
#### 2.4.1 DETERMINING THE TASK CONSTRAINTS

Using the defined criterion we extract the following task constraints: the frame of reference (as explained in Section 2.4.1), the relative importance of position and force on each axis of the object (see Section 2.4.1), and a weighting factor between the two, used to modulate the controller’s stiffness throughout the task (Section 2.4.1). The procedure is summarized in Alg. 2.1.

##### EXTRACTION OF THE REFERENCE FRAME

For choosing a frame of reference we compare the computed criteria and choose at each time index  $t$ ,  $t = 1 \dots T$  the value of the highest criterion for all the variables considered  $\max(C(\xi_{d,t}^i))$ , see Fig. 2.3 (b). Thus the vector of obtained maximum values  $\max(C(\xi_{d,t}^i))$  is analyzed separately for each dimension  $d$ , using a time window of arbitrary size (in this case  $w_1 = 100$  time steps). We consider that in each time window the reference frame is given by the object  $o$  with the highest number of occurrences of its corresponding criterion  $\max(C(\xi_{d,t}^o))$ . In this example there are two changes of reference frame, as shown in Fig. 2.4 (a): for the first 100 time steps the reference frame  $R$  is given by object  $o_2$ , for the next 200 time steps there is a change to  $o_1$ , and for the rest of the motion the RF is changed to  $o_2$ .

The changes in the reference frame determine a set of *segmentation points*  $\psi_s$ ,  $s = 1 \dots S$  which delimit the actions performed on each object. In this example there are 3 actions (one performed on object 1 and two performed on object 2) determined by the change of RF. Each segmentation point corresponds to a state that contains the time index  $t_s$  when the change occurred and the id of the reference frame used up to that point  $\psi_s = [t_s, R_s]$ .



**Figure 2.4** The reference frame and variables of interest are given by the maximum criterion in a time window  $\omega_i$ .

---

#### EXTRACTION OF THE RELEVANT TASK VARIABLES

---

The criterion defined in Eq. 2.3 allows us to compare in a relative manner the influence of variables of different types (like force vs. position), and that vary across different scales, see Fig. 2.3 (a). The aim is to be able to quantify their relevance with respect to the task, so as to give more importance to the variable of interest in the controller and to adjust it when a change occurs.

For determining the relevant task variables, we analyze the criterion on each dimension  $d$  using a time window of arbitrary size (in this case  $w_2 = 100$  time steps). Similarly to extracting the reference frame, we consider the relevant variable in each time window to be the one that has the highest occurrence of its corresponding maximum criterion in that interval. In the given example, there are several changes between position and force as variables of interest (see Fig. 2.4 (b)).

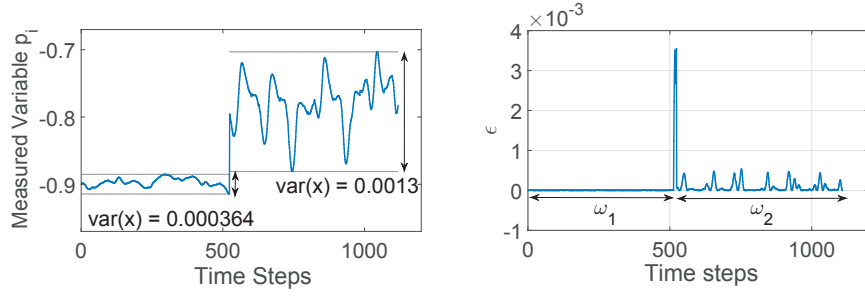
The changes in the variable of interest determine additional *segmentation points* which together with the initial points determined by the change of reference frame delimit individual atomic actions such as reaching movements. In the example described above, there are 3 segmentation points corresponding to the change of the variable of interest (see Fig. 2.4 (b)). The first two points are identical to the segmentation points  $\psi_1$  and  $\psi_2$  found by the change in the reference frame. The next point  $\psi_3$  marks a change from a force-based part of the task to a position based part. The final point  $\psi_4$  concludes the motion. The points are sorted according to the time index when the segmentation occurred. The information about the variable of interest is added to the vector  $\psi_s = [t_s, R_s, \xi_{d,l}^s]$ . The current  $\xi_{d,l}^s$  now contains only the data between the previous and current segmentation points.

---

#### EXTRACTION OF THE STIFFNESS MODULATION FACTOR

---

Determining the axis-specific relative importance between the two variables can be done by computing a weighting factor  $\lambda$  that balances the contribution



**Figure 2.5** Automatically adjusting the window size based on monitoring changes in the observed variance

of the force and position according to the relevance determined above. Thus, for each dimension  $d$  the value of  $\lambda_d \in \mathbb{R}^D$  is given by the normalized difference between the criterion computed for position and the one computed for force

$$\lambda_d = C(x_d) - C(F_d) \quad (2.6)$$

Thus the value of  $\lambda \in [0, 1]$  becomes a weighting factor for the controller's stiffness  $K$ . Therefore we can use an impedance controller for reproducing the motion with the factors described above representing continuous constraints, that can be directly embedded in the robot's control.

$$\tau = J^T \cdot R \cdot (\lambda K(x - x_r) + F) \quad (2.7)$$

The corresponding  $\lambda$  profile for each segment of the motion is added to the constraints vector  $\psi_s = [t_s, RF_s, \xi_{d,k}^s, \lambda_s]$

---

#### CHOICE OF TIME-WINDOW SIZE

In the example presented above the size of the time window was chosen arbitrarily. When performing manual tuning our aim was to determine a time window that would result in avoiding very sudden changes from an important variable to another. For example switching from force control to position control for less than 10 ms will not have an effect on the task.

However a variable time window is desirable. We propose a way of determining a suitable time window by comparing the average variance with the instantaneous variance, therefore monitoring the rate of change in the signal. For example in the signal presented in Fig. 2.5(a), choosing a large time window (e.g. 1200 time steps) leads to losing information because the average variance in the first part of the signal is different and not representative for the second part of the signal. Therefore the average variance in a local time window ( $var_{tw}$ ) should be similar with the instantaneous variance computed at each time step ( $var_{ts}$ ). A change in the average variance determines a step

---

**Algorithm 2.1** Task Constraints Extraction

---

```
Bootstrapping(Set of  $N$  demonstrations:  $\xi_{d,l}^i = \{F_d^i, x_d^i\}$ )  
                                 $1 \rightarrow N$   
Do DTW, dataset length  $T$   
Criteria:  $C(\xi_{d,l}^i) = Var_{win}(\xi_{d,l}^i) - Var_{trial}(\xi_{d,l}^i)$   
 $s = 0$  % number of segmentation points  
% Determine the reference frame:  
for  $t = 1 : \omega_1 : T$  do  
     $R(t) = R_i$  for which  $C_{max} = \max_{t:t+\omega_1} (C(\xi_l^i))$   
    if  $RF(t) \neq RF(t-1)$  then  
         $s = s + 1$ ; % Create a new segmentation point  
         $\psi_s = [t_s, R_i]$  % add the current constraints  
    end if  
end for  
% Determine the variable of interest:  
for each dimension  $d = 1 : D$  do  
    for  $t = 1 : \omega_2 : T$  do  
        add  $\xi_{d,k}^i$  to the current constraints vector  
         $\psi_s = [t_s, R_i, \xi_{d,l}^i]$  for which  $C_{max} = \max_{t:t+\omega_2} (C(\xi_{d,l}^i))$   
        if  $\xi_{d,l}^i(t) \neq \xi_{d,l}^i(t-1)$  then  
            Insert a new segmentation point  
        end if  
    end for  
    % Determine the stiffness modulation factor:  
    for each segment  $s$  do  
        add  $\lambda_{d,s}(t) = C(\xi_{d,1}(t) - \xi_{d,2}(t))$  to the constraints vector  
         $\psi_s = [t_s, R_i, \xi_k^i, \lambda_{d,s}]$   
    end for  
end for  
return  $\psi_{1:s}$   
end
```

---

change in the instantaneous value. Therefore we can compute a suitable time window using a variable  $\epsilon$  defined as:  $\epsilon = |var_{tw} - var_{ts}|$ . A significant change in this measure determines starting a new window. According to this variable (see Fig. 2.5(b)) we were able to determine two windows ( $\omega_1 = 513$  samples and  $\omega_2 = 595$  samples for the given example, based on an abrupt change in  $\epsilon$ ).

## 2.4.2 CONSTRAINT-BASED MOTION LEARNING

---

In our work, segmentation of the demonstrated data occurs whenever there is a change in the extracted constraints. This is a natural manner of segmenting as the points in which either the reference frame or the variables of interest change, delimit atomic actions (e.g. the force sensed at the end effector might be relevant in the first part of the task while after the segmentation point, end effector's position could become more relevant). Segmenting and interpreting the data in a stochastic manner allows regenerating the motion according to the measures determined to be important as well as finding optimal control strategies with respect to the variables of interest (see Table 2.1, Columns 1 and 2).

When encoding the motion profile we aim to preserve the exact behavior seen during demonstration. We therefore choose to encode variables that show a temporal coupling (like position and orientation, that change synchronously towards a target posture (*the attractor*)) using our Coupled Dynamical Systems (CDS) approach [Shukla and Billard \(2012\)](#). This encompasses the following advantages: (a) the motion is encoded in a time-invariant manner and ensures asymptotical stability at the target of both dynamical systems; (b) the motion follows the demonstrated dynamics even if the execution starts from unknown regions of the space, far from the demonstrated motion, without the need to replan or re-scale the trajectory; (c) the temporal-correlated behavior of the two variables is preserved and thus a perturbation in one of the systems does not cause an unsynchronized behavior, the robot being able to adapt online to changes in the environment.

With respect to a given reference frame  $R$  extracted previously the CDS approach determines an attractor (a relative positioning and learns the motion profile with respect to this frame). In the given example there are two attractors with respect to the grater object and one for the bowl.

---

#### LEARNING THE MOTION PROFILE

---

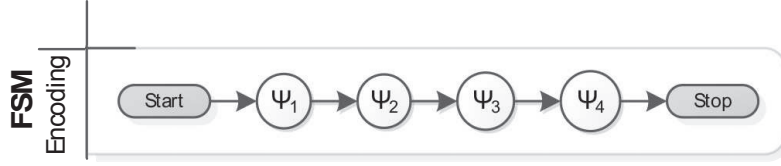
We choose to encode the motion using a coupled dynamical system approach, as described in [Shukla and Billard \(2012\)](#), which allows us to preserve the coupled evolution of position and orientation towards the target posture, that was observed in the demonstrations. The force profile is encoded separately, as a function of the position. This allows the robot to execute the task in changing conditions and to generalize to situations not seen during training (Fig. 2.1).

Each individual variable is encoded as a non-linear dynamical system of the form  $\dot{x} = f(x)$ , which encodes the mapping between a variable and its first derivative thus removing the explicit time dependency. Here  $x$  and  $\dot{x} \in \mathbb{R}^D$  represent the cartesian position and velocity of the end effector. The function  $f : \mathbb{R}^D \mapsto \mathbb{R}^D$  (initially unknown, but implicit in the demonstrated behavior) is a continuous and continuously differentiable function stable only at the attractor  $x^*$ . The non-linear behavior of function  $f$  is encoded using a mixture of  $k$  Gaussians, specified by a vector  $\theta_x^k = [\pi_x^k, \mu_x^k, \Sigma_x^k]$ , representing the parameters of the GMMs (priors, means, covariance matrices), such that  $P(x, \dot{x} | \theta_x^k)$  represents the dynamics of system 1. Based on this encoding the velocity  $\dot{x}$  is thus computed as  $\dot{x} = E\{p(\dot{x} | x; \theta_x^k)\}$ . The model is learned through maximization of likelihood under stability constraints (see [Shukla and Billard \(2012\)](#) for details).

In our case the absolute position of the attractor in each segment is estimated from the initial set  $\xi_0$  (in  $R_0$ ) as the average of all the points from the  $N$  demonstrations, on each dimension  $d$ , at the segmentation time  $t_s$ , resulting in:  $x_d^* = \text{avg}_{1 \rightarrow N}(x_d(t_s))$ . The motion is encoded in the attractor's reference frame  $R_*$ ,

State	Constraints	Motion Encoding
$\psi_1$	$[t_{s_1}, R_1, F, \lambda_1]$	$C_{\psi_1} = [C_x, \theta_F^k, \theta_\lambda^k]$
$\psi_2$	$[t_{s_2}, R_2, x, \lambda_2]$	$C_{\psi_2} = [C_x, \theta_\lambda^k]$
$\psi_3$	$[t_{s_3}, R_2, F, \lambda_3]$	$C_{\psi_3} = [C_x, \theta_F^k, \theta_\lambda^k]$
$\psi_4$	$[t_{s_4}, R_1, x, \lambda_4]$	$C_{\psi_4} = [C_x, \theta_\lambda^k]$

**Table 2.1** Final task parametrization for the given example, consisting of states  $\psi_s$ , the extracted constraints and the corresponding statistical encoding to be used by the controller in each segment,  $C_{\psi_s}$ .



**Figure 2.6** Finite State Machine used for executing the task. Each state encodes the determined constraints. We consider that the order of the demonstrated actions is implicit for the task flow.

such that the attractor becomes  $x^* = 0$ . The axis of the attractor's reference frame are not necessarily aligned with those of  $R_i$  and the origin is located at  $x^*$ . In a grating task for example there are two attractors with respect to the grating surface: the *top* (initial point touched on the grater) and the *bottom* (after passing the blade).

Similarly we encode the rotation specified by an axis-angle representation  $r \in \mathbb{R}^4$ , as  $P(r, \dot{r}|\theta_r^k)$ , with respect to an estimated attractor  $x^*$ . Finally  $P(\gamma(x), r|\theta_c^k)$  represents a coupling function between the two systems, learned using maximization of likelihood. During the execution the system updates the dynamics of system 1 through GMR, second the coupling is updated and this determines updating the second system (in this case the orientation) (see Alg. 2.2).

The model can be further parameterized to control the speed and amplitude of the robot's behavior under perturbation, using two scalars  $\alpha$ ,  $\beta$ . While in the original implementation in Shukla and Billard (2012) these parameters are learned from recording good trials and perturbed demonstrations, here we can estimate them based on the variance information, such that in regions with high variability the adaptation is slower than in regions with low variability. Thus, in the proposed impedance controller, the reference trajectory for the reaching segments is given by the learned CDS model. This ensures that the learned model follows the original dynamics of the demonstrated motion, and it is stable at the target. The synchronous evolution is ensured through the coupling function. The complete CDS encoding of the motion in a sub-part of the task is thus specified by the vector:  $C_x = [\theta_x^k, \theta_r^k, \theta_\xi^k, x^*, r^*, \alpha, \beta]$ .

---

**Algorithm 2.2** Constraint-based task execution
 

---

```

FSM Execution( $\psi_i, C_{\psi_i}, i = 1 : s$ )
  do
    read robot current position  $\xi_{d,1}$  and EE force  $\xi_{d,2}$ 
    read objects positions
    for all task segments  $s$  do
      Use current state's constraints  $\psi_s = [t_s, R_s, \xi_s^d, \lambda_s]$ 
      Transform data to  $R_s$ 
      % Compute the next desired robot position  $\{x(t+1), r(t+1)\}$ ,
      % using CDS (Shukla and Billard, 2012)
      if current attractor  $\bar{x}, \bar{r}$  not reached then
        % Compute next end effector position
         $\dot{x} = E\{\dot{p}(x; \theta_x^k)\}$ ;
         $x(t+1) = x(t) + \dot{x}(t)\Delta t$ 
        % Infer orientation based on current position
         $\bar{r} = E\{p(r|\gamma(x); \theta_c^k)\}$ ;
        % Compute next end effector orientation
         $\dot{r} = E\{\dot{p}(r|\beta(r - \bar{r}); \theta_r^k)\}$ ;
         $r(t+1) = r(t) + \dot{r}(t)\Delta t$ 
        % Determine stiffness modulation based on current position
         $\lambda = E\{p(\lambda|x)\}$ 
        if Force is important on dimension  $d$  then
          % Predict force based on current position
           $F = E\{p(F|x)\}$ 
        end if
        Transform all data back to  $RF_0$ 
        Update robot's motion (according to eq. 2.7)
      end if
    else Go to the next state
  end for
until Task completed
end

```

---



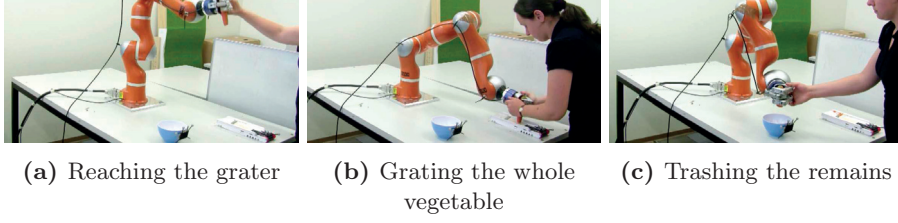
---

**LEARNING THE FORCE PROFILE**


---

For segments of the task, and across the dimensions in which force becomes important, we use GMM to learn a joint distribution of the variables  $F$  and  $x$ . We choose to encode the force profile with respect to the axis in which we see noticeable changes in position. In the grating task for example, force control is performed along the Z axis of the object; there is no modification in position along the Y axis (i.e. along the width of the grater, but the highest variance is observed with respect to the motion along the X axis (the grater's length), which is thus the variable with respect to which we encode the force profile.

We use a model comprising a mixture of  $K$  Gaussian components, such that:  $p(F, x) = \sum_{k=1}^K (\pi_F^k \cdot p(F, x; \mu_F^k, \Sigma_F^k))$ , where  $\pi_F^k$ ,  $\mu_F^k$  and  $\Sigma_F^k$  represent the priors, the mean and the covariance matrix for the Gaussian model. These parameters are learned through (EM) Expectation – Maximization algorithm. The vector  $\theta_F^k = [\pi_F^k, \mu_F^k, \Sigma_F^k]$  is added to the  $C_{\psi_s} = [\theta_F^k]$ . During the execution, GMR is used for predicting the force to be applied based on the current position:  $E\{p(F|x)\}$ . Unlike the encoding of position, for the force there is no attractor, as force control is performed along a trajectory.



**Figure 2.7** Atomic actions in the *Vegetable Grating Task*. The user demonstrates the task, using different starting configurations of the objects and the robot.

---

#### LEARNING THE STIFFNESS PROFILE

We encode the stiffness modulation factor  $\lambda$  similarly to encoding the force, by learning a joint distribution  $p(\lambda, x)$  using a mixture of  $k$  gaussians. The model is parameterized by the vector  $\theta_\lambda^k = [\pi_\lambda^k, \mu_\lambda^k, \Sigma_\lambda^k]$ , representing the priors, means and covariance matrices.

#### 2.4.3 CONSTRAINT-BASED EXECUTION

---

We assume that the order of the actions is implicit in the demonstration, thus the reproduction is based on the determined sequence of  $\psi_{1:S}$  points. A finite State Machine containing the inferred states is generated, as shown in Fig. 2.6. A state is generated for each change of constraints and contains: (a) the extracted constraints, and (b) the learned motion models, as they are summarized in Table 2.1, Column 3. Typically the transition between states occurs when the attractor of the current state is reached. This implies that reaching the determined relative frame is the main factor for advancing the execution. However the variables that were not determined as important for control might still hold complementary information, useful for state transitioning. The constraint-based task execution is presented in Alg. 2.2.

### 2.5 Validation

---

This approach was validated on two robot experiments performed using a 7 degrees of freedom (DOF) KUKA Light Weight Robot arm (LWR), with the provided Cartesian Impedance controller. The controller takes as parameters the desired position, force and stiffness and it automatically adjust the damping and dynamics terms for stability. The two experiments consisting of a kitchen task, *grating vegetables*, and an office task *removing a battery from a charging stand*, differ in duration, number of variables used for control and objects involved. We performed a quantitative evaluation of the extracted constraints with respect to the learned models, and a qualitative assessment with respect to the task performance.

### 2.5.1 EXPERIMENT I. VEGETABLE GRATING TASK

---

#### TASK DESCRIPTION

---

The task consisted of several atomic actions, presented in Fig. 2.7: reaching from the initial position to the slicer (the motion takes around 3 to 5 seconds), a repetitive slicing motion (on average around 30 seconds), a reaching motion from the slicer to the trashing container (on average 2 seconds).

Two objects were used: a grater ( $o_1$ ) and a bowl ( $o_2$ ). Data was recorded from the robot at 100 Hz, using kinesthetic demonstration and consisting of: end effector position  $x \in \mathbb{R}^3$  and orientation ( $r \in \mathbb{R}^{3 \times 3}$ ), and external forces estimated at the end effector ( $F \in \mathbb{R}^3$ ). The objects were tracked at 100 Hz using an OptiTrack motion capture system.

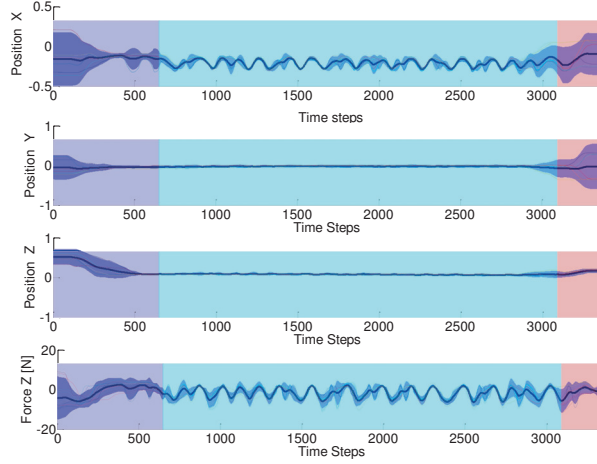
The variability of the task consisted in: (1) starting each demonstration from a different initial position of the robot, and placing the objects in different positions in the reachable space of the robot (we recorded data for 3 different positions of the objects, placed on average 30, 45 and 65 cm apart from the initial position); (2) using vegetables of different sizes and types (we recorded data for 3 types of vegetables (carrots, zucchinis and cucumbers). The vegetables varied in length, from a minimum of 10 cm for a carrot to a maximum of 35 cm for a cucumber, and with about 2 cm in diameter); the variability of the manipulated object affected the force applied by the user when providing demonstrations and the duration of the demonstration. The task lasted until the vegetable was fully grated; (3) inherent user variability between demonstrations. A total of  $N = 18$  demonstrations were recorded, 6 for each vegetable type, using 3 different objects poses.

#### EXTRACTED CONSTRAINTS

---

For extracting the task constraints we evaluated the 3D measurements of position and force projected in the reference frame of each object. Following the approach described in Section 2.4, the criterion on each axis was evaluated in a time window of width  $w = 200$  time steps (2 seconds) for determining the reference frame. This resulted in one segmentation point. The motions of reaching and grating were expressed in the reference frame of object 1, the grater, and the motion of reaching the trash container was expressed in the reference frame of object 2, the bowl.

Similarly, we evaluated the criterion on each dimension, using a time window of width  $w = 300$  time steps (3 seconds) for determining the variable of interest. The results showed that the force on the vertical axis became important in the second part of the task (grating and trashing), while only position was important in the first part of the motion (corresponding to reaching the grater).



**Figure 2.8** The obtained segmentation overlapped on the demonstration data

The change in the variable of interest determined a new segmentation point. A final point concludes the motion. Therefore 3 segmentation points  $\psi_s$  were determined for this task (see Fig. 2.8), involving the 3 different states.

Two attractors were determined relative to the grater: one near the handle (*Grater top*); one at the bottom (*Grater bottom*), after passing over the blade. Similarly at the end of the motion the positioning was relative to the trash-ing bowl. We thus obtained an attractor-based encoding of each action. The learned dynamics for reaching the grater  $o_1$  and the trash  $o_2$  respectively are shown in Fig. 9 (a) and Fig. 9 (b), with generalization across different starting postures. Generalization with respect to a moving target is shown in Fig. 9(c); the force and stiffness modulation are presented in Fig. 2.10.

A finite state machine was generated as described in Section 2.4.3. The advancement of the FSM happened when the current attractor was reached, or when the number of grating passes was completed. For evaluation purposes the number of times the grating was performed was an additional condition for the transition between states  $\psi_1$  and  $\psi_2$ .

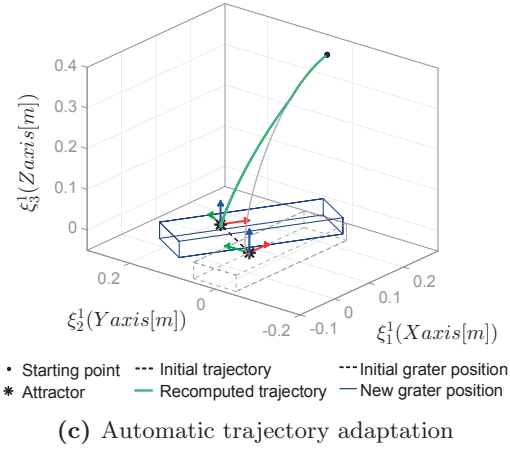
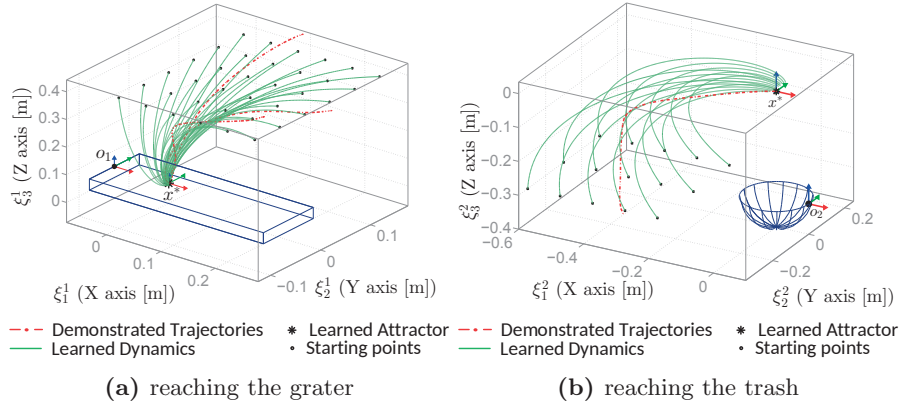
## TASK EVALUATION

---

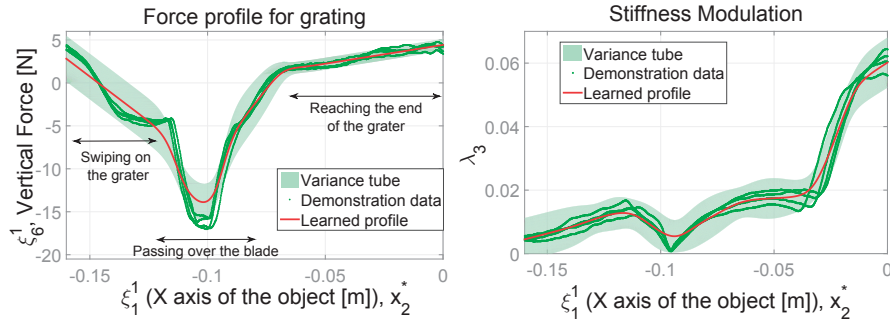
We performed both a qualitative and quantitative assessments and evaluated (1) the correct extraction of task constraints; and (2) the ability of the system to generalize to new object locations and different vegetables.

### Evaluation of the extraction of constraints

We validated whether the model had correctly extracted the dimensions onto which to provide either force or position control, by comparing the robot’s quantitative performance in executing the task when using the proposed approach or other simple control schemes. For the quantitative assessment we measured



**Figure 2.9** Learned dynamics. Figures (a) and (b) show generalization with respect to different starting locations; figure (c) shows the automatic adaptation of the trajectory with respect to changing positions of the object.



**Figure 2.10** Force profile and stiffness modulation used when grating

the effects of the determined variables as the determined constraints.

For evaluating the framework we compared our approach with standard control modes: a position controller and an impedance controller with fixed stiffness values. For these two control modes,  $N = 5$  different demonstrations were provided, using gravity compensation mode (*gcp*) and robot's execution was evaluated during motion replays ( $Rep_i, i = 1 \dots 5$ ) in the different setups: position control (*pos*) and impedance control (*imp*). The performance under these control modes was compared to the developed approach (*amp*). Several replays were performed for each demonstrated motion. We constantly compensated for the decrease of the vegetable's height, during replays. Each group of 1 demonstration followed by 5 replays were performed on the same vegetable. A single vegetable type was used, and the task was demonstrated using 5 passes over the grating surface during each trial.

For all the trials we measured: the original and final weight of the vegetable ( $u_{init}, u_{fin}[g]$ ); the original and final height ( $h_{init}, h_{fin}[cm]$ ). The original values were measured before the demonstration was performed, while the final values were measured at the end of the last replay round. For each round of demonstration and replay we measured the weight of the grated part ( $\Delta u[g]$ ) with a precision of  $\pm 1g$  and counted the number of successful passes (*SP*).

We evaluated the performance with respect to the following measures:

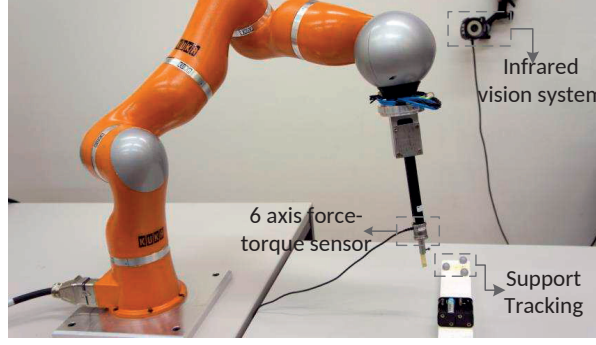
1.  $u_{ratio}[\%]$  the ratio of the grated vegetable ( $u_{grated} = \sum \Delta u$ ) as a percentage of the initial weight.
2.  $h_{ratio}[\%]$  the percentage of the vegetable length being grated ( $h_{init} - h_{fin}$ ) with respect to the initial length.
3.  $SP_{ratio}[\%]$  the percentage of successful passes (SP) out of the total passes performed.

Results are presented in Table 2.2. Using a standard position controller (Trials 1 - 5) for replaying the motion gave good results in a very low number of cases: mean (M) = 12% and standard deviation (SD) = 10.95 successful passes, while the amount of vegetable grated was below one gram per trial (M = 0.80g, SD = 0.83). When replaying the recorded motion using an impedance controller the number of successful passes increased (M = 52.5%, SD = 25.16).

These results were compared against the proposed approach (see Table 2.2, Trial 6), using the parametrization learned from demonstrations. The grating performance was assessed using the same performance metrics as for the standard control modes. The overall performance was better with respect to the amount of grated vegetable, and the number of successful passes.

Type	Control	Trial 1			Trial 2			Trial 3			Trial 4			Trial 5			Trial 6 – amp		
		$\Delta u$ [g]	SP	$SP_{ratio}$ [%]	$\Delta u$ [g]	SP	$SP_{ratio}$ [%]	$\Delta u$ [g]	SP	$SP_{ratio}$ [%]	$\Delta u$ [g]	SP	$SP_{ratio}$ [%]	$\Delta u$ [g]	SP	$SP_{ratio}$ [%]	$\Delta u$ [g]	SP	$SP_{ratio}$ [%]
N1	gcp	4	5	100	7	5	100	9	5	100	6	5	100	6	5	100	7	5	100
Rep1	pos	1	1	20	2	1	20	1	1	20	0	0	0	0	0	0	4	4	80
Rep2	imp	2	3	60	2	2	40	7	4	80	5	4	80	2	2	40	5	4	80
Rep3	imp	3	2	40	5	3	60	6	4	80	3	2	40	1	1	20	8	5	100
Rep4	imp	4	4	80							1	1	20	1	1	20	9	5	100
Rep5	imp	7	4	80							1	1	20	5	4	80			
$u_{ratio}$ [%]		21.00			21.62			31.08			17.78			18.07			35.86		
$h_{ratio}$ [%]		42.06			35.65			35.00			42.30			26.92			48.15		

**Table 2.2** Evaluation of the control modes. For Trials 1 - 5 we compared the demonstrated motion  $D_i$  provided using the robots gravity compensation mode (*gcp*), with a standard position control mode (*pos*), and with an impedance controller with fixed stiffness (*imp*). Trial 6, illustrates the performance of the proposed controller, learned from the  $N = 18$  demonstrations (*amp*).



**Figure 2.11** Experimental setup for removing a battery from a charging stand.

### Evaluation of the generalization ability

We tested whether the automatic segmentation of the task and the extraction of reference frame was correct and led to a correct reproduction when the position of the objects was changed. The robot regenerated the complete sequence and managed to complete the overall task comprising the 3 segments even when the objects were located in arbitrary positions and orientations, none of which were seen during training.

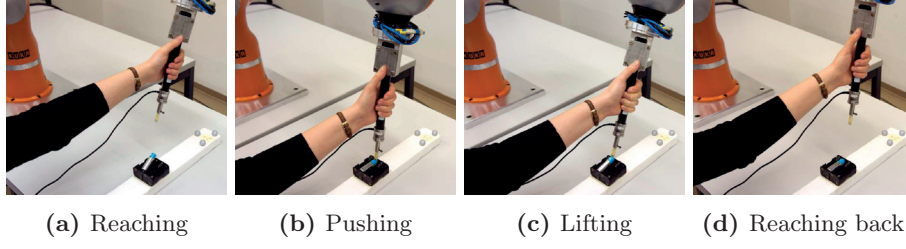
The importance of being able to change the reference frame is illustrated in Fig. 2.1, when using different positions and orientations of the two objects. In this case we performed a pure qualitative assessment by placing the objects in random positions and orientations in the robot’s reachable space, and using different vegetables. We measured the number of successful passes over the grater (using a normal and a larger surface).

### 2.5.2 EXPERIMENT II. BATTERY REMOVAL FROM CHARGER

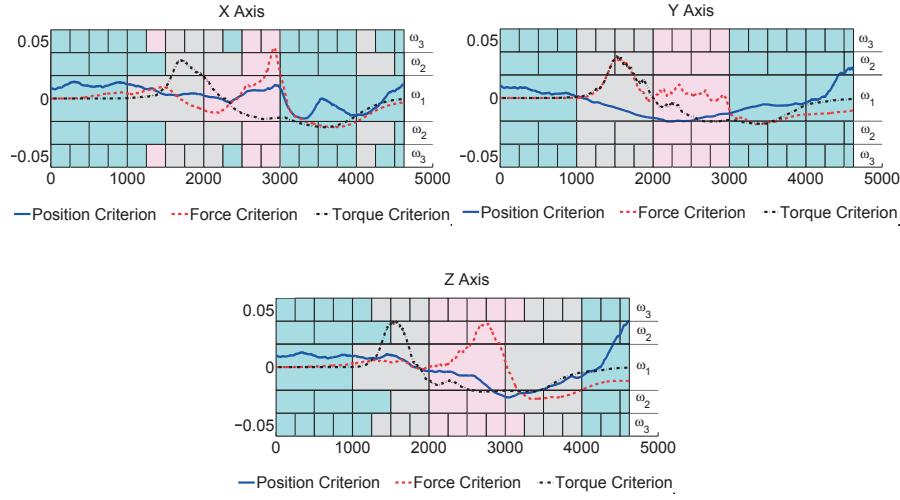
We tested the ability of the proposed method to properly extract constraints on a second task, i.e. removing a battery from a charging stand, see Fig. 2.11. The task was very fast paced. From the first segment to the last segment the task lasted on average less than 5 seconds.

In this example we used a single object  $o$ , the battery stand. We recorded data at 1 kHz, from human demonstrations by using vision to track the motion of the tool and of the object. Additionally we mounted a 6 axis force torque sensor on the tool to record precise interaction forces (Fig. 2.11). The steps of the task are shown in Fig. 2.12. The data-set consisted of 9 variables, 3D measurements of end effector position, force and torque. We computed the criterion as described in Section 2.4, using a time window of 1000 time steps, for position, force and torque on each axis of the object (see Fig. 2.13 and 2.15).

For the first part of the task (reaching) the criterion for position was dominant on all axes. For the following part (pushing and lifting the battery) there



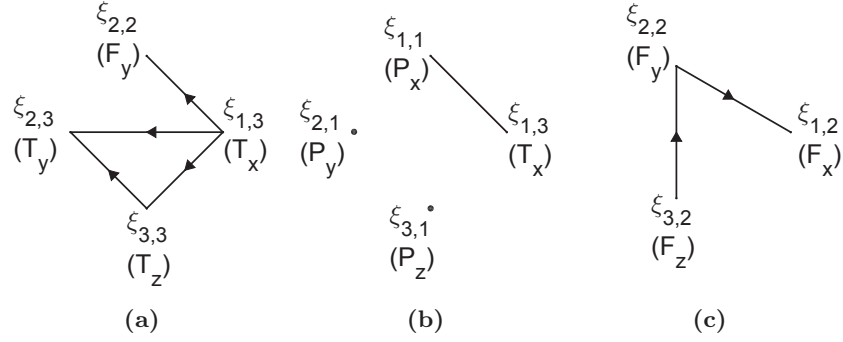
**Figure 2.12** Atomic actions in performing the task. The task typically consists of reaching for the battery stand, applying a force that tensions the spring inside the support (pushing), taking out the battery (lifting), and reaching away



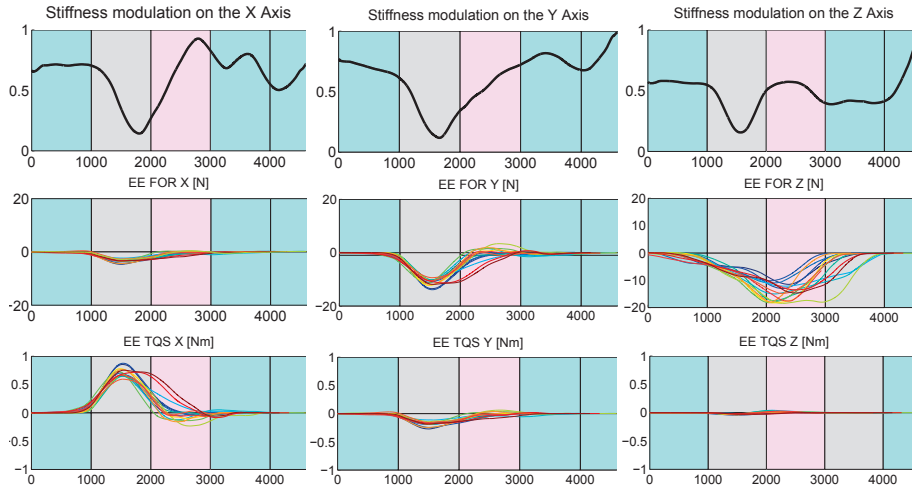
**Figure 2.13** Computed Criteria. We contrast the contribution of Position, Force and Torque as variables of interest. Segmentation obtained using time window of various sizes:  $\omega_1 = 1000$  time steps;  $\omega_2 = 500$  time steps;  $\omega_3 = 250$  time steps. We retain the segments obtained after using the time window  $\omega_1$ .

was a clear separation between the two segments on the X and Z axis of the object (see Fig. 2.13 (a), (c), marked by changing the variable of interest (i.e torque than force), while on the Y axis (perpendicular to the object) torque and force were equally important with a small relative difference in their criterion (Fig. 2.13 (b)). In this case, the proposed approach, does not offer a clear decomposition of the task, suitable for hybrid force–position control.

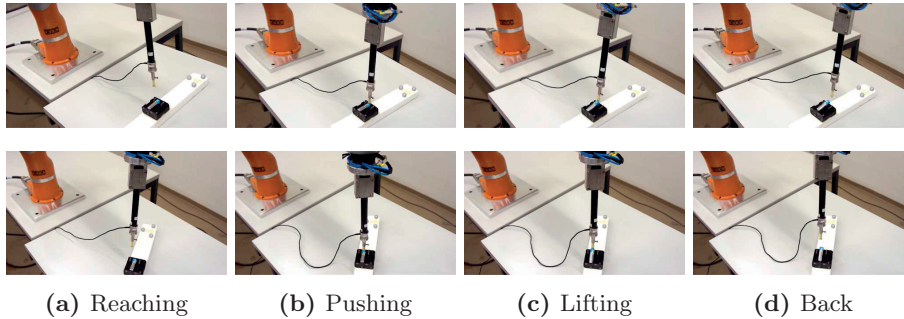
The method offers a relative weighting between the importance of different variables acting on the same axis. However to use a hybrid controller, we need to determine the relative importance between axes, as in this case the forces and torques acting sideways were a reaction to the motion of taking out the battery. For this we propose studying the causal relation between the variables of interest determined above, across all the  $N$  demonstrations, in order to: (1) have a relative weighting of the axis’s importance; (2) determine on which of the other axis the motion should be conditioned on.



**Figure 2.14** Causality relationships corresponding to the "push" and "lift" segments. The oriented arrow shows the start variable to be causal for the end variable. An un-oriented edge shows double causality.



**Figure 2.15** Segmentation for the battery extraction task



**Figure 2.16** Robot task execution using different configurations of the object with respect to the robot's base.

For analyzing the causality in the data we have used an existing Matlab toolbox (Seth, 2010a). Fig. 2.14 (a) shows the relationship between the variables of interest determined on each axis for the "push" segment. The force component on the X axis along the object (corresponding to torque around the X axis of the end effector) was causal for the force components around other axes. The amplitude of the causal interaction was 0.37 for the torque around the Y axis and 0.1793 for the force on the Z axis, thus proving that the interaction is stronger in the XY plane of the battery charger.

Secondly we studied the connectivity of the most important variable with all the other secondary variables (i.e the change of position on all axis, see Fig. 2.14 (b)), which showed a causality relation in both ways. This allowed us:

- to reduce the number of axis on which we perform force control in this segment to one (the X axis)
- to automatically determine that it should be encoded based on a change of position and along which axis.

Similarly analyzing the causal structure in the data for the "lifting" segment (Fig. 2.14 (c)) allowed us to reduce the dimensionality of this model.

Fig. 2.16 shows robot reproduction and generalization to different positions of the battery charger stand.

## 2.6 Discussion

---

Our approach of extracting continuous soft constraints from human demonstration was tested on a cooking task encompassing 3 segments and on an office task with 4 segments. The tasks differed in duration and the set of important variables. The proposed method extracted the necessary control information for encoding and performing the tasks without using prior knowledge. The tasks were executed using a time-invariant encoding, and an impedance controller parameterized by the continuous constraints. We further discuss aspects that influence our approach.

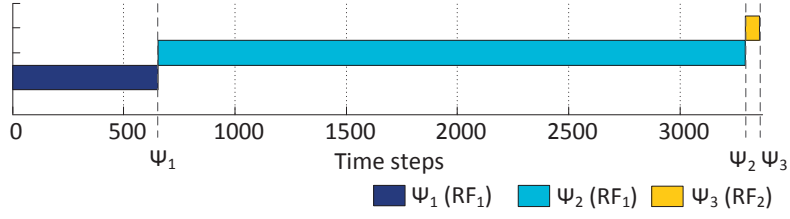
### 2.6.1 OPEN PARAMETERS

---

This work relies on several open parameters: the variables taken into account for segmentation, the choice of window size, and the termination condition. We address each separately.

#### Variables included in the analysis

The variables included in the analysis are specified by the user. In the work presented above we focused on position and force-torque measurements,



**Figure 2.17** Segmentation points and controller type obtained when accounting for 4 variables: end effector position, force, torque, and velocity.

however the approach can be extended to account for other variables. For the grating task, for instance, we computed the variance over trials and time window for 2 other measures: the torques sensed at the end effector, and the end effector velocity (a total of  $L = 4$  variables). The analysis, using the same approach presented in Section 2.4, showed that using the extra information provided by the velocity, or torque data did not significantly modify the segmentation points. The information related to the end effector orientation, even if it was not used for segmentation, it was retained for each action and incorporated in the dynamical systems used for reaching. The attractor for each action was specified in both position and orientation. The arm reached it using a coupled dynamical systems implementation (Shukla and Billard, 2012), in which a different dynamics was learned for both position and orientation, as well as a coupling function ensuring synchronization.

### Choice of window size

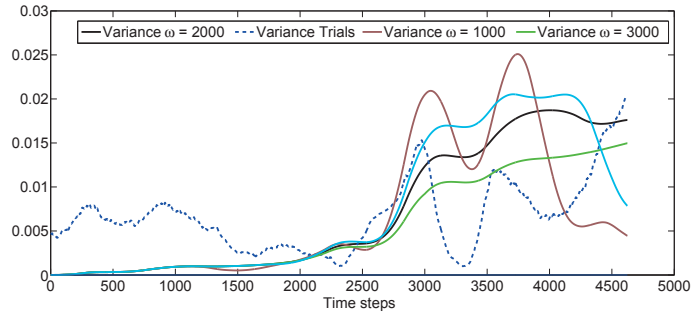
In the current implementation the window size was chosen by the user. Its size might influence the number and location of the segmentation points obtained. A small window size can lead to over segmentation, while a high window size can leave aside important aspects of the task.

Properly scaling the window depends highly on the task pace, such that for the two tasks analyzed in this chapter we used a window size equal to our sampling rate.

This might not always be applicable, therefore an automatic way of obtaining an adaptive time window was proposed in Section III. This however required to set a threshold of the minimum amount of change and hence introduced yet another open parameter. In figure 2.18 we show how various time window sizes affect the variance computation.

### Ending condition for repetitive tasks

While in the grating task, reaching the first attractor was needed for starting the grating, still the complementary force information indicated that at the end of the segment the end effector was in contact. Similarly, during the grating



**Figure 2.18** The change of time window variance with respect to the window size. This representation corresponds to the criterion for position on the X axis of the battery task.

motion, mainly the vertical force was the important variable for control.

However the vertical position of the end-effector with respect to the grater, held complementary information for ending this action. Namely for each grater pass we observed a decrease in height by approximately  $2mm$ . The task was demonstrated until the vegetable was fully grated, which implied finishing the grating action at the same height above the grater. Therefore we could consider this information as an ending condition for the repetitive motion.

### 2.6.2 ADVANTAGES

We further emphasize specific advantages of the proposed method.

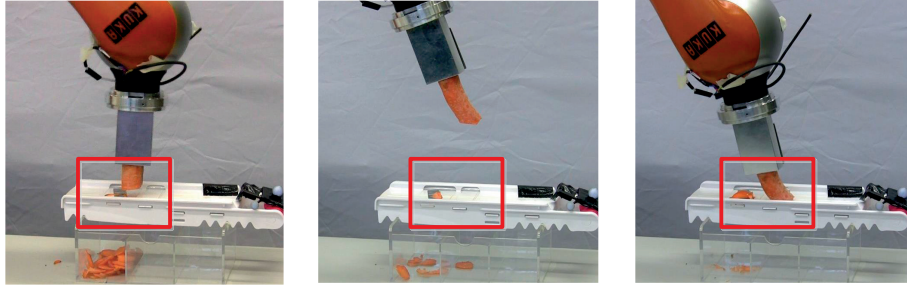
#### Task representation

The method developed in this work bootstraps information for learning, thus automating this part of a Learning from Demonstration (LfD) procedure which was usually done manually, while the decision of choosing certain dimensions for encoding a model was typically hardcoded.

It thus decreases the task complexity by focusing on learning just the variables that are important for each region of the task (i.e. encode just end effector position for a reaching motion vs. accounting for position and force on a certain axis in manipulation sub-tasks). It determines the chain of actions in the task and the conditions for the transition between actions. Automatically extracting this information contributes to both simplifying the control and to automating this part of the the learning procedure.

#### Stiffness modulation

Moreover the choice of the actual values of stiffness (which in our case is modulated throughout the task by the  $\lambda$  factor), is not intuitive and requires learning. Additionally by applying the same method to extract different rela-



**Figure 2.19** Problems encountered when using standard control modes, mostly due to the size variation in the vegetable (from left to right): robot missed the grating target, incomplete slicing, high force applied, causes the vegetable to bend or break.

tionships in force/torque and position control in two different tasks confirms that the method is agnostic to the particular choice of frame of reference of position versus force control.

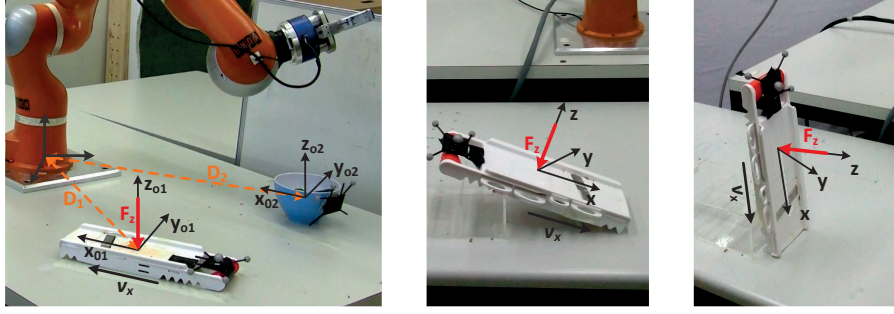
Modulating the arm’s stiffness is important for several reasons. Firstly it allows us to apply the determined decomposition of force and position control. Secondly proper stiffness contributes to successfully executing the task. For example a robot that is too stiff in the grating segment would break the carrot or other soft vegetables (like a cucumber) during grating, while a robot that lacks sufficient stiffness would not be able to pass over the grater’s blade and therefore not manage to perform the task (see Fig. 2.19).

Lastly it is a safety issue: a stiff robot is required to be able to perform some parts of the task, but a less stiff robot when reaching the trash for example is safer, in case of colliding with a human.

### Human Robot Interaction considerations

The decomposition of position versus force control might be intuitive for an engineer, but it would be hard for a naive user to make it explicit. The LfD approach taken in this work allows the human to demonstrate a complex task to a robot in a natural manner, while the robot can transfer the demonstrated task into a mathematical and computational framework interpretable by its control system.

From an HRI perspective, the proposed method can facilitate teaching interactions as it allows the user to demonstrate the whole task rather than individual actions. A fragmented demonstration can be demanding when the user has to focus on actively teaching the robot how to perform the task. As multiple demonstrations are required for generalization, it is more convenient for the user to demonstrate the whole task, rather than individual actions, such as reaching movements.



**Figure 2.20** The change of reference frame with respect to object's location.

### Task Generalization

Determining the frame of reference to be used in each action allows the robot to easily generalize to changing configurations of the objects. Proper execution is ensured as control is performed with respect to this frame attached to the object (see Figure. 2.20).

However the proposed approach has a two-level specification of the reference frame, by determining an object of interest and one or more attractors (i.e. relative positioning), with respect to this object. There can be multiple attractors with respect to a single object. For example in the grating task we needed to reach the grater at a certain point above the blade, but the grating motion ended at a point just after passing the blade. The two points determined different actions performed with respect to the same object, and thus refining the task encoding. Relating the attractors to the initial frame, rather than storing only the attractor points with respect to the world, allowed us to implicitly capture properties of the object, such as rigidity.

Additionally, for the first task, we tested the developed controller for a different grating surface and a softer vegetable. This resulted in proper grating. Furthermore in the current implementation the choice of modeling the force as conditioned on the position was ad-hoc, prior information. The possibility to learn and extract automatically that there is a correlation between these two variables and the directionality of the correlation was explored in the second robotic experiment, in Section 2.5.2.

### 2.6.3 LIMITATIONS

A major limitation of this work is the fact that it does not use any high level information about the objects used, the environment, the task specification or the desired effect. Thus the method is limited to relating only the arm behavior to how the manipulation should be performed on an object. However it is not suitable for modeling effects on the object. Visual information could have been

used for relating the effects that applying a force has on the state of the object. Moreover the method does not directly apply to tasks where the "lack of change" is important (such as controlling for zero force on one axis) as being key to task completion. However this can be addressed by studying the relative importance of each axis, extending the approach proposed in Section 2.5.2. Lastly the demonstration setup can become an impediment for the user. Often during a demonstration the user has to adjust the position of the robot, maneuvering its 7 degrees of freedom, until it feels comfortable to demonstrate the task. This can affect the ability of the user to provide good demonstrations, as well as the demonstrated trajectories.

## 2.7 Conclusions

---

The presented approach for extracting task constraints takes advantage of the existing variance in the demonstrated data, and proposes a criterion for detecting regions of coherence across demonstrations. Objects upon which an action was performed are determined. The action is further encoded in the local frame of reference, in a time-invariant manner, preserving the flow of actions in the task.

In particular, we compared different measurements (like position and force) and modulated their contribution to the controller used in reproducing the motion, by using a weighting factor that adapts the robot's stiffness. Also by weighting the relative importance of each of the task variables when expressed in the reference system of the objects involved in the task we can determine the suitable reference frame to be used in each segment.

Finally a set of segmentation points were obtained by splitting the motion whenever a change in the reference frame or in the variables of interest occurred. The approach was validated on a kitchen task (grating vegetables), and an office task (removing a battery from a charging stand) achieving good generalization results, and managing to capture the dynamics of a fast task.

# CONSTRAINT–REPRESENTATION OF COORDINATED BEHAVIOR

The work presented in this chapter has been published in:

*Pais Ureche, A. L., and Billard, A. (2018) Constraints Extraction from Asymmetrical Bimanual Tasks and Their Use in Coordinated Behavior, Robotics and Autonomous Systems, vol. 103, pp 222-235, 2018.*

## 3.1 Forward

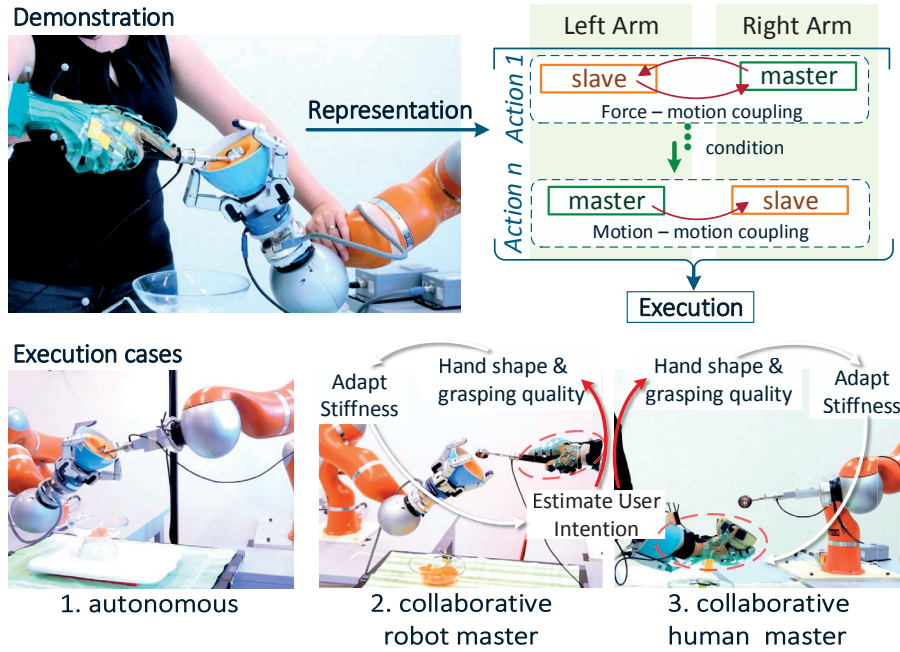
---

In this chapter we extend our approach of extracting task constraints (described in Chapter 2, (Ureche et al., 2015)) to asymmetrical bimanual tasks. Such tasks require continuous coordination between the arms which results in a relative movement or contact force, often transmitted through an object.

We start by decomposing the task in a set of actions and identifying for every action the *coordination features* as relationships between the sets of unimanual constraints corresponding to each arm. This leads to automatically determining the role of the arms as master or slave; the type of coupling as simple motion coordination, or force–motion coordination as well as the coupling function; and the pre-condition that enables the transition between actions. We use this representation for autonomous execution.

Secondly we aim to use the same constraint–representation for executing the task in collaboration with a human user. For this we extend the set of features with *the embodiment features* which allow the robot to anticipate and adapt to the user’s actions. These features are a representation of the user’s specific manner to use the tool during each action. For example the grasping quality is an indication of whether the grasp is adapted for exerting forces and torques across directions of interest. A robot able to adapt its stiffness in response to a user’s intention to apply a force, contributes to an intuitive and reliable interaction.

We encode the task based on the extracted features and we execute it both autonomously and collaboratively. We validate our approach on common bimanual daily tasks: scooping, peeling and mixing.



**Figure 3.1** We record bimanual demonstrations of asymmetrical tasks, using a custom setup that consists of a kinesthetically guided robot arm, and a human arm wearing a sensorized glove. We extract a task representation encoding arm coordination features and human’s dexterous use of the tool. We execute the task autonomously or collaboratively using this representation.

## 3.2 Introduction

Bimanual tasks rely on the coordination between the arms. In particular, asymmetrical bimanual tasks are both common and natural for humans: i.e. we can scoop a fruit with one hand, but the task becomes easier when the other hand is holding it. The hands interact indirectly, transmitting a desired relative movement or contact force through an object. Thus the action of each arm is characterized by a motion profile, and use of force which we automatically determine using our previously proposed approach (Ureche et al., 2015). However these unimanual features are interrelated as one arm adapts to the other, switching their *roles* as master and slave, and changing the type of *coupling* from motion coordination to force–motion coordination.

In this chapter we focus on extracting *coordination features* from human demonstrations. We use them for 3 execution cases: (1) autonomous execution by a bimanual robot, (2) collaborative execution with a human partner in which the human acts as master, or (3) the robot acts as master.

In the last two cases a reliable interaction requires the robot to anticipate and adapt to the counterpart’s intention to apply a force before this is actually applied in the task. For example in the scooping task a robot arm holding the fruit can adapt its stiffness in response to a force that the human arm is expected

to exert. We thus analyze the way humans use the tools in relation to the constraints extracted before. Based on the hand shape and tactile signature we compute a grasping quality metric. A high value of this metric in the direction in which force is a constraint indicates that the user is ready for the task and his hand is shaped appropriately. This allows the robot to update its stiffness according to the user’s state. The approach is summarized in Fig. 3.1.

We address these aspects by taking advantage of factors implicit in human behavior when employing tools with high dexterity, and working towards a goal. The role of the dominant and non-dominant hands is not hardcoded, but assigned depending on the task constraints (Hughes et al., 2013). Therefore it can change during manipulation, based on a force–motion relationship (Johansson et al., 2006). With respect to handedness, position control is often employed by the non-dominant hand while force control is commonly used by the dominant hand (Ferrand and Jaric, 2006). However the force coordination is stronger within rather than between arms (Krishnan and Jaric, 2010; Jaric et al., 2006). A change in the task is typically initiated by the non-dominant hand (de Poel et al., 2006). However the passive arm sets the frame of reference for the active arm (Guiard, 1987), establishing a master–slave relationship.

Additionally when explaining to someone how to perform an action which requires maneuvering a new tool, people often indicate that the tool should be held in a certain way, thus making the hand features explicit. The grasp that the humans use is often adapted for applying forces and torques across a desired direction (de Souza et al., 2015). The same tool is held differently when used in different actions, adopting distinctive hand shapes and making contact with particular parts of the hand (de Souza et al., 2015). In the tasks we study in this chapter (scooping, peeling and mixing), the tool is always in hand, but the grasp changes continuously, as the hand adapts to the requirements of the current action: i.e. enclosing on the tool before applying a force or switching from a precision to a power grasp.

This chapter builds upon our previous work on automatic task segmentation and constraints extraction (Ureche et al., 2015) for unimanual tasks. Here we extend the framework to target the extraction of bimanual constraints. In particular, we focus on learning the change in the master–slave relationship between the two arms, on determining coupled dimensions and transition conditions between the actions, that ensure coordination. Additionally we use this constraint based representation in both autonomous and collaborative execution modes. We achieve this by analyzing the human grasping behavior and updating the robot’s stiffness for ensuring an intuitive interaction in collaborative mode.

Consequently our approach is applicable as a middle layer between planning and control, contributing to:

- (1) abstracting a representation of the coordinated behavior applicable to different asymmetrical bimanual tasks

- (2) using a common representation when executing the task autonomously and in physical coordination with a human
- (3) validating the approach on a real robotic platform

We tested the approach (described in Section 3.4) on real life tasks Section 3.5. We discuss our results and conclusions in Sections 3.6 and 3.7, and the state of the art in Section 3.3.

### 3.3 Related Work

---

Demonstrating bimanual tasks is often problematic as recording data requires kinesthetically driving two robots, potentially with hands. This can be demanding given the high number of DOF (i.e. a demonstrator needs to use both hands for unscrewing a light bulb, using a 16 DOF Allegro hand on a stationary robotic arm (Li et al., 2014)). Conversely the lack of kinesthetic interaction leads to a correspondence problem.

Common approaches are: teleoperation (Peters et al., 2003), suitable for arm motions, but not for manipulation; or demonstrating gestures using motion sensors and refining them kinesthetically (Calinon and Billard, 2007b). Alternatively custom setups allow directly demonstrating force patterns. One such example is transmitting stiffness patterns through a coupling device that connects the human and robot arm in conjunction with EMG for detecting the grasping state of the hand (Yang et al., 2015). In our work we also use a custom setup for kinesthetically demonstrating the task. The setup consists of a robotic arm from which we record pose and force–torque information, in conjunction with the hand shape and tactile signature from a glove covered with pressure sensors. We modified the tool to embed a 6 axis force torque sensor. This setup allows the human to freely manipulate the tool in a dexterous way. We analyze the forces applied both as a feature of the task, as well as in conjunction with the tool use. Based on a grasp quality metric we show that the position of the tool in hand changes continuously as it adapts to the requirements of the current action, unlike having only two discreet states: hand opened or closed. This information facilitates the interaction during collaborative execution.

#### 3.3.1 COORDINATION IN BIMANUAL TASKS

---

Coordinated behavior can be represented through features such as: stable postures (Gribovskaya and Billard, 2008); keyframes (or keypoints) as important "snapshots" of the task (Asfour et al., 2008); the grasping state of the hand (Jkel et al., 2010); or spatial and temporal constraints (Calinon and Billard, 2007b; Asfour et al., 2008; Park and Lee, 2015; Berthet-Rayne et al., 2016). While coordination is typically continuous, there are instances when it can be

represented through discreet stable postures at the trajectory level, i.e. in symmetrical tasks.

In reference (Gribovskaya and Billard, 2008) the authors extract stable postures by analyzing the rate of change in the demonstrations. The movement is described by a generic variable (e.g. the relative distance, or phase between the arms), which remains constant during an action (Gribovskaya and Billard, 2008) and the encoding is time-dependent. However in our work, the spatial constraints are not rigid, the coordination is action-specific and continuous, done with respect to different reference frames. We use a time-independent encoding in which the synchronization between the arms becomes implicit.

Similarly to the stable postures approach, keypoints of a task and time dependencies between the arms are identified as features using an HMM (Hidden Markov Model) approach (Asfour et al., 2008). In our work we focus on the importance of the continuous coordination between the arms throughout an action, especially required during manipulation actions. Additionally in our case the spectrum of task features encompasses a sequence of actions characterized by the coupled trajectories of the two arms, force-motion coupling during actions that require exerting forces and stiffness modulation of the two arms.

In reference (Likar et al., 2015) the authors employ iterative learning control for online adaptation to inaccuracies in the environment during the execution of bimanual tasks that require exerting forces. In our case we obtain a decomposition of force and position controlled dimensions for each arm by extracting the reference frame used in each action. Additionally we compute a stiffness modulation factor that weights the contribution of force and position continuously during each action. An alternative approach to controlling the arms separately is controlling the closed kinematic chain that results in bimanual manipulation while ensuring the exertion of proper forces (Liu et al., 2016). While this method is suitable for manipulation actions, in our work we consider tasks that encompass a sequence of actions that don't always form closed kinematic chains.

Typically the passive arm defines the reference for the active arm (Calinon et al., 2012). In our work, we automatically detected the reference frame to be used in each action and based on this information we determine the role of the arms as master or slave. In reference (Silvrío et al., 2015) the authors highlight the importance of properly choosing the reference frames and of encoding the task of one arm relative to the other end effector, especially allowing the arms to react to perturbations applied to the opposite arm. In our work we also stress this aspect of adaption especially to perturbation in the environment, which can be avoided by properly assigning reference frames and maintaining the precedence between the arms.

In asymmetrical tasks the master-slave role is also reflected in the behavior of each arm (i.e. performing manipulation or assisting (Xu et al., 2012)). Typically one arm is having an assisting role, and therefore adjusts its stiffness to resist the motion of the active arm. A user might not always be consistent in this

aspect allowing the passive arm a relatively high range of movement between demonstrations. However the user might be very conservative in the force that the active arm needs to apply, as this is essential for the task. We extract this information as different types of coupling between the arms (motion - motion vs. force - motion coupling). The coupling changes between actions, and require the adaptation of the both arms.

### 3.3.2 COORDINATION IN PHYSICALLY COLLABORATIVE TASKS

---

Physical human-robot collaboration consists of transmitting motion through an object and relies mostly on modelling force and torque data (Rozo et al., 2016) (i.e a force-velocity dependency is used for collaborative carrying an object (Evrard et al., 2009)). The robot can predict and adapt to the human, and assist in execution (Berthet-Rayne et al., 2016). Impedance modulation is used for dealing with the uncertainty from the human input (Ficuciello et al., 2015). In our case we estimate the user’s intention to apply a force and modulate the stiffness accordingly by monitoring the user’s hand and computing the grasping quality in relation to the force applied.

The hand state (grasping or not) is action-specific. It has been used for segmentation based on thresholds for the wrist and fingers velocities (Jkel et al., 2010) or on observed object states (Zollner et al., 2004). Prior information improves the segmentation accuracy: predefining the roles of the hands (Zollner et al., 2004) or annotating data in critical tasks, i.e. surgery (Dergachyova et al., 2016). By contrast, we show that even when the tool remains in hand across actions the hand shape adapts to the task requirements (e.g. different grasps are employed in scooping and trashing).

### 3.3.3 TASK REPRESENTATIONS AND EXECUTION

---

Specific representations of bimanual tasks include: graphs (Jkel et al., 2010), macro operators for specifying the roles of each arm and the coordinated action (Zollner et al., 2004), symbolic representations based on changes of the objects states (Zollner and Dillmann, 2003); hierarchical state machines (Steffen et al., 2010), while dealing with platform-specific aspects: i.e. the common manipulation space of the arms (Colomé and Torras, 2014), or decomposing the actions in different subspaces for each arm (Zacharias et al., 2010).

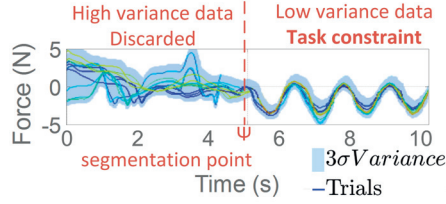
Our representation enables execution using hybrid control and fits a sub-symbolic level encoding the task through probabilistic models, similar to (Jkel et al., 2010). The bootstrapping is based only on the sensory information without a model of the environment. However adding high-level information can be done at the planning level (Nyga and Beetz, 2015), making use of language or previously acquired knowledge (Wrgtter et al., 2015). This requires estimat-

ing the object’s state (Hebert et al., 2013), the effect that the task has on the environment and replicating it (Paxton et al., 2016).

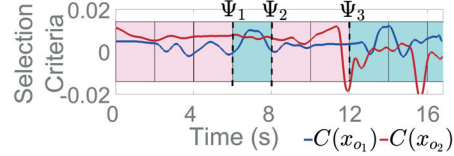
The constraints are used to direct task learning often using time-dependant models (Gribovskaya et al., 2011; Calinon and Billard, 2007b; Smith et al., 2014). Alternatively task parameterized gaussian mixture models (TP-GMM), for representing position and orientation of both arms in one compact model (Silvrío et al., 2015). We use a time-independent encoding following a coupled dynamical systems approach (Shukla and Billard, 2012), aimed to preserve the coordinated behavior. Typically the choice of the coupled variables is arbitrary: i.e. coupling finger and arm motion when reaching for an object (Shukla and Billard, 2012); or multi-level eye-arm-hand coordination (Lukic et al., 2014). In contrast in our work we identify the coupled dimensions.

### 3.3.4 SUMMARY OF THE EXTRACTION OF TASK CONSTRAINTS

We provide a summary of the extraction of unimanual constraints and the corresponding encoding (Ureche et al., 2015) as used throughout this chapter.



**Figure 3.2** Regions of high and low variance (constraint) in sensor data



**Figure 3.3** Segmentation based on maximum criterion

**Unimanual Constraints** are determined by identifying regions of consistent behavior (low variance) across demonstrations (see Fig. 3.2). We project all data onto each reference frame  $R_i$ , of the objects  $N_o$  and the opposite arm. For each dimension 1 : 3 of the position and force measurements we compute a **selection criterion**  $C$  given by the difference between the variance in a time window  $\omega$  and the variance over trials.

$$C(R_i x_{1:3}) = Var_{t:t+\omega}(R_i x_{1:3}) - Var_{1:T}(R_i x_{1:3}) \quad (3.1)$$

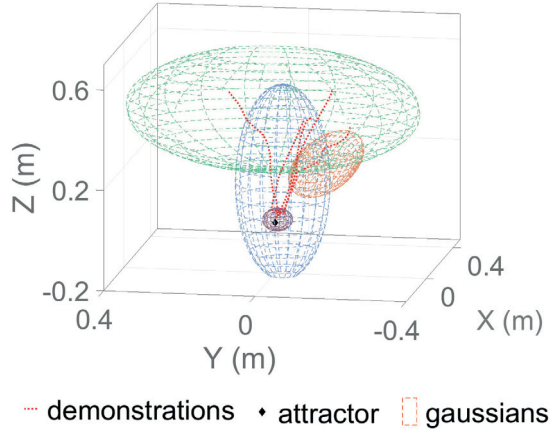
The reference frame  $R$  is given by the object with the maximum corresponding criterion (see Fig. 3.8). The variable of interest for each axis  $\nu$  is given by the maximum criterion of either position or force. A stiffness modulation factor  $\lambda$  weights the contribution of position and force.

Variable	Description
$x_p, x_o \in \mathbb{R}^3$	end effector position and orientation
$\dot{x}_p, \dot{x}_o \in \mathbb{R}^3$	end effector translational and rotational velocities
$\gamma_{p,o}$	coupling function between the position and orientation
$\gamma_{\nu^M, \nu^S}$	coupling function between the master and the slave
$F_R, F_L \in \mathbb{R}^3$	right arm (R) and left arm (L) cartesian forces
$T_R, T_L \in \mathbb{R}^3$	right arm (R) and left arm (L) cartesian torques
$F_e \in \mathbb{R}$	estimated force on the axis where force is a constraint
$F_d \in \mathbb{R}$	desired force on a force constrained axis
$w_p, w_o \in \mathbb{R}^3$	wrist position and orientation
$\theta \in \mathbb{R}^{22}$	finger joint angles
$\phi \in \mathbb{R}^{34}$	hand tactile signature
$o_p^i, o_o^i \in \mathbb{R}^3$	position and orientation of objects $o_i \in 1 \dots N_o$
$N_D$	Total number of demonstrations
$N_\Psi$	Total number of actions
$N_o$	Total number of objects
$\Psi_i$	The set of actions in the task $i \in 1 \dots N_\Psi$
$R, x^*$	reference frame, and attractor frame
$\nu \in \mathbb{R}^3$	vector of important variables for each axis
$\lambda \in \mathbb{R}^3$	normalized stiffness modulation, $\lambda_{1:3} \in [0, 1]$
$C \in \mathbb{R}^3$	selection criteria for each axis
$\kappa$	transition condition
$role$	arm role: <i>master slave uncoordinated</i>
$\rho_{\{\nu^R, \nu^L\}}$	coordinated variables between the arms
$\vartheta \in \mathbb{R}$	normalized grasp quality for each force constrained axis
$\alpha, \beta \in [0 \dots 1]$	controller gains
$\pi, \mu, \Sigma$	GMM parameters: priors, means and covariance matrix

**Table 3.1** Summary of the notation used throughout the chapter

$$\begin{aligned}
R_{t:t+\omega} &: \max(C(R_i x_{1:3})) \\
\nu_{1:3} &: \max(C(x_{1:3}), C(F_{1:3})) \\
\lambda_{1:3} &: C(x_{1:3}) - C(F_{1:3})
\end{aligned} \tag{3.2}$$

Changes in the constraints indicate segmentation points, determining the action sequence  $\Psi_i, i \in [1..N_\Psi]$ . Fig. 3.3 shows an example of two selection criteria and the segmentation obtained corresponding to changes of the maximum criterion.



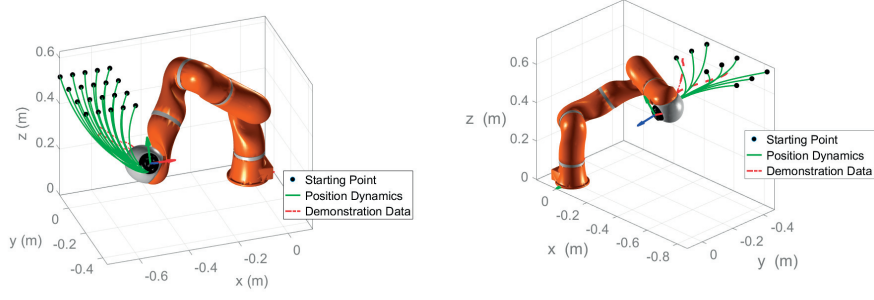
**Figure 3.4** gaussian encoding of trajectories

**Trajectory Encoding** We encode the trajectory of each arm using a Coupled Dynamical System approach (CDS) (Shukla and Billard, 2012). The system has 3 components. The position  $x_p \in \mathbb{R}^3$  and orientation  $x_o \in \mathbb{R}^3$  are represented by a first order autonomous dynamical system of the form:

$$\dot{x} = f(x). \tag{3.3}$$

The function  $f$  is encoded as a Gaussian Mixture Model (GMM) with  $K$  components, specified by the priors  $\pi$ , means  $\mu$ , and covariance matrices  $\Sigma$  (see Fig. 3.4). A function  $\gamma_{\{p,o\}}$  couples the two previously learned dynamics, such that a desired orientation  $\tilde{x}_o$  is inferred given the current position  $x_p$ .

$$\begin{aligned}
\dot{x}_p &= E\{p(x_p|x_p; \Omega_{x_p}^K)\}, & \Omega_{x_p}^K &= [\pi_{x_p}^K, \mu_{x_p}^K, \Sigma_{x_p}^K] \\
\dot{x}_o &= E\{p(x_o|\beta(x_o - \tilde{x}_o), \Omega_{x_o}^K)\}, & \Omega_{x_o}^K &= [\pi_{x_o}^K, \mu_{x_o}^K, \Sigma_{x_o}^K] \\
\gamma_{\{p,o\}} &= \|\cdot\|, & & \\
\tilde{x}_o &= E\{p(x_p|\gamma_{\{p,o\}}; \Omega_c^K)\}, & \Omega_c^K &= [\pi_c^K, \mu_c^K, \Sigma_c^K]
\end{aligned} \tag{3.4}$$

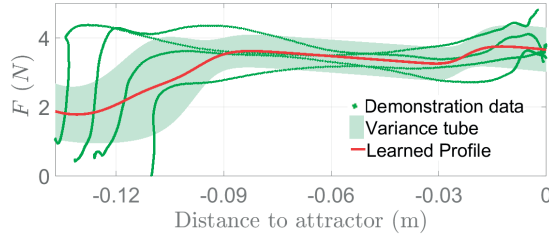


**Figure 3.5** CDS motion, generalization to different starting positions

**Trajectory Computation** For each arm we compute the next desired pose by integrating the translational and rotational velocities from the models (eq. 3.5). The gains  $\alpha$ ,  $\beta$  control the amplitude and speed of the system.

$$\begin{aligned}
 x_p(t+1) &= x_p(t) + \dot{x}_p(t)\Delta t && \% \text{ update position} \\
 \tilde{x}_o &= E\{p(x_o|\gamma(x_p); \Omega_c^K)\} && \% \text{ update coupling} \\
 \dot{x}_o &= E\{p(\dot{x}_o|\beta(x_o - \tilde{x}_o); \Omega_{x_o}^K)\} && \% \text{ update orientation} \\
 x_o(t+1) &= x_o(t) + \alpha\dot{x}_o(t)\Delta t
 \end{aligned} \tag{3.5}$$

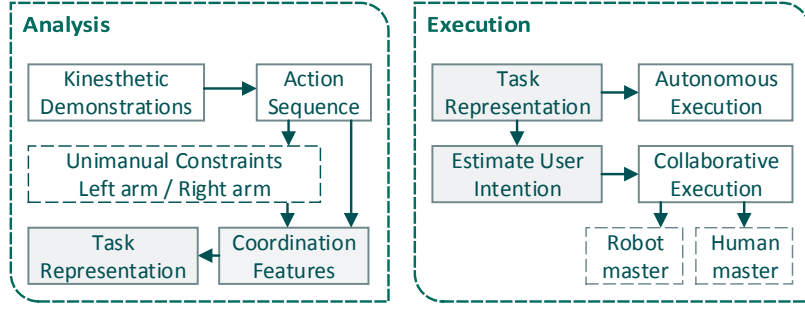
The model ensures asymptotic stability when reaching the attractors in both position and orientation. The coupling ensures synchronicity. The model is robust to temporal (Khansari-Zadeh and Billard, 2011) and spatial perturbations (Khansari-Zadeh and Billard, 2012) and can generalize to different starting positions (see Fig. 3.5).



**Figure 3.6** Example of GMM encoding of the task force given the distance to the attractor

**Force and Stiffness Encoding** The desired force and stiffness are encoded across the directions where force is a variable of interest (in the reference frame  $R$  extracted previously) based on the distance to the attractor (see Fig. 3.6).

$$\begin{aligned}
 F_d &= E\{p(F|x)\} \\
 \lambda &= E\{p(\lambda|x)\};
 \end{aligned} \tag{3.6}$$



**Figure 3.7** Pipeline of the proposed approach

### 3.4 Method

We focus on asymmetrical bimanual tasks performed in physical contact. For each arm we consider a Cartesian impedance controller given by:

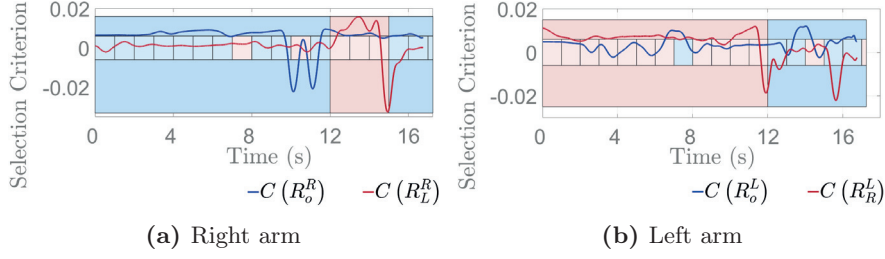
$$\tau = J^T(\lambda K_b(x - x_r) + F_d) \quad (3.7)$$

where  $\tau \in \mathbb{R}^7$  is the joint control input,  $J \in \mathbb{R}^{6 \times 7}$  the Jacobian. For each arm the controller is parameterized with constraints extracted from demonstration (Ureche et al., 2015), such that: the desired position  $x_r \in \mathbb{R}^6$ , force  $F \in \mathbb{R}^6$  and stiffness modulation  $\lambda \in \mathbb{R}^6$  are computed by querying corresponding models (Ureche et al., 2015). The models are learned with respect to the reference frame relative to which the arm moves and force models are learned only for the directions in which force is a variable of interest.

In this work we determine the role of each arm as master or slave, and a function coupling the motion of the master  $x_r^M$  to that of the slave  $x_r^S$ , ensuring precedence. We then determine a transition condition for switching between actions. Additionally we analyze the dexterous use of the tool as an indication of the user’s intention to apply a force. We execute the task autonomously and in physical coordination with a human. The approach is summarized in Fig. 3.7.

We record  $N_D$  kinesthetic demonstrations of the task in which the left arm (L) arm is maneuvering the tool (while wearing a Cyberglove covered with Tekscan pressure sensors) and the right robot arm (R) arm is backdriving a robotic arm (we use a 7 Degrees of Freedom (DOF) KUKA Light Weight Robot (LWR)). For the left arm we record joint angles of the human hand  $\theta \in \mathbb{R}^{22}$ , tactile signature for each phalange and the palm  $\phi \in \mathbb{R}^{34}$ ; wrist position and orientation  $w_p, w_o \in \mathbb{R}^3$  and forces and torques at the tool  $F_t, T_t \in \mathbb{R}^3$ . For the right arm we record end effector, position and orientation  $x_p, x_o \in \mathbb{R}^3$ , and cartesian forces and torques  $F_e, T_e \in \mathbb{R}^3$ . We track the position and orientation  $o_p, o_o \in \mathbb{R}^3$  of  $N_o$  objects using an OptiTrack vision system.

We present the approach in relation to an experiment consisting of a scooping



**Figure 3.8** Extraction of the reference frame  $R$ . We compare the arm motion in the object frame  $R_o$  (blue) versus the opposite arm (red).  $R$  is given by the maximum criterion in a time window of 1s

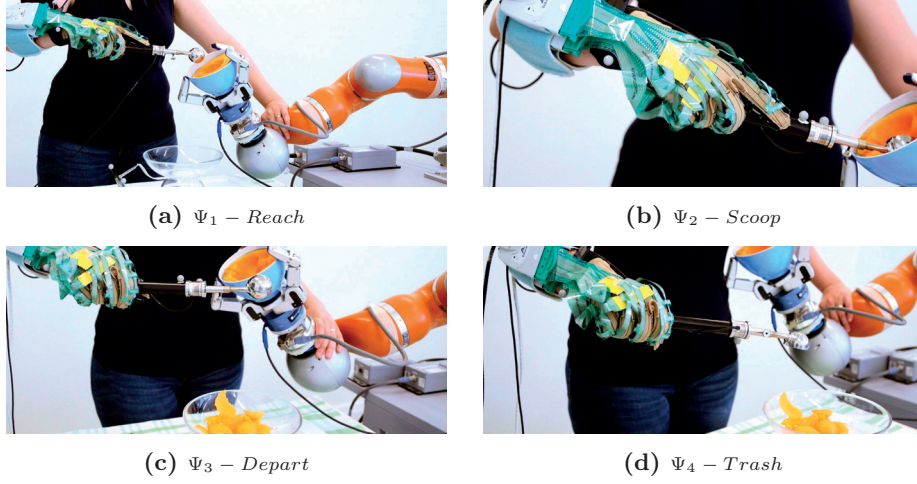
Right arm (Holding)				Left arm (Scooping)	
	$R^R$	$\nu$	role	$R^L$	$\nu$
$\Psi_1$	$R_o^R$	$[x_x, x_y, x_z]$	master – slave	$R_R^L$	$[x_x, x_y, x_z]$
$\Psi_2$	$R_o^R$	$[x_x, x_y, x_z]$	master – slave	$R_R^L$	$[x_x, F_y, F_z]$
$\Psi_3$	$R_L^R$	$[x_x, x_y, x_z]$	slave – master	$R_o^L$	$[x_x, x_y, x_z]$
$\Psi_4$	$R_o^R$	$[x_x, x_y, x_z]$	uncoordinated	$R_o^L$	$[x_x, x_y, x_z]$

**Table 3.2** Unimanual constraints and the determined role for each arm

task. We recorded  $N_D = 10$  demonstrations, with an average duration of 17s. We obtained a decomposition in 4 actions (Ureche et al., 2015), shown in Fig 3.9: *reaching* for the initial configuration; *scooping*; *departing* by switching the position on top of the trashing bowl; and *trashing*. The corresponding constraints are listed in Table 3.2. We obtained 2 changes of reference frame for the right arm (see Fig. 3.8a): at 12s from from object to the left arm, and back to the object at 15s; and one change for the left arm: at 12s from the right arm to the object frame (Fig. 3.8b). The right arm was position controlled during all actions  $\nu_{\Psi_{1:4}}^R = \{x_{1:3}\}$ . The left arm applied a vertical force and torque during scooping  $\nu_2^L = \{x_1, F_2, T_3\}$  and used position control during the remaining actions  $\nu_{\Psi_{1,3,4}}^L = \{x_{1:3}\}$ .

The master-slave role ensures that both arms respect precedence when reaching their targets. We exemplify this in Figure 3.10, showcasing the reaching action  $\Psi_1$  from the scooping task. The arm holding the mellon needs to reach a target above the bowl. The arm holding the scoop needs to reach above the first arm. When their roles are assigned accordingly (first arm master, second arm slave) then the master starts and drives the motion. Precedence is thus preserved when a perturbation occurs, which moves the bowl closer to the scooping arm. In the second case, when the arms are uncoordinated and the same perturbation is applied to the bowl, the scooping arm reaches first as the target is closer, and the holding arm no longer has space to converge.

Therefore typically one arm sets the reference frame for the other. This defines it as a *master*, as a change in its pose determines the second arm to



**Figure 3.9** The decomposition of the task into actions

follow (i.e. *slave* behavior). We determine the arm roles from the extracted reference frames, such that an arm  $i$  is master for an arm  $j$  if the reference frame of its motion is given by an object  $o$  in the environment, and it sets the reference frame for the motion of the other arm  $j$ ; it becomes slave when this relationship is inverted; the two arms are uncoordinated when moving independently with respect to one or more objects (eq. 3.8). With each action that requires changing the reference frames, the roles also change.

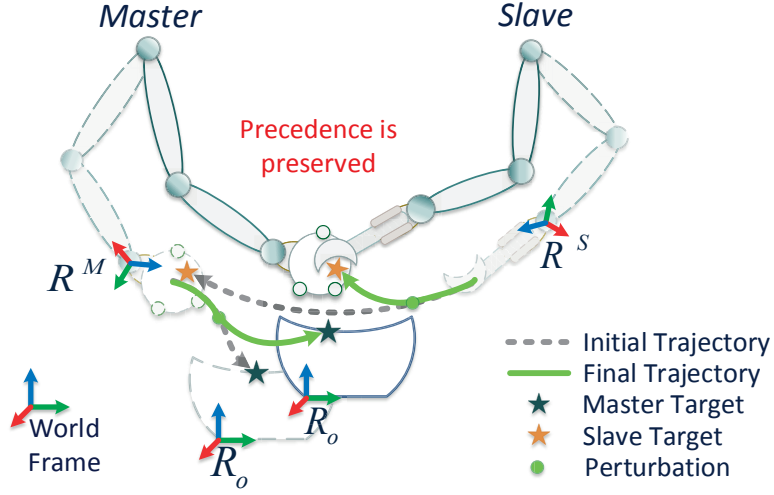
$$role_{\{arm_i, arm_j\}} = \begin{cases} master - slave, & \{R_o^i, R_i^j\} \\ slave - master, & \{R_i^j, R_o^j\} \\ uncoordinated, & \{R_o^i, R_o^j\} \end{cases} \quad (3.8)$$

In the scooping task there were two role changes (Table 3.2). The right arm (holding) was master during the reaching and scooping actions, moving with respect to the trashing bowl. The roles inverted in the depart action. The scooping arm became master, moving on top of the trashing bowl, while the right arm made room by moving aside. During trashing the arms were uncoordinated, moving relative to the trashing bowl: the scooping arm dropped the scooped piece, the holding arm moved backwards.

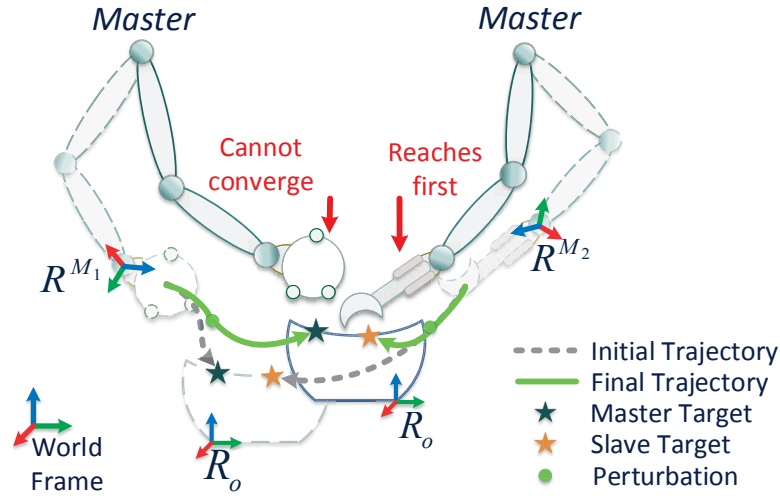
### 3.4.1 MASTER-SLAVE COUPLING BETWEEN THE ARMS

---

The motion of the arms is continuously coupled enabling adaptation during manipulation.

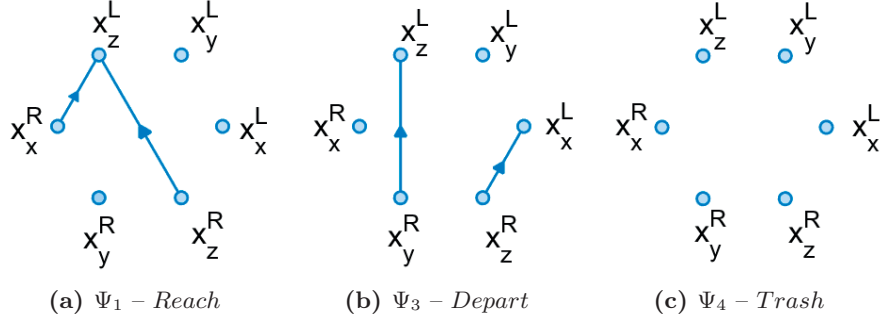


(a) Coupled. Master arm moves wrt. the bowl, slave wrt. master

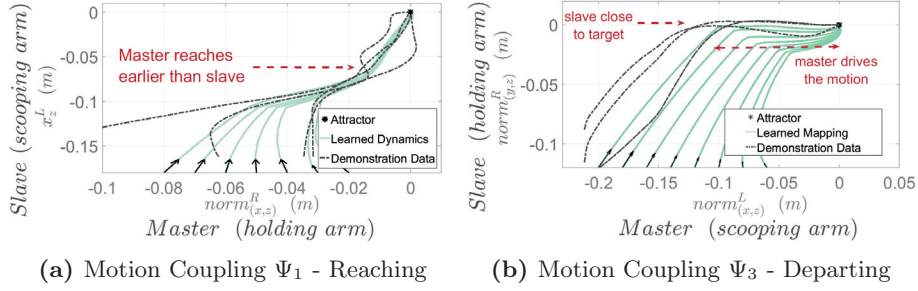


(b) Uncoupled. Both arms move relative to the external bowl

**Figure 3.10** Importance of the master-slave role in respecting precedence in the motion of the two arms. (a) master arm moves with respect to the bowl and slave arm relative master. When the bowl changes position the precedence is preserved; (b) both targets are set relative the bowl (i.e. both arms master). When the bowl moves closer to the arm on the right, this one reaches faster while the other arm has no place to converge.



**Figure 3.11** Motion-motion coupling for the reaching actions. Coupled dimensions in  $\Psi_1$  and  $\Psi_3$ , and no coordination in  $\Psi_4$



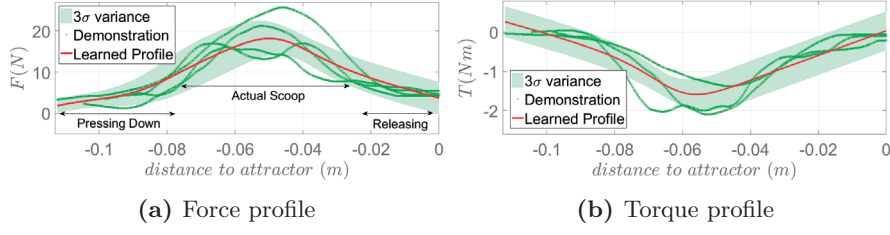
**Figure 3.12** Coupling functions between the master and the slave in the reach and depart actions. In each case the profiles are encoded as autonomous dynamical systems, taking for each arm the norm of the coupled dimensions obtained in Fig. 3.11. The holding and scooping arm switch their master-slave roles.

#### MOTION-MOTION COUPLING

For actions in which both arms employ position control we determined the coupled dimensions by analyzing the pair-wise interactions between the components of  $\nu^M, \nu^S$  using Granger Causality (Seth, 2010b). For the scooping task the dependencies are shown in Fig. 3.11: in  $\Psi_1$  the scooping arm was conditioned by reaching the vertical plane of the holding arm; a horizontal translation of the two arms in  $\Psi_3$ ; and no coordination in  $\Psi_4$ .

We further determined a continuous coupling function  $\gamma_{\{\nu^M, \nu^S\}}$  by encoding the norm of the coupled variables using an SEDS model (stable estimator of dynamical system (Khansari-Zadeh and Billard, 2011)). In the reaching action (Fig. 3.12(a)) the master got in the vicinity of its attractor sooner, allowing the slave to position relative to it. In the departing action (Fig. 3.12 (b)) the slave moved a smaller distance, but converged simultaneously with the master.

This coupled the position of the master and the slave as they reached their respective attractors (shown in Fig. 3.12). We thus use eq. 3.5 for controlling the master arm  $x_p^M, x_o^M$ , while the velocity of the slave arm adapted given the position of the master (eq. 3.9):



**Figure 3.13** Force–motion coupling in the scooping action. The scooping arm (slave) applies a force and torque profile with respect to the holding arm (master)

$$\begin{aligned} x_p^S(t+1) &= x_p^S(t) + \gamma \dot{x}_p^S(t); \\ x_o^S(t+1) &= x_o^S(t) + \alpha \dot{x}_o^S(t); \end{aligned} \quad (3.9)$$

Three aspects of coordinated behavior become implicit: *continuous coupling* - the slave adapts to the master throughout an action; *end-state coupling* - both arms reach the desired configuration simultaneously; *temporal coupling* - perturbing one of the arms does not cause a desynchronization.

---

#### FORCE–MOTION COUPLING

In actions in which force was applied (i.e.  $\Psi_2$ , scooping), the coupling was determined directly by the variables of interest. The scooping arm applied the force in the reference frame of the holding arm, while the holding arm was maintaining its position. The time independent encoding of the force/torque applied with respect to the distance to the attractor is shown in Fig. 3.13 (a) and (b).

---

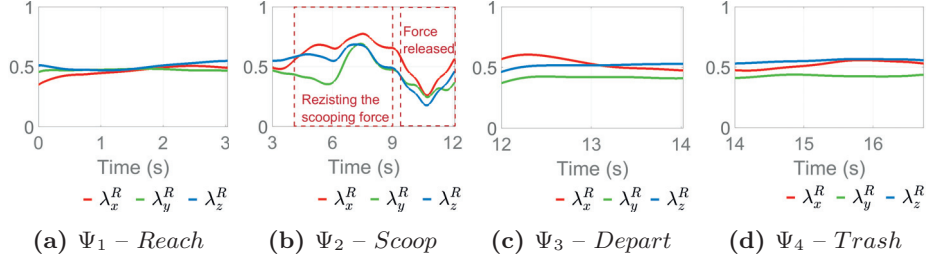
#### STIFFNESS MODULATION

For the holding arm the estimated stiffness modulation increased gradually as the scooping arm applied more force and decreased when the force was released (see Fig. 3.14). For the scooping arm the estimated stiffness is low on the axes on which force control should be used and higher for the position controlled axis ((Fig. 3.15) (b)).

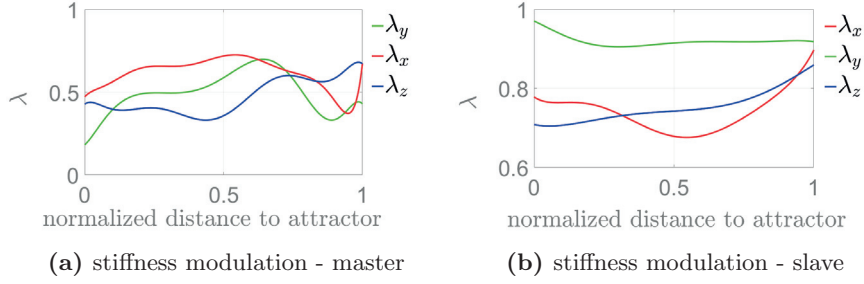
In the case of autonomous execution stiffness of both robot arms was updated based on the encoded profiles  $\lambda^{M,S} = E\{p(\lambda|x)\}$  (Fig. 3.15).

In the collaborative case we updated the stiffness based on the eq. 3.10, which also takes into account the state of the user given its current grasp on the tool:

$$\lambda_h = \begin{cases} \lambda_{\Psi_i} + \vartheta F_e, & F \in \nu_{\Psi_i}^S \\ \vartheta F_e, & \text{dist}(x^S, x^{*S}) > x^S(t_s) \& F \notin \nu_{\Psi_i}^S \end{cases} \quad (3.10)$$



**Figure 3.14** Stiffness modulation for the passive arm: average stiffness in the reaching actions  $\Psi_1, \Psi_3, \Psi_4$ , while during manipulation ( $\Psi_2$ ), the stiffness adapts to the force applied by the active arm.

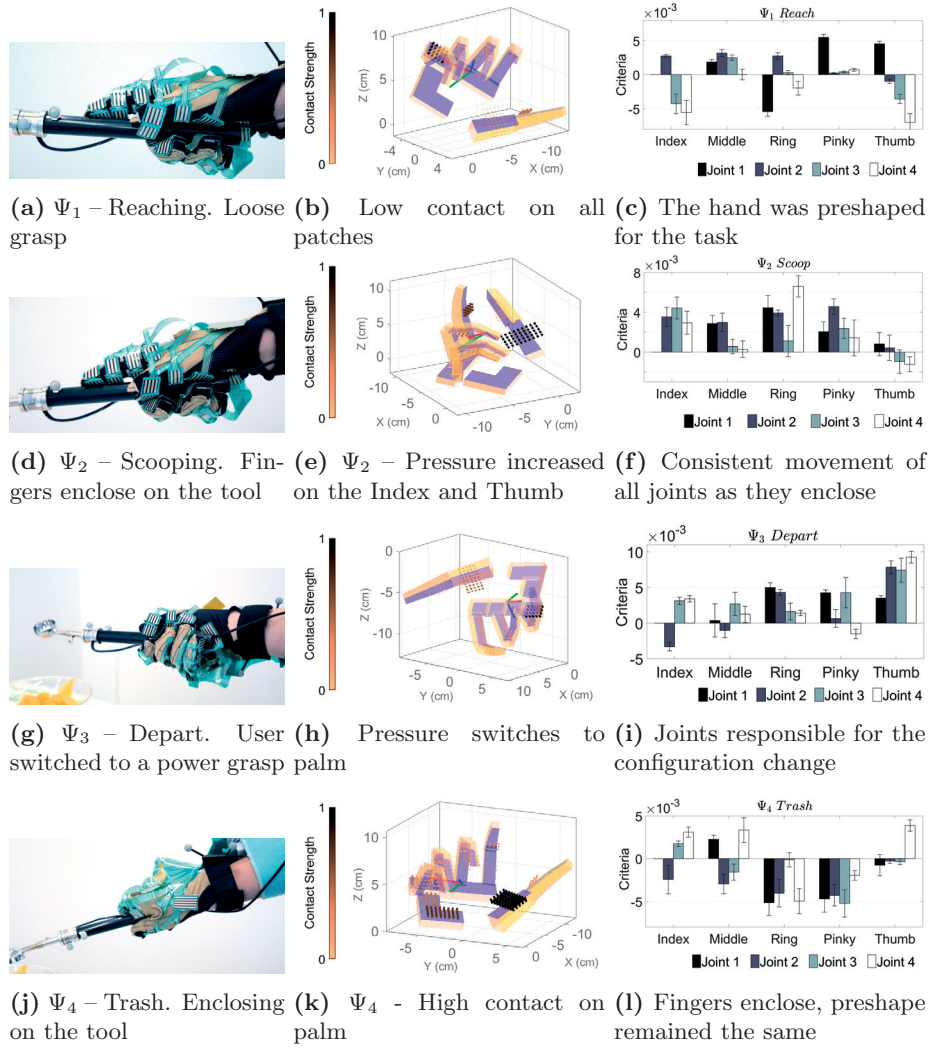


**Figure 3.15** Stiffness modulation for the two arms during the  $\Psi_2$  scooping phase with respect to the distance to the attractor.

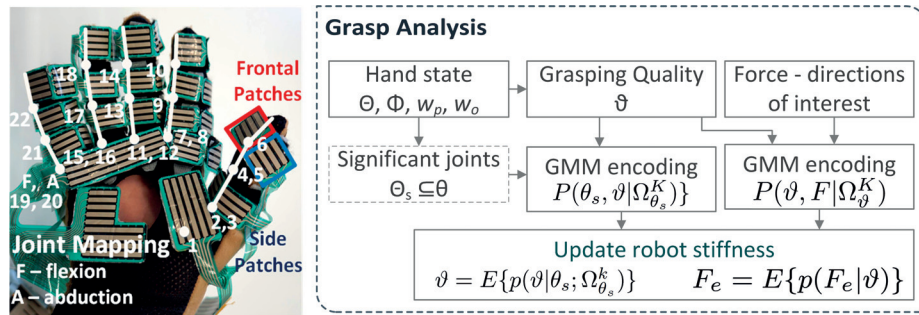
where  $\lambda_{\Psi_i}$  is the previous stiffness profile,  $\vartheta \in [0, 1]$  represents a grasping quality metric across the dimensions where force or torque are constraints, while  $F_e$  is the estimated force that the user could apply on the force-constrained axis given the current hand configuration. This allows the robot to update its stiffness according to the user's intention to apply a force, such that a low  $\vartheta$  or  $F_e$  lead to a low robot stiffness, which allows the user to freely reposition it. Conversely high values of these variables suggest the user is ready for the task.

### 3.4.2 ENCODING OF THE HAND SHAPE AND GRASPING QUALITY

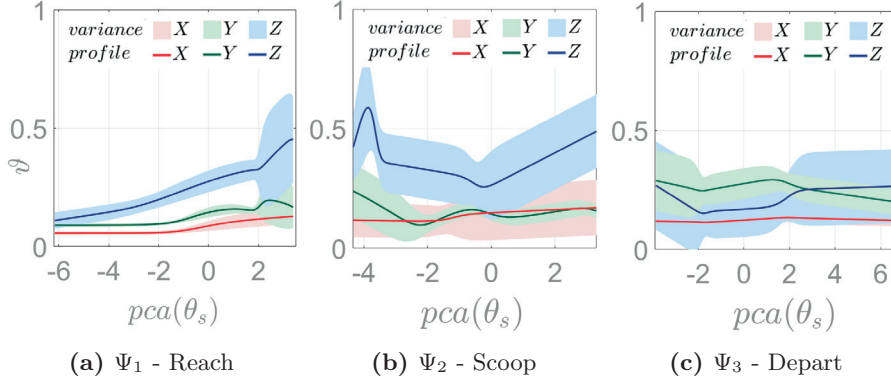
From the hand state (finger joint angles  $\theta \in \mathbb{R}^{22}$ , tactile signature  $\phi \in \mathbb{R}^{34}$ , wrist position and orientation  $w_p, w_o$ ) we compute the grasping quality metric  $\vartheta$  for the task directions where force or torque are variables of interest, using the approach described in (Borst et al., 1999; de Souza et al., 2015)). This value indicates if the current grasp is shaped for applying forces on the desired axes. Conversely a change in the hand shape influences the grasping quality. We thus retain a subset of significant joints  $\theta_s \subseteq \theta$  determined using the criterion in eq. 3.1. We encode the dependency between these two variables in a GMM  $P(\theta_s, \vartheta | \Omega_{\theta_s}^K)$ , see Fig. 3.18. Additionally since  $\vartheta$  is an indication of the task force, we encode a second GMM  $P(\vartheta, F | \Omega_{\vartheta}^K)$ . We use these two models (see



**Figure 3.16** (left column) The grasp changed over actions from a directional grasp for the scooping action to a power grasp while departing, and trashing; (center column) pressure was higher during scooping and trashing, while contact localization changed from thumb and index in the first case to palm in the second case; (right column) averaged selection criterion for each of the finger joints. A positive criterion indicates joints that moved consistently across demonstrations



**Figure 3.17** (left) glove and joint mapping; (right) grasp assessment pipeline



**Figure 3.18** Normalized grasping quality  $\vartheta$  given the set of significant joints for each action  $\theta_s$ . The value of  $\vartheta$  on the vertical Z axis increased during reaching and was highest in the scooping action as the user prepared for and applied task forces.  $\vartheta$  decreased in the departing action.

Fig. 3.17) to update the stiffness of the robot (eq. 3.10) as follows:

$$\vartheta = E\{p(\vartheta|\theta_s, \phi_s)\} \quad \% \vartheta \text{ from hand shape} \quad (3.11)$$

$$F_e = E\{p(F_e|\vartheta)\} \quad \% \text{ force given current } \vartheta \quad (3.12)$$

For the scooping task we obtained four grasps corresponding to each action (see Fig. 3.16), and encoding in Fig. 3.18.

### 3.4.3 TRANSITION CONDITIONS

During autonomous execution we switch between actions when reaching an attractor in either position ( $\bar{x}$ ) or in force ( $\bar{F}$ ) depending on the variables of interest  $\nu$  in the following action (eq. 3.13).

$$\kappa_{\Psi_i \rightarrow i+1}^{S,M} = \begin{cases} \text{norm}(d(x, \bar{x})) \leq \epsilon, & x, F \in \nu_{\Psi_i}^S \text{ \& } x \in \nu_{\Psi_{i+1}}^S \\ F \geq \bar{F}, & x \in \nu_{\Psi_i}^S \text{ \& } F \in \nu_{\Psi_{i+1}}^S \end{cases} \quad (3.13)$$

where  $\bar{F}$  was the force at the segmentation time  $t_s$ .

In the collaborative case the attractor in force is given by the user's ability to apply or resist the task forces (eq. 3.14).

$$\kappa_h = \begin{cases} F_e > \bar{F} & F \in \nu_{\Psi_{i+1}}^S \\ F_e > \bar{F}_{\Psi_i} & F \in \nu_{\Psi_i}^S \end{cases} \quad (3.14)$$

The approach is summarized in Algorithm 3.1.

---

**Algorithm 3.1** Extraction of coordination features
 

---

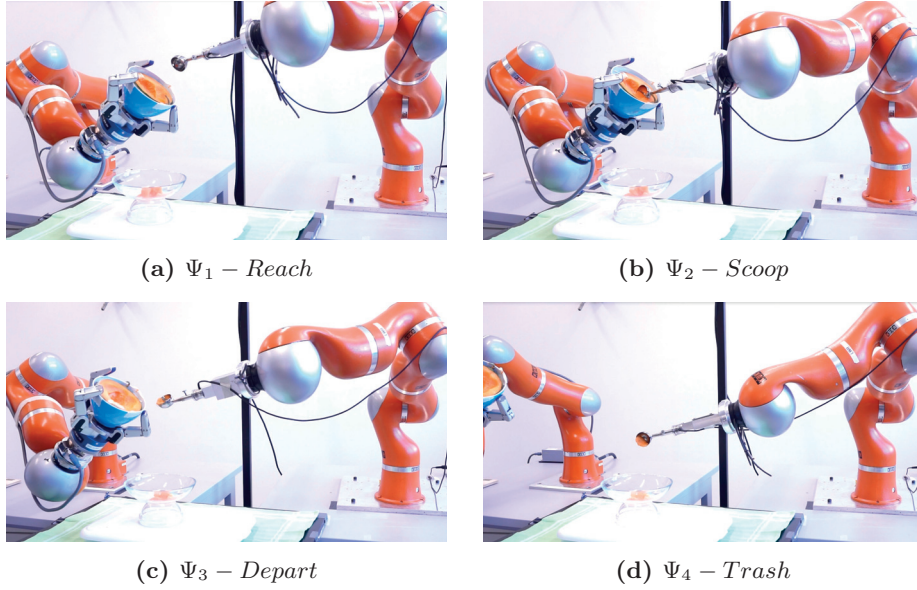
Coordination features(*Set of actions*  $\Psi_i$ ,  $i = 1 \dots N_\Psi$ ,)

```

for each action  $\Psi_i$ ,  $i = 1 \dots N_\Psi$  do
  | Get current unimanual constraints for arms A, B:
  |   ◦ reference frames:  $R_{\Psi_i}^A$ ,  $R_{\Psi_i}^B$ 
  |   ◦ control variables:  $\nu_{\Psi_i}^A$ ,  $\nu_{\Psi_i}^B$ 
  |
  | % Determine arm roles (eq. 3.8):
  | if  $R^A \rightarrow R_o^A$  and  $R^B \rightarrow R_o^B$  then
  | |  $A \Rightarrow$  master % motion in the object frame
  | |  $B \Rightarrow$  master % motion in the object frame
  | else if  $R^A \rightarrow R_o^A$  and  $R^B \rightarrow R_A^B$  then
  | |  $A \Rightarrow$  master % motion in the object frame
  | |  $B \Rightarrow$  slave % motion in the frame of robot A
  | else if  $R^A \rightarrow R_B^A$  and  $R^B \rightarrow R_o^B$  then
  | |  $A \Rightarrow$  slave % motion in the frame of robot B
  | |  $B \Rightarrow$  master % motion in the object frame
  | end if
  |
  | % Determine coupling:
  | if  $A \Rightarrow$  master and  $B \Rightarrow$  master then
  | | break % uncoordinated motion
  | else if  $\nu^A = x_{1:3}$ ,  $\nu^B = x_{1:3}$  % position control on all axes then
  | | % motion-motion coupling
  | |  $\{\nu_s^A, \nu_s^B\} =$  significant pairwise causal interactions  $\{\nu_{1:3}^A, \nu_{1:3}^B\}$ 
  | | encode norm of  $\nu_s^A$ ,  $\nu_s^B$  as a SEDS model (Khansari-Zadeh and Billard, 2012)
  | else if force is a control variable  $F \in \nu^A$  or  $F \in \nu^B$  then
  | | % force-motion coupling
  | | encode F wrt. distance to attractor, in the master RF
  | end if
  |
  | % Determine stiffness modulation
  | encode  $\lambda$  wrt. distance to attractor
  | encode  $\vartheta$  given the set of significant joint angles  $\theta_s$ 
  | encode the estimated force  $F_e$  given  $\vartheta$ 
  |
  | % Determine transition condition  $\kappa$  for each arm (eq. 3.13):
  | if ( $x$  or  $F \in \nu_{\Psi_i}$ ) & ( $x_{1:3} \in \nu_{\Psi_{i+1}}$ ) then
  | |  $\kappa: d(x, x^*) \leq \epsilon$  % distance to attractor
  | else if ( $x \in \nu_{\Psi_i}$ ) & ( $F \in \nu_{\Psi_{i+1}}^S$ ) then
  | |  $\kappa: F \geq F^*$  % motion ends in contact
  | end if
  | % Transition to the following action
  |  $\Psi_i \rightarrow \Psi_{i+1}: \{\kappa^M, \kappa^S\} = \text{true}$ 
end for
end

```

---



**Figure 3.19** Autonomous execution, snapshots of each action

## 3.5 Validation

---

We evaluate the execution of the scooping task in the three execution cases. Additionally we showcase the extraction of constraints for two other experiments: peeling and mixing.

### 3.5.1 MELLON SCOOPING

---

**Autonomous Execution** For the autonomous execution we used two 7 DOF Kuka LWR robot arms and a 4 DOF Barret hand for holding the mellow (snapshots in Fig 3.19). The scooping tool was rigidly attached, with an embedded 6 axis force–torque sensor.

We obtained a success rate of 8 out of 10 consecutive trials, also shown in the accompanying video. The first failed trial was due to not managing to completely remove the scooped piece. In the second case the robot removed just a tiny amount, due to scooping close to the skin.

#### **Collaborative Execution - Robot master**

In this scenario the robot held the mellow, while the human was performing the scoop (Fig. 3.20). The master arm initiated the motion and waited for the human counterpart to complete its current action. The robot increased its stiffness based on the anticipated intention of the human to apply a force. The success rate was 10 out of 10 trials (illustrated in the accompanying video).



(a)  $\Psi_1 - Reach$



(b)  $\Psi_2 - Scoop$

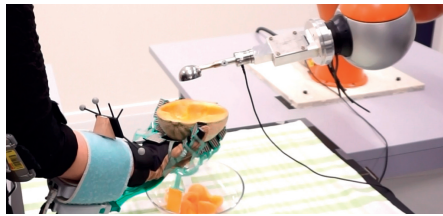


(c)  $\Psi_3 - Depart$

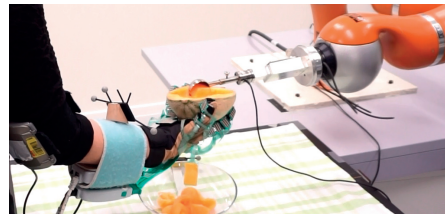


(d)  $\Psi_4 - Trash$

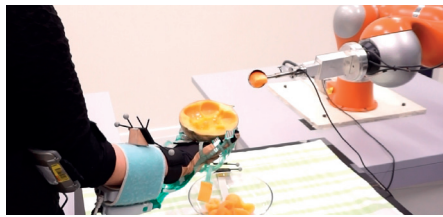
**Figure 3.20** Collaborative execution, robot master



(a)  $\Psi_1 - Reach$



(b)  $\Psi_2 - Scoop$

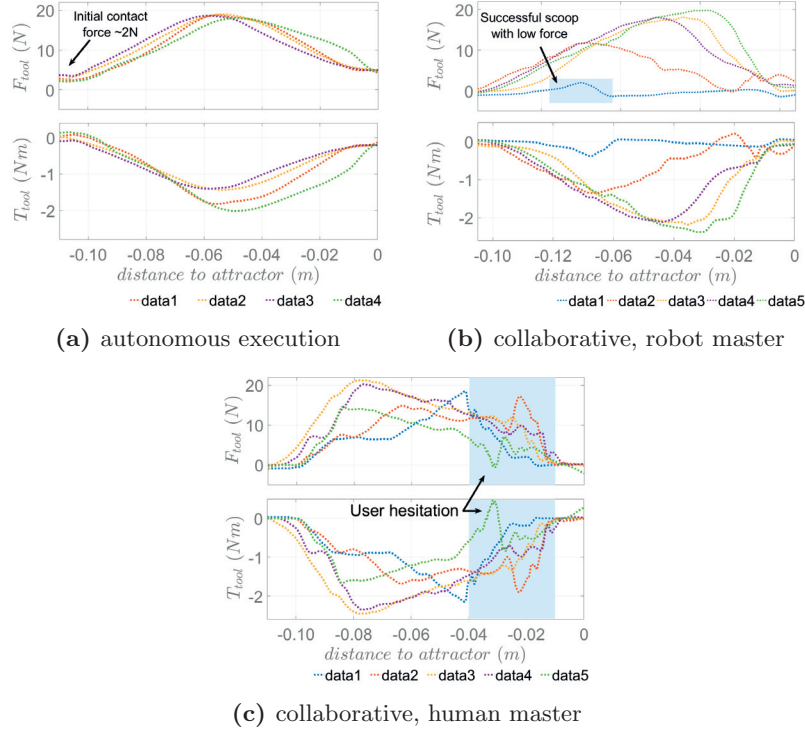


(c)  $\Psi_3 - Depart$



(d)  $\Psi_4 - Trash$

**Figure 3.21** Snapshots taken during the task execution: (top row) autonomous execution; (middle row) collaborative execution, robot master; (bottom row) collaborative execution, human master



**Figure 3.22** Forces and torques applied by the scooping tool in the 3 execution cases. The human when maneuvering the tool could better adapt to the environment, therefore achieving successful scoops with low forces (i.e. trial 1, when scooping on a new melon). Conversely when the human was holding the melon, the high variance comes from trembling in the human arm and improper adaptation of the stiffness in response to the robot applied forces (c). This happens particularly at the end of the motion when the robot arm starts going up removing the scooped piece.

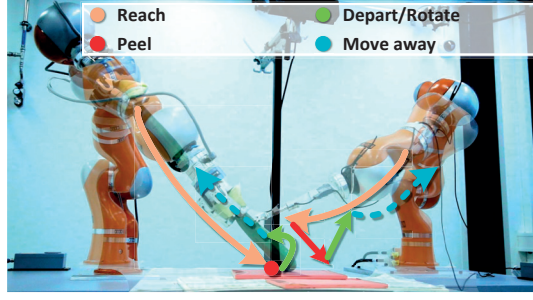
### Collaborative Execution - Human master

The robot arm scooped, while the human had to adapt to the applied force (Fig. 3.21). The success rate was 8 out of 10, due to the human hand trembling in the first failed trial, and the robot scooping a small amount due to improper positioning in the second failed trial.

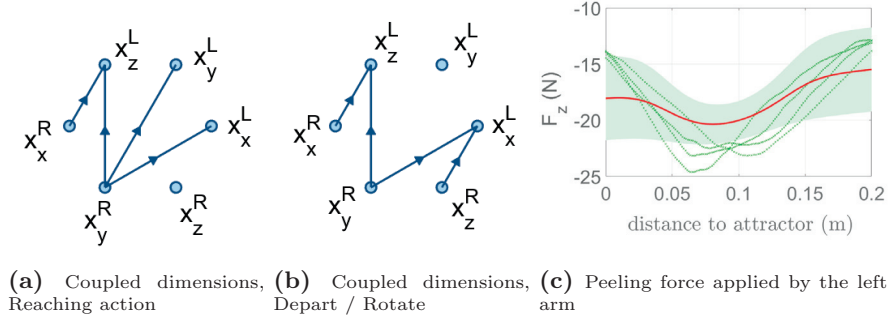
We provide a comparison of the forces applied in the 3 cases in Fig. 3.22. Overall there was a high variance of the forces in the two collaborative cases (Fig. 3.22b and 3.22c) compared to the autonomous case (Fig. 3.22a). This was due to better estimating the task conditions in case (b), but not adapting well to the robot in case (c).

### 3.5.2 VEGETABLE PEELING

We apply the extraction of task constraints to an additional experiment: peeling a vegetable, as shown in fig. 3.24. The task was originally segmented



**Figure 3.23** Typical motions for the 4 actions in the peeling task.



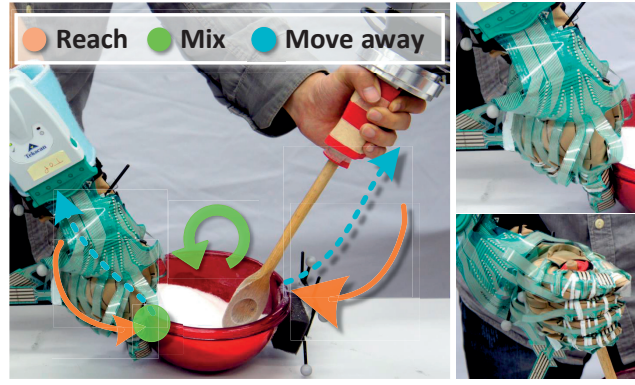
**Figure 3.24** Constraints for the peeling task.

using a BP-HMM approach (Figuerola and Billard, 2016), and the constraints were extracted for each action individually (Ureche et al., 2015). Four actions were obtained: reaching, peeling, departing while the holding arm rotates, and retracting.

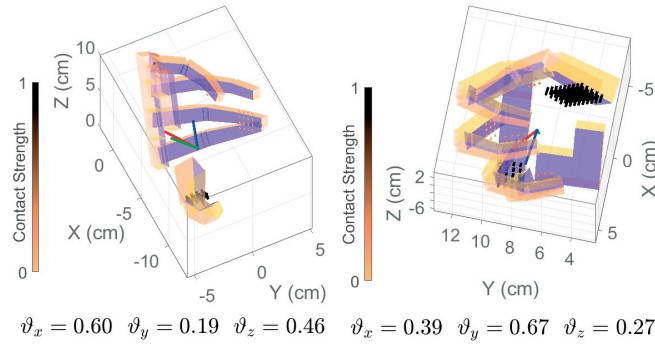
The right arm holding the vegetable acted as master throughout the task. Force constraints are used by both arms. The right arm ends the reaching action in contact with the table, and maintains contact by applying a constant force during the peeling and rotating actions. The left arm applied a force perpendicular to the zucchini in the peeling phase (Fig. 3.24c). The coupled dimensions in the third action (Fig. 3.24b) show that the right arm’s motion determines the left arm to retract backwards and down during the rotation. Using the constraints we obtained a success rate of 10 out of 10 trials.

### 3.5.3 BOWL MIXING

Lastly we performed an experiment of mixing in a bowl using a spoon, while the other arm was holding the bowl. The task took about 20 seconds to complete (Figure 3.25a). We obtained a decomposition in 3 actions: reaching, mixing and moving away. The holding arm acted as master throughout the task, applying a vertical force for maintaining contact with the table and using position control otherwise. The mixing arm was slave and employed force control during the mixing action.

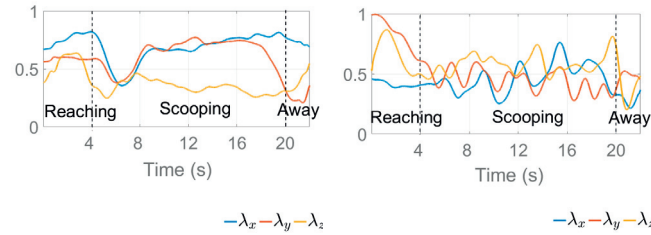


(a) actions and grasp close-ups



(b) directional grasp

(c) mixing power grasp



(d) Master - stiffness modulation

(e) Slave- stiffness modulation

**Figure 3.25** Bowl mixing task

Fig. 3.25b and 3.25c show the hand shape used for holding, with the correspondingly activated tactile patches. The grasp was adapted to applying a high force on the X axis ( $\vartheta_x = 0.6$ ) for stabilizing motions in the plane of the table, and a medium grasping quality ( $\vartheta = 0.46$ ) on the vertical axis ensuring contact with the environment.

We show the stiffness modulation of the master and slave arms in Fig. 3.25d and 3.25e respectively. The master arm had a low stiffness on the vertical axis for applying a force that maintains contact with the table and high stiffness on the other two axes. However residual motions of the bowl were the result of the low stiffness of the human arm. The stiffness of the slave arm changed continuously during each mixing pass.

## 3.6 Discussion

---

We described an approach for obtaining coordination constraints from demonstrations of asymmetric bimanual tasks. The approach is incremental, by detecting relations between the sets of unimanual constraints. The method proved efficient in the examples we explored, however we discuss multiple factors that posed limitations, and future work.

### 3.6.1 ADVANTAGES

---

The obtained representation allowed the robot to execute the task both autonomously as well as in physical collaboration with a human. Using the hand information in conjunction with the task constraints was important for the task success. Estimating the human’s intention based only on distance from its corresponding attractors, might not be sufficient, as shown in Fig. 3.26. The robot could correctly adapt its stiffness when the human approached from a demonstrated pose. But it would not adapt when approaching from above. However in both cases the user employed the same grasp, adapted for applying high forces. This is due to the fact that different actions require different ways of holding the tool (de Souza et al., 2015).

Thus the hand is shaped to apply a desired motion or force in accordance to the constraints of the current action. Therefore the grasp has a complementary role to the constraints. It is informative on how the tool should be used to achieve the desired effects on the object. This information can allow the robot to predict the human’s intent to apply a force and adjust accordingly.

In our experiment the tools (the fruit and the scoop) were already grasped when the task started and remained in hand throughout the task. Therefore the hand preshape was already task-specific, however the grasp continuously adapted to the current constraints. Additionally the estimated force ensured that the robot was able to adapt to scooping objects of different consistencies. For example the user would apply significantly less force when scooping cream vs. mellon, however the grasping quality alone does not give a direct indication of the amplitude of the force.

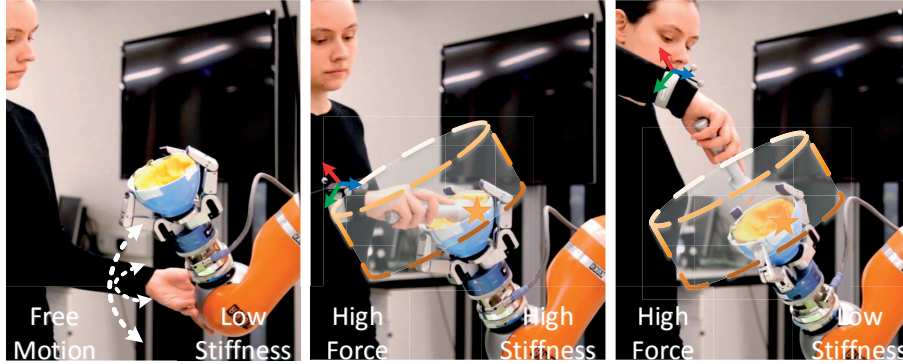
### 3.6.2 LIMITATIONS

---

The method described in this work applies only to asymmetrical bimanual tasks in which the two arms maneuver different objects either for reaching different targets or for performing actions in physical contact.

#### **Task modeling**

The proposed approach modelled directly the demonstrated behavior however this might not be the most efficient manner to execute the task. However



**Figure 3.26** Stiffness update based on vision only estimation of the wrist position. (left) free motion for safe interaction; (center) the human wrist enters the vicinity of the estimated attractor following the demonstrated behavior. The robot is able to increase stiffness; (right) the user is ready to apply high force, but being further from the attractor the robot does not increase its stiffness.

we consider that the behavior that the user demonstrated is the one that should be reproduced. We don't focus on determining if this behavior is optimal for the task, or if certain gestures should not be included in the task model.

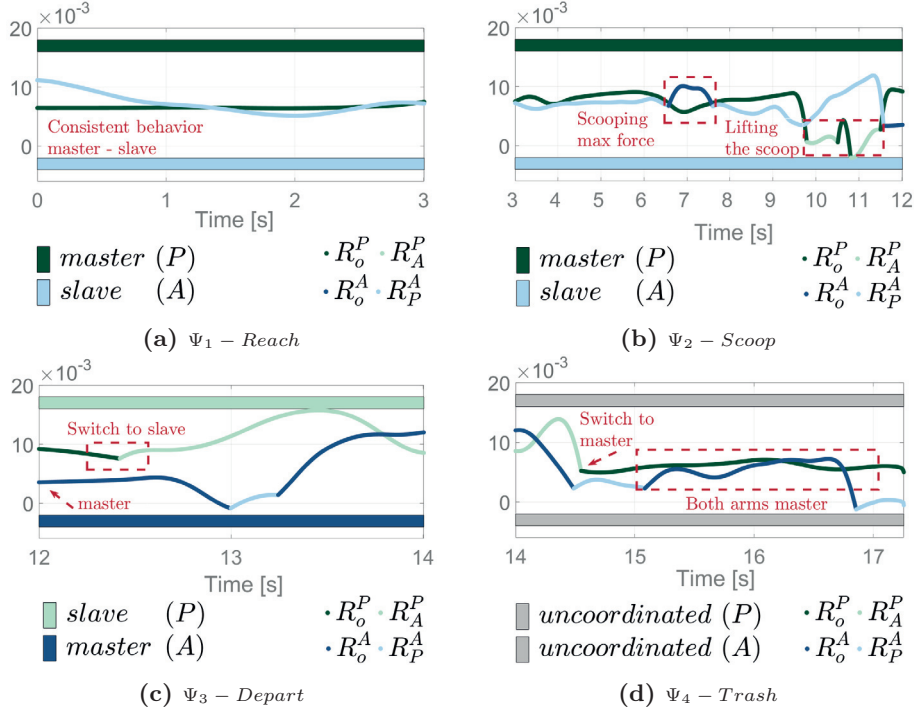
For example in the case of the scooping experiment, the departing and reaching back actions could have been modeled in a single action as they serve the same purpose thus avoiding the change of models and reference frames. While these changes occur in complex tasks requiring multiple subtasks it is preferable to design a way to aggregate actions with respect to the current goal.

Similarly, in the "bowl-mixing task" the arm holding the bowl showcased some residual motions as the active arm was mixing. This was due to the lower stiffness of the human arm during demonstration, and was not necessary for successfully completing the task.

Moreover the effect on the object was modeled indirectly through the exerted forces. However even though this was a feature of the task, it does not necessarily ensure that an autonomous execution would always be successful (i.e. obtaining a plastic deformation, where the scooped part is actually removed, but in a changing context: using a hard pumpkin instead of a melon). This could be achieved by making use of higher-level information about the actual state of the object and correlating it with the applied forces. Conversely, when executing the task collaboratively, the human might have to apply higher forces than what was demonstrated to achieve the goal. In this case our encoding of the coordinated behavior could ensure successful execution, regardless of the fact that the robot lacks a representation of the high-level goal.

### Hardware setup

The setup used for recording demonstrations is not suitable for demonstrating dexterous manipulation for two hands. This would require two data gloves



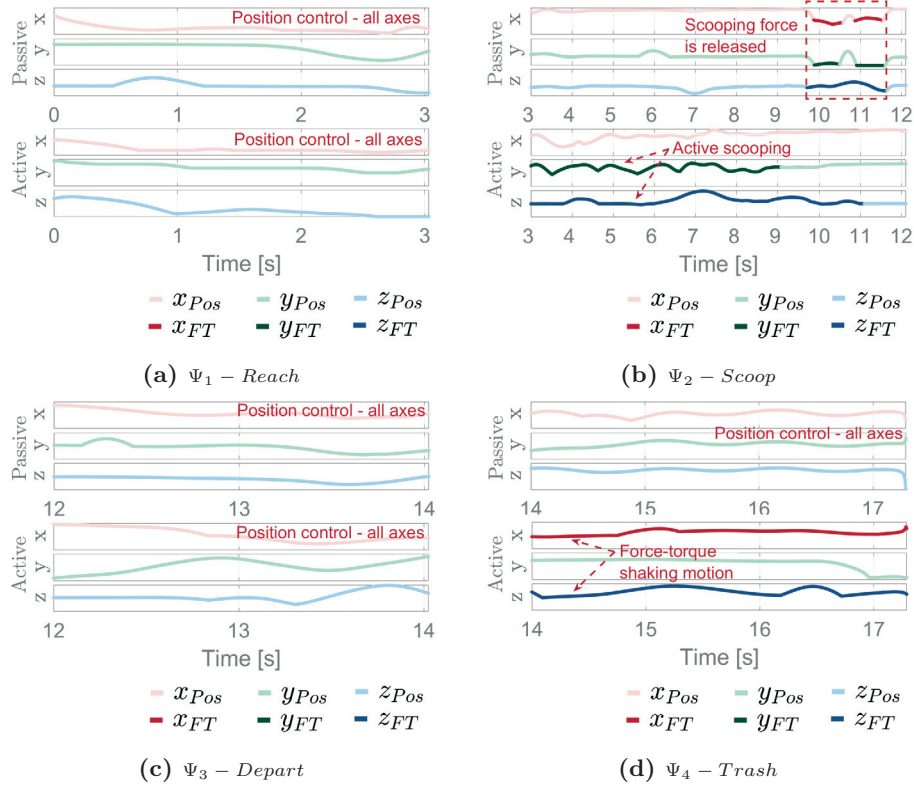
**Figure 3.27** The line plots show the maximum criterion at each time step corresponding to the change of reference frame. Dark green correspond to the criterion of the holding arm moving with respect to the the bowl, and light green moving wrt. the active arm. Similarly for the arm holding the tool, the dark blue line corresponds to moving wrt. the bowl, and light blue wrt. the holding arm. The patches show the arm roles for each action, as attributed during segmentation.

and two sensorized tools that capture directly the motion of the human hand and the forces exerted by the arm. However in this case transferring the task to the robot (especially the dexterous aspect) raises different challenges, such as determining the appropriate mapping between the human and the robotic hand, which we don't address here. The setup is also a downside during collaborative execution as the user always has to wear the glove for the robot to access the hand state.

### Algorithm

In the current work we don't explicitly consider the end effector orientation when performing segmentation. However this information is retained for each action and incorporated in the behavior of the robot when reaching a target, through our dynamical systems implementation (Shukla and Billard, 2012).

Also our algorithm is sensitive to the way the user holds the tool and to changing the grasp in a consistent way across demonstrations, as this influences our extracted vector of important joint angles  $\theta_s$ . Various users might feel more comfortable holding the tool in different ways, or not varying the grasp across



**Figure 3.28** The maximum criterion at each time step corresponding to the variable of interest for each arm. Light red, green, and blue lines correspond to position control on the X, Y and Z axis respectively. The dark colored lines correspond to force control.

actions, even if this behavior is not optimal for the task.

Moreover constraints in configuration space are important for safe task execution. However the method described here does not extract these type of constraints (such as self-collision avoidance). But if these aspects related to arm kinematics are known they could be accounted for during the execution phase.

Lastly we don't consider all the possible combinations of subsystems when studying coordination. While this reduces our search space, it might let interesting correlations escape unobserved (such as the coordination between fingers, or the motion of one arm might influence the finger movement of the opposite hand).

### Choice of window size

Our algorithm is sensitive to the window size used for segmentation. A small window size can lead to oversegmentation, while a large window size has a smoothing effect. In Fig. 3.27 we show the maximum criterion (for the choice of reference frame) obtained at each time step before applying a time window for performing the segmentation.

From this criteria we can identify subtle events: (1) the active arm became master for a short period of time ( $< 1s$ ) which corresponded to the maximum force being applied; (2) the passive arm switched shortly to a slave behavior as the active arm finished scooping and was moving up; (3) the master/slave role switched during the departing action; (4) the motion became uncoordinated as both arms switched to the object reference frame.

These changes were smoothed out in our segmentation as we used a time window equal to our sampling rate, with no visible effect in this low paced task. However in other tasks it might be important to catch these events. The axis-specific control variables also change according to the action requirements (see Fig. 3.28). Position is the relevant variable in reaching actions ( $\Psi_1, \Psi_3$ ). During scooping the active arm employed force and torque across the Y and Z axis; the passive arm was position controlled. A change to force control for the holding arm occurred as the active arm released the scooping force. The last action (departing) does not end in contact, the arm holding the tool accelerates and shakes to drop the scooped piece, thus inducing dynamic forces. These can be filtered while in this case the transition condition depends on the arms reaching their respective attractors.

### 3.6.3 STABILITY CONSIDERATIONS

---

The motion of each arm is generated using a coupled dynamical systems (CDS) representation, with 3 components: a position dynamics, a orientation dynamics and a coupling between the position and orientation. The stability of a CDS system has been addressed previously in Shukla and Billard (2012) by analyzing the stability of its components.

We further encode the coupling between the arms as a SEDS (stable estimator of dynamical systems) (Khansari-Zadeh and Billard, 2011). SEDS ensures global asymptotical stability in reaching the attractor (see Khansari-Zadeh and Billard (2011) for a formal proof), robustness to perturbations and online adaptation for obstacle avoidance (Khansari-Zadeh and Billard, 2012). This applies both to changes in the object's position as well as to changes in the motion of the human hand during collaborative execution.

During the task execution we use the cartesian impedance controller provided through the Kuka Fast Research Interface (FRI 1.0):  $\tau = J^T(K_m(x - x_m) + F_m) + D + f_{dynamics}(q, \dot{q}, \ddot{q})$ , in which the stiffness  $K_m$ , position and  $x_m$ , force  $F_m$  are model based, while the last two terms are compensated by the controller.

### 3.6.4 FUTURE WORK

---

As previously mentioned, constraints alone might not be sufficient for obtaining a generic task representation. Therefore one future direction focuses

on including high-level information about the state of the manipulated objects coming from vision or other sensors. This can influence the system’s ability to generalization: such as obtaining the same effect using different tools, or modifying the placement of the scoop inside the mellow as a function of the remaining amount of fruit pulp. This can also lead to practical metric of task completion. Such meta-information is essential for reasoning about the task, inferring missing information, or even correlating the action with semantic data, whereas in the current work, the action labels were manually added.

Secondly this technique applied to collaborative tasks has the potential to improve interaction, by making the robot’s behavior more predictable for a human partner.

### 3.7 Conclusions

---

In this chapter we presented an approach for abstracting a representation of asymmetrical bimanual tasks from user demonstrations. While the motion of each arm is characterized by its own set of constraints, we are particularly interested in coordination features, which we identify as relationships between the unimanual constraints.

We form a task prototype based on constraints, motions models and embodiment features that represent the user specific way of performing the task. We tested the proposed approach on two common cooking tasks. We showed that the same prototype can be instantiated when performing the task on a bimanual platform, as well as in collaboration with a human. However this approach has limitations with respect to the efficiency of the encoding as well as the user’s ability to demonstrate the task in the proposed manner.

Lastly we investigated how the motion of the two arms can be coupled for actions that have different requirements. We also showed that the roles governing the motion change, as well as the type of coupling.



# USER SKILL ASSESSMENT BASED ON TASK CONSTRAINTS

The work presented in this chapter is currently under review:

*Pais Ureche, A. L., and Billard, A. (2017) **Automatic skill assessment in learning from demonstration.** [Under Submission, IJSR 2017]*

## 4.1 Forward

---

In this chapter we explore an alternative use of the soft task constraints introduced previously. The constraints are identified based on a notion of consistency in the execution of multiple demonstrations. Here we perform a user study to investigate firstly how consistent behavior relates to applying the required task forces and to maneuvering the tool, and secondly whether it affects the performance of the subject as perceived by himself or by an external rater. Thus the proposed approach constitutes an automatic assessment of the user performance through objective task-specific metrics.

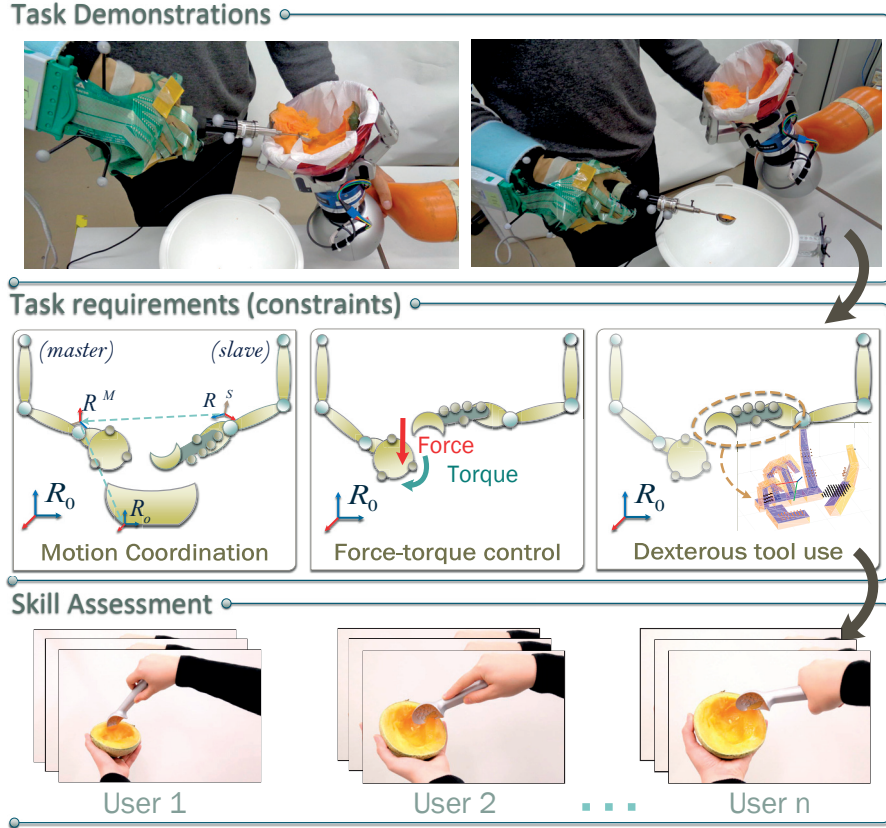
We test the approach on a daily bimanual task, in a user study involving 37 participants<sup>1</sup>. We compare our metrics with two subjective evaluations: user's self-assessed skill, and skill assessed by video raters.

Our work is based on the observation that Programming by demonstration (PbD/LfD) often relies on experts performing the task, however users might be more or less skilled in performing the same task, especially when force control and dexterous tool use are required. This can impact the quality of the demonstrations, of the learned models and of the interaction. Despite this fact user performance is typically evaluated through hardcoded metrics, making the assessment difficult.

We then show that the user skill impacts robot performance while executing the learned task and that the hand state can be an indicator of user performance in relation to the task constraints. We then use the skill information to classify the users hand state seen during task demonstrations. We show that in the case of collaborative execution signal the expected level of human performance given the current constraints.

---

<sup>1</sup>The data and code from this experiment are provided on the following [link](#).



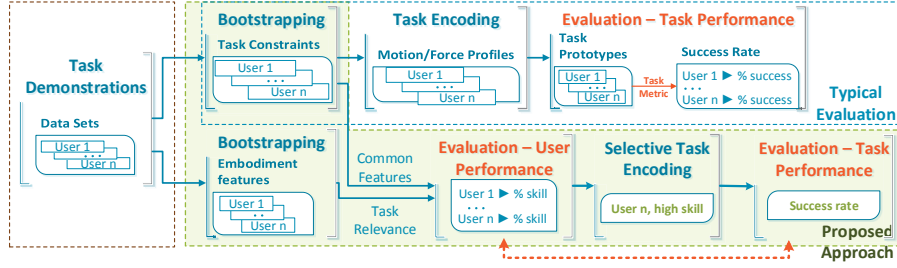
**Figure 4.1** We record demonstrations from multiple users. For each we extract a constraint-based representation consisting of: the action sequence, the reference frame for each arm, the relevant variables in each action, and the stiffness modulation (Ureche et al., 2015). We evaluate performance across users given the different strategies they adopt, assessing how consistent they are through consecutive trials and how their performance is correlated with various factors such as the force they apply, or the way they manipulate the tool.

## 4.2 Introduction

When learning a task through Programming by Demonstration (PbD/LfD) the aim is obtaining an accurate execution while giving the robot the ability to generalize to various contexts. The demonstrator is often an expert, and the task is typically learned from good demonstrations.

In this chapter we address the fact that multiple users can be successful in providing demonstrations however some perform the task with ease, while others struggle to obtain the desired effect. Users might adopt different strategies of using the tool, adapted to the local conditions, which result in successful demonstrations. However applying the same strategy might not result in a good execution under different conditions.

We consider our previous approach Ureche et al. (2015) which identifies regions of low variability across multiple demonstrations as task constraints. For



**Figure 4.2** Typically user performance is linked to task performance evaluated at the end of the learning cycle. In our approach we bootstrap task constraints and embodiment features related to the way the user manipulates the tool. We determine user performance based on these two sets of features and show that it is linked to robot performance during execution.

a given task the constraints remain the same across demonstrators. Therefore this notion of *consistency* (i.e. regions of low variability) in relation to the task constraints can constitute an indication of the ability to perform the task properly.

We thus make the hypothesis that a skilled user shows consistency over trials. This most likely originates from prior knowledge of the task and results in the ability to reproduce the skill properly from the beginning. In contrast, an unskilled user who tries different strategies, shows little to no consistency across multiple demonstrations, thus leading to over segmentation.

This aspect is in line with other observations of human skilled performance. In sports for example skill is defined as a "consistent production" of movements or gestures that were learned and that serve the task goal (McMorris, 2004). Thus a skill is acquired when a subject is able to show consistency in performing it (McMorris, 2004). Moreover subjects who already have a cognitive representation of the task are better able to control their voluntary motions thus showing more consistent structures and better controlled force and position profiles (Seegelke and Schack, 2016).

Therefore we also investigate the way consistent performance is linked to other aspects of task execution, namely: exerting forces, modulating the arm's stiffness, maneuvering the tool (as different actions require holding the tool in different ways (de Souza et al., 2015)) or the time required to complete the task.

Manipulation tasks, such as scooping a fruit, require the two arms to coordinate for obtaining a physical effect, by adjusting their relative pose, force and impedance, which represent the task constraints (Ureche et al., 2015; Pais and Billard, 2015). However the way the tool is employed favors applying these constraints (see Fig. 4.1). Moreover a human learning to use a new tool is often shown the best way to hold it by an experienced person.

Typically performance is evaluated indirectly at execution time through specific task success metrics. In our work we propose performing an assessment directly on demonstration data, by correlating user's behavior with the task

constraints (see Fig. 4.2).

We show that the two evaluations are correlated thus making user performance a good indicator of the robot performance in autonomous execution. For example the fact that a user did not implicitly emphasize the constraints during demonstration (i.e. by applying forces randomly rather than on the direction of interest for the task), can influence the robot’s ability to generalize.

Conversely we show that a robot aware of the task constraints can use this information for estimating the performance level based on the user’s hand state.

Our approach contributes to task learning by:

- (1) providing *objective task-specific metrics* related to automatically extracted constraints, instead of hardcoded metrics or a ground truth model;
- (2) identifying patterns that unskilled users have in common thus revealing difficult aspects of the task.
- (3) using the performance estimation both for selectively learning parts of the task from different users and for evaluating user behavior in realtime;

We structure our work around addressing the following research questions:

RQ1 Can the user performance during demonstration be reliably assessed based on objective task constraints?

RQ2 Is the user performance during the demonstration directly correlated with the robot’s ability to execute the task?

RQ3 Can the user performance be predicted from the ability to dexterously manipulate the tool?

We present our method for assessing user performance and the experiment we conduct for evaluating it in Section 4.4. We further investigate causes of poor performance in Section 4.5.

We then relate our user performance assessment with robot performance during autonomous task execution in Section 4.6.

Finally we use the computed performance to label and classify users’ hand state during demonstrations and show that this information can be used to reliably estimate performance levels in Section 4.7. Implications and limitations are discussed in Section 4.8. Section 4.3 presents related work.

## 4.3 Related Work

---

We address the evaluation of human’s performance during kinesthetic teaching interactions. Despite successfully completing a task, users might not always provide demonstrations that generalize to new contexts.

### 4.3.1 USER ASSESSMENT IN TEACHING INTERACTIONS

---

Teaching interactions can be evaluated objectively during the execution phase with respect to whether the task has been transferred successfully (i.e. the robot’s ability to reproduce the task) (Kronander and Billard, 2014), or subjectively based on the quality of the interaction, as perceived by the user (Pais et al., 2013). In our work we propose a method of assessing the user performance through objective metrics, during the demonstration phase. We show that this assessment is correlated with the robot’s performance during the execution and that performance can increase when selectively learning actions based on the user assessment.

Teaching interaction and implicitly the quality of the demonstration data can be improved by: providing instructions to guide teaching (Cakmak and Thomaz, 2014a); asking questions (Cakmak and Thomaz, 2012a); using measures of demonstration quality (Kaiser et al., 1995).

However all these approaches assume prior knowledge of the task, and of what makes a good demonstration. In our work we minimize the use of prior information about the task by automatically extracting the constraints and assessing the user’s performance relative to them.

Additionally we explore information relative to the way a user is performing the task, particularly using the tool, as a means of achieving the goal. For example choosing a particular configuration of the arms when performing a bimanual task can affect the strategy people use to stabilize the system (Saha and Morasso, 2010).

### 4.3.2 USER ASSESSMENT DURING AN INTERACTION

---

Kinesthetic demonstrations are a particular case of human robot interaction (HRI). In HRI assessing the user performance can affect the system’s efficiency, robustness, and learning ability when dealing with uncertainty (Kannan and Parker, 2007). However few works focus on characterizing and quantifying user behavior in force control tasks. Physical interaction during a kinesthetic demonstration becomes challenging as the user should be skilled not only in performing the task but also in maneuvering the robot to continuously apply the proper forces.

Common objective metrics used in HRI to quantify human performance focus on optimizing various measurements: time to task completion (Salcudean et al., 1997; Murphy and Schreckenghost, 2013) – however depending on the task characteristics this information might not be as relevant as the quality of the demonstration; distance traveled with the tool, which should be minimized in precision tasks, such as surgery (Jog et al., 2011); relative to respecting position and force (Salcudean et al., 1997); optimal paths with respect to a known geometric configuration (Chen and Zelinsky, 2003); relative to contact errors (Steinfeld et al., 2006) as an indicator of accuracy in manipulation tasks; relative to the task goal (i.e. in the context of rendering forces for a teleoperated suturing task (Mohareri et al., 2014)).

While task relevant, these metrics are handcoded, enforcing a certain way of performing the task. In our work we emphasize the possibility of automatically sequencing the task and obtaining a representation based on constraints. Performance is evaluated based on the ability to enforce these constraints.

In Jain et al. (2015) objective and automatic performance measures for a human operating with a robot are proposed by segmenting video data of the human performance and identifying specific steps. However this method requires ground truth, and does not take into account interaction forces.

Subjective evaluation in HRI implies user-related metrics such as "trust" or the "degree of mental computation" (Murphy and Schreckenghost, 2013; Steinfeld et al., 2006). Alternatively, teaching interactions are a particular case of human-robot team interactions. Team-specific metrics are proposed in (Olsen and Goodrich, 2003) valuing a decrease in the human's interaction effort.

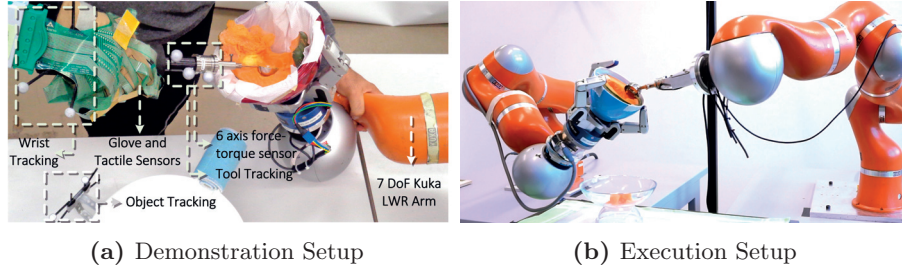
### 4.3.3 PARTICULARITIES OF BIMANUAL BEHAVIOR

---

In this chapter we focus on an asymmetrical bimanual task which requires manipulating the tool for exerting relative forces between the arms. Skill in this case influences arm motion and impacts performance when operating machinery (Suzuki et al., 2008). In bimanual tasks the arms work in synergy (Kazennikov et al., 2002), synchronizing towards reaching a goal (Perrig et al., 1999) while showcasing spatial and temporal coupling (Franz et al., 1991; Kazennikov et al., 2002). Decoupling in arm motion might indicate hesitation.

Apart from motion coordination, modification in control strategies may occur (Dimitriou et al., 2011). These can be considered a "*decoupling*" in the movement pattern (Mutha and Sainburg, 2009) and can be observed in the way the motion is being performed.

These factors have implications in the way a task is demonstrated to a robot, as users who are not skilled themselves in performing a task may showcase many instances of decoupling.



**Figure 4.3** During demonstrations the subject is kinesthetically driving a KUKA LWR arm used for holding. The tool is maneuvered by the opposite hand while wearing a glove covered with tactile sensing. Vision is used for tracking the tool, the wrist and the bowl. Two Kuka LWR arms with FT sensors, and vision tracking are used for autonomous execution.

## 4.4 User performance assessment

---

The ability of a robot to learn and generalize a newly demonstrated task depends greatly on the quality of the demonstrations. Therefore this experiment was carried out to study whether skilled performance of a person can be assessed through consistency in relation to the task constraints and to evaluate the impact it has on the robot’s performance.

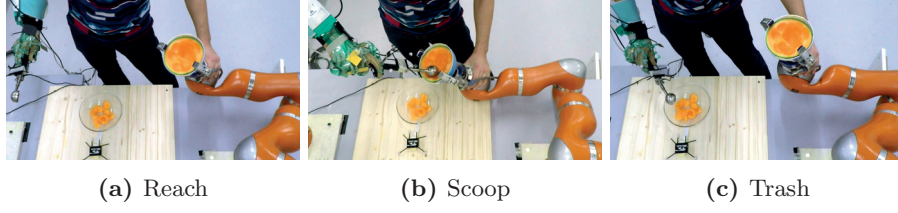
### 4.4.1 STUDY DESIGN

---

The experiment consisted of an asymmetrical bimanual task: scooping. Properly completing the task required coordinating the arms, and maneuvering the tool to exert appropriate forces.

We thus test the hypothesis that consistency in the execution can be used as an indicator of skilled performance and that it is further related to other task aspects such as exerting proper forces and manipulating the tool.

**Experimental Setup** For recording demonstrations we used the setup shown in Figure 4.3a. A 7 degrees of freedom (DoF) Kuka LWR robotic arm, and a Barret hand (4 DoF), was used for holding the mellon to be scooped. The demonstrator could kinesthetically guide the arm with his left hand. The subject scooped with the other arm, wearing a data glove covered with Tekscan tactile sensors on the front and side of the phalanges. Force–torque sensors were mounted both on the tool and on the robot’s arm. We tracked the tool, human wrist and trashing bowl using an Optitrack Vision System. External cameras recorded the subject’s performance. For executing the task we used two 7 DoF KUKA LWR arms. The first arm with the 4 DoF Barret hand was used for holding. The scooping tool was rigidly attached to the second arm. A vision tracked bowl was used as external object (Fig. 4.3b).



**Figure 4.4** Typical steps in the scooping task

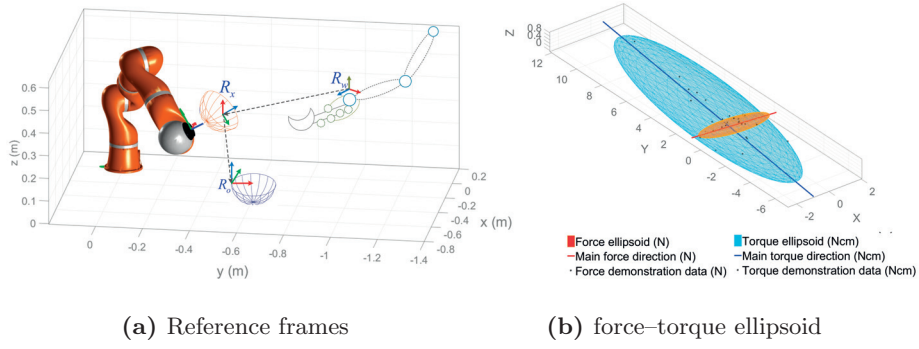
**Study Protocol** The participants were told to start the task from a comfortable position, scoop a piece of the pulp, and drop it in the bowl<sup>2</sup>. This delimits 3 actions  $\Psi_1 - Reach$ ,  $\Psi_2 - Scoop$ ,  $\Psi_3 - Trash$ , as shown in Figure 4.4. No specific instructions were given on how to achieve these actions. The participants were requested to provide a minimum of 10 demonstrations, and were allowed to continue performing the task up to 20 times if desired. We thus collected a total of 480 demonstrations with most of the subjects performing between 12 and 15 trials. The participants filled in a post-experiment questionnaire (in English), for evaluating their overall perception of the task. Each demonstration was filmed and raters who have not done the experiment, were asked to rate the overall performance of each subject as well as during individual trials.

**Participants** The study involved  $N = 37$  participants (28 male, 9 female), age  $28.75 \pm 3.88$ , right-handed, part of the university staff pursuing a master, PhD or post doc.

**Measurements** For each demonstration we recorded the following data:

1. the position, orientation  $r_p, r_o \in \mathbb{R}^3$  of the robot's end effector;
2. the forces  $F_e \in \mathbb{R}^6$  on the robot's end effector;
3. the motion of the wrist  $w_p, w_o \in \mathbb{R}^3$ ;
4. the forces and torques acting on the tool  $F_t \in \mathbb{R}^6$ ;
5. the tool pose  $t_p, t_o \in \mathbb{R}^3$ ;
6. the bowl pose  $o_p, o_o \in \mathbb{R}^3$ ;
7. the finger joint angles  $\theta \in \mathbb{R}^{23}$
8. tactile readings: averaged tactile pressure on the frontal patches  $\phi_f \in \mathbb{R}^{18}$  and side patches  $\phi_s \in \mathbb{R}^{18}$ ;
9. the time length of each demonstration  $T (s)$ ;
10. the scooped quantity ( $g$ );

<sup>2</sup>The data recording started when the tool was already in hand, such that we didn't assess the initial reaching for the tool nor the grasping phase.



**Figure 4.5** Constraints extraction for the scooping task. The human arm  $R_w$  moves with respect to the robot  $R_x$ ; the robot moves relative to the bowl on the table  $R_o$ . The directions to apply force and torque are illustrated on the right.

From the first 6 measurements we determined a constraint representation of the task by using our previously proposed approach (Ureche et al., 2015). We automatically segmented the task actions and extracted soft constraints that consisted of: the reference frame used for manipulation, the relevant variables with respect to this frame (illustrated in Fig. 4.5) and a stiffness modulation factor for each arm.

## Metrics

We propose 4 sets of metrics for comparing our automatic assessment of performance (metrics A) with: objective task measurements (metrics B); the user’s self-assessed performance (metrics C); and with the performance assessed by video raters (metrics D).

### A. Metrics related to the autonomous extraction of task constraints:

- (1) number of segments  $\Psi, a \in [1..N_\Psi]$
- (2) important variables in each action  $\nu \in \mathbb{R}^3$ :
- (3) stiffness modulation in each action  $\lambda \in \mathbb{R}^3$
- (4) user skill  $\{skilled, unskilled\}$
- (5) metrics regarding dexterous tool use:
  1. grasp adaptability  $\vartheta \in \mathbb{R}^6$
  2. maximum pressure per patch
  3. demonstration quality  $\{low, high\}$

For each subject we determined the task constraints based on the total number of demonstrations, using our previous approach (Ureche et al., 2015). For each arm we used the state of the end effector:  $\{r_p, r_o, F_e\}$  for the robot and

$\{t_p, t_o, F_f\}$  for the tool to determine the constraints consisting of: the reference frame relative to which the arm moved;  $\nu$  the important variable on each axis (position, force or torque); and a stiffness modulation factor  $\lambda \in [0 \dots 1]$  which weights the contribution of position and force on each axis. Lower stiffness is expected for dimensions where force control should be used and higher for position controlled axes.

A segmentation point was determined by either a change in the reference frame (e.g. when scooping the tool moves relative to the holding arm, but when trashing the motion is done relative to the bowl), or by a change in the variables of interest (i.e. switching from position to force control). Over-segmentation can be caused by the subject changing the control strategy. For each user the value of  $\Psi_a$  indicated the total number of segments determined automatically. We compared this number with hand segmented data as ground truth delimiting the actions shown in Fig. 4.4,  $\Psi_g, g \in 1..3$ . Based on the number of segments we attribute each subject a *skill* value, such that a *skilled* user completes each action in one segment  $N_{\Psi_a} = N_{\Psi_g}$ , while an *unskilled* user shows over segmentation.

The metrics regarding dexterous tool use were computed for each action  $\Psi_g, g \in 1..3$  and for each demonstration. The grasp adaptability  $\vartheta$  was computed according to (de Souza et al., 2015), based on the hand shape, the tactile signature, the position of the tool in hand and the position of the wrist with respect to the robot frame. It represents a measure of how adapted the grasp was to exert forces or torques across the dimensions of interest. Therefore a high  $\vartheta$  is expected along the axis in  $\nu$  where force should have been exerted, and low for the rest. Based on this observation we marked each demonstration as 'low' quality, if  $\vartheta < 0.7$  on a dimension where force control should have been applied, and 'high' quality if the tool was properly used.

## B. Objective task measurements:

- (1) action duration  $t_{\Psi_i}(s), i \in 1..N_{\Psi_g}$
- (2) scooped amount  $w(g)$

The task duration represented the length of each demonstration for each user. The duration of each action  $\Psi_g$ , represents an average over demonstrations as the action set is obtained after segmentation, which requires aligning the demonstration data using Dynamic Time Warping (DTW). The total scooped amount was weighted for each subject at the end of the experiment. An average value was computed given the total number of demonstrations.

## C. Self-rating post-experiment questionnaire:

The questionnaire involved 3 parts evaluating general task aspects, usability and task load. The general evaluation included 4 questions with a 5 level Likert scale answers:

1. How easy was to teach the robot?
2. How familiar were you with the scoop tool?
3. How would you rate your performance?
4. How often do you perform cooking tasks?
5. Which aspect of the task posed most difficulties?  
(maneuvering the robotic arm / wearing the glove / maneuvering the tool)
6. Overall impression (free text)

For assessing usability we employed the SUS test (Brooke, 1996b). For measuring the physical, mental, and temporal task load we used the NASA TLX test (Hart and Staveland, 1988a).

#### D. Video Rating

The video raters were shown the demonstrations ordered per subject. They rated each demonstration individually. After the last demonstration they rated the subject’s overall performance.

The demonstration rating involved 4 questions:

1. Rate the scooped amount: (too little/normal/too much)
2. Did this person perform the task with ease (yes/no)
3. How was the task pace (too slow/normal/too fast)
4. The applied force was: (too little/normal/too much)

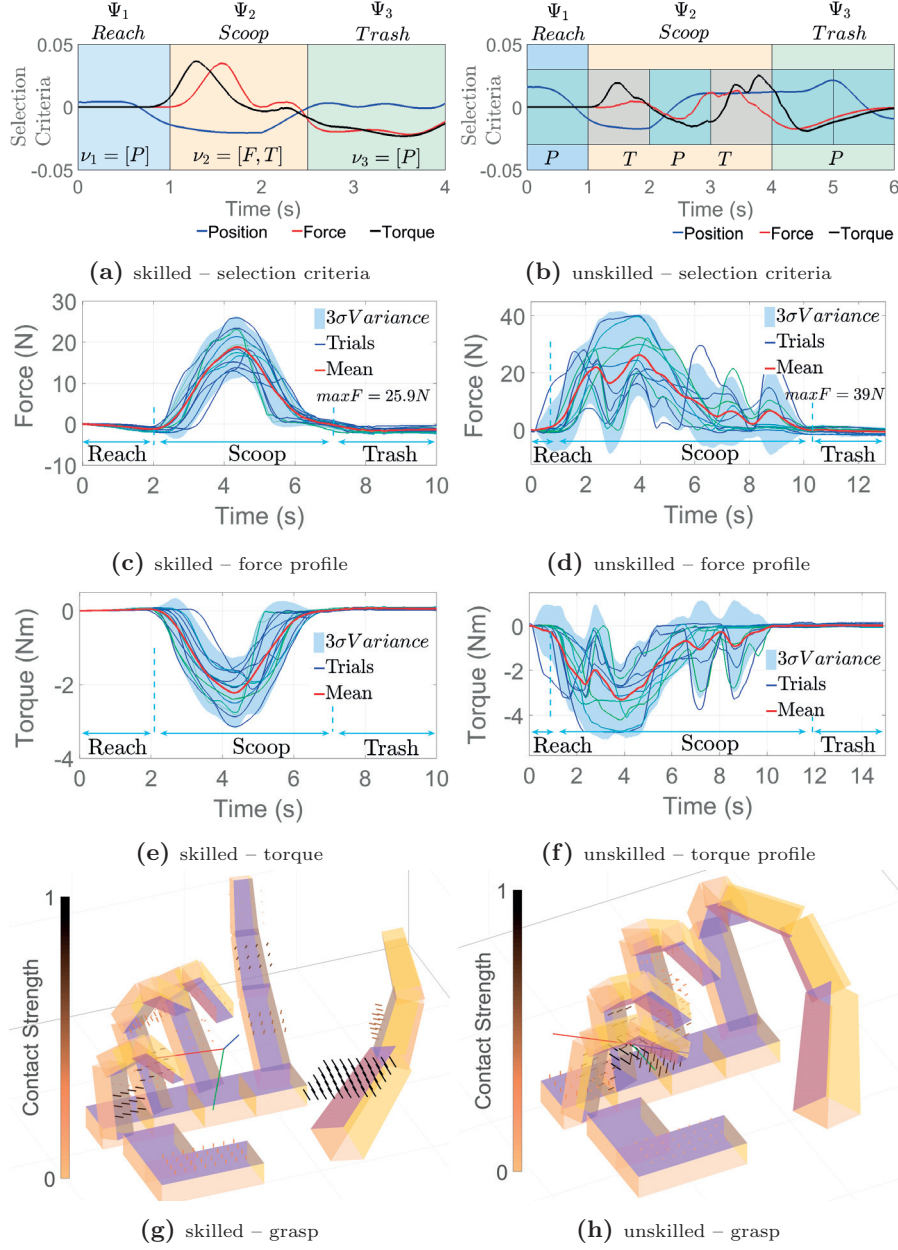
The subject’s overall evaluation comprised 4 questions:

1. Was this subject consistent over trials? (yes/no)
2. Did this subject improve over trials? (yes/no)
3. Could this subject manage the setup well? (yes/no)
4. What was the main issue this subject had: (arm coordination / grasping the tool / direction of movement / none of the above)

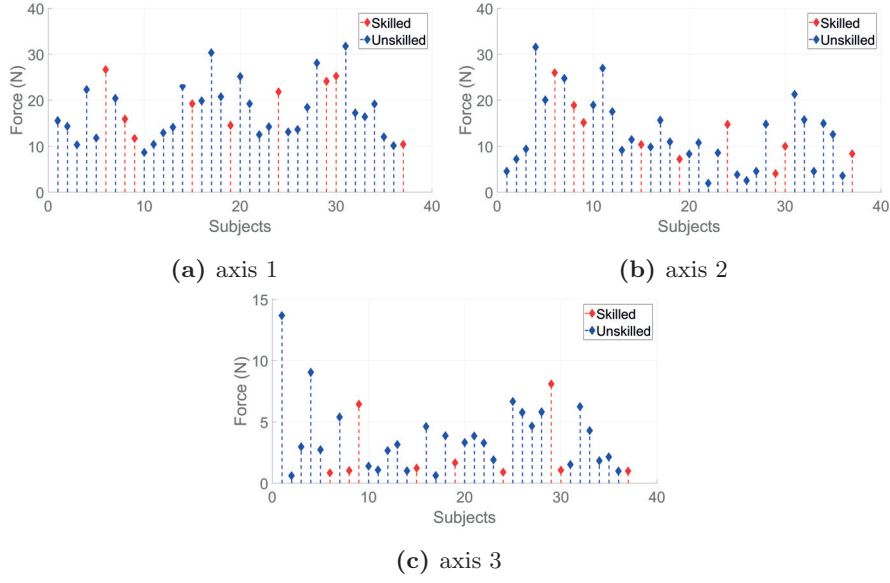
#### 4.4.2 DATA ANALYSIS

---

We analyze the data averaged per users and per demonstration. We compute Anova statistics using as factors the automatically determined skill *auto-skill*, the user self-assessed skill through the questionnaire *self-skill* and the skill assessed through video rating *rated-skill*. Each of the factors mentioned above has two levels: ‘*skilled*’, ‘*unskilled*’. We also compute Spearman correlations.



**Figure 4.6** Comparison between skilled (left column) and unskilled (right column) users. Change of important variables (left column): a skilled user employed position control in *reaching*, and *trashing* actions and force control in *scooping*. An unskilled user changed the control strategy during *scooping*, passing from applying a torque to position control and back to applying a torque; force and torque profiles – columns 2 and 3; hand shape and pressure for a skilled and unskilled user in column 4.



**Figure 4.7** Maximum force applied by skilled and unskilled subjects

#### 4.4.3 RESULTS

---

We analyzed the data for each subject and we present results in relation to the 4 categories of objective metrics, thus addressing the first research question.

#### USER PERFORMANCE BASED ON CONSTRAINTS

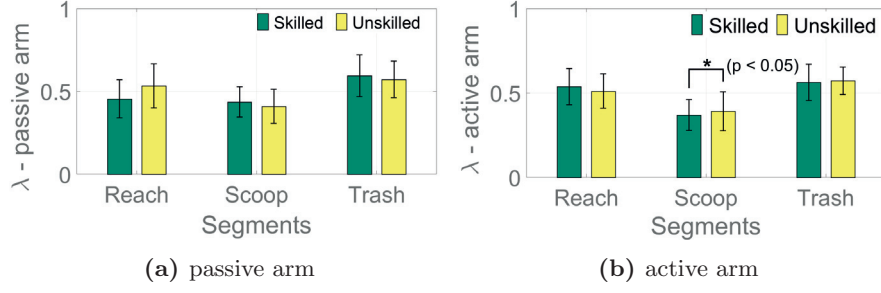
---

##### Action sequence and task constraints

Applying our constraints extraction method (Ureche et al., 2015) showed that each user completed the reaching and trashing actions in one segment ( $\Psi_{1,3}$ ). For these actions the automatic segmentation corresponded with the ground truth ( $N_{\Psi_a} = N_{\Psi_g}$ ). During the scooping action over-segmentation occurred for some subjects. This was caused by changes in the important variables especially along axes where force and torque should have been applied (see Fig. 4.6). Nine out of all demonstrators completed the scooping action in one segment and were marked as *skilled*, cumulating 110 demonstrations, while the other 28 subjects were marked as *unskilled* (for a total of 370 demonstrations).

##### Force applied

Comparing skilled and unskilled users with respect to the force (see Fig. 4.6c vs. Fig. 4.6d) and torque profiles (Fig. 4.6e and Fig. 4.6f) showed that skilled users applied the force for a shorter time, compared to unskilled users, suggesting that their movements were more precise. Unskilled users applied either smaller, or higher forces than skilled users.



**Figure 4.8** Stiffness modulation of skilled and unskilled subjects

Averaged per user skilled users applied  $18.83N \pm 5.99$  on the direction where force was a variable of interest. Some unskilled users (13 out of 28) applied considerably less force  $12.18N \pm 7.79$ , while 15 applied more force  $21.81N \pm 7.67$  (see Fig. 4.7).

For the second axis the average maximum value of force applied by the skilled users was  $12.72N$ , while the unskilled users were divided in two groups: 16 subjects applied less  $12N$  (average value  $6.93N \pm 3.25$ ), while the rest 12 subjects applied  $19.54N \pm 5.68$ .

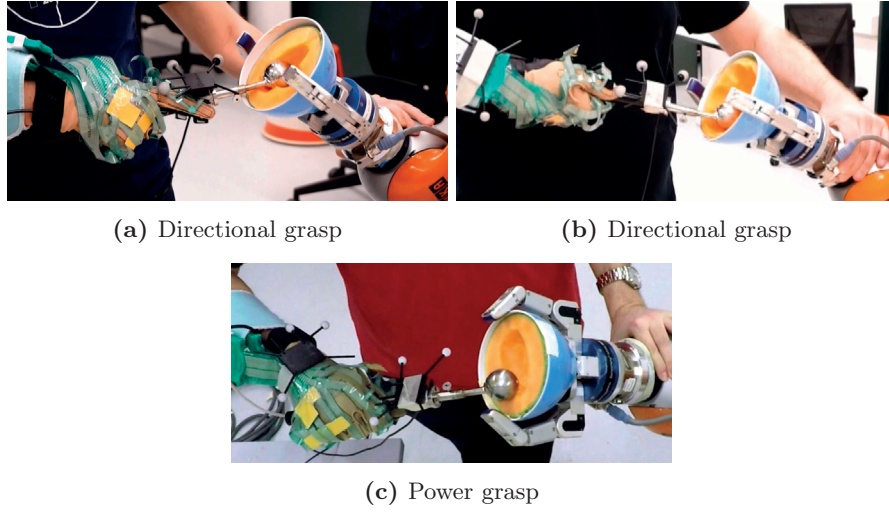
In the case of the 3rd axis where force was not a variable of interest, all of the 9 skilled users applied less than  $10N$ , while 7 out of 9 skilled users applied on average  $1.10N \pm 0.27$ . In the case of unskilled users the maximum value of force applied on this axis was  $13.65N$  and the average was  $3.75N \pm 2.85$ .

Overall the subjects that we marked as skilled were better able to control their force for the important axes and they were not applying too much force. In comparison, the unskilled subjects applied either too much or too little force on the main axis while on the secondary axes they had higher values than the skilled users. The differences are significant across users on all axes:  $F(36, 479) = 22.68$ ,  $p - value < 0.001$ , axis 2:  $F(36, 479) = 43.01$ ,  $p - value < 0.001$ , and for the 3rd axis  $F(36, 479) = 6$ ,  $p - value < 0.001$ . For the computed skill factor (*auto-skill*) the effect was significant only in the case of the axis where force was a variable of interest:  $F(1, 479) = 5.52$ ,  $p - value = 0.019$ .

### Stiffness modulation

Overall for the arm holding the tool the skilled subjects displayed a lower average stiffness during Scooping ( $\bar{\lambda} = 0.37 \pm 0.09$ ) on the axis on which force was becoming an active constraint, compared to unskilled users ( $\bar{\lambda} = 0.39 \pm 0.12$ ), see Fig. 4.8b. Conversely the skilled users were stiffer than unskilled users for one of the remaining axis ( $\bar{\lambda} = 0.41 \pm 0.08$  versus  $\bar{\lambda} = 0.38 \pm 0.08$ ), while for the third axis there was no significant difference ( $\bar{\lambda} = 0.42 \pm 0.10$  versus  $\bar{\lambda} = 0.41 \pm 0.08$ ).

For the holding arm the skilled users were stiffer on the vertical axis ( $\bar{\lambda} = 0.44 \pm 0.09$ ) compared to unskilled users ( $\bar{\lambda} = 0.41 \pm 0.10$ ) Fig. 4.8a. The stiffness of the passive arm was inversely correlated with the scooped weight  $\rho = -0.36$  and directly correlated with the total demos  $\rho = 0.3$ , suggesting



**Figure 4.9** Subjects employed a variety of grasps. The adopted hand shape has an effect on their ability to maneuver the tool. The first two images are examples of directional grasps in which one of the fingers is used to direct the motion: the index (a) and the thumb (b). The first grasp is well suited for this task. The last image shows a power grasp.

that people who were able to properly maneuver the robot arm were capable of scooping more and were willing to provide more demonstrations.

This confirms earlier results as part of acquiring a skill is learning in which direction to apply the correct amount of stiffness (Erden and Billard, 2015).

### Dexterous use of the tool

In this task the force was applied using a tool which could be held by the subject in a dexterous way. The hand shape influenced the ability to maneuver the tool. This determined the pattern of tactile activation and could influence way the force was applied. We related these measures through the grasping quality  $\vartheta$ . For the first 2 task segments this was computed in the reference frame of the robot and represents the adaptability of the hand to applying forces with respect to this frame. Examples of grasps are shown in Fig. 4.9.

For skilled subjects the average value of the grasping quality along the axis where force would be applied (the Y axis of the robot) was  $\vartheta_{skilled} = 0.78 \pm 0.28$ , with just two subjects providing low average values of 0.44 and 0.45 respectively. In the case of unskilled users the average was  $\vartheta_{unskilled} = 1.02 \pm 0.5$ . While the overall value is higher, this group was very diverse, with 6 subjects having an average below 0.5 and 5 subjects having values above 1.5.

In the case of skilled subjects the value of  $\vartheta_{skilled}$  was correlated with applying higher task forces (Spearman  $\rho = 0.45$ ), while for the group of unskilled subjects there is no correlation along this direction ( $\rho = 0.01$ ). This suggests that even when they were holding the tool properly, still there were other factors that were not allowing them to exert proper forces for completing the task.

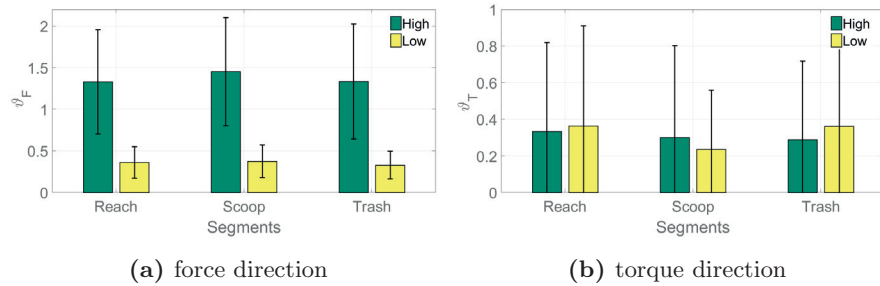
	$\Psi_1 : \text{Reaching}$ $RF_{Robot}$		$\Psi_2 : \text{Scooping}$ $RF_{Robot}$		$\Psi_3 : \text{Trashing}$ $RF_{Bowl}$	
	<b>Skilled</b> mean $\pm$ std	<b>Unskilled</b> mean $\pm$ std	<b>Skilled</b> mean $\pm$ std	<b>Unskilled</b> mean $\pm$ std	<b>Skilled</b> mean $\pm$ std	<b>Unskilled</b> mean $\pm$ std
$\vartheta_x$	$0.83 \pm 0.45$	$0.80 \pm 0.40$	$0.78 \pm 0.36$	$0.92 \pm 0.44$	$0.74 \pm 0.33$	$0.71 \pm 0.44$
$\vartheta_y$	$0.67 \pm 0.29$	$0.82 \pm 0.41$	$0.78 \pm 0.28$	$1.02 \pm 0.50$	$0.86 \pm 0.43$	$0.88 \pm 0.37$
$\vartheta_z$	$0.43 \pm 0.21$	$0.54 \pm 0.30$	$0.43 \pm 0.31$	$0.54 \pm 0.29$	$0.51 \pm 0.17$	$0.49 \pm 0.24$
$\vartheta_{rx}$	$0.47 \pm 0.43$	$0.39 \pm 0.36$	$0.32 \pm 0.26$	$0.25 \pm 0.16$	$0.31 \pm 0.40$	$0.31 \pm 0.28$
$\vartheta_{ry}$	$0.47 \pm 0.45$	$0.33 \pm 0.34$	$0.32 \pm 0.26$	$0.26 \pm 0.24$	$0.32 \pm 0.27$	$0.37 \pm 0.38$
$\vartheta_{rz}$	$0.51 \pm 0.45$	$0.59 \pm 0.68$	$0.33 \pm 0.27$	$0.34 \pm 0.27$	$0.56 \pm 0.53$	$0.66 \pm 0.68$

**Table 4.1** Average values for the grasp adaptability metric per user for each segment of the task, across the directions of the local frame of interest.

For the other axes the values for skilled and unskilled users were:  $\lambda_z = 0.43 \pm 0.31$  for skilled user, and  $\lambda_z = 0.54 \pm 0.29$  for unskilled users. However here for skilled subjects a high value of  $\lambda$  was correlated to scooping lower amounts ( $\rho = -0.37$ ), while for unskilled users there was a positive correlation with the scooped quantity ( $\rho = 0.25$ ) and with applying a high force ( $\rho = 0.52$ ), suggesting that the two groups used different hand shapes. These results are summarized in Table 4.1.

There was little difference in the grasping quality for the *Reaching* and *Scooping* actions, given that the grasp was already preshaped. When passing from *Scooping* to *Trashing* there was a change of reference frame as the scooping arm was no longer moving with respect to the holding arm, but positioning itself with respect to the trashing bowl. Force was no longer a variable of interest, still the motion was similar, moving downwards in the bowl reference frame.

We further analyzed the data per demonstration. We marked a demonstration as 'low' or 'high' quality using a threshold of 0.7 for the grasping quality. Most unskilled subjects provided at least one high quality demonstration. We summarize the effects of the skill and demonstration rating on the computed measures in Table 4.2.



**Figure 4.10** Grasping quality per action, averaged for high and low quality demonstrations

	Skill Rating		Demonstration Rating	
	$F_{stat}$	$p - value$	$F_{stat}$	$p - value$
$\vartheta_{F_x}$	2.53	$p = 0.113$	15.30	$p < 0.001$
$\vartheta_{F_y}$	8.56	$p = 0.004$	514.31	$p < 0.05$
$\vartheta_{F_z}$	2.36	$p = 0.125$	00.03	$p = 0.860$
$\vartheta_{T_x}$	9.71	$p = 0.002$	00.32	$p = 0.570$
$\vartheta_{T_y}$	1.28	$p = 0.259$	12.05	$p < 0.001$
$\vartheta_{T_z}$	0.03	$p = 0.870$	00.27	$p = 0.601$
$max_F$	05.52	$p = 0.019$	0.89	$p = 0.345$
$max_T$	05.58	$p = 0.019$	0.66	$p = 0.418$
$P_{Thumb}$	09.08	$p = 0.003$	00.31	$p = 0.581$
$P_{Index}$	36.06	$p < 0.001$	00.74	$p = 0.390$
$P_{Middle}$	00.28	$p = 0.596$	00.39	$p = 0.535$
$P_{Ring}$	07.65	$p = 0.006$	13.39	$p < 0.001$
$P_{Pinky}$	00.30	$p = 0.583$	08.69	$p = 0.003$
$P_{Palm}$	13.80	$p < 0.001$	05.19	$p = 0.023$
$t_{\Psi_1}$	2.17	$p = 0.150$	09.21	$p = 0.005$
$t_{\Psi_2}$	1.30	$p = 0.263$	11.49	$p = 0.002$
$t_{\Psi_3}$	0.07	$p = 0.792$	03.28	$p = 0.079$

**Table 4.2** Effect of the *skill* (two levels: 'skilled', 'unskilled') and demonstration rating (two levels: 'low', 'high') on the computed metrics per demonstration. We highlight significant interactions ( $p - value < 0.05$ ).

	Low skill	High skill
	mean $\pm$ std	mean $\pm$ std
$\Psi_1 : Reaching$	1.10 $\pm$ 0.33	2.03 $\pm$ 1.86
$\Psi_2 : Scooping$	3.44 $\pm$ 1.24	6.86 $\pm$ 8.88
$\Psi_3 : Trashing$	4.72 $\pm$ 0.81	5.05 $\pm$ 3.68
Total task time	9.51 $\pm$ 2.02	15.16 $\pm$ 12.57

**Table 4.3** Time (in seconds) required per segment and for the whole task, for skilled and unskilled subjects.

### Task timing

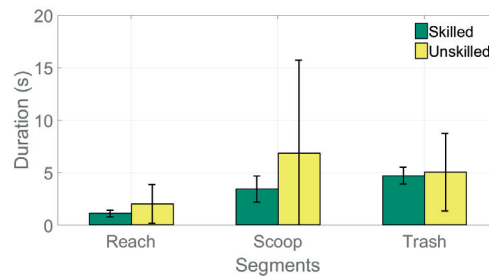
The total task time was lower for skilled subjects ( $9.51s \pm 2.02$ ) compared to unskilled subjects ( $15.15s \pm 12.57$ ). Duration per segment was also different among skilled and unskilled demonstrators (see Table 4.3). All subjects took between 1 and 2 seconds to complete the first reaching action. The duration of the second scooping action constituted the biggest difference among subjects, with an average of  $3.44s \pm 1.24$  for skilled subjects versus  $6.86s \pm 8.88$  for unskilled subjects. The effect of skill on action duration was not significant (see Table 4.2), however there was a significant effect of the demonstration quality on the duration of the reaching and scooping actions (Fig. 4.11).

When considering the skilled and unskilled users separately, the duration of the scooping segment was inversely correlated with the stiffness of the active arm  $\rho = -0.41$  for skilled subjects and  $\rho = -0.13$  for unskilled subjects. Overall, the segment duration was inversely correlated with the grasping quality for the torque direction ( $\rho = -0.34$ ), suggesting that the ability to exert proper torques might contribute to completing the task faster. The segment duration was also correlated with the subjects age  $\rho = 0.31$

### Scooped amount

The average scooped weight was weakly correlated with our assessment of consistency (Spearman  $\rho = 0.20$ ). For consistent subjects the average scooped weight was  $11.49 \pm 3.74g$ , with a minimum of  $7g$  per scoop and a maximum of  $17.9g$  per scoop. For subjects that showed inconsistency the differences in the scooped amount are higher: mean  $9.70 \pm 3.97$ . The minimum scooped amount was  $2.83g$  and the maximum was  $20.36g$  per trial.

The big differences between users with respect to the scooped amount were mostly justified by the fact that there were few subjects who have applied a high force and managed to remove a big amount of the pulp even if they struggled to



**Figure 4.11** Duration per action. Unskilled users took longer time to perform the task than skilled users.

do so. On the contrary there are subjects who tried different strategies, were not very successful with either of them and thus scooped little. Overall the scooped amount was correlated with the force across the direction of interest ( $\rho = 0.52$ ), however this correlation is higher for the subjects showing consistency ( $\rho = 0.61$ ) than for the inconsistent ones ( $\rho = 0.49$ ).

Additionally the scooped amount was inversely correlated with the stiffness across the axis where force was a variable of interest  $\rho = -0.43$ , meaning that subjects able to properly control their stiffness would scoop more. However the scooped quantity was not correlated to the grasping quality with respect to the direction of force. There was also no correlation between the scooped weight and the total task time or the duration of the scooping segment.

---

#### POST-EXPERIMENT QUESTIONNAIRE RESULTS

---

We present the results with respect to the 3 categories from the post-experiment questionnaire.

##### General evaluation

The average self-rating of the participants skill was  $3.51 \pm 0.65$ , on a scale of 1 (very bad) to 5 (very good). No subject rated their performance as very bad, and only one rated as bad. Most subjects rated themselves as medium (18) or good (16) and only two as very good.

Most participants cook often: 18 daily, 17 weekly and 2 monthly. On average the subjects were familiar with the tool ( $3.02 \pm 1.25$ ) on a scale of 1 to 5, with no significant difference between the lower skilled - i.e. levels 1 - 3 of the self assessed skill ( $3.00 \pm 1.20$ ) and highly skilled - levels 4 and 5 ( $3.05 \pm 1.34$ ). A total of 6 subjects had never used the tool before, while 4 were very familiar with it.

Most subjects provided free text impressions: 22 positive, 7 negative, while 8 subjects did not provide comments. Examples are given in Table 4.4. The type of comment was directly correlated with the self assessed skill ( $r = 0.23$ ). Additionally the type of comment has an effect on how easy the participants perceived the teaching procedure to be  $F(1, 36) = 4.76$ ,  $p = 0.01$ . Most negative comments were provided by subjects not familiar with the tool (implicitly nor with the task), and by those reporting problems in maneuvering the tool.

Choosing between the robot arm, glove or tool as the aspect that posed most difficulties was aimed at highlighting possible issues in working with the given setup. Interestingly, the participants rated their performance lowest when they indicated a problem in manipulating the tool (see Fig. 4.12a), suggesting they perceived this as an important aspect of the task, however negative comments are mostly related to maneuvering the robotic arm. Furthermore subjects that had problems with the robot arm or glove also rated the teaching procedure lower ( $2.43 \pm 1.18$ ) than those having difficulties with the tool  $3.20 \pm 1.64$ .

Overall impressions (free text)	
Positive remarks	Negative remarks
"Very easy and quick experiment to perform."	"The glove and the robot arm were limiting the movements, they were not like real moves I would do with my bare hands."
"I felt good being able to teach a robot in such a way."	"It was an easy task to do but harder to do on the robot."
"I was comfortable to use the system."	"Because of the glove, I felt I am doing something alien."
"I felt comfortable and it didn't take too much time."	"I had difficulties using the tool. However I easily controlled the robot."
"Great, I found the robotic arm to be very easy to handle."	"It was easy to learn, but moving the arm was more difficult."
"Actually I believe it would have been more difficult to use my left hand to handle the melon because I could not have the same grip as the robotic arm."	"I found the task a bit unnatural for me as I had to adapt my movements to the constraints imposed by the kinematics of the robot. Moreover, the weight of the sensors wore on my right arm affected my motions."
"The task was generally easy to do but it became even easier when gained more familiarity with the robot."	

**Table 4.4** Samples of free text impressions from the participants

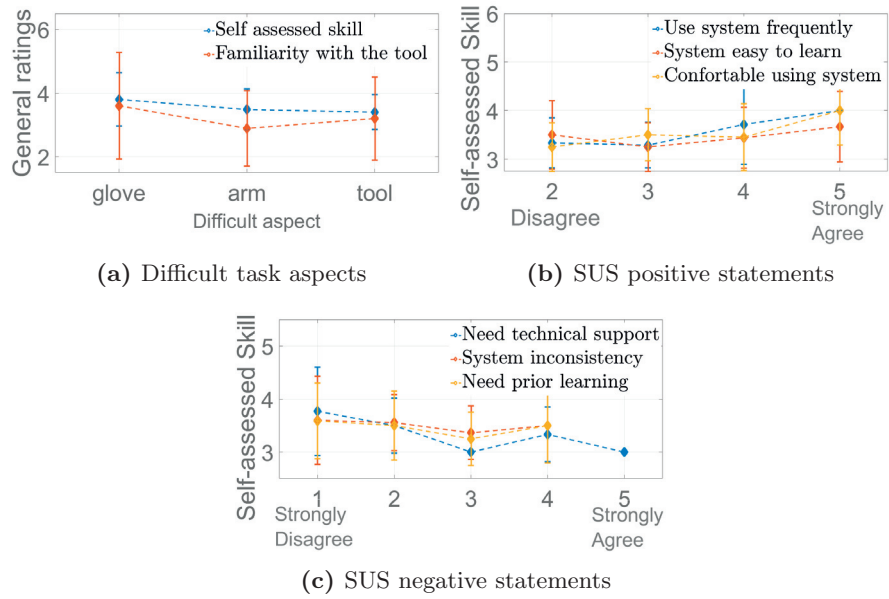
Moreover identifying the use of tool as a difficult aspect was not linked with how familiar participants were with it (Fig. 4.12a).

With respect to the statistics computed per user the gender had a significant effect on the duration of the scooping segment ( $F(1,36) = 4.31$ ,  $p - value = 0.045$ ), with women taking slightly longer to complete the segment than men. Also gender influenced the maximum force applied on the Z axis ( $F(1,36) = 4.32$ ,  $p - value = 0.044$ ), with women applying on average more force than men.

### SUS Ratings

The results of the SUS ratings are summarized in Table 4.5, grouped in two levels of self assessed skill: *low self skill* for levels 1 - 3 , and *high self skill* – levels 4 and 5. We further analyze Spearman correlations between these factors.

Overall the participants rated the system more positively when they also rated their performance higher. As a result a high self-assessed skill was correlated with high levels of the positive statements in the SUS scale (see Fig. 4.12b). Skilled participants were *confident* with the system and found it *easy to use*. These two factors were correlated with being open to using the system more often ( $\rho = 0.56$ ,  $\rho = 0.52$ ) and with providing a positive comment ( $\rho = 0.30$ ,  $\rho = 0.15$ ). Additionally finding the system *easy to use* was highly correlated with thinking that other people would learn to use it quickly ( $\rho = 0.62$ ), but it was inversely correlated with how easy it was to teach ( $\rho = -0.53$ ). However subjects confident in using the system performed the task much faster



**Figure 4.12** General evaluation and comparing SUS ratings for positive and negative statements

	Low skill mean $\pm$ std	High skill mean $\pm$ std
<b>Positive statements scores</b>		
Use system frequently	3.05 $\pm$ 0.70	3.50 $\pm$ 1.04
Easy to use	3.57 $\pm$ 1.01	4.00 $\pm$ 0.84
Well integrated system	3.52 $\pm$ 0.96	3.88 $\pm$ 0.83
Easy to learn to use	4.00 $\pm$ 0.81	4.38 $\pm$ 0.84
Confident using system	3.52 $\pm$ 0.84	3.88 $\pm$ 0.83
<b>Negative statements scores</b>		
System too complex	2.00 $\pm$ 0.81	2.05 $\pm$ 0.80
Need technical support	2.63 $\pm$ 1.34	1.72 $\pm$ 0.95
System inconsistencies	2.10 $\pm$ 0.99	1.88 $\pm$ 0.96
System cumbersome	3.10 $\pm$ 1.04	2.72 $\pm$ 1.48
Need previous knowledge	1.78 $\pm$ 0.91	1.72 $\pm$ 0.82
<b>Total Score</b>	29.31 $\pm$ 9.46	29.77 $\pm$ 9.43

**Table 4.5** Results of the System Usability Evaluation (SUS), averaged for the low and high self-assessed skill ratings.

	Low self skill	High self skill
	mean $\pm$ std	mean $\pm$ std
Mental load	04.94 $\pm$ 3.23	5.61 $\pm$ 3.82
Physical Load	09.57 $\pm$ 5.38	8.16 $\pm$ 4.24
Temporal Load	04.42 $\pm$ 3.84	3.61 $\pm$ 3.44
Success	12.52 $\pm$ 4.67	6.72 $\pm$ 5.51
Effort	08.57 $\pm$ 5.51	5.33 $\pm$ 3.72
Frustration	02.94 $\pm$ 3.06	4.11 $\pm$ 4.48
<b>Total Score</b>	43.00 $\pm$ 25.72	33.55 $\pm$ 25.24

**Table 4.6** Task Load Index (TLX)

(10.30s  $\pm$  2.07) compared to subjects who felt a low level of confidence (25.85s).

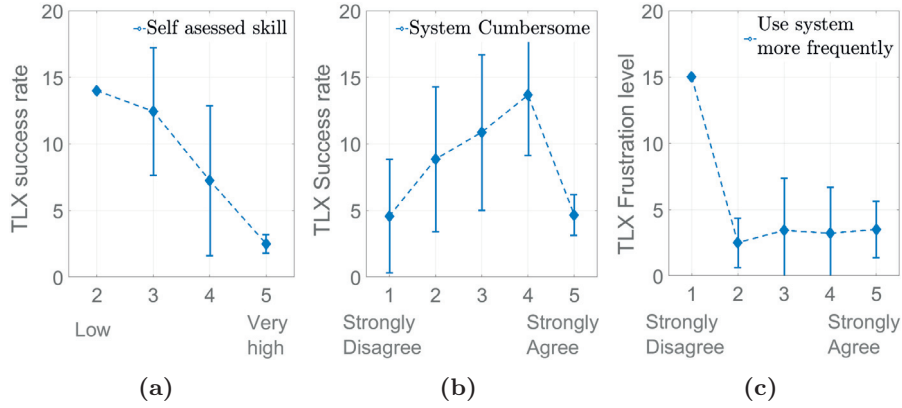
On the contrary a low self assessed skill was linked to rating higher the negative statements in the SUS questionnaire (see Fig. 4.12c). Unskilled participants highlighted the need for technical support and prior learning. Rating the system as being *too complex* was correlated with finding it *inconsistent* ( $\rho = 0.30$ ) and cumbersome ( $\rho = 0.57$ ). Also the wish to use the system more frequently was inversely correlated with rating the system as *inconsistent* ( $\rho = -0.51$ ) and cumbersome ( $\rho = -0.52$ ).

Lastly, subjects that scooped higher amounts were less likely to see the *need for technical support* (Spearman  $\rho = -0.26$ ), or to rate the system as *inconsistent* ( $\rho = -0.30$ ). The scooped amount was also correlated with reporting *confident in using the system* ( $\rho = 0.34$ ), the desire to *use the system more frequently* ( $\rho = 0.36$ ) and only slightly correlated with their *self-skill* assessment ( $\rho = 0.28$ ).

However for the subgroup of subjects who were consistent in the execution, and thus labeled as *skilled* by our automatic analysis (*auto-skill*), the scooped amount was correlated with their *self-skill* rating ( $\rho = 0.60$ ), with being confident with the system ( $\rho = 0.45$ ) and with the desire to use the system more frequently ( $\rho = 0.76$ ). Scooping a higher amount was correlated with perceiving the task pace as higher ( $\rho = 0.67$ ).

### TLX Ratings

The perceived mental load was higher for the subjects who rated themselves as skilled (see Table 4.6). The mental load was inversely correlated with the need of technical feedback ( $\rho = -0.2$ ), which had a significant effect on this metric ( $F(4, 32) = 4.19$ ,  $p < 0.01$ ). The lower skilled subjects perceived a higher physical and temporal load than the skilled subjects. The rating on the teaching procedure had an impact on the perceived temporal demand ( $F(4, 32) = 4.87$ ,  $p = 0.01$ ), such that the subjects who considered demonstrating the task was easy also perceived the task pace higher ( $\rho = 0.29$ ). Perceiving a higher physical



**Figure 4.13** Influence of SUS factors on TLX ratings

load was correlated with scooping a higher amount ( $\rho = 0.23$ ).

Surprisingly the low skilled participants (*self-skill* rating) indicated a higher success rate in achieving what they were asked to do (TLX success rate) compared to skilled subjects. This happened despite rating their own performance as low ( $F(3, 33) = 4.48, p = 0.01$ ), the two being inversely correlated ( $\rho = -0.51$ ), see Fig. 4.13a. The more complex they perceived the system to be the higher they rated their success rate ( $F(4, 32) = 4.91, p < 0.01$ ), see Fig. 4.13b.

Lastly the lower skilled subjects perceived their effort as higher than skilled subjects, but their frustration level was lower. The frustration level was linked to being open to use system more frequently ( $F(4, 32) = 2.90, p < 0.05$ ), see Fig. 4.13c.

## VIDEO RATING RESULTS

### Ratings per user

After watching all the demonstrations done by a subject the raters were asked to perform an overall assessment of that particular subject with respect to 4 aspects: consistency in execution over trials, improvement over trials, ability to manage the robotic setup and the most common issue during the execution (either of the following: arm coordination, tool grasping, direction of movement or no issue). Please see Metrics D in Section 4.4.1 for the exact questions. Table 4.7 summarizes the Cohen's Kappa agreement rates between the raters.

Overall the raters agreed on whether the subject was consistent (kappa = 0.78). All the subjects marked by our approach as skilled were also marked by rater 1 as consistent. In the case of rater 2 one such subject was marked as unskilled. However for the subjects marked as unskilled by our approach, only one was marked as inconsistent by rater 1 and 7 by rater 2. Their agreement rate for unskilled subjects was 0.75.

	Cohen's Kappa
Consistency over trials	0.78
Improvement over trials	0.59
Ability to manage the setup	0.72
Issues in arm coordination	0.75
Issues in tool grasping	0.78
Issues in movement	0.75
No issue	0.56

**Table 4.7** Agreement rate for subject rating. All values are above 0.5.

	<i>rated-skill</i>	
	$F_{stat}$	$p - value$
<i>improve over trials</i>	1.86	$p = 0.17$
<i>manage setup</i>	5.58	$p < 0.001$
<i>grasp problems</i>	0.81	$p = 0.44$
<i>movement problems</i>	2.31	$p = 0.11$

**Table 4.8** Effect of the *rated-skill* on the video ratings per user. We highlight significant interactions.

We considered a subject as consistent when marked by both raters as such and correlated these values with our metric of skill (auto-skill) (Spearman correlation). The raters showed a medium correlation of 0.58 for 16 subjects, however for the first 11 subjects and the last 10 the correlation was low. This was expected as the raters required time to adapt to different performances and understand which aspects could vary in the task, while in the end it was mostly due to the raters fatigue.

The consistency in execution (*rated - skill*) was also inversely correlated with the total task time ( $\rho = -0.22$ ) suggesting that a skilled person finishes the task faster. There was also an inverse correlation ( $\rho = -0.42$ ) with the maximum force applied by the users on an axis on which force was not a variable of interest, showing that the video raters could correctly identify this aspect as an aspect of successful execution. Lastly there was a direct correlation with the scooped weight ( $\rho = 0.30$ ), and with several factors from the post-experiment questionnaire: confidence in using the system ( $\rho = 0.24$ ), and how easy it was to teach the robot ( $\rho = 0.21$ ).

The ability to improve over trials was correlated with the scooped weight ( $\rho = 0.27$ ) and also with the grasp adaptability to applying torques ( $\rho = 0.30$ ). The ability to manage the setup was correlated with several of the subjects answers to the questionnaire. There was a direct correlation with rating the

	Cohen's Kappa
Scooped amount	0.62
Task performed with ease	0.77
Task pace	0.73
Applied force	0.73

**Table 4.9** Agreement rate for demonstration rating. All values are above 0.5.

system as being easy to use ( $\rho = 0.24$ ) and with the desire to use the system more frequently ( $\rho = 0.30$ ). It was also inversely correlated with the TLX mental demand ( $\rho = -0.22$ ), physical demand ( $\rho = -0.23$ ), TLX task pace ( $\rho = -0.33$ ) and TLX effort ( $\rho = -0.22$ ), indicating an agreement between the way the subjects and the raters perceive the task performance. Likewise the identified problems in grasping by the video raters are inversely correlated with the TLX physical demand as indicated by the subjects ( $\rho = -0.38$ ), while problems in movement are inversely correlated with the TLX mental demand ( $\rho = -0.21$ ).

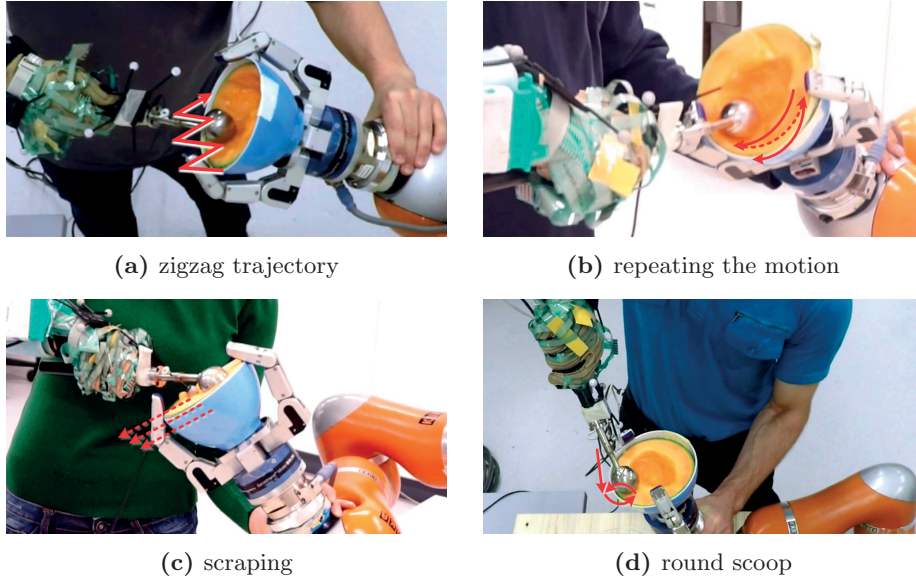
Overall the raters showcased good agreement rates between themselves, however their ratings are only weakly to medium correlated with our sensor metrics and with the subjects self assessment through the questionnaire.

#### Ratings per demonstration

For each demonstration the raters had to assess 4 factors: the scooped amount, if the person performed the task with ease, the task pace, and the force applied. Overall their agreement rates (summarized in Table 4.9) were above 0.5, with the highest value for assessing whether the task was performed with ease. This is related to our extraction of task constraints, as struggling to perform the task introduces variability and leads to over-segmentation. Conversely, consistency leads to *fluency* in execution.

We further assessed how these factors relate to the corresponding sensor metrics. The estimated scooped amount was slightly correlated with the measured amount (Spearman  $\rho = 0.25$ ) and also with the maximum force and torque ( $\rho = 0.28$  and  $0.25$  respectively). Also the estimated scooped weight was inversely correlated with the number of segments ( $\rho = -0.23$ ) suggesting that a smooth execution also could occasionally lead to scooping higher amounts.

The force estimated by the raters was not correlated with the maximum task force ( $\rho = 0.14$ ). The estimated task pace per demonstration was inversely correlated with the average task duration ( $\rho = -0.25$ ).



**Figure 4.14** Motion strategies adopted by unskilled users. In the first 3 cases subjects adjusted their trajectory as they were applying too little force. In the last case the subject applied too much force as he consistently positioned the scoop pressing down with the tip, rather than with the cutting edge.

## 4.5 Possible causes of poor performance

---

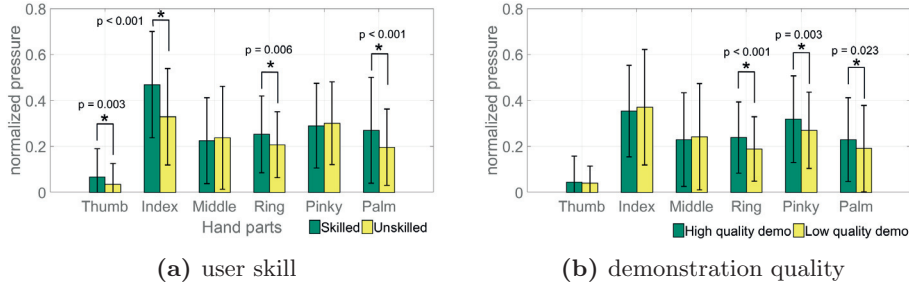
The metrics computed above can help a robot characterize skilled users through a notion of consistency in execution. This aspect is related to users able to respect the task constraints when exerting forces on an object and manipulating tools. This information can help a robot distinguish between poor and good performance. We further identify traits of unskilled demonstrators and strategies for task adaptation by performing a qualitative evaluation.

### 4.5.1 MOTION STRATEGY

---

One aspect of the adopted motion strategies is the coordination between the arms. While skilled users typically move their two arms to reach a point above the trashing bowl, unskilled subjects either keep the holding arm stationary above the bowl and only move their active arm, either the inverse (active arm remains always on top of the bowl, performing small movements while the passive arm moves aside to free space when necessary).

A second aspect related to motion strategy is the trajectory employed when applying a force. In Fig. 4.14 we illustrate various strategies adopted by unskilled users. In the first and second case (Fig. 4.14a and 4.14b) the subjects applied too little force and therefore had to modify their trajectories to be able to scoop, either by moving sideways or by repeating the motion. In the third



**Figure 4.15** Comparing normalized pressure values on each hand part, for two factors: subjects skill and the demonstration rating.

case (Fig. 4.14c) the subject performed a linear motion outwards, rather than a scooping motion. This was mostly due to not being able to adapt the stiffness of the passive arm (which on average was low for this subject  $\lambda = 0.40 \pm 0.06$ ) while the active arm was applying a force. With this strategy instead of adapting to a vertical force, the arm has maintain the position while resisting a torque.

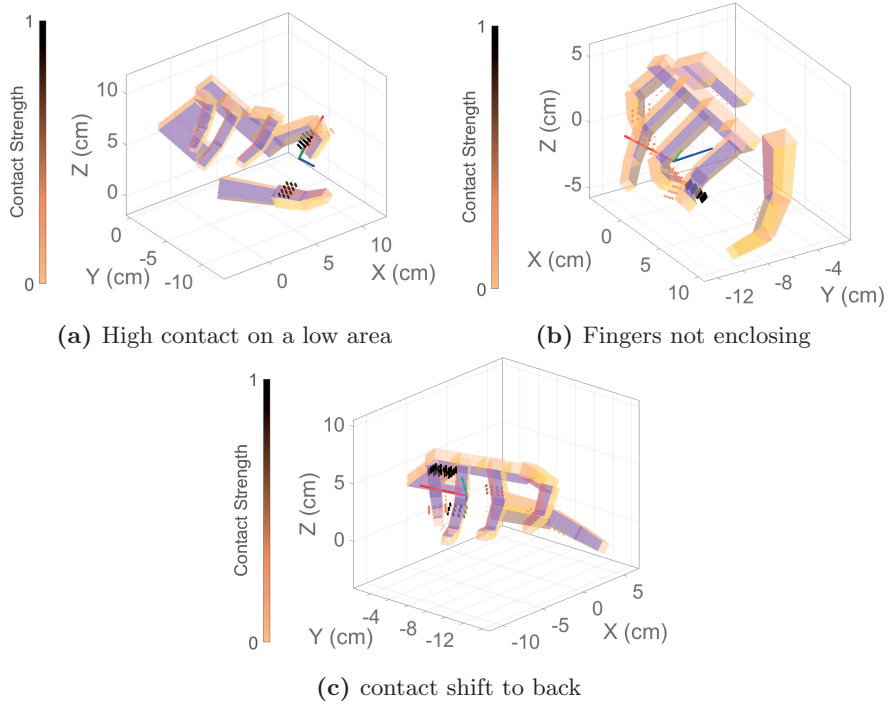
The last aspect of the motion strategy is related to the approach direction. In the last image (Fig. 4.14d) the subject approaches the mellon from above. The task became harder starting with this tool position and orientation as it required too much force. The subject applied a force of  $23.05N$  and a torque of  $1.3Nm$ , while his grasping quality related to the torque dimension was very low  $\vartheta_T = 0.225$ .

#### 4.5.2 TOOL USE IN RELATION TO THE TASK CONSTRAINTS

Over demonstrations, for skilled subjects the force applied on the direction of interest was correlated with the pressure on the palm (Spearman  $\rho = 0.50$ ), thumb ( $\rho = 0.37$ ) and middle fingers ( $\rho = 0.27$ ). This showed a clear tendency to use these hand parts when manipulating the tool since there is no correlation with the pressure on the ring ( $\rho = 0.04$ ) and pinky fingers ( $\rho = -0.24$ ). However the pressure on the ring and pinky are correlated with applying torques ( $\rho = 0.49$ ,  $\rho = 0.67$ ). For the index finger, the pressure is correlated with the maximum vertical force applied on the mellon ( $\rho = 0.34$ ).

In the case of unskilled subjects the correlations were much weaker:  $\rho = 0.14$  for the palm and  $\rho = 0.12$  for the middle, while the vertical force was not correlated with the pressure on the index finger  $\rho = -0.17$ . However the highest correlation values between the pressure and force were found for applying forces on the Y axis: index finger  $\rho = 0.48$ , ring  $\rho = 0.37$ , and pinky  $\rho = 0.54$ .

In Fig. 4.15a we showcase the difference in the applied pressure for the skilled and unskilled subjects for each hand part. The effect of the user skill was significant for the following areas: thumb ( $F(1, 480) = 9.08$ ,  $p - value = 0.003$ ); index ( $F(1, 480) = 36.06$ ,  $p - value < 0.001$ ); ring ( $F(1, 480) = 7.65$ ,  $p - value = 0.006$ ); and palm ( $F(1, 480) = 13.80$ ,  $p - value < 0.001$ ).



**Figure 4.16** Common ways of misusing the tool among unskilled demonstrators.

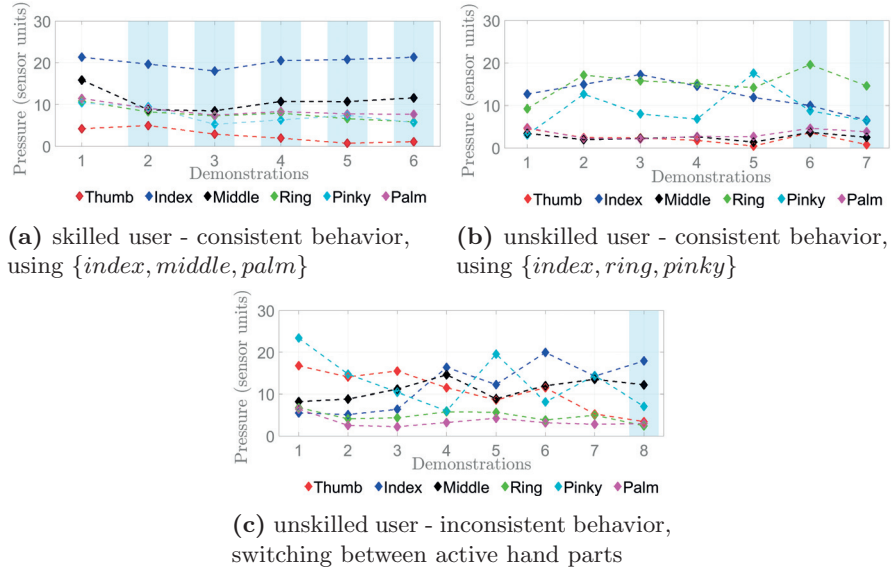
For the demonstration quality factor (Fig. 4.15b), significant differences were obtained for the pressure on the ring ( $F(1, 480) = 13.39$ ,  $p - value < 0.001$ ); pinky ( $F(1, 480) = 8.69$ ,  $p - value = 0.003$ ); and palm ( $F(1, 480) = 5.19$ ,  $p - value = 0.023$ ).

Overall skilled and unskilled subjects used different strategies in manipulating the tool, and they relied on using different parts of the hand.

### 4.5.3 CONTACT LOCALIZATION

The grasping quality was computed based on the hand shape, tactile signature and hand localization with respect to the object on which force should be exerted. Here we evaluate these aspects separately, aiming to find patterns that lead to improper usage of the tool.

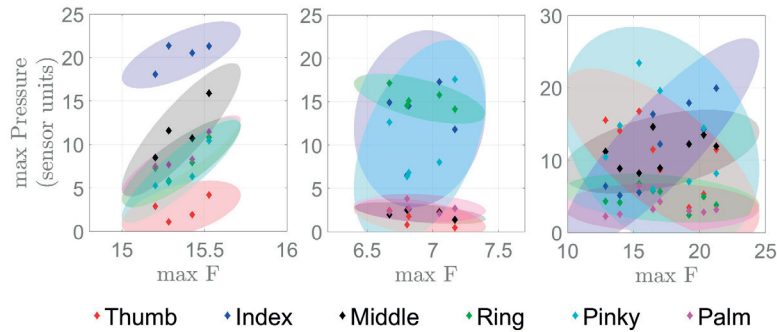
Analyzing the demonstrations with a 'low' rating we observed 3 common types of holding the tool which led to low grasping qualities, also illustrated in Fig. 4.16. In the first case (Fig. 4.16a) the demonstrator employed a pinch grasp, with the contact localized on the thumb and index. Exerting a high pressure on a low area (no contact on the palm and little contact on other phalanges), made it hard to maintain a good grip on the tool. In the second case (Fig. 4.16b) the demonstrator employed a power grasp, however not all the fingers were properly enclosed around the tool. In the last type of common grasp (shown in Fig. 4.16c) the user shifted the maximum contact to the palm,



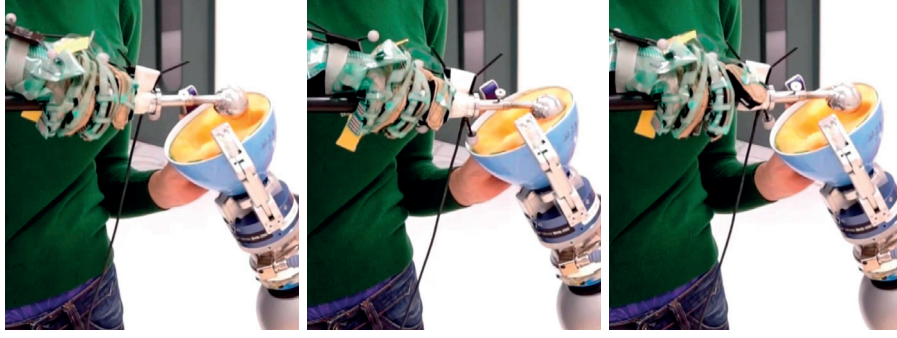
**Figure 4.17** Averaged pressure across demonstrations for each hand part. The contact localization across trials was used to compare the consistency of skilled and unskilled users. The pressure was averaged per fingers and palm during the scooping segment. We highlighted the trials rated as 'high' quality

pinky and ring fingers, while the thumb, index and middle have little to no contact. This type of grasp was not suitable for applying the required torque.

Most skilled users preferred a grasp that favored the distribution of pressure across hand parts while the maximum contact was applied on the index, middle and palm and they were consistent across trials (such as Fig. 4.17a). In unskilled users two behaviors were often encountered: either they preferred exerting more force on the index, ring, and pinky (leading to the tool misuse shown in Fig. 4.16c) and this behavior was consistent across trials (Fig. 4.17b); either the way they held the tool and thus the tactile signature varied between trials (Fig. 4.17c). In the first two cases these hand parts were also used when applying the



**Figure 4.18** Pressure on each finger corresponding to the maximum applied force. First two subjects show consistency, while the last subject changed the strategy in using the tool.



**Figure 4.19** Re-grasping during the scooping action.

maximum force (see Fig. 4.17), but not always for the last case. In Fig. 4.18 we show the pressure on each hand part corresponding to the maximum applied force for 3 different subjects. Some were consistent across trials, while others switched the active hand parts trying out different grasps.

#### 4.5.4 RE-GRASPING

---

Subjects often employ re-grasping as a strategy of dealing with poor performance. Re-grasping can occur during an action, when switching to a different action or between trials. We analyze these cases separately.

##### **Re-grasping during an action**

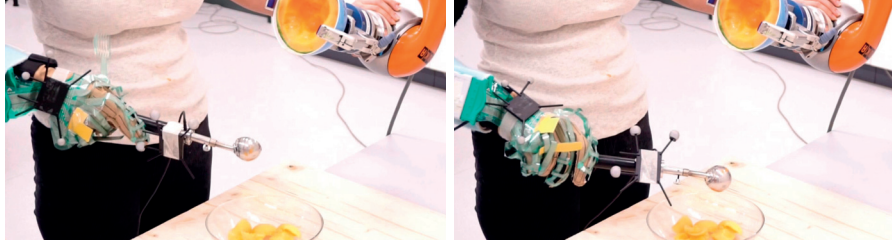
Fig. 4.19 shows an example of re-grasping while scooping. This behavior was observed often in 3 subjects and it was observed in situations when the tool got stuck while the subject was applying low torques and holding the tool loosely. Therefore the subject had to re-grasp to continue the task. In this particular case the applied torque was very low ( $0.07Nm$ ). Even if changing the grasp was an indication of adaptation to the task, all cases of re-grasping during an action were marked as low performance by the video raters, as this behavior was interpreted as hesitation.

##### **Re-grasping between actions**

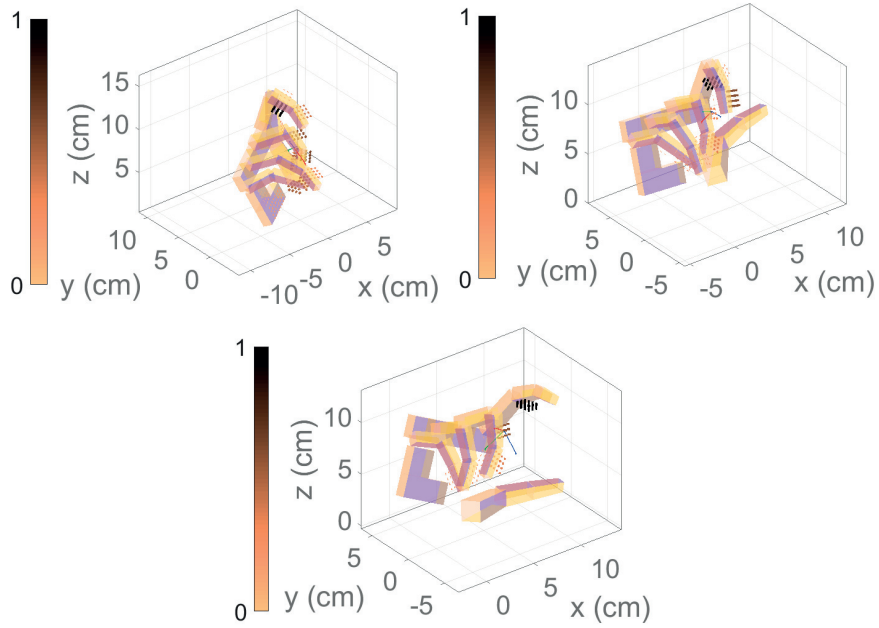
In Fig. 4.20 we show an example of a subject switching from a directional grasp while scooping to a power grasp while trashing. This happened as the requirements of each action are different. The first grasp allowed the subject to apply high force in the mellon reference frame ( $\vartheta_F = 0.96$ ). In the trashing action the motion was performed with respect to the reference frame of the bowl, and changing the grasp facilitates in this case the vertical motion ( $\vartheta = 1.13$ ).

##### **Re-grasping between trials**

Most subjects changed the position of the tool in hand while preparing to



**Figure 4.20** Re-grasping between actions in the same demonstration. The subject switches from a directional grasp to a power grasp.

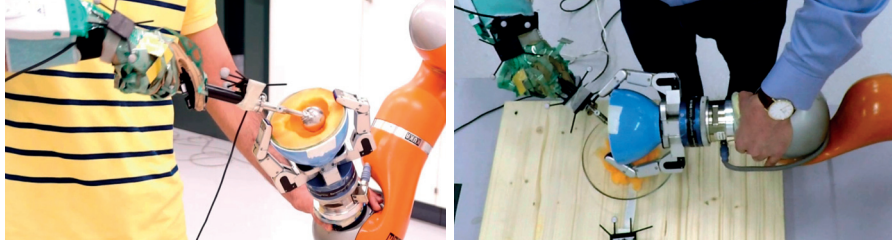


**Figure 4.21** Re-grasping trials as a form of adaptation to the task constraints. The subject starts by using a power grasp (left), switches to an intermediary grasp (center), and to a directional grasp (right).

start a new trial. This was correlated with an increase in performance over trials, and with marking a subject as having improved by the video raters. In Fig. 4.21 we show the change in hand shape for the same subject in different trials. The subject managed to increase his grasping quality on both the force ( $\vartheta_F = 0.55/0.64/0.70$ ) and the torque dimension ( $\vartheta_T = 0.12/0.27/0.44$ ). Video raters also marked this subject as having improved over trials.

#### 4.5.5 VISUAL FEEDBACK

The way the subjects coordinated their arms also impacted their ability to use visual feedback and thus see what they were scooping. In Fig. 4.22 we compare a skilled subject who always kept the bowl upwards and was able to cover the entire surface efficiently while scooping, with a subject holding



**Figure 4.22** Comparison between a subject who used visual feedback with one who did not (i.e. the holding arm was pointing down and the subject had to rely only on kinesthetic information).

the bowl downwards and thus having no visual feedback. This difference was reflected in the quantity being scooped (160g vs. 99g), despite applying similar amount of force ( $\sim 14N$  for both subjects). The video raters rated the first subject as good performance and the second as very low performance, despite their subjective ratings being similar.

## 4.6 Robot performance during task execution

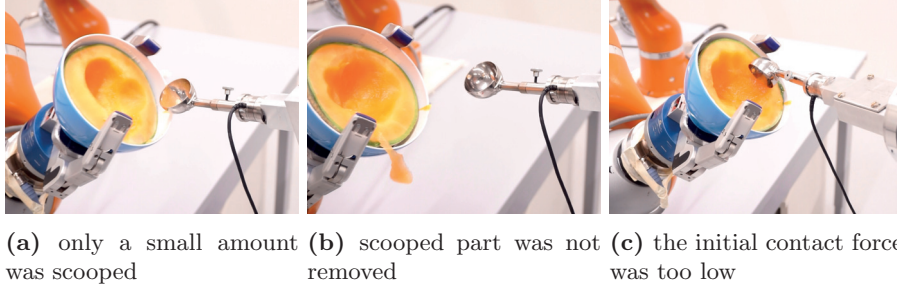
In this section, we address our second research question, by evaluating robot performance during task execution in 3 cases:

1. learning the task from an unskilled user;
2. learning from a skilled user
3. learning selectively from good demonstrations regardless of user skill

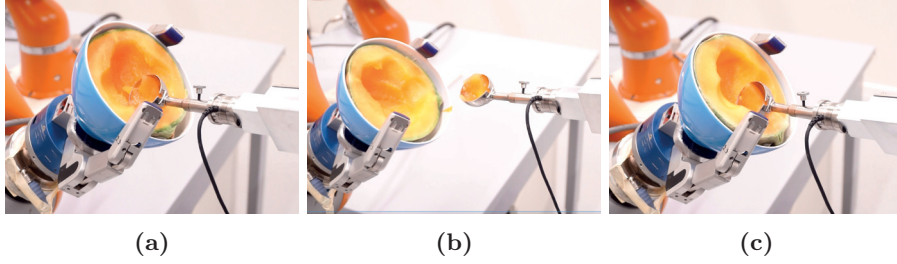
We encoded the task using time independent models of the end effector motion, cartesian force and stiffness. For the trajectories we used a coupled dynamical systems approach (Shukla and Billard, 2012). We encoded the position and orientation of each end effector as a first order dynamical system of the form  $\dot{x} = f(x)$ . The function  $f$  is estimated using a Gaussian Mixture Model (GMM). The force profiles are learned only for the directions in which force is a variable of interest and are encoded in a GMM as a function of position. Similarly we use a GMM encoding for the stiffness as a function of end effector position (Ureche et al., 2015).

For quantifying the robot’s success rate while executing the task we measured the scooped quantity. We marked a trial as successful if the robot was able to scoop at least  $2g$  and to completely remove the scooped part. For each case we performed the scoops on a new melon which we rotated between the trials.

For the first case we have performed 10 trials, out of which just 4 were successful. The total scooped amount was  $11g$ . In 4 of the trials nothing was scooped; in 2 of the trials the scooped amount was about  $1g$ , while in other 4 trials the scooped amount was between 2 and  $4g$ . The reasons of failure



**Figure 4.23** Failure illustration when using the force-torque encoding from the *unskilled* user.



**Figure 4.24** We show snapshots of the robot’s performance when learning from a *skilled* user: images (a) and (b) and when learning only from good demonstrations (c).

are illustrated in Fig. 4.23. They can be summarized as: applying a low initial contact force which meant that the scoop did not go very deep inside the mellon, especially when scooping closer to the skin; applying a low force towards the end of the motion which resulted in the scooped piece not being completely removed; lastly, scooping small amounts of about 1g was also considered a failed trial.

In the second case we performed 10 trials with data from a *skilled* user. The total scooped amount was 46g, averaging  $4.6 \pm 2.1g$  per trial. In the last case we used data only from demonstrations marked as high quality. We performed 5 trials, and scooped a total amount of 35g, averaging  $7 \pm 2.23g$  per trial. Overall the performance when using data from the unskilled user was significantly lower than in the following two cases. Conversely using data from good demonstrations resulted in proper execution (see Fig. 4.24) and Table 4.10.

These results answer our second research question, namely that the robot’s ability to execute the task is correlated with the user’s ability to provide good demonstrations.

## 4.7 Performance estimation based on hand state

---

As emphasized in the previous section, performance in manipulation tasks depends considerably on respecting the task constraints. Consequently holding

Task model	Trials	Success rate (%)	Total weight (g)	Average weight (g)
unskilled user	10	40	11	$2.1 \pm 1.2$
skilled user	10	100	46	$4.6 \pm 2.1$
selective learning	5	100	35	$7 \pm 2.23$

**Table 4.10** Robot performance in the 3 execution cases. While both the second and third case aimed a high success rate, the best result relative to the scooped weight per trial was obtained when using models learned from good demonstrations (highlighted).

the tool in a way that allows easily applying forces and torques across the correct directions results in good performance. This confirms previous results showing that the grasp on the tool is always task dependent (El-Khoury et al., 2015).

We thus focus on classifying the hand states (consisting of finger joint angles, pressure on frontal and side patches) seen during the demonstrations. Given that the grasp changes dynamically throughout the task (by enclosing on the tool, re-grasping, or changing the action), for each demonstration we take as datapoints the sampled hand state at every half a second during the reaching and scooping actions ( $\Psi_1$  and  $\Psi_2$ )<sup>3</sup>, aiming a total of 27880 points. We label the demonstration data as “good” or “bad performance” by discretizing the grasping quality using a threshold of 0.8.

We compare the performance of two classification methods: support vector machine (SVM), and a feedforward neural network (NN) (see Table 4.11). We trained each classifier separately for four cases, using only:

- (1) pressure on the frontal patches (18 features);
- (2) pressure on the front and side patches (36 features);
- (3) finger joint angles (23 features);
- (4) and all features combined (59 total features)

Classification in all cases was above chance level (50%). We further discuss particularities of each method.

#### 4.7.1 CLASSIFICATION WITH SVM

We trained a support vector machine (SVM), using an RBF kernel function. Using a training–testing ratio of 20/80 we obtained an accuracy of: 83.94% on training data vs. 73.56 on the testing set for case (1); 92.14% vs. 78.15% for

<sup>3</sup>We don’t include data from the last action  $\Psi_3$  trashing, as the constraints change: the reference frame for the human arm is given by the trashing bowl, and the arm is performing a reaching motion. The grasping quality in this case is computed with respect to the bowl frame and is thus irrelevant for the force controlled action.

Features	Feedforward neural network		Support Vector Machine	
	Training set	Testing set	Training set	Testing set
Tactile front patches	86.96	71.39	83.59	76.35
Front & side patches	94.33	75.67	92.83	81.94
Finger joint angles	79.41	75.05	98.56	94.72
All features combined	98.43	83.23	99.54	89.56

**Table 4.11** Comparison of the classification performance (%) obtained using a feedforward neural network and SVM. We highlight the best obtained values.

NN	Neurons per layer (L)				Performance (%)	
	L1	L2	L3	L4	Train set	Test set
2 layers	60	2			98	83
3 layers	60	10	2		95	80
4 layers	60	10	30	2	95	81

**Table 4.12** Performance using various structures for the neural network. We highlight the best obtained values.

case (2); 98.45% vs. 92.14% for case (3); and 99.65% vs. 84.28 for case (4). Increasing the training–testing ratio to 30/70 (8364 data points vs. 19516 data points) increased accuracy as follows: 83.68% on training data vs. 74.40% on testing data for case (1); 92.54% vs. 79.41% in case (2); 98.47% vs. 92.96% for case (3); 99.56% vs. 85.90% for case (4). We obtained the best results using 40% training data and 60% testing data, see Table 4.11. Further increasing the training–testing ratio did not improve significantly the results. The training time was 34.72s for case (1), 15.51s for case (2), 26.25s for case (3) and 114.95s for case (4).

Frontal pressure alone was not enough to discriminate between grasps. The best accuracy on testing set in this case was 76.35%, and increased when adding the information on the lateral patches placed on the side of the fingers (75.67%). The hand shape given by the finger joint angles was the most informative when deciding if a grasp was adapted to the task (94.72% accuracy on testing set). The best performance obtained when including all hand features was 89.56%.

#### 4.7.2 CLASSIFICATION WITH FEEDFORWARD NEURAL NETWORK

Implementation was done using Google Tensor Flow (Abadi et al., 2016). We have tested several configurations with different numbers of neurons in each layer and different activation functions, both linear and non-linear.

**Number of layers** With a data ratio of 30/70 we obtained the best performance with 2 layers (98% on training data and 83% on testing data). For a data ratio of 50/50 the best performance was obtained with 4 layers (95% on training data and 85% on testing data). For a data ratio of 60/40 we obtained 93% on training data and 83% on testing data. Adding more data in the training set did not significantly improve accuracy. Also adding more than 4 layers did not improve accuracy. For 5 and 6 layers networks we obtained 94% performance on training data and 80% on testing data.

**Number of neurons per layer** The configurations that led to the best results are presented in Table 4.12. In all cases at the output we had 2 neurons.

**Activation function** We tested different non-linear activation functions, *ReLU*, *softmax* and *softsign*. We observed consistently better results when the input and output layers were using the *sigsign* function. This can be explained by the cut-off nature of this function. This enabled a clear separation between active and non-active patches and, on the output, between the active and passive neuron. For each combination of parameters we ran 10000 iterations and the model converged in each case. Overall the SVM performed slightly better (about 5% increase in accuracy) than the feedforward neural network. For both methods similar trends were observed across training cases. Classification rate was lowest when including only tactile data and increased when all features were taken into account.

The results presented in this section answer our last research question, namely that the hand state can be used to estimate user performance.

## 4.8 Discussion

---

Our hypothesis was only partially supported by our results, and specifically by the results of video rating performed by naive users. Even if in sports sciences consistency in performance is considered an indicator of skill (McMorris, 2004), this proved difficult to assess.

In our case consistency was not directly linked to an external measurement, such as the scooped amount. Moreover this notion of consistency was also not easy to assess by video rating. This was due to the fact that no specific set of rules were used to define "skilled performance" or "consistency". For the first set of raters the concept of "skill" was left ambiguous, while for the second group of raters assessing "consistency" also proved problematic as they were not aware of the sources of variability in the task. Therefore their rating was very subjective and could not easily relate to our metric.

On the contrary, in sports, there are specific, well defined standards that should be met by a skilled performance. These are well known by experts

and often unfamiliar to novices or naive viewers. For example complex figure skating routines might appear flawless to an unaccustomed person, but very small mistakes, sometimes imperceptible to an untrained judge, can lead to very different scores given by the official judges.

Lastly the task addressed in this experiment was very common, despite requiring arm coordination and exerting forces. This increased the raters tolerance in their assessment, compared to a precision task that requires a very exact assessment.

In summary this method would be more suitable as a qualitative performance assessment than a quantitative one. We further summarize the advantages of the proposed approach and discuss limitations and future work.

#### 4.8.1 ADVANTAGES

---

The proposed method gives the robot the ability to quantify human performance during task demonstrations. This was shown to improve the teaching outcome by selectively learning from good demonstrations of different users. While in this case we used a ground truth pre-segmented data for comparison, the common features of the task remain constant across skilled users. The assessment can be performed automatically with respect to the task constraints. This represents an objective task-specific evaluation, unlike using metrics pre-defined by the user. Therefore the method is generic and applicable to a variety of manipulation tasks. Moreover it provides insight into the humans behavior during manipulation tasks.

Additionally given enough examples the robot can estimate the expected quality of user performance continuously, by monitoring the hand state. Since the performance estimation can be done as soon as the tool is in hand (i.e. even before a force is actually applied in the task) makes it suitable for estimating if the user is ready to start the task. This can be applied when executing a task collaboratively, when training a new user on performing the task, or in cases when the robot needs to become assistive. The approach has the potential to make the interaction more reliable and predictable for the human. For example a robot can increase its stiffness in response to a human's intention to apply a force, before actually doing so.

#### 4.8.2 LIMITATIONS

---

We further discuss several limitations in our approach.

##### **Task Modeling**

Firstly, in our work we only focused on the robot performance achieved when using a certain encoding of the task variables, known to generalize poorly

when poor quality data is provided. Alternative methods of task learning might compensate for the data quality, such as learning from failed demonstrations (Grollman and Billard, 2012).

Secondly, the method cannot differentiate between a user preference of doing the task in a different way. Some users had a low value of force or torque on the expected axis, but applied higher values on other axes. This might correspond to using a different strategy. For example applying a horizontal force instead of torque corresponds to "scraping" instead of "scooping".

Lastly when computing the grasping quality the tool is always considered cylindrical. No complex model of the tool is taken into account.

### Human Factors not accounted for in the assessment

Several limitations with respect to the user assessment might influence the approach overall. Firstly in this work we assess the skill of the human in demonstrating the task, and not the skill actually in performing it unrestrained.

Wearing the glove might limit the tactile perception of the user making the scooping task harder. Several users complained about the weight of the glove and transceiver that they had to wear on their arm (see Table 4.4). Users did not always change the grasp as expected, possibly because the setup was interfering with their natural motions. Also maneuvering a robotic arm for holding the mellon, might have affected the natural coordination and adaptation between the arms.

Secondly users might prefer a certain way of doing the task, which is not necessarily the most efficient. The current framework does not offer a way of differentiating a preferred style from an unskilled performance. However consistency (i.e. relatively small variability) can hint towards a user preference and can be prioritized during model learning.

User performance is not always *clean*. Ideally we would expect to obtain a clear decomposition into hybrid control. This was only observed for a low number of subjects. Most subjects have components of force and torque on all axes, however most are resulting FT. This issue of distinguishing between the important and resulting forces can be addressed as proposed in (Ureche et al., 2015) (see Chapter 2), by analysing causal interactions between the variables.

Lastly, there are multiple human factors that could influence the quality of the demonstrations, that we do not assess here, either because they are hard to quantify and measure, either because they require a long term evaluation. For example: *aging* as this can influence the coordination ability, as well as the strength of the grip (Gorniak and Alberts, 2013), however a proper assessment can only be done through a long term study; *handedness*; which we could not assess due to our setup designed for right handed users only; *skill in performing the actual task* without the robotic equipment; *task features* features required by the task, in our case we tested on a single task, but in a different one (like knitting for example) the coordination might be more complex.

### Setup Limitations

The setup was custom built and the tactile patches used for measuring the pressure exerted on the tool were not firmly attached to the glove. Additionally the tactile patches are not bendable. Bending a patch leads to saturating the value of the pressure reading.

However bending of some patches might happen accidentally when the user moves the hand freely. This depends highly on the hand size of the participants (the length of the fingers and the thickness of the hands which can modify the position of the patches). To better suit the individual characteristics a calibration procedure has been devised, but proved impractical due to the long duration (approximately 1 hour per subject), while the experiment duration was about 15 minutes. Therefore a default calibration of a person with an averaged sized hand has been used for all subjects.

Lastly the need to always wear the glove for monitoring to be possible makes the manipulation more difficult such that fine movements or fine adjustments of force are no longer possible. Thus the approach would only be suitable for tasks that require relatively high forces (such as scooping in our case), but not for fine manipulation.

## 4.9 Conclusions

---

In this chapter we presented a method for assessing user performance when demonstrating the task to a robot. We provide objective metrics that directly relate the user's behavior when manipulating the tool with the task constraints. The constraints are automatically extracted, rather than using hardcoded task specific metrics. For a known task prototype the robot can estimate the user's behavior from the use of the tool.

Skilled demonstrators in contrast with unskilled users showcase: a better ability to maneuver the tool in order to apply the force required by the task; a low number of changes in the extracted constraints, especially in the variables of interest; task constraints remain consistent during the same action.

While the demonstrations are successful, still a robot learning from these data would not always be successful in applying that strategy in a slightly different context. However failure can be linked to the wrong use of the tool. This results in applying forces that are not optimal for the task and as such the task is not successful when being reproduced by a robot.

Other aspects of user performance and the way it influences the task should also be studied. For example a person who performs poorly a task requiring arm coordination and force control might also be prone at performing poorly other tasks. These suggests several directions worth investigating: (a) providing feedback to the user on which aspect of the performance should be improved (i.e. the grasp used on the tool, the force applied, the direction of the motion etc.); (b)

using the robot to train these skills while having a quantitative feedback; or (c) use the robot as an assistive device that complements the human's performance while reinforcing the task constraints such as applying more force.

Secondly humans might have a certain preference in executing the task that they would like to see displayed in the robot's behavior. Encoding the task with respect to the constraints might affect the way it is perceived by a human, by favoring a robotic-looking execution, rather than a natural-looking behavior.

# INTERACTION DYNAMICS IN PbD

The work presented in this chapter has been published in:

*Pais, A. L., Argall, B.D. and Billard, A. (2013) Assessing Interaction Dynamics in the Context of Robot Programming by Demonstration. International Journal of Social Robotics, November 2013, Volume 5, Issue 4, pp 477 – 490.*

## 5.1 Forward

---

In this chapter we focus on improving human–robot interactions through robot feedback provided during demonstrations. While in the previous chapters we have discussed approaches for extracting task constraints from kinesthetic demonstrations, here we assume that the robot already has an understanding of the important aspects of the task. Therefore the demonstrations that the user provides should fit these requirements.

The task that we are addressing is teaching a robot various configurations of the hand and fingers that would allow it to hold a cup and adjust to perturbations without letting it fall. The key aspect is maintaining a good contact between the fingertips of the robot and the cup while the fingers are backdriven by the demonstrator into different positions.

## 5.2 Introduction

---

Programming by Demonstration (PbD) methods contribute to Human-Robot Interaction (HRI), by making robots accessible to naive users, who have little knowledge of a robotic platform or programming language. Necessary tools are provided so that a robot is able to learn how to accomplish a task by simply observing the necessary gestures. This paper focuses on evaluating the user-friendliness of our framework for teaching a robot how to refine its manipulation skills (Sauser et al., 2012). Specifically we seek to identify the factors that make the interaction more engaging for the teacher. An engaged user may be more willing to teach the robot longer, and may pay more attention to the procedure, which may improve robot’s performance (Gielniak and Thomaz, 2011).

Evaluating a robot teaching by demonstration procedure can be done with respect to (1) *the quality of the demonstration* as a measure of the amount of useful data that can be included in learning the task (Sauser et al., 2012); (2) *the teaching efficiency*, which is a measure of how well the robot can reproduce the demonstrated task (Calinon and Billard, 2007a) and (3) the *perceived user satisfaction*, which is the aspect addressed in this paper.

The framework that we are evaluating consists of a multi-step iterative learning procedure, in which a human shows a robot multiple ways of holding a can, via tactile feedback, and several rounds of demonstration. The teaching procedure consists of three phases:

- (1) *demonstration*, in which the user shows the robot different ways of holding an object by moving the robot’s fingers, using their passive compliance capability. A certain contact signature corresponds to each demonstrated posture, and is reflected by the activation of the robot’s tactile sensors on the fingertips;
- (2) *replay*, in which the robot replays the sequence of hand postures, to record data that is not influenced by the touch of the teacher; and
- (3) *testing*, in which the adequacy of the learned model is reflected by the robot’s ability to adapt the fingers’ positions in response to perturbations in the position of the object.

Alongside the teaching procedure users are provided with various feedback modalities (detailed in Section 5.5) that expresses the robot’s current state.

The following section reviews works on identifying human factors involved in HRI teaching applications, that are the basis of the work presented here. Section 5.4 presents user study results validating a set of facial expressions on the humanoid robot iCub, that are later used as feedback in our framework. Section 5.5 describes our PbD interface and assesses the HRI development during teaching. Section 5.6 presents conclusions.

## 5.3 Related Work

---

From a human perspective, teaching a robot by demonstrating a task is a natural approach as it resembles the way humans teach another person (Peacock, 2001). From a robot’s perspective, learning can occur (a) by observing gestures, natural language, and other cues offered by the teacher or (b) by experience, being directly guided through the task. Natural methods for robot task learning include (Nicolescu and Mataric, 2003): instructive demonstrations, generalization over multiple demonstrations and practice trials. In our work we take a similar approach by including demonstrations, rounds of replay, and testing. These guidelines are complemented by stressing the importance of

using social cues as a natural way of structuring and guiding the robot’s learning (Breazeal, 2009). The robot should make its states transparent to the tutor by using communicative acts, while the instructor builds a mental model of what the robot has learned. While this highlights the importance of bi-directional teaching (Dautenhahn, 1998), that allows for the improvement of both learner and teacher, it also raises two main concerns: (1) finding the appropriate type of feedback for the robot to provide so that the teacher easily understands the effects that teaching has on the robot and (2) designing the interaction so that the tutor does not lose interest in teaching.

To address the first question, various ways of providing feedback in tutoring applications have been tested: *gazing* at what the teacher is doing (Breazeal, 2009); *emotional reactions* that influence human performance in collaborative tasks (Ushida, 2010); *verbal cues* that increased the frequency and accuracy of demonstrations in a dancing task (Leyzberg et al., 2011). Given that proper feedback is provided, the social component goes as far as attributing emotional states to artificial objects (Giusti and Marti, 2006), thus increasing the user’s implication. In our case, holding an object requires good contact on all fingertips and, in particular, on fingers placed in opposition on the object to ensure the stability of the grasp. Therefore, we take a similar approach to (Breazeal, 2009) and make this information (i.e. how good the contact is at the fingertips) transparent to the user, by correlating it with different feedback modalities. This helps the user create a mental model of the level of adaptation the robot achieves throughout multiple rounds of demonstration, replay and testing.

Addressing the second question of whether the interaction is sustainable is particularly relevant in demonstrating a task to a robot because the user should be engaged for the proper amount of time to deliver the required number of demonstrations. Initial user curiosity might drive the interaction (Hanson, 2005), but a sustained interaction is subject to six factors (Robins et al., 2005) responsible for keeping the user engaged. The first two factors, described in (Robins et al., 2005), address the problem of setting up the interaction, by: (1) providing contextual objects and knowledge, shown to dramatically improve human participation, as well as (2) initiating the interaction. The other four factors focus on regulating the interaction by: (3) having the robot provide responses in a timely manner and having a mechanism for managing role-switching, (4) using feedback to express robot’s states, (5) using turn-taking for sustaining a certain rhythm in the interaction and (6) confirming robot’s engagement by showing attention. Using these factors increases the complexity of the interaction which may promote accepting the robot as an interaction partner (Dautenhahn and Werry, 2000).

In our work we aim to add social components to a programming by demonstration interaction such that it keeps the user engaged and willing to deliver better quality demonstrations, see Experiment II. In designing the interaction we use four out of the six factors mentioned above, throughout the whole teach-

ing procedure: first, the user is given contextual knowledge about the task to be performed; second, the robot responds in a timely manner to the user’s actions; third, the teaching procedure is implicitly designed for turn taking by alternating the user’s lead in the demonstration and testing phases with the robot’s lead in the replay step; and fourth, the robot’s states are conveyed to the user.

We test three active ways in which to convey the robot’s internal states, namely via verbal feedback from a knowledgeable person, a graphical user interface and robot facial expressions. These modalities are contrasted against a control group in which no feedback was offered. For using adequate expressions a prior user study is conducted to validate a set of 20 custom face displays and choose the best recognized ones, see Experiment I. Adding social components to the teaching paradigm (Calinon and Billard, 2007a; Breazeal, 2009; Cakmak and Thomaz, 2012b), changes the classical approach to teach robots, where the robot is passive and learns solely from observing the teacher performing the task. The active feedback provided by the robot contributes to a novel view of human-robot team work, where both agents work cooperatively to achieve the same goal, namely transfer of skills.

## 5.4 Experiment I. Facial displays validation

---

Validating a robot’s expressive capabilities is a necessary step before using them in real applications, as embodiment particularities can influence both the way the user perceives the expressions as well as the recognition accuracy (Bartneck et al., 2004). Thus we conducted an experiment to assess to what extent humans can decode and interpret facial emotion expressions on the iCub robot. The goal was to determine a subset of best recognized expressions that we could later use to provide feedback in a PbD framework, described in Section 5.5. The underlying model for building the emotional displays and the implementation are described next.

### 5.4.1 ICUB FACIAL DISPLAYS

---

#### Emotion Representation

When using robot emotions it is important to represent them in a way humans could easily understand. Russell (1980) determined that humans have an innate capability of representing affect and thus proposed a circumplex model of clustering emotions, containing 28 facial expressions positioned in a two dimensional space. The first dimension emerges in studies of intra-personal behavior, and it is easily interpretable regardless of the users’ culture, while the second dimension is validated on inter-personal behavior (Russell, 1991). The dimensions are considered implicit in the human understanding of emotion (Russell, 1991)

and are given by (a) valence, pleasure or positivity and (b) activity, arousal or activation (Russell, 1991). Our work will refer to this first axis as *valence* and the second as *arousal*.

The design of emotion displays used in this study was based on Russell’s model of arousal and valence Russell (1997) because: (1) it provides an easy mapping between emotion features and robot expressive capabilities, (2) these dimensions are easily interpretable as discussed above, and (3) these dimensions emerge in inter-personal behavior, making the emotions validated in this study suitable for communicating internal states in HRI. In robotics applications, the arousal and valence dimensions are explored in different contexts. The first dimension can be communicated through haptic interaction (Yohanan and MacLean, 2011), while the emotional valence of a situation can lead to perceiving a robot as being empathetic (Cramer et al., 2010).

### Expressions Implementation

The facial expressions were implemented on the humanoid robot iCub using LEDs for representing the eyebrows and mouth, and actuators for controlling the eyelids opening angle. The changes along the arousal dimension were modeled by the opening of the eyelids and the curvature of the eyebrows, while the changes along the valence axis were mapped to changes in the lip curvature. LEDs are used to project the eyebrows and mouth facial features onto the face shell. The projection makes the line of consecutive individual LEDs appear continuous. There are 19 LEDs for the mouth and 4 sets of 5 LEDs for the eyebrows. An overview of all the implemented expressions is shown in Fig. 5.1.

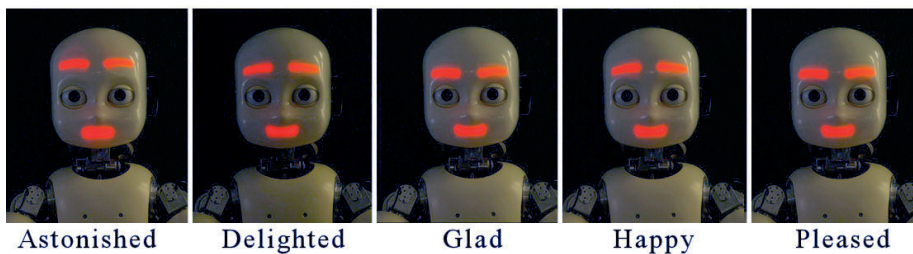
#### 5.4.2 STUDY DESIGN

---

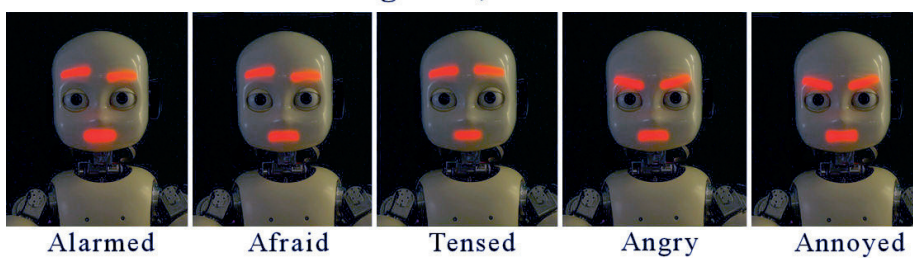
A subset of 20 out of 28 expressions in Russell’s original model were chosen arbitrarily as representing the maximum set of iCub displays that could be easily distinguishable. The designed expressions fit 2 valence levels (positive and negative) and 3 arousal levels (low, medium, and high). The displays were investigated, according to four categories: (1) positive, and intense: astonishment, delightedness, gladness, happiness, and pleased; (2) negative, and intense: alarmed, afraid, tensed, angry, and annoyed; (3) negative, not intense: miserable, depressed, sad, gloomy, and bored; (4) positive, not intense: satisfied, content, serene, calm, relaxed.

This way of dividing emotions allowed us to assess the degree of granularity that we could use for the expressions to still be interpretable by the users. Thus we evaluated the recognition rates on different levels of granularity: 2 classes, if only the distinction between positively and negatively valenced emotions was considered, 3 classes according to the arousal levels; 4 classes, given by Russell’s categories and 20 classes when classification by emotion name was considered.

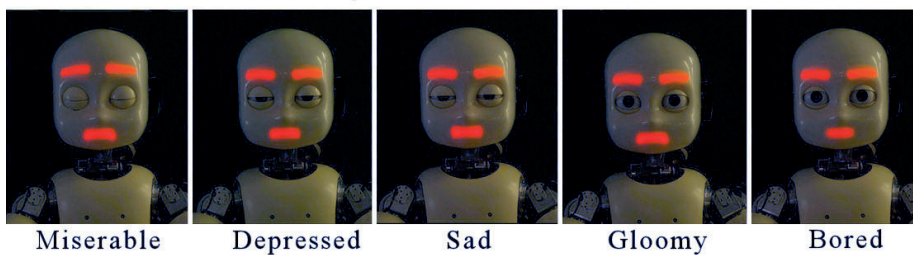
### **I. Positive, Intense**



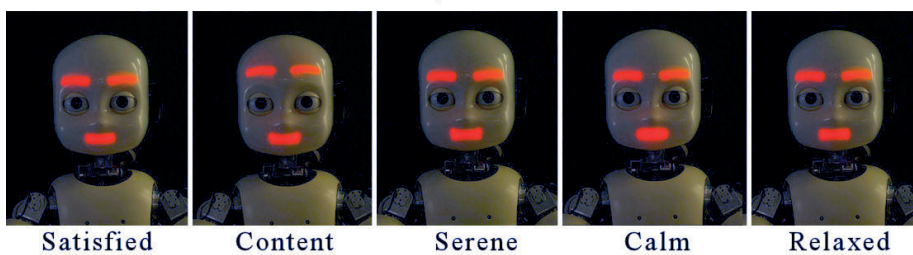
### **II. Negative, Intense**



### **III. Negative, Not Intense**



### **IV. Positive, Not Intense**



**Figure 5.1** Snapshot of each implemented expression, according to the four categories in Russell's model.

The study addressed the overall question of how easily the iCub’s facial expressions could be recognized if conveyed only through features like lip curvature, eyebrows and eyelids. We made the following untested assumptions: (1) the designed mapping between human emotions and robot displays was correct, implying that the implemented expressions were as close as possible to the human ones; (2) subjects were able to identify these emotions in humans. Based on these assumptions, our working hypotheses were:

H1: The categories in Russell’s model of emotions are identifiable in robot expressions by most humans.

H2: Subjects claiming to be skilled in recognizing human emotions might also be skilled in recognizing robot displays.

H3: The time a user requires for classifying an emotion is correlated with the arousal level of that emotion.

## Participants

The experiment involved 23 participants (5 females and 18 males), from various places of origin (13 European, 6 Asian, 4 North American), with an average age of  $M = 27.52$ , standard deviation  $SD = 5.43$  (minimum of 21 and maximum of 48).

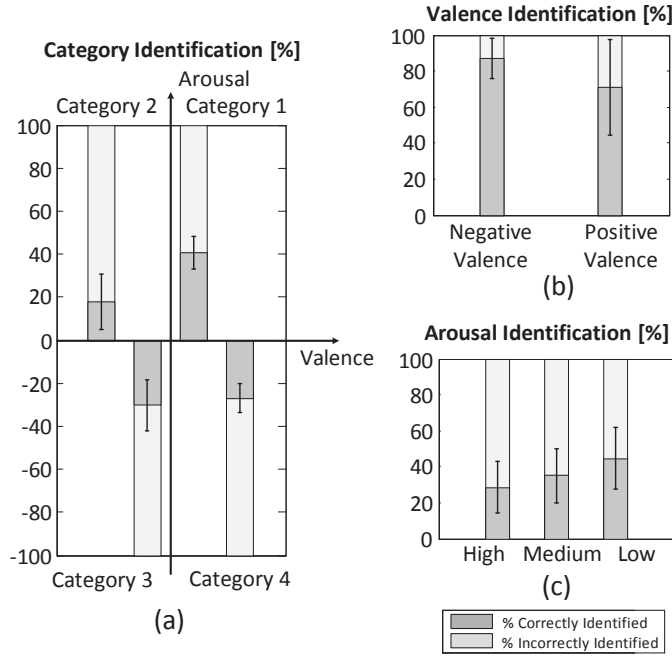
## Study Protocol

In a pre-experiment questionnaire the subjects had to assess their skill in understanding human emotions. The questions were:

1. How often can you read a person’s facial expressions?  
(Never/rarely/often/always)
2. How often do you check for emotional cues while interacting with a person?  
(Never/rarely/often/always)
3. What is easier for you to recognize from a person’s facial expression?  
(Sadness/happiness/both)

The answer to each of the first two questions was marked with a score from 0 to 3, for the third question a point was given for being able to recognize sadness or happiness, two points for both or minus two for none. The sum of the points obtained represented a general evaluation of the responders’ confidence levels (self-assessed skill) in recognizing human emotions. Based on this score participants were divided in three skill levels: low, 4 subjects; medium, 9 subjects; and high, 10 subjects.

In the second part of the study, the subjects were shown the facial displays, and for each asked to: classify the display as positive or negative valence, to assign an arousal level, and a name from a given list, and to rate the arousal level



**Figure 5.2** Recognition Rates [%] for: (a) Russell's Categories, (b) Valence, (c) Arousal levels

in comparison to the previous emotion. Each participant was exposed to a sequence of 60 facial displays, consisting of 20 different expressions, each repeated 3 times. The order in which the expressions were displayed was randomized, while avoiding the consecutive display of identical or closely related emotions. Participants were facing the robot during the whole experiment. The subject controlled the moment when the displayed emotion changed. They were not shown examples of iCub facial expressions prior to taking the survey. The time between the emotion display and the selection of each answer was recorded. Participants were not told that the experiment was timed, to avoid rushed answers. The survey required up to 40 minutes per user for completion. The study language was English, however as not all subjects were native speakers, some required clarifications for emotion names. Commonly hard to distinguish emotion terms were "content vs. serene"; "calm vs. relaxed"; and "sad vs. gloomy". In a post-experiment questionnaire the subjects were asked to rate their general expectations of HRI when these facial displays would be provided. On a 5 level Likert scale(Likert, 1932) subjects rated the *Interaction* (ranging from distracting to engaging), and the *Aesthetical* component (ranging from unpleasant to pleasant).

### Measurements

The coding of each emotion was done using an initially assigned value for valence (P = positive or N = negative), one of three arousal levels (L = low, M = medium, and H = high), and a name label, based on Russell's mapping

of emotions to the arousal and valence axes (See Table 5.1, columns 1 and 2). For each facial emotional expression we recorded the arousal, valence levels and the name label attributed by the user, and the time the user took to assign a value. Secondly we recorded the user’s answers to the pre and post-experiment questionnaires.

### 5.4.3 RESULTS

---

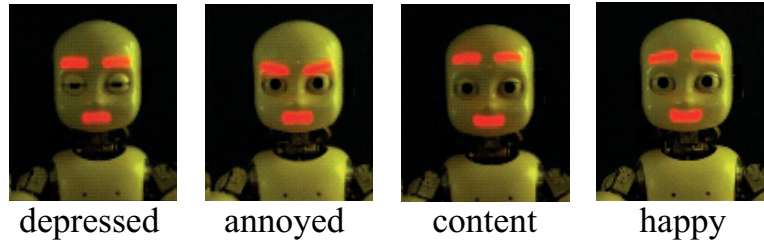
Results are presented in relation to the working hypotheses, and consist of evaluating the recognition rates for each emotion, and in making a subjective evaluation of the user’s experience while seeing the displays.

#### RECOGNITION RATES

---

To determine whether participants were able to correctly identify emotions in Russell’s model (hypothesis H1), recognition rates were evaluated over multiple categories, in order to assess how well people can differentiate between different levels of granularity. Recognition rates for the valence level (Table 5.1, 3rd column), arousal level (4th column) and name (6th column) were computed by comparing the score attributed by the user for each level and the name label with the initially assigned values for each emotion. A good match was marked with 1 and a no-match with 0. The rates presented in Table 5.1 represent the percentage of recognized displays (number of matches) from the 60 total displayed emotions. Similarly, the recognition score for both valence and arousal levels (5th column), represents the number of correct matches for both levels, from the total number of displayed emotions.

Recognition rates vary across categories (see Fig. 5.2(a)). The best recognized emotion from each category is shown in Fig. 5.3. Recognition rates for positive emotions tended to decrease as the arousal increased, while with negative emotions, the opposite trend was observed. Participants could identify the emotion valence (positive vs. negative) for more than two thirds of the emotions ( $M = 78.84\%$ ,  $SD = 21.34\%$ ); see Fig. 5.2(b). This correlates well with the fact that all participants agreed that they were capable to recognize when someone was happy. Similarly, participants correctly associated Depressed, Miserable and Sad with a negative emotion, even though they did not always label the displayed emotion correctly. This again correlates well with participants’ ability to recognize when someone was sad. Analysis of recognition rates for each of the three arousal levels (see Fig. 5.2(c)) shows that participants had a tendency to better recognize low arousal ( $M = 43.47\%$ ,  $SD = 19.14\%$ ) and medium arousal ( $M = 35.93\%$ ,  $SD = 15.63\%$ ) emotions, than high arousal emotions ( $M = 28.62\%$ ,  $SD = 14.56\%$ ). In other words, the less intense the emotion (whether positive or negative), the better it was recognized. This observation



**Figure 5.3** The best recognized facial displays with respect to the valence level from each of the four categories

did not seem to match the observation that participants were good at recognizing positive vs. negative emotions, and generally at associating emotions to the correct Russell category. We suspect that these poor results are due to the fact that participants may confuse some closely related emotions. The confusion matrix for the intensity levels showed that in 53.62% of the cases the negative-medium emotions were mistaken for negative-high emotions, and positive-low for negative-low (18.55%), while negative-low emotions were equally assigned to negative-low or negative-medium. The name recognition rates for each emotion showed rather poor results, with an average of 20%. This is partially justified by the difficulties subjects had in understanding the different terms used for the given emotions.

Results presented in this subsection partially support hypothesis H1 for low levels of granularity (e.g. differentiating positive emotions vs. negative displays). While category recognition rates were above chance level (5%), they were overall poor. This is likely due to the simplicity of the LED coding which does not allow rendering the full complexity of human facial expressions.

## HUMAN FACTORS INFLUENCE ON RECOGNITION RATES

---

To test hypotheses H2 and H3, we tested the influence of human factors on the recognition rates, mainly the user's self assessed *skill* in recognizing human emotions, the *reaction times* (the time necessary to assign the appropriate levels to each displayed emotion), and the user perceived *aesthetics* of the displays.

### A. Evaluation of User's Skill

We hypothesized that if participants felt confident in their general ability to assess emotions, they would also be more competent at recognizing robot emotions. Thus, we made a more general assessment about how confident participants were at recognizing emotions in general. Almost half of the participants declared themselves as confident in their ability to detect a sad person ( $M = 52.17\%$ ,  $SD = 0.51\%$ ). The vast majority of participants claimed to be able to recognize when a person was happy ( $M = 82.60\%$ ,  $SD = 0.38\%$ ). Most

participants declared that they were often able to recognize facial expressions and they often searched for facial cues while interacting with a human partner ( $M = 82.60\%$ ,  $SD = 13.27\%$ ).

We tested the influence on the category-based recognition rates of 3 factors<sup>1</sup> that aimed significant effects: (1) skill ( $F(2, 1379) = 69.9$ ,  $p = 0.001$ ), (2) valence level ( $F(1, 1379) = 4.15$ ,  $p = 0.04$ ) and (3) arousal level ( $F(2, 1379) = 3.04$ ,  $p = 0.01$ ). The recognition rates are presented in relation to the 3 levels of skill in Fig. 5.4(a). The users' self assessed skill in recognizing human emotions was not correlated with the recognition rates, showing that hypothesis H2 was not supported.

The degree of engagement that the users assign to the human-robot interaction when facial cues are involved is correlated with the recognition rates. Thus, people who rated the robot-expressed emotions as being very engaging were also good at recognizing emotions ( $F(3, 1316) = 98.124$ ,  $p < 0.01$ ). The effect of how aesthetic the interaction is when facial expressions are used is also significant ( $F(4, 1315) = 50.96$ ,  $p = 0.001$ ). Age was also found to have a significant impact on identifying the emotion valence, ( $F(1, 1369) = 98.575$ ,  $p = 0.001$ ), and arousal level ( $F(2, 1369) = 164.784$ ,  $p = 0.002$ ), showing that identification rates decrease with age.

## B. Evaluation of Users' Reaction Times

We tested the effect of 3 factors on users' reaction times: the emotions' arousal and valence levels and users' skill. The average time required to classify valence was 10.41s for negative emotions and 16.7s for positive emotions, suggesting that negative emotions were easier to understand. The average time necessary for assigning an arousal level was significantly lower for high arousal emotions (10s) compared to low arousal emotions (20s). The arousal level had a significant impact on the time the user took to rate the displayed emotion ( $F(2, 1375) = 10.34$ , and  $p = 0.002$ ). Skill however, did not have a significant effect on the arousal level classification time, but only on the valence classification time ( $F(2, 1377) = 5.495$ ,  $p = 0.004$ ); see Fig. 5.4(b). Average valence identification time for people that consider themselves not skilled in recognizing human emotions was 10s, while for high skilled people was almost 30s, suggesting that people who considered themselves skilled in recognizing human emotions might be more motivated during the interaction. In addition users that rated the interaction as engaging took a longer time to recognize if an emotion was positive or negative (Fig. 5.5(a)), but had better recognition times for emotion arousal level than those who rated the interaction as distracting (see Fig. 5.5(b)). Hypothesis H3, stating that the time to decision required for classifying an emotion into a category was negatively correlated with the arousal level of

<sup>1</sup>Analysis was based on ANOVA, a statistical technique used for testing the null hypothesis that there is no difference between groups. It is based on comparing the mean value of a common component. When the null hypothesis is false, the result is significant, implying an F value greater than 1, and a p-value  $p \leq \alpha$ , e.g.  $\alpha = 0.05$ .

Coding	Emotion	Valence [%]	Arousal [%]	Both [%]	Name [%]
1. P_H	Astonish	68.12	44.93	31.88	39.13
2. P_H	Delight	89.86	36.23	36.23	11.59
3. P_M	Glad	89.86	50.72	50.72	07.25
4. P_M	Happy	91.3	47.83	46.38	15.94
5. P_M	Pleased	86.96	42.03	39.13	10.14
6. N_H	Alarmed	63.77	13.04	08.70	11.59
7. N_H	Afraid	92.75	20.29	20.29	0
8. N_M	Tense	81.16	43.48	39.13	02.90
9. N_M	Angry	85.51	13.04	13.04	76.81
10.N_M	Annoyed	98.55	10.14	08.70	10.14
11.N_M	Miserable	95.65	23.19	21.74	15.94
12.N_M	Sad	89.86	47.83	44.93	17.39
13.N_L	Gloomy	88.41	37.68	30.43	05.80
14.N_L	Bored	73.91	56.52	40.58	18.84
15.N_L	Depressed	98.55	13.04	13.04	14.49
16.P_M	Satisfied	84.06	43.48	36.23	05.80
17.P_M	Content	95.65	30.43	30.43	10.14
18.P_L	Serene	34.78	50.72	24.64	02.09
19.P_L	Calm	39.13	49.28	18.84	15.94
20.P_L	Relaxed	28.99	60.87	24.64	07.25

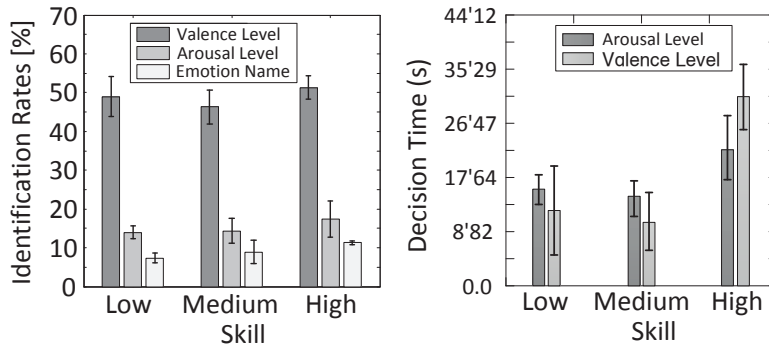
**Table 5.1** Percentage of correctly identified emotions by valence and arousal levels, by both arousal and valence, and by name. The coding indicates a positive (P) or negative (N) valence and low (L), medium (M) or high(H) arousal level

that emotion, was supported by the results presented in this subsection.

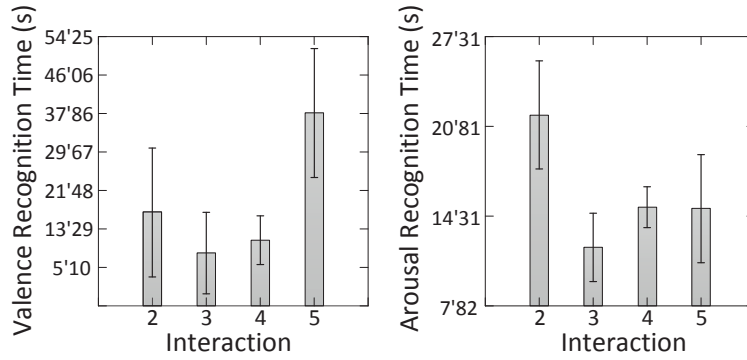
### C. User-perceived Aesthetic Component

In the last part of the experiment, participants were asked to rate the *aesthetics* of the interaction (ranging from unpleasant to pleasant) when robot facial displays were provided. The aesthetics component was rated lowest by persons that rarely check for expressions of emotion in humans (2 subjects). The highest rating was given by the group of subjects that always check for emotional expressions in other persons (16 participants). This group also had the best recognition rates for valence ( $M = 53\%$ ,  $SD = 0.2$ ) and arousal levels ( $M = 19.6\%$ ,  $M = 0.8$ ).

Overall, above chance recognition rates occurred for all categories, with the



**Figure 5.4** Effect of the user self assessed skill of recognizing emotions on (a) the emotion arousal level and (b) the time necessary to assign arousal and valence levels to a facial display

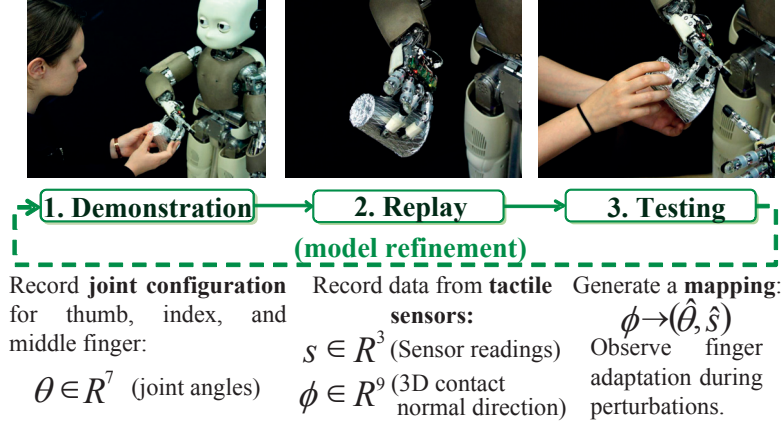


**Figure 5.5** Effect of the perceived interaction (ranging from 1 (distracting) to 5 (engaging)) on the recognition time for (a) emotion valence (b) emotion arousal level

best rates found for the smallest level of granularity (i.e. classification in two classes, positive and negative emotions).


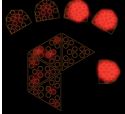


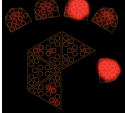




## 5.5 Experiment II. Robot feedback during teaching interactions

The second experiment was carried out to study the impact of providing different types of robot feedback on the effectiveness of a teaching by demonstration framework, as well as on user satisfaction. The goal is to have human-users, with no prior experience of interacting with the iCub platform, be able to teach the robot how to refine its manipulation capabilities and achieve a satisfactory model of holding a certain object, after providing the robot with several rounds of kinesthetic teaching.



**Figure 5.6** PbD framework for teaching a manipulation task to a robot. A human shows the robot various ways of holding a can through tactile guidance. The robot replays the demonstrated motion and learns a model of the task that can be tested and further refined by providing additional demonstrations

A multi step training procedure, illustrated in Fig. 5.6 was used to iteratively build a training data-set from teacher’s demonstrations and learner’s replay. The teaching procedure consisted of three steps. The first step was the *demonstration*, in which the user demonstrated the robot different finger positioning on the object using tactile guidance. The robot held the object with 3 fingers of the right arm (the thumb, index and middle finger), maintaining contact just on the fingertips. The information recorded in this step consisted of a set  $\Theta \in R^7$  of robot finger joint angles. The second step was the *replay*, in which the robot replayed the demonstrated motion in order to record for each posture the corresponding tactile-sensor signature, without being influenced by the additional pressure provided by the teacher. The contact information was recorded using the pressure response of the tactile sensors on the robot’s fingertips. Each fingertip has 12 tactile nodes that were activated on contact with the object, providing an 8-bit pressure value. Information recorded at this stage consisted of sensor readings  $s \in R^3$ , representing an averaged value for each fingertip, and a vector  $\phi \in R^9$  representing the computed 3D contact normal direction. Based on the information recorded in the first 2 steps, the robot used statistical techniques to learn a mapping between the tactile response on its fingers and the corresponding finger positions  $\phi \rightarrow (\hat{\theta}, \hat{s})$ , as described in (Sauser et al., 2012). When a perturbation occurred the contact signature changed. The learned model allowed the robot to predict a new hand configuration based on the new sensed contact. The third step was the *testing*, in which the participant could test the learned model by perturbing the position of the object. The displacement of the robot’s fingers in response to perturbation gave an indication of the adequacy of the model. The obtained model could be further refined by providing additional rounds of demonstration, replay and testing.

Situation Example	Verbal Feedback	GUI Feedback	Facial Feedback
Good contact on all fingers 	Good contact and posture. You can show the robot more postures.		 Happy
Contact lost on one finger 	Be careful, one finger is no longer in contact. You need to press harder on all fingertips.		 Content
Contact lost on all fingers 	The robot dropped the can. You need to readjust the hand posture.		 Annoyed

**Figure 5.7** The usability of the PbD framework was tested using different modalities of providing feedback to the user. The experimental setups according to the 3 major situations in the experiment: verbal feedback, GUI feedback, facial feedback. These setups were contrasted against a no feedback situation

The tactile information was important because of the way it was accounted for in the learning algorithm. According to the reliability measure introduced by [Sauser et al. \(2012\)](#) the stronger a contact sensor reading was, the more reliable it was considered to be. This implied discarding weak contact readings. Thus providing the user with a valid representation of this information would dramatically improve the amount of useful information provided through demonstration. This would be reflected in the learned model by achieving better adaptation.

### 5.5.1 STUDY DESIGN

The experiment was performed on the iCub robot. We studied four conditions (experimental setups), shown in Fig. 5.7, which reflected the type of feedback being provided. In the first setup (**E1**) no feedback was provided by the robot, nor by the experimenter. This setup was called *no-feedback*. In the second setup (**E2**) rich verbal feedback was given by a knowledgeable experimenter whenever it was considered necessary (*verbal-feedback*). In the third setup (**E3**), a Graphical User Interface (GUI) was used consisting of a diagram of the tactile nodes on each fingertip. The GUI provided a real-time continuous feedback on the tactile sensing intensity and area of activation, by highlighting the activated tactile nodes. The subject knew when the object was in contact with the robot's fingertips and could see the variation in the contact area (*GUI-feedback*). In the last setup (**E4**), robot facial expressions were provided as discretized feedback to the subject on the adequacy of his/her teaching (*facial-feedback*). Three facial expressions were used from the ones validated in the previous experiment, and having the highest recognition rate on the valence

axis in three of the categories tested previously. The expressions were mapped to contact sensing as a 3 levels discrete feedback as follows: the *happy* expression was used when all 3 fingers of the robot were in contact with the object, the *content* expression was used when one finger lost contact or the overall contact was weak, and the *annoyed* expression was used when at least two fingers lost contact. The types of feedback described above were provided for the whole duration of the interaction, in all phases of the teaching procedure.

The study addressed two research questions:

RQ1: Does the feedback provided influence the teaching procedure and the learned manipulation model?

RQ2: Does the effect that the type of feedback has on the subjective usability ratings change in relation to task performance?

## Participants

The participants ( $N = 57$ , 14 females and 43 males) were selected from university staff and represented the 25-35 years age group. The selection criterion was to not be directly working with robots. Participants were distributed as follows: 12 took the experiment in the first setup (no feedback), 16 were assigned to verbal-feedback, 14 to GUI-feedback and 15 to facial feedback.

## Study Protocol

Before beginning the experiment, participants were given general guidelines and were shown a descriptive movie of the teaching procedure. For all setups, the experiment consisted of providing three rounds of demonstration through kinesthetic teaching, of 90 seconds each. Each demonstration round was followed by the robot's replay of the recorded motion. The model learning took place offline after each replay step and was followed by a round of 90 seconds of testing. A post-experiment questionnaire was employed to assess users' satisfaction with the outcome of the teaching task. The total length of the experiment for each participant was 40 to 45 minutes.

## Measurements

For each round robot measurements consisted of joint angles values for the 3 fingers used in the task, and the contact signature consisting of tactile response and 3D normals. Four objective metrics were computed based on these measures, as defined in [Sauser et al. \(2012\)](#): (1) *range of motion*, (2) *contact times*, (3) *joint shakiness* and (4) *contact error*. The *range of motion* is based on the difference between the minimum and maximum joint angle values for each finger. These ranges of joint angles are combined in 4 groups by summing the proximal and distal ranges of motion for thumb, index and middle fingers and separately for the thumb opposition angle. This measure allowed us to compute

the percent of the range of motion that was actually demonstrated (when the robot was holding the object) out of the total possible range of motion for a given joint group.

Several metrics have been computed related to *contact times*: (a) the percent of time two fingers and (b) three fingers were in contact with the object, out of the total demonstration time; and (c) the time in force closure, representing the percentage of the total demonstration time in which the three fingers were in contact with the object and the resulting grasp attained force closure [Bicchi \(1995\)](#). The time in force closure was used as a measure of grasp stability and adaptation quality. The grasping quality was evaluated as described in [Ponce et al. \(1996\)](#). *Joint shakiness* represented a measure of the instances of jerky movements. It was evaluated in the testing phase and represented the difference between the raw and smoothed joint velocities averaged across the testing period. *Contact error* represented the difference between the contact value that was predicted (the target) and what the controller executed (the actual) contact value. It gives an overall assessment of the adaptation provided.

Responses from standardized post experiment questionnaires were used to assess user satisfaction. The questionnaires involved: (1) NASA (Task Load Index) TLX ([Hart and Staveland, 1988b](#)), (2) System Usability Scale (SUS) ([Brooke, 1996a](#)) and (3) AttrakDiff ([Hassenzahl et al., 2003](#)). The questionnaires were given in English and clarifications have been provided when necessary. NASA-TLX [Hart and Staveland \(1988b\)](#) is commonly used in studies of interface design. It is a workload assessment tool used for evaluating how the user perceived the physical, mental, and temporal demand during a task, and perceived levels of effort, performance and frustration. It consists of 6 questions, answered with a rating on a 21 point-scale, providing an overall workload score. The SUS questionnaire ([Brooke, 1996a](#)) was used for assessing the overall satisfaction with the system. It consisted of 10 statements (5 positives, 5 negatives) rated on a five-point Likert scale ([Likert, 1932](#)). Positive questions are given a rank according to the value of their index position minus 1, while negative questions, have a contribution of 5 minus their index position. The score was computed by summing the contribution of each individual component and multiplying the sum by 2.5. AttrakDiff ([Hassenzahl et al., 2003](#)) is a method for assessing complementary aspects of the user experience: (1) pragmatic quality, (2) hedonic quality and (3) attractiveness. However, in this study the hedonic quality of identity was not tested, due to the fact that the robot together with the interface being examined do not represent a commercial application. Thus, the modified version of the questionnaire consisted of 19 pairs of sets of opposite words, which users evaluated on a seven-step scale ranging from -3 to 3. Finally, the participants' assessment of the teaching procedure was evaluated separately by answering 4 questions considering: how easy was the teaching, how satisfied the participant was with the resulted model, if the robot behaved as expected, and how comfortable the participant felt while providing the demonstrations.

## 5.5.2 RESULTS

---

Results are presented both with respect to objective, task-specific metrics, as well as subjective user evaluation. Task completion time is constant among users as the teaching and testing rounds were time restricted to 90 seconds.

### MEASURES OF PERFORMANCE

---

All the task specific metrics presented below are computed based on joint and pressure values of the three fingers that are in contact with the object. They are evaluated for each round of teaching, and represent an evaluation of the learned model. Analysis of variance (ANOVA) was conducted using the measures of performance as dependant variables and the type of feedback as main factor.

#### Range of motion

The range of motion is a percentage representing how much each joint group moved with respect to the total possible range of motion for that group. The robot's ability to adapt over a higher range of motion shows that a higher range of postures was demonstrated by the user. Detailed statistics are presented in Table 5.2. The best results were obtained for the verbal feedback setup (E2). Participants that were given graphical or facial display feedback (E3 and E4) explored a significantly lower range of possible motion comparable to the case when they were given no feedback at all (E1), as seen in Fig. 5.8(a). A main effect of the experimental setup was found on the Range of Motion of each finger, see Table 5.2, last column.

#### Contact Times

The percentage of time when two fingers and three fingers are in contact with the object, out of the total testing time, was evaluated. A high time is an indication of a good adaptation, while a poorly trained motion results in the robot being stiff in that region and losing contact with the object when perturbed. The experimental setup used had a significant effect on all the contact times metrics defined, as seen in Fig. 5.8(b). The percentage of time when 2 fingers were in contact with the object was lowest when the participant was not given any feedback ( $M = 0.98, SD = 0.03, F(3, 171) = 7.58, p < 0.001$ ) and similarly when three fingers were in contact ( $F(3, 171) = 10.84, p < 0.001$ ). However an important observation is the fact that the percentage of time three fingers were in contact with the object was highest when the graphical user interface (E3) was used as feedback ( $M = 0.99, SD = 0.01$ ), while the second best result was obtained for both the facial display (E4) setup ( $M = 0.97, SD = 0.005$ ) and the verbal feedback (E2) setup ( $M = 0.97, SD = 0.018$ ). These

results together with the negative correlation existing between the time 3 fingers are in contact and average range of motion (Pearson  $r = -0.42$ ), in the case of E3 and  $r = -0.38$  for E4, suggest that while the feedback provided may have been distracting, keeping the user focused on the display rather than on exploring the motion space, helped improve contact accuracy.

A decreasing trend was observed for the time in force closure as more feedback was being provided and similarly in the grasping quality, as shown in Fig. 5.9(b).

### Shakiness

The Shakiness is also an indication of proper adaptation, with lower values being desirable. The average Range of Motion and average Shakiness are inversely correlated (Pearson  $r = -0.58$ ). Detailed results are presented in Table 5.2. A significant interaction effect of the experimental setup on the Shakiness values was observed for all joint groups (see Fig. 5.9(a)) The lowest shakiness values were found in the verbal feedback setup, followed by facial feedback.

### Contact Error

Contact error decreased considerably as more feedback was provided, as seen in Fig. 5.9(c), yielding the significant effect ( $F(3, 83) = 3.78$ ,  $p = 0.01$ ) that the experimental setup had on achieving a more stable contact and a smoother adaptation. The lowest contact error was achieved when verbal feedback was provided ( $M = 3.23$ ,  $SD = 0.62$ ), while the highest contact error ( $M = 3.58$ ,  $SD = 0.85$ ) is associated with facial feedback.

---

## INTERACTION DURING DEMONSTRATION

---

User's behavior while providing demonstrations was of particular interest as it would influence the quality of the teaching. We were interested in finding factors that will keep the user engaged in the interaction, in order to assure good quality demonstrations and also to be willing to provide an optimal number of demonstrations for the robot to be able to properly learn the task. The *demonstration* phase is important for recording proper joint angles. In the *replay* step, the robot will replay the recorded motion while also recording tactile information and thus generating a set of data not influenced by the tutor. For the teacher this step can give a clear understanding of what the robot has recorded (e.g. if the demonstrator moved too fast, only some points in the trajectory will be recorded and this will result in a shaky reproduction). Users' initial attitudes in relation to the feedback being provided influenced the learning by modifying user reaction times, the exploratory motions performed or the observed test patterns, as discussed below.

Experimental Setups						
Objective Measures	E1. No Fb	E2. Verbal Fb	E3. GUI Fb	E4. Expr Fb	$F_{statistics}$	p-value
Range of Motion [Deg]						
Thumb Opposition	42.24 ± 26.38	94.50 ± 29.48	44.01 ± 24.36	32.66 ± 17.75	F(3,171)=59.25	$p < 0.001$
Thumb Finger	29.65 ± 13.85	38.70 ± 07.43	32.20 ± 13.47	27.99 ± 10.99	F(3,271)=7.91	$p < 0.001$
Index Finger	24.36 ± 10.75	33.81 ± 06.03	33.23 ± 17.81	30.44 ± 14.39	F(3,171)=4.10	$p = 0.008$
Middle Finger	27.28 ± 13.74	35.59 ± 06.09	34.24 ± 16.27	26.25 ± 13.40	F(3,171)=6.036	$p = 0.001$
Contact Times [% out of Total Time]						
2-Fingers Contact	0.98 ± 0.03	0.99 ± 0.004	0.99 ± 0.003	0.99 ± 0.03	F(3,171)=7.58	$p < 0.001$
3-Fingers Contact	0.96 ± 0.05	0.97 ± 0.018	0.99 ± 0.01	0.97 ± 0.005	F(3,171)=10.84	$p < 0.001$
Time in Force Closure	0.67 ± 0.31	0.72 ± 0.15	0.38 ± 0.24	0.58 ± 0.26	F(3,171)=35.159	$p < 0.001$
Joint Shakiness [Deg/s]						
Thumb Opposition	0.029 ± 0.015	0.015 ± 0.004	0.025 ± 0.010	0.023 ± 0.008	F(3,171)=15.091	$p < 0.001$
Thumb Finger	0.128 ± 0.068	0.080 ± 0.020	0.108 ± 0.045	0.118 ± 0.042	F(3,171)=9.327	$p < 0.001$
Index Finger	0.110 ± 0.049	0.065 ± 0.021	0.097 ± 0.036	0.097 ± 0.038	F(3,171)=12.779	$p < 0.001$
Middle Finger	0.093 ± 0.038	0.060 ± 0.016	0.094 ± 0.042	0.098 ± 0.034	F(3,171)=12.835	$p < 0.001$
Grasping Quality (*10 <sup>-3</sup> )	0.39 ± 0.04	0.6 ± 0.22	0.22 ± 0.19	0.20 ± 0.12	F(3,171)=23.845	$p < 0.001$

**Table 5.2** Objective Metrics, averaged across all rounds in the testing phase

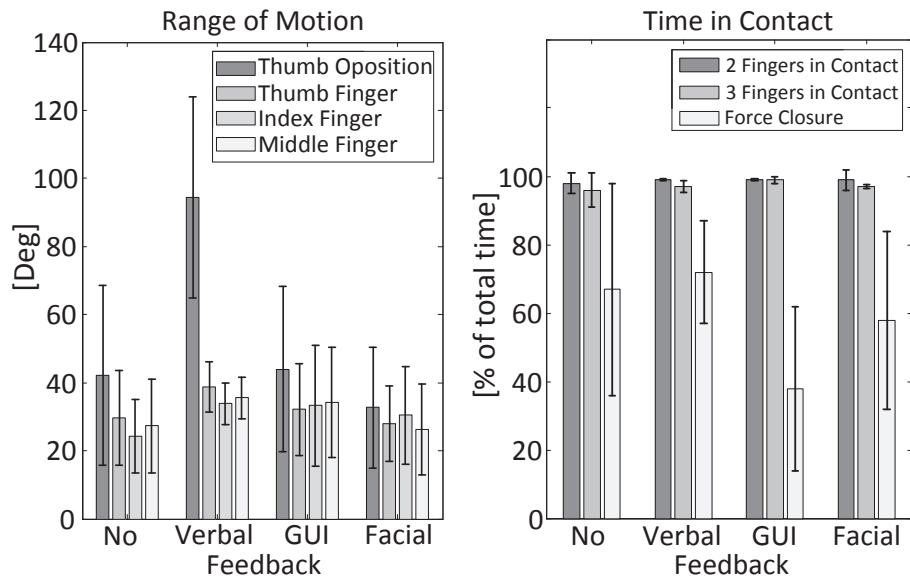
### Exploratory motions

According to our observations, (consistent with the ones mentioned in [Hanson \(2005\)](#)), in all cases the initial interaction with the robot was driven by users' curiosity. The subjects were not familiar with any humanoid robotic platform, and were not given time to familiarize with our robot before the experiment. However in the first round of providing demonstrations, they performed a lot of exploratory motions: either pushing the robot to the joints limits, or on the contrary starting from small motions, to try to understand how to control all the degrees of freedom in the robot's fingers. This behavior resulted in frequent lost contact, shaky motions, and an overall poor demonstration. Losing contact between the robot's fingers and object results in poor replay and thus less pairs of postures and contact signatures to be included in the model in the first round of teaching. The improvement rates increase with the rounds of teaching. In several cases, assessing the model improvement across users, regardless of the setup, showed that the improvement rate dropped in the third round of teaching, even if the user was now familiar with the robot capabilities. This might have been due to user fatigue or might be a result of seeing little adaptation while testing the previously obtained models. Exploratory motions performed by the user are necessary in order to get familiar with the robot and to understand the robot limits. In the case of facial feedback, seeing that the robot was responsive to user actions seemed to encourage subjects to use caution when teaching, which however negatively influenced the objective metrics: e.g. the range of motion, see Fig. 5.8(a).

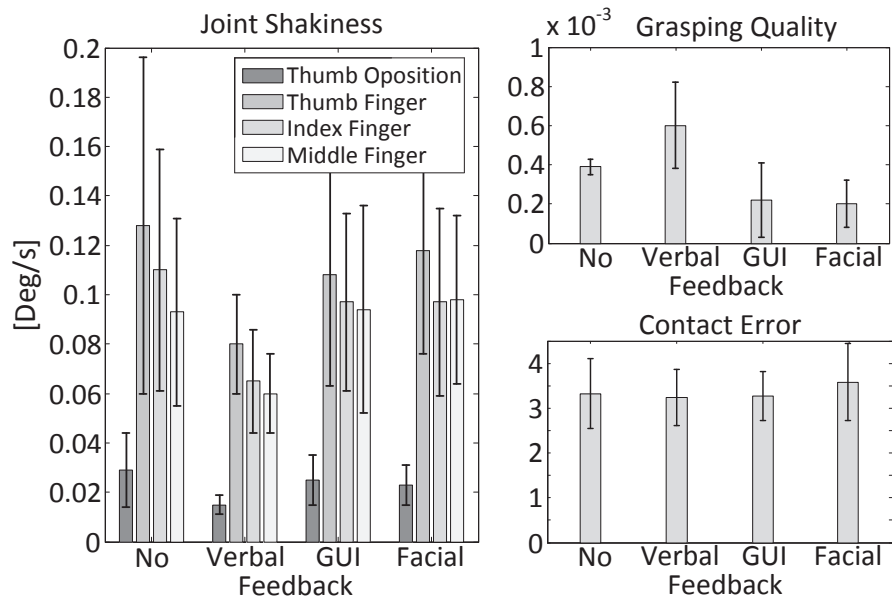
The subjects were asked to perform a minimum of 3 demonstrations, but were not limited to an upper number. Interestingly, only 3 subjects decided to perform a 4th demonstration (2 from the verbal feedback setup and one from the GUI setup). Their overall performance ratings during the testing phase were not the best in comparison with other subjects, but they managed to successfully control the robot degrees of freedom so as to teach a wide range of motions.

### Model testing

After each learning session the users were asked to test the obtained model in order to decide what should be improved in the next round of teaching. In almost all of the testing cases ( $M = 92\%$   $SD = 14.7$ ), regardless of the experimental setup, the user pushed the robot outside the trained range of motion. During teaching, 4 types of movements were possible: left and right translational movements, and left and right rotational movements. However in more than 80% of the cases, regardless of the feedback provided, in the first round of demonstration only translational movements were trained, but in the testing phase, rotational movements for which no adaptation occurred were tested as well. During the second and third round of demonstration, rotation movements started to be taught, with a higher frequency on the verbal feedback



**Figure 5.8** (a) Range of motion and (b) Contact Times evaluated for each experimental setup.



**Figure 5.9** (a) Joint Shakiness (b) Grasping Quality and (c) Contact Error, evaluated for each experimental setup

	TLX Factors and Overall Score	
	E3. GUI Fb	E4. Expr Fb
	mean $\pm$ std	mean $\pm$ std
Mental Load	08.33 $\pm$ 04.79	10.18 $\pm$ 04.35
Physical Load	04.38 $\pm$ 02.32	08.31 $\pm$ 06.61
Temporal Load	07.07 $\pm$ 03.20	06.43 $\pm$ 04.30
Performance	09.84 $\pm$ 05.65	09.56 $\pm$ 04.70
Effort	09.00 $\pm$ 03.46	08.87 $\pm$ 04.68
Frustration	08.61 $\pm$ 04.94	05.93 $\pm$ 05.01
Total Score	47.23 $\pm$ 24.36	49.28 $\pm$ 29.65

**Table 5.3** NASA Task Load Index (TLX)

setup. In 2 cases of users from the E1 setup (no feedback), rotational movements were not trained at all.

### User Reaction Times

Results showed that human adaptation time was better when either facial feedback or graphical display feedback was being provided. The time between the moments in which the contact was lost and when the human adjusted the fingers positions was lower. The user provided a motion such as to immediately correct the posture. However this may result in a shaky, sudden motion, thus explaining the high shakiness in these two experimental setups (see Fig. 5.9(a)). The fastest response time occurred in the case of facial feedback ( $M = 1.35s$ ,  $SD = 0.52$ ), while the slowest response was recorded for the no feedback case of ( $M = 7.56s$ ,  $SD = 3.81$ ).

### SUBJECTIVE EVALUATION

For the first two experimental setups (no feedback and verbal feedback) a general interaction assessment was made verbally by the participants. More than 80% of the participants characterized the interaction as "interesting", "motivating" and "captivating". They also described the shortcomings of the interaction as being the "lack of previous knowledge about the robot" and "the little time available for providing demonstrations". As we were interested in finding the best robot-provided feedback that would improve the interaction, the participants in the other two experimental setups were subject to a more thorough evaluation, being asked to fill in standardized usability questionnaires. Results are presented below.

The effect of experimental setup on task load was not significant. Results (see Table 5.3) show that mental demand and physical demand were perceived

<b>System Usability Evaluation</b>		
	E3. GUI Fb	E4. Expr Fb
	mean $\pm$ std	mean $\pm$ std
Use Freq.	2.93 $\pm$ 1.22	3.06 $\pm$ 0.85
Sys. Complex.	2.26 $\pm$ 0.96	1.81 $\pm$ 0.98
Ease of Use	3.20 $\pm$ 1.42	3.50 $\pm$ 1.26
Techn. Support	2.20 $\pm$ 1.26	2.31 $\pm$ 1.30
Funct. Integ.	3.40 $\pm$ 0.82	3.37 $\pm$ 0.71
Sys. Inconsis.	2.20 $\pm$ 1.01	2.12 $\pm$ 1.08
Learn to Use	2.93 $\pm$ 1.48	3.25 $\pm$ 1.12
Cumbersome	1.86 $\pm$ 0.99	1.62 $\pm$ 0.80
Confidence	3.06 $\pm$ 1.33	3.00 $\pm$ 1.03
Prev. Knowl.	1.80 $\pm$ 1.32	1.81 $\pm$ 0.91
Total Score	64.66 $\pm$ 15.20	64.68 $\pm$ 8.41

**Table 5.4** System Usability Evaluation (SUS)

as higher when facial feedback was provided (E4 setup) compared to the case when a graphical display was used (E3 setup). However, the level of frustration perceived was much lower when facial expression feedback was provided and similarly the effort perceived was lower, suggesting that it represents a more natural means of interaction.

The experimental did not have a significant effect on the SUS ratings. However the participants in E4 rated the interface more positively on two key aspects than the users in E3: the usage frequency (namely they would like to use the system more frequently) and the ease of learning the functionality of the system. Results of the SUS questionnaires are summarized in Table 5.4. An assessment of how attractive the users found the teaching framework was made and results are reported in Table 5.5. The users taking part in the facially-displayed feedback setup (E4) rated the interface higher on hedonic quality and attractiveness, than the users given only graphically-displayed feedback (E3). What is more, in the group of words describing the attractiveness, they all assigned the maximum value for the positive attributes ("pleasant", "likeable" "inviting", and "creative"), suggesting that the E4 setup was more motivating and appealing.

Results from evaluating the teaching procedure are presented in Table 5.6. The participants in the facial feedback experimental setup E4 reported an increased satisfaction with the resulted model ( $M = 3.31$ ,  $SD = 0.94$ ) than those offered only the GUI feedback ( $M = 2.86$ ,  $SD = 1.12$ ), even though the performances in terms of objective metrics were clearly lower. Moreover the subjects in E4 reported an increased perception of the fact that the robot behaved as they expected. This suggests that seeing a responsive robot increased the users

<b>AttrakDiff Ratings</b>		
	E3. GUI Fb	E4. Expr Fb
	mean $\pm$ std	mean $\pm$ std
Pragmatic Quality PQ	0.56 $\pm$ 0.57	0.40 $\pm$ 0.35
Hedonic Quality HQ	0.47 $\pm$ 0.43	0.75 $\pm$ 0.66
ATT Score	0.74 $\pm$ 0.40	1.07 $\pm$ 0.64

**Table 5.5** AttrakDiff Ratings

<b>Teaching Procedure</b>		
	E3. GUI Fb	E4. Expr Fb
	mean $\pm$ std	mean $\pm$ std
Ease of Teaching	03.40 $\pm$ 01.12	03.12 $\pm$ 01.08
Satisfaction	02.80 $\pm$ 01.26	03.31 $\pm$ 00.60
Expectation	02.86 $\pm$ 01.12	03.31 $\pm$ 00.94
Comfortability	02.93 $\pm$ 01.48	03.50 $\pm$ 01.15

**Table 5.6** User Evaluation of the Teaching Procedure

contentment with respect to the interaction. The subjects that took part in E4 reported being significantly more comfortable ( $M = 3.5, SD = 1.15$ ) than participants in E3 ( $M = 2.93, SD = 1.48$ ), suggesting that facially displayed emotions facilitated a positive interaction.

## 5.6 Discussion

The work presented in this chapter paper addressed the problem of finding a suitable type of feedback that would facilitate robot’s learning in a PbD context. Making the human-robot interaction rewarding and keeping the user engaged contributes to improving robot’s learning. Two user studies were presented.

### 5.6.1 EXPERIMENT I. FACIAL EXPRESSIONS

The first experiment evaluated the correct classification of 20 robot expressed facial emotions into given categories. The study targeted testing the assessment that users can relate to robot displayed emotions just as well as they can do with human emotions, and also that they perceive the relative order of emotions, when the valence and arousal levels vary. Results showed that this hypothesis is confirmed only for small levels of granularity, implying fewer emotion categories.

For robot expressed emotions, through LEDs, there was a good recognition rate along Russell’s valence axis (differentiating between positive and negative emotions) and a poor recognition rate along the arousal axis. We found little to no support for the second hypothesis that a high user’s self assessed skill in recognizing human emotions might positively impact the ability to recognize robot expressions. The third hypothesis, that intense emotions take a very small reaction time was supported.

### Limitations

Limitations of this study are threefold. First, the LED display used for generating the facial expressions could not portray a good enough range of human emotions. We aimed to determine a small set of best recognized facial displays however the displayed faces raised problems in terms of ambiguity of the LED display. The expression of the same emotion might look different when using another robotic platform.

Second, the lack of prior interaction with the robot or its expressions made the respondents unsure when assigning extreme intensity values for the displayed emotions without having a prior idea of the possible range.

Third, we did not assess participants’ ability to recognize the same facial expression when displayed by a human face.

## 5.6.2 EXPERIMENT II. ROBOT FEEDBACK

---

The second user study was conducted to assess the usability of a teaching by demonstration interface, that was not initially based on a user-centered design. In our approach, similar to other robot teaching tasks, the interaction was initiated by the human. We designed the interaction in a way that would ease teaching for the human user, by having rounds of demonstration, robot replay and testing. This allowed not only the iterative refinement of the obtained model, but it also helped the user to understand what the robot has learned at each step and what needs to be improved in the next demonstration. Different feedback modalities were used to reflect the strength of the contact between the robot’s fingers and the object: verbal feedback, graphical user interface feedback, facial displayed feedback and no feedback at all.

Results presented confirmed that the type of feedback provided by the robot influenced both subjective and objective metrics. According to objective metrics, satisfactory results were obtained in all study cases. During testing, 3 fingers are in contact with the object in more than 95% of the time, force closure grasps are attained for more than one third of the testing time, and no large differences can be seen between shakiness and grasping quality across setups. While in most cases the verbal feedback from a knowledgeable person proved the best, this is not feasible in real world applications.

### Advantages of robot–provided feedback

Providing feedback in a natural manner helped the participants to perceive the interaction as less restricting and have a lower temporal pressure. According to the subjective metrics evaluation, the experimental setup influenced the ease of the interaction, user demand and friendliness. Thus for a naive user who was not familiar with the robot this might be the best way of obtaining a satisfactory object manipulation model, in a comfortable and rewarding interaction.

Moreover the feedback provided by the robot is similar to the social cues that humans might use when teaching another person, have the advantage of giving the user an intuitive understanding of the robot’s limits. This might well compensate for a lack of prior knowledge, while keeping the user focused and motivated in the interaction for longer periods of time.

### Limitations of the provided feedback

The different ways of providing feedback that we explored in this study convey different types of information and thus make use of user’s attention in different ways. In the case of *verbal feedback* we provide auditory information in the form of specific instructions such as: ”you should press more”, ”make sure all fingers are in contact” or ”move this finger more”. This made it easy for the subject to focus on the demonstration, while following instructions. It also gave the subjects more confidence when maneuvering the robot and it might be the reason why the verbal feedback yielded the best results. However this setup makes the user dependent on an external expert, present at all times, which is unpractical in the real world.

*GUI feedback* makes use of visual information provided on a screen. This makes the subject switch from looking at the robot’s hand to looking at the screen. Some subjects chose to look mostly at the screen while blindly driving the robot’s finger joints. This made them report a low mental and physical demand. Additionally this setup favoured obtaining the best values for the contact times compared to the rest of the setups. This was due to the fact that the contact information was conveyed directly, with a high granularity. The pressure information could be visualized on 255 levels of corresponding to different shades of red, for each of the 12 taxels on each fingertip. Also visualizing the taxels individually (grouped by fingertip) gave the subject an idea about the area of contact of each finger and how this shifted when the finger joints moved. However the fact that the subjects tended to ignore looking at the robot’s hand was reflected in a higher joint shakiness and the fact that the grasps were not always optimal for the task. This increased the subjects’ frustration when testing the obtained model. Additionally the *GUI feedback* required technical knowledge and understanding of the mapping of touch sensors to the displayed interface. However this was mostly intuitive for the participants in our study since they mostly had an engineering background.

The *facial feedback* setup also makes use of the subject’s visual attention. In this case the subject has to switch from looking downwards to the robot’s hand to looking upwards to the robot’s face. This proved to be difficult for most subjects, and this was reflected in perceiving a higher physical and mental demand. Moreover the granularity of the feedback was lower in this case compared to the *GUI feedback*. Few expressions were used (thus leading to a lower granularity of the feedback), each of them corresponded to a range of possible contact values. This aspect might have influenced the *time in contact* metrics. Nevertheless, the feedback was intuitive and engaging, according to the subjects.

Lastly, in the case of *GUI* and *facial feedback* the complexity of the interaction is increased by the fact that the subject needs to take decisions on their own (such as which joints to move, how hard to press etc.), based on the feedback provided, unlike the case of verbal feedback where they mostly follow instructions or corrective feedback given by the experimenter.

## 5.7 Conclusions

---

We conducted a user study in which we contrasted 4 conditions: *no feedback*, *verbal feedback* provided by a knowledgeable user, *GUI feedback* displaying a realtime map of the tactile contacts and the current pressure intensity, and *robot-provided feedback* through facial displays of emotion correlated with the intensity of the tactile sensing. The facial displays were initially validated through another user study in which 20 emotions were tested and the 4 best recognized ones were chosen to be used for providing feedback.

The results showed that both the verbal feedback and robot feedback proved to be effective ways of making the user aware of the state of the robot and thus improving the quality of the demonstrations. Additionally the robot provided feedback kept the users engaged throughout the interaction, improving ratings of subjective metrics regarding the perceived easiness to use the system and their satisfaction with using the system.

Future work in the direction of using social cues in PbD should address the question of what is the optimum level of feedback that should be provided to the user. Particularly in our experiment mapping facial displays to how strong the contact on the fingertips was had a great impact on improving the time the fingers were in contact. However this was not enough for our task success since the task also required exploring the range of motion. Therefore mapping the range of motion to another social cue, such as voice or hand gestures done with the other hand, might have increased the task success rate even further. Subsequently task performance could be improved by assessing how the type of feedback influences the users’ approach of the task. Namely providing feedback to systematically guide the users’ training and testing could lead to an improved robot performance.

# CONCLUSIONS

## 6.1 Contributions

---

Throughout this thesis we have described approaches for automatically obtaining and using constraint-based task representations for facilitating robot's control and improving the interaction with the user. To summarize, this thesis described 4 contributions regarding task representation and user interaction:

---

### CONTRIBUTIONS WITH RESPECT TO TASK REPRESENTATION

---

**Bootstrapping unimanual and bimanual constraints.** From kinesthetic demonstrations of tasks we extracted the action sequence and soft constraints that parameterized a Cartesian impedance controller, obtaining a hybrid decomposition into force and position control in the object frame. Embedding the constraints in realtime during execution allowed the robot to adapt to changing conditions, such as different positions of the objects, of the arms or slight changes in the tools being used (i.e. grating on different surfaces). We extended this framework to bimanual tasks by studying coordination as relationships between the constraints of each arm. We used the constraint-based representation to execute the task autonomously.

**Collaborative execution based on the task constraints.** We extended the constraint-based representation obtained previously to be used in collaborative tasks, when a robot would execute the role of the master or of the slave in physical collaboration with a human user. We tracked the state of the human hand using a glove and tactile sensors and we predicted human intention by analyzing if the way the user manipulated the tool was aligned with the task constraints.

---

### CONTRIBUTIONS WITH RESPECT TO USER INTERACTION

---

**Automatic user performance assessment in manipulation tasks** We used the constraint-based representation for assessing user performance and

determining skilled and unskilled users. We quantified the performance by analyzing the way users manipulated the tool in relation to the task constraints. The analysis was performed directly on demonstration data, thus allowing the robot to selectively learn parts of the task from different users, which resulted in improved performance during autonomous execution.

**Sustained interaction dynamics through robot feedback** We provided the robot the ability to express its state relative to an important task variable (fingertip pressure in this case) as feedback provided to the user through various modalities such as facial displays of emotion, or GUI rendering. We contrasted these modalities with a no-feedback and a verbal feedback provided by a human and evaluate the outcome of the teaching interaction in a user study. Results showed that the feedback provided improved the quality of the demonstrations, as well as the user experience.

## 6.2 Limitations

---

### Offline vs. online performance

One of the main limitations of this work is the fact that the extraction of constraints and model encoding are performed offline, after enough demonstrations have been collected. While this gives reliable results, still it make the overall time required for acquiring a task to be quite significant, leaving the robot unable to react to the user’s action or to perform another task during this interval.

### Constraints on the demonstrations

The approach described in this paper requires the demonstrations to include all the necessary actions performed in the same order, for the variance based analysis to work. This requirement is constraining for the user who has to repeat the same sequence of actions multiple times. It also structures the way tasks need to be performed which is not a typical human behavior. Moreover the demonstrations are not put in the context of more complex tasks and are mostly performed using the same or slightly different tools and objects. We extract the task constraints without having an explicit model of the object makes the representation generic, however the extracted reference frame links the current action with an object.

### Problems posed by the experimental setups

Our approaches facilitate human interaction but depend heavily on the possibility to accurately observe the motion of the human. Most of the setups used in this work are custom made, requiring combining different sensors, instead

of being more self-contained. This makes them impractical and hard to integrate in daily life, and sometimes even difficult for the user to maneuver when demonstrating a task.

### Performing experiments with naive subjects

Oftentimes users on one hand have their own mental representations of a task, and on the other hand they lack a representation of the robot capabilities. Asking them to do a particular task might lead to a different performance than what was expected in the experiment. For example in the *grasp adaptation experiment* (Chapter 5) some users preferred demonstrating the task while guiding the robot’s hand with just one of their hands. This leads to severely limiting the range of motion that can be explored due to the limitations of the human hand. Similarly in the vegetable scooping experiment the users preferred holding the tool in ways that were familiar to them, even if that led to changing the task completely (i.e. performing scraping instead of scooping). This behavior is more likely to occur in real world interactions and thus algorithms should be able to handle these situations.

Furthermore, subjects are not always good at performing self-assessment. This was the case when we asked the subjects to assess their own skill in recognizing robot displayed emotions (Chapter 5) or to assess their performance in demonstrating the scooping task (Chapter 4). This factor might influence the way the users perceive the interaction and the robot’s performance.

## 6.3 Future Work

---

While our proposed constraint-based task representation provided useful knowledge about daily activities here we highlight potential improvements and future directions.

### REASONING WITH CONSTRAINTS

---

One of the first fundamental improvements would be to provide the robot the ability to segment and extract task constraints online, while incrementally observing multiple demonstrations. Secondly the constraints could serve not only in executing a task, but also in the high-level planning of a task that consists of multiple subtasks. For example a humanoid robot could properly position itself for executing a task that requires its arms to apply a force; could allocate unimanual tasks to each arm independently, and could reason about the required resources for completing complex tasks.

The task constraints together with information about the objects could be used to disambiguate between the use of different objects for similar purposes (such as mixing in a bowl, a glass or a pan). Also a constraint-representation

of a task could be parameterized and used in a different context, such as mixing ingredients in a bowl and egg beating. The two tasks are very similar in nature, they both require a mixing motion while maintaining a vertical contact with the bowl, however the mixing speed is different, and the task goal (or success metric) is also different.

Moreover knowing the task constraints could allow a robot to arbitrarily allocate parts of the task to multiple arms while enforcing the multi-arm coordination. For example in the task of mixing ingredients in a bowl the holding and mixing actions are continuous while the task might require the mixing arm to stop and to pour additional ingredients. These discrete operations could be allocated to a different arm. Additionally there are cases in which a single arm might not manage to fulfil the task constraints, such as opening a bag or a drawer. A second arm could be used for achieving the task goal.

Lastly knowing the constraints of a task the robot could acquire additional data by passively observing the users perform task and linking the observed behavior with the effects on the environment, on the objects, or on following the task sequence.

---

#### USER PROFILING FOR CUSTOMIZED INTERACTION

---

Different users might perform the same task in a different way, by choosing different objects, different tools, or using them in a different way. Differences across users might be significant and might showcase preferences in performing the task. Allowing the robot to associate knowledge about the task constraints with user preferences could facilitate a customized interaction and on the long term lead to an increased user satisfaction.

---

#### TASK ASSISTANCE AND TRAINING

---

Lastly, having a constraint-based representation of the task could allow the robot to train a naive user in performing it well, by reinforcing the constraints during training phases. Alternatively the robot could provide assistance to users suffering from various disabilities affecting the proper functioning of the arms, by ensuring that the task constraints are properly used (e.g. applying more force in parts of the task where the user is not able to do this). This behavior could also lead to initiative tasking in collaborative tasks.

---

## 6.4 Final Words

---

We conclude by highlighting several aspects of robot behavior that prove indispensable for a meaningful a long-term interaction with human users.

#### COMPREHENSIVE VIEW OF THE DAILY ACTIVITIES

---

A robot in a domestic environment needs to have a comprehensive understanding of the activities that are routinely performed and the way their goals are achieved. In daily activities humans rarely perform all the actions in a task or execute them in the same order. More often tasks are done in parallel, mixing actions that serve different goals. Therefore tasks can be represented on different levels of granularity. For example cutting an onion requires a sequence of atomic actions such as reaching, grabbing a knife, removing the skin, cutting etc. However cutting the onion task can be part of making a salad which can contribute to cooking dinner, or even to a bigger long term task such as house holding. The robot needs to be able to reason not in isolation on small tasks, but switch between these levels of granularity, schedule, plan and develop long-term strategies.

#### ADAPTABILITY AND INITIATIVE TAKING

---

Humans behavior is flexible and adaptive. People often find creative uses for old tools to make them serve new purposes. For example a spoon can be used for mixing in a cup of tea, but when this is not at hand the task can be done with a kitchen knife or even a letter opening knife. A robot needs to be able to show the same level of adaptation and flexibility. This aspect is particularly important since lay users expect robots to be able to perform actions that extend far beyond their current capabilities.



## APPENDIX. INITIAL VIDEO RATING FOR THE USER STUDY IN CHAPTER 4

An initial video rating was performed by 10 persons (5 male, 5 female). The aim was to obtain a performance rating for each demonstration. However the question used to assess this aspect ("How well did this person perform the current trial?") was confusing for the raters. In order to not influence the raters they were not given a clear definition of what was a "skilled performance" assessed here. This led to raters having a lower agreement rate for this aspect as some of them gave a rating based on the scooped quantity, while others looked at how the task was performed. However they had a rather high agreement rate on other questions (such as identifying the task pace or indicating if too much or too little force was applied). We present these results below and discuss subgroups of subject for which the agreement rates were higher.

### 7.1 Video rating assessment

---

The video rating was performed in 2 cases: 5 raters were shown the demonstrations in random order, and 5 raters were shown the demonstrations ordered per subject. In each case 2 participants rated the full sequence of demonstrations, while 3 were given batches of one third of the total demonstrations. Therefore each video has received 3 ratings for each rating case for a total of 2964 total ratings.

The rating of each demonstration involved 4 questions:

1. How well did this person perform the current trial?  
(scale 1 (very bad) to 5 (very well))
2. How was the task pace  
(too slow/normal/too fast)
3. Were there problems with the following aspects:
  - arm coordination (yes/no)
  - grasping the tool (yes/no)
  - direction of movement (yes/no)
4. The applied force was: too little/normal/too much

The raters shown the demonstrations in order, also had to rate the overall performance for each subject:

1. Overall performance (5 level Likert scale)
2. Did this subject improve over trials? (yes/no)
3. Could this subject manage the setup well? (yes/no)

## 7.2 Video rating results

---

### Ratings per demonstration

The average skill rating from videos was  $2.69 \pm 1.10$ . Out of the total 2964 ratings 282 were very low performance, 757 low performance, 960 medium, 716 high, and 249 very high. The rating case (random or ordered) affected the performance rating ( $F(1, 2963) = 128.32, p < 0.001$ ), such that the raters seeing the demonstrations in order attributed lower scores per demonstration ( $2.74 \pm 1.08$ ) than those seeing them randomly  $3.18 \pm 1.06$ . Averaged per demonstration 10 were marked as very low performance, 120 as low, 213 as medium, 144 as high and 7 as very high.

The average inter-rater agreement for attributing a skill level was Cohen's kappa 0.33. The highest agreement rate was 0.73 for determining coordination problems. In the case of observing grasping problems kappa was 0.66, however the agreement was higher in the case of skilled rather than unskilled subjects. Movement problems were easier to detect in unskilled subjects (kappa = 0.64). The raters also agreed more on estimating the applied force of the skilled subjects (kappa = 0.67). Results are summarized in Table 7.1.

The attributed skill is correlated with the estimated level of force ( $r = 0.43$ ). However this estimation of force from video rating was also correlated with the actual force ( $r = 0.32$ ) and the torque ( $r = 0.31$ ) applied across the direction of interest in the task, suggesting that raters could have a good understanding of the task performance only by analyzing video recordings. The skill rating had a significant effect on all the other measures: task pace ( $F(1, 492) = 11.60, p < 0.001$ ), identifying coordination problems ( $F(1, 492) = 43.24, p < 0.001$ ), grasping problems ( $F(1, 492) = 30.29, p < 0.001$ ), movement problems ( $F(1, 492) = 29.28, p < 0.001$ ) and estimating force applied ( $F(1, 492) = 31.29, p < 0.001$ ).

Grasping problems were commonly identified among demonstrations previously rated as *low* and *very low* performance. In the case of medium and high skilled performance problems were mostly related to the direction of movement (Fig. 7.1a). The 3 types of problems also affected the pace ( $F(1, 492) = 25.17, p < 0.05$ ) and force estimated by the raters ( $F(1, 492) = 9.88, p < 0.05$ ), such

	Cohen's kappa		
	all subjects	skilled	unskilled
Skill	0.34	0.35	0.34
Task pace	0.64	0.63	0.65
Coordination problems	0.74	0.74	0.74
Grasping problems	0.66	0.73	0.64
Movement problems	0.63	0.60	0.64
Estimated force	0.63	0.67	0.61

**Table 7.1** Inter-rater agreement for the video assessment. We highlight agreement values greater than 0.65.

that identified problems led to a lower force rating and a lower task pace (see Fig. 7.1).

Identified problems in the movement were correlated with a higher number of subsegments ( $F(1, 492) = 8.02, p < 0.05$ ). Problems in grasping were correlated with applying a higher force in the directions which were not important for the task ( $F(1, 492) = 7.03, p < 0.05$ ), and lower force on the direction of interest ( $F(1, 492) = 3.41, p = 0.06$ ).

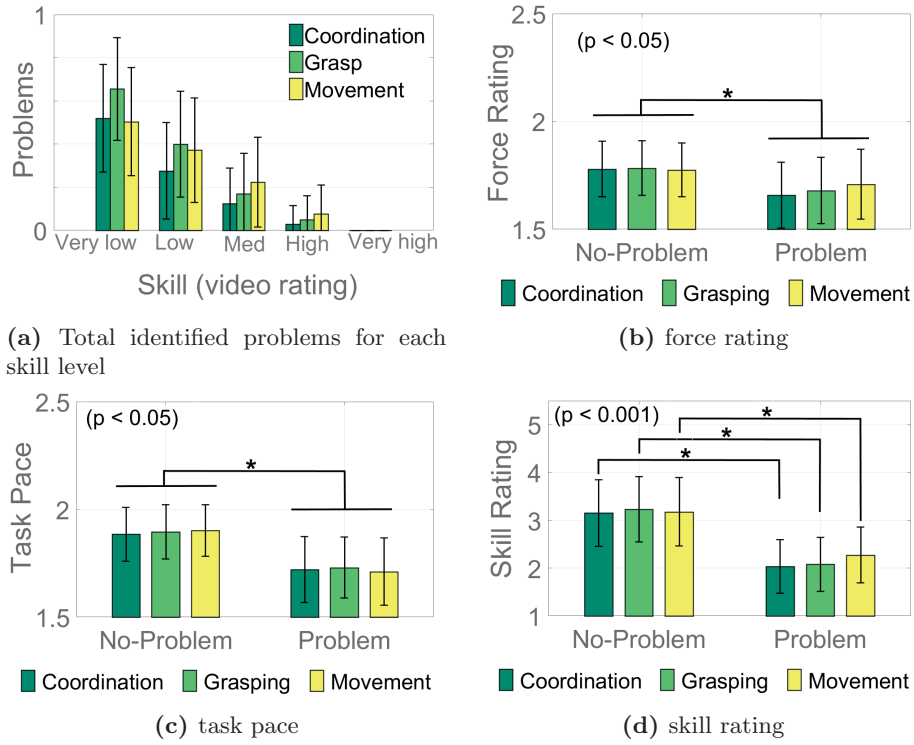
### Ratings per subject

Five video raters watched the sequence of demonstrations in order for each subject. At the end they had to rate the overall performance of that subject. Two of the raters watched the full sequence of demonstrations for all subjects. Each of the following 3 raters watched only a batch of videos corresponding to 12 subjects (for batches 1 and 2) and 13 subjects for batch 3. Each batch contained 3 skilled subjects (as rated automatically) while the rest were unskilled.

We compute the inter-rater agreement (Cohen Kappa) between each 2 raters when taking into account their rating of all subjects, or of subjects only in a given batch, for assigning a level of skill, assessing the subject's improvement over trials and the subject's ability to manage the setup (see Table 7.2 for full results).

For the skill level and taking into account all subjects, the highest agreement rate observed was 0.41 between raters 2 and 3. Looking at individual batches we notice that the agreement rates improve over batches (average 0.30 for batch 1, 0.43 for batch 2 and 0.45 for batch 3). The highest observed agreement was 0.54 between raters 1 and 2 for the second batch.

The generally low agreement rates could be explained by two factors. Firstly no instructions were given to the raters on what a successful scoop was. Therefore the raters were expected to have an internal understanding and representation of the task, the actions required to perform it and the result that should be observed. Differences in this representation led too raters looking at var-



**Figure 7.1** Identified problems are reflected in lower ratings of the estimated force, task pace and skill. Issues in movement affect mostly the force and skill rating, while grasping issues affect the task pace

Cohen's kappa					
	Raters	all subjects	batch 1	batch 2	batch 3
Skill	$R_1 - R_2$	0.33	0.27	0.54	0.45
	$R_1 - R_3$	0.37	0.18	0.33	0.44
	$R_2 - R_3$	0.41	0.45	0.41	0.45
	average	0.37	0.30	0.43	0.45
Improvement	$R_1 - R_2$	0.32	0.36	0.30	0.30
	$R_1 - R_3$	0.56	0.45	0.46	0.76
	$R_2 - R_3$	0.32	0.36	0.38	0.23
	average	0.40	0.39	0.38	0.43
Manage setup	$R_1 - R_2$	0.64	0.63	0.61	0.69
	$R_1 - R_3$	0.62	0.63	0.53	0.69
	$R_2 - R_3$	0.70	0.81	0.61	0.69
	average	0.65	0.69	0.58	0.69

**Table 7.2** Inter-rater agreement evaluating the full performance of a subject. We highlight agreement values greater than 0.50.

		Cohen's kappa					
		Raters	all subjects		batch 1	batch 2	batch 3
			skilled	unskilled	unskilled	unskilled	unskilled
Video rating assessment	Skill	$R_1 - R_2$	0.25	0.35	0.25	0.55	0.37
		$R_1 - R_3$	0.33	0.44	0.12	0.33	0.50
		$R_2 - R_3$	0.16	0.48	0.50	0.50	0.55
		average	0.25	0.42	0.29	0.46	0.47
	Improvement	$R_1 - R_2$	0.50	0.39	0.50	0.40	0.30
		$R_1 - R_3$	0.55	0.57	0.50	0.50	0.70
		$R_2 - R_3$	0.50	0.25	0.25	0.30	0.20
		average	0.50	0.40	0.41	0.40	0.40
	Manage setup	$R_1 - R_2$	0.77	0.60	0.50	0.60	0.70
		$R_1 - R_3$	0.77	0.57	0.50	0.40	0.80
		$R_2 - R_3$	0.77	0.67	0.75	0.60	0.70
		average	0.77	0.61	0.58	0.53	0.73

**Table 7.3** Inter-rater agreement for the subjects overall performance when considering subgroups of skilled or unskilled users as marked by our automatic analysis. We highlight agreement values greater than 0.50.

ious aspects: the amount that was scooped, the confidence that the subject displayed when performing the task, and not necessarily the fluidity and ease of the motion. Similarly the subjects were not given specific instructions on how to perform the task, which resulted in a multitude of approaches, ranging from holding the tool in a different way to different strategies in performing the motion. Secondly the fact that the agreement rate increased over batches is an indication that the raters needed many examples of the task as a "calibration" step to even their expectations.

Higher agreement rates were observed when estimating the subject's ability to improve over trials, with the highest values of 0.76 between raters 1 and 3 for the third batch of subjects.

The highest agreement rates were obtained for rating the subject's ability to manage the setup (all values are above 0.5 in this case). The highest value is 0.81 as the agreement between raters 2 and 3 for batch 1. This is an indication of the fact that despite the considerable equipment involved the raters were able to consistently pinpoint problems related to the setup and alongside the task execution.

We further analyze the agreement rate between all the pairs of raters when considering subgroups of skilled or unskilled users as marked by our automatic analysis (see Table 7.3).

The agreement rate between the video raters was higher when assigning a skill level or assessing the improvement for the subjects labeled as unskilled by

our approach, than those labeled as skilled (highest agreement rates 0.48, and 0.57 respectively). For the ability to manage the setup the inverse trend was observed. It was easier to rate the skilled subjects (average kappa value 0.77) than the unskilled ones (average kappa value 0.61).

For the individual batches we analyzed the agreement rates only for the subjects labeled as unskilled. For both the video raters assigned skill and the improvement over trials the highest agreement rate was observed for batch 3, confirming our previous observation that raters actually need many examples of the task to even their expectations. Similarly the ability to manage the setup was better estimated for batch 3, with the maximum agreement rate of 0.80.

We do not present the results of the agreement rate for the skilled subjects in batches, as there were only 3 skilled subjects in each batch. However a notable exception was a Cohen’s kappa value of 1.00 obtained as agreement in rating the skill between raters 2 and 3 for batch 2.

On a level of 1 (very low) to 5 (very high) the raters marked 1 subject as very low performance, 12 as low, 16 as medium, 8 as high, and 0 as very high. The overall performance was correlated with the skill computed from sensor metrics ( $r = 0.36$ ) and with the scooped weight ( $r = 0.44$ ), but only weakly correlated with the subjects self-assessed skill ( $r = 0.16$ ).

On average 19 users were considered to have improved over trials, while 18 did not. Rating a subject as better over trials was linked with the subject’s own perception of the task as being easy to teach ( $r = 0.27$ ), and with the TLX stress factor ( $r = 0.38$ ).

The raters appreciated that 27 users did not have any problem manipulating the setup, while 10 might have had. The ability to manage the setup well was directly correlated with the grasping quality across the torque direction ( $r = 0.4$ ), as well as with the stiffness of the robot arm holding the mellon ( $r = 0.25$ ), and the stiffness of the arm maneuvering the tool ( $r = 0.20$ ).

We then corroborated the setup management with the user’s self assessment. Giving the impression that a subject can manage the setup was linked to a lower need of technical support ( $r = 0.20$ ), the TLX success factor ( $r = 0.22$ ), and the TLX effort factor ( $r = 0.24$ ). Additionally the users able to manage the setup completed the task on average in 12.47s, compared to 17.32s for those who did not.

---

## REFERENCES

- Abadi, M., A. Agarwal, P. Barham, E. Brevdo, Z. Chen, C. Citro, G. S. Corrado, A. Davis, J. Dean, M. Devin, et al. Tensorflow: Large-scale machine learning on heterogeneous distributed systems. *arXiv preprint arXiv:1603.04467*, 2016.
- Akgun, B. and A. Thomaz. Simultaneously learning actions and goals from demonstration. *Autonomous Robots*, 40(2):211–227, 2016. ISSN 1573-7527. doi: 10.1007/s10514-015-9448-x. URL <http://dx.doi.org/10.1007/s10514-015-9448-x>.
- Allavena, R. E., A. B. Schaffer-White, H. Long, and J. I. Alawneh. Technical skills training for veterinary students: A comparison of simulators and video for teaching standardized cardiac dissection. *Journal of Veterinary Medical Education*, 5(5):1–12, 2017. doi: 10.3138/jvme.0516-095R. URL <https://doi.org/10.3138/jvme.0516-095R>. PMID: 28581914.
- Alotaibi, M. and I. Choudhury. A social robotics children diabetes management and educational system for saudi arabia: System architecture. In *2015 Second International Conference on Computer Science, Computer Engineering, and Social Media (CSCESM)*, pages 170–174, Sept 2015. doi: 10.1109/CSCESM.2015.7331888.
- Amershi, S., M. Cakmak, W. B. Knox, and T. Kulesza. Power to the people: The role of humans in interactive machine learning. *AI Magazine*, 35(4): 105–120, 2014. URL <http://www.aaai.org/ojs/index.php/aimagazine/article/view/2513>.
- Argall, B., B. Browning, and M. Veloso. *Learning by demonstration with critique from a human teacher*, pages 57–64. 9 2007. ISBN 1595936173. doi: 10.1145/1228716.1228725.
- Argall, B. D., B. Browning, and M. M. Veloso. Teacher feedback to scaffold and refine demonstrated motion primitives on a mobile robot. *Robotics and Autonomous Systems*, 59(3):243 – 255, 2011. ISSN 0921-8890. doi: <https://doi.org/10.1016/j.robot.2010.11.004>. URL <http://www.sciencedirect.com/science/article/pii/S0921889010001971>.
- Arsenio, A. Learning task sequences from scratch: applications to the control of tools and toys by a humanoid robot. In *Control Applications, 2004. Proceedings of the 2004 IEEE International Conference on*, volume 1, pages 400–405 Vol.1, 2004. doi: 10.1109/CCA.2004.1387244.
- Asfour, T., P. Azad, F. Gyarfas, and R. Dillmann. Imitation learning of dual-arm manipulation tasks in humanoid robots. *International Journal of Humanoid Robotics*, 05(02):183–202, 2008. doi: 10.1142/S0219843608001431.

- Atashzar, S. F., M. Shahbazi, F. Rahimi, M. Delrobaei, J. Lee, R. V. Patel, and M. Jog. Effect of kinesthetic force feedback and visual sensory input on writer's cramp. In *2013 6th International IEEE/EMBS Conference on Neural Engineering (NER)*, pages 883–886, Nov 2013. doi: 10.1109/NER.2013.6696076.
- Bartneck, C., J. Reichenbach, and A. V. Breemen. In your face, robot! the influence of a character's embodiment on how users perceive its emotional expressions. In *In Design and Emotion 2004 Conference*, 2004.
- Basoeki, F., F. DallaLibera, and H. Ishiguro. How do people expect humanoids to respond to touch? *International Journal of Social Robotics*, 7(5):743–765, 2015. ISSN 1875-4805. doi: 10.1007/s12369-015-0318-7. URL <http://dx.doi.org/10.1007/s12369-015-0318-7>.
- Becker-Asano, C. and H. Ishiguro. Evaluating facial displays of emotion for the android robot geminoid F. In *2011 IEEE Workshop on Affective Computational Intelligence, WACI 2011, Paris, France, April 14, 2011*, pages 22–29, 2011. doi: 10.1109/WACI.2011.5953147. URL <http://dx.doi.org/10.1109/WACI.2011.5953147>.
- Beetz, M., L. Mösenlechner, and M. Tenorth. CRAM – A Cognitive Robot Abstract Machine for Everyday Manipulation in Human Environments. In *IEEE/RSJ International Conference on Intelligent Robots and Systems.*, 2010.
- Bennewitz, M., W. Burgard, G. Cielniak, and S. Thrun. Learning motion patterns of people for compliant robot motion. *International Journal of Robotics Research*, 24:31–48, 2005.
- Berthet-Rayne, P., M. Power, H. King, and G. Z. Yang. Hubot: A three state human-robot collaborative framework for bimanual surgical tasks based on learned models. In *2016 IEEE International Conference on Robotics and Automation (ICRA)*, pages 715–722, May 2016. doi: 10.1109/ICRA.2016.7487198.
- Bianchi, M., G. Valenza, A. Lanata, A. Greco, M. Nardelli, A. Bicchi, and E. P. Scilingo. On the role of affective properties in hedonic and discriminant haptic systems. *International Journal of Social Robotics*, 9(1):87–95, 2017. ISSN 1875-4805. doi: 10.1007/s12369-016-0371-x. URL <http://dx.doi.org/10.1007/s12369-016-0371-x>.
- Bicchi, A. On the closure properties of robotic grasping. *The Int. J. of Robotics Research*, 14(4):319–334, 1995.
- Bobick, A. F. and A. D. Wilson. A state-based approach to the representation and recognition of gesture. *IEEE TRANSACTIONS ON PATTERN ANALYSIS AND MACHINE INTELLIGENCE*, 19:1325–1337, 1997.
- Borst, C., M. Fischer, and G. Hirzinger. A fast and robust grasp planner for arbitrary 3d objects. In *Robotics and Automation, 1999. Proceedings. 1999 IEEE International Conference on*, volume 3, pages 1890–1896 vol.3, 1999. doi: 10.1109/ROBOT.1999.770384.
- Breazeal, C. Role of expressive behaviour for robots that learn from people. *Philosophical Transactions of the Royal Society B*, 364:3527–3538, 2009.

- Breazeal, C., A. Brooks, J. Gray, G. Hoffman, C. Kidd, H. Lee, J. Lieberman, A. Lockerd, and D. Chilongo. Tutelage and collaboration for humanoid robots. *International Journal of Humanoid Robotics*, 01(02):315–348, 2004. doi: 10.1142/S0219843604000150. URL <http://www.worldscientific.com/doi/abs/10.1142/S0219843604000150>.
- Brooke, J. SUS - a quick and dirty usability scale. In *Usability Evaluation in Industry*, pages 189–194, 1996a.
- Brooke, J. SUS - a quick and dirty usability scale. In *Usability Evaluation in Industry*, pages 189–194, 1996b.
- Cabibihan, J., M. C. Carrozza, P. Dario, S. Pattofatto, M. Jomaa, and A. Benallal. The uncanny valley and the search for human skin-like materials for a prosthetic fingertip. In *2006 6th IEEE-RAS International Conference on Humanoid Robots*, pages 474–477, Dec 2006. doi: 10.1109/ICHR.2006.321315.
- Cabibihan, J.-J., I. Ahmed, and S. S. Ge. Force and motion analyses of the human patting gesture for robotic social touching. In *2011 IEEE 5th International Conference on Cybernetics and Intelligent Systems (CIS)*, pages 165–169, Sept 2011. doi: 10.1109/ICCIS.2011.6070321.
- Cakmak, M. and L. Takayama. Teaching people how to teach robots: The effect of instructional materials and dialog design. In *Proceedings of the 2014 ACM/IEEE International Conference on Human-robot Interaction, HRI '14*, pages 431–438, New York, NY, USA, 2014. ACM. ISBN 978-1-4503-2658-2. doi: 10.1145/2559636.2559675. URL <http://doi.acm.org/10.1145/2559636.2559675>.
- Cakmak, M. and A. L. Thomaz. Designing robot learners that ask good questions. In *Proceedings of the Seventh Annual ACM/IEEE International Conference on Human-Robot Interaction, HRI '12*, pages 17–24, New York, NY, USA, 2012a. ACM. ISBN 978-1-4503-1063-5. doi: 10.1145/2157689.2157693.
- Cakmak, M. and A. L. Thomaz. Eliciting good teaching from humans for machine learners. *Artificial Intelligence*, 217:198 – 215, 2014a. ISSN 0004-3702. doi: <http://dx.doi.org/10.1016/j.artint.2014.08.005>.
- Cakmak, M. and A. L. Thomaz. Eliciting good teaching from humans for machine learners. *Artificial Intelligence*, 217:198 – 215, 2014b. ISSN 0004-3702. doi: <http://dx.doi.org/10.1016/j.artint.2014.08.005>. URL <http://www.sciencedirect.com/science/article/pii/S0004370214001143>.
- Cakmak, M. and A. L. Thomaz. Designing robot learners that ask good questions. In *HRI*, pages 17–24, 2012b.
- Cakmak, M., N. DePalma, R. I. Arriaga, and A. L. Thomaz. Exploiting social partners in robot learning. *Autonomous Robots*, 29(3):309–329, 2010. ISSN 1573-7527. doi: 10.1007/s10514-010-9197-9. URL <http://dx.doi.org/10.1007/s10514-010-9197-9>.
- Calinon, S. and A. Billard. What is the Teacher’s Role in Robot Programming by Demonstration? - toward Benchmarks for Improved Learning. *Interaction Studies. Special Issue on Psychological Benchmarks in Human-Robot Interaction*, 8(3), 2007a.

- Calinon, S. and A. Billard. What is the teacher’s role in robot programming by demonstration? - Toward benchmarks for improved learning. *Interaction Studies. Special Issue on Psychological Benchmarks in Human-Robot Interaction*, 8(3):441–464, 2007b.
- Calinon, S. and A. Billard. Active teaching in robot programming by demonstration. In *RO-MAN 2007 - The 16th IEEE International Symposium on Robot and Human Interactive Communication*, pages 702–707, Aug 2007c. doi: 10.1109/ROMAN.2007.4415177.
- Calinon, S., F. Guenter, and A. Billard. On Learning the Statistical Representation of a Task and Generalizing it to Various Contexts. In *Proceedings of the IEEE International Conference on Robotics and Automation (ICRA)*, pages 2978–2983, 2006.
- Calinon, S., F. Guenter, and A. Billard. On learning, representing and generalizing a task in a humanoid robot. *IEEE Transactions on Systems, Man and Cybernetics, Part B. Special issue on robot learning by observation, demonstration and imitation*, 37(2):286–298, 2007.
- Calinon, S., I. Sardellitti, and D. Caldwell. Learning-based control strategy for safe human-robot interaction exploiting task and robot redundancies. In *Intelligent Robots and Systems (IROS), 2010 IEEE/RSJ International Conference on*, pages 249–254, 2010.
- Calinon, S., Z. Li, T. Alizadeh, N. G. Tsagarakis, and D. G. Caldwell. Statistical dynamical systems for skills acquisition in humanoids. In *2012 12th IEEE-RAS International Conference on Humanoid Robots (Humanoids 2012)*, pages 323–329, Nov 2012. doi: 10.1109/HUMANOIDS.2012.6651539.
- Calinon, S. *Continuous extraction of task constraints in a robot programming by demonstration framework*. PhD thesis, EPFL, July 2007.
- Chen, J. and A. Zelinsky. Programing by demonstration: Coping with suboptimal teaching actions. *The International Journal of Robotics Research*, 22(5): 299–319, 2003. doi: 10.1177/0278364903022005002.
- Chen, T. L., C.-H. King, A. L. Thomaz, and C. C. Kemp. Touched by a robot: An investigation of subjective responses to robot-initiated touch. In *Proceedings of the 6th International Conference on Human-robot Interaction, HRI ’11*, pages 457–464, New York, NY, USA, 2011. ACM. ISBN 978-1-4503-0561-7. doi: 10.1145/1957656.1957818. URL <http://doi.acm.org/10.1145/1957656.1957818>.
- Colomé, A. and C. Torras. *Computational Kinematics: Proceedings of the 6th International Workshop on Computational Kinematics (CK2013)*, chapter Positioning Two Redundant Arms for Cooperative Manipulation of Objects, pages 121–129. Springer Netherlands, Dordrecht, 2014. ISBN 978-94-007-7214-4. doi: 10.1007/978-94-007-7214-4\_14.
- Coninx, A., P. Baxter, Elettra, Oleari, S. Bellini, B. Bierman, O. B. Henkemans, L. Canamero, P. Cosi, V. Enescu, R. R. Espinoza, A. Hiolle, R. Humbert, B. Kiefer, I. Kruijff-Korabayov, R. Looije, M. Mosconi, M. Neerincx, G. Paci, G. Patsis, C. Pozzi, F. Sacchitelli, H. Sahli, A. Sanna, G. Somavilla, F. Tesser, Y. Demiris, and T. Belpaeme. Towards long-term social child-robot interaction: Using multi-activity switching to engage young users. *Journal of Human-Robot Interaction*, o.A.:o.A., 2016. In press.

- Corrigan, L. J., C. Basedow, D. Kster, A. Kappas, C. Peters, and G. Castellano. Perception matters! engagement in task orientated social robotics. In *2015 24th IEEE International Symposium on Robot and Human Interactive Communication (RO-MAN)*, pages 375–380, Aug 2015. doi: 10.1109/ROMAN.2015.7333665.
- Cramer, H., J. Goddijn, B. Wielinga, and V. Evers. Effects of (in)accurate empathy and situational valence on attitudes towards robots. In *Proceedings of the 5th ACM/IEEE international conference on Human-robot interaction*, pages 141–142, 2010.
- Dantam, N. and M. Stilman. The motion grammar: Analysis of a linguistic method for robot control. *IEEE Transactions on Robotics*, 29(3):704–718, 2013. ISSN 1552-3098.
- Dautenhahn, K. The art of designing socially intelligent agents - science, fiction and the human in the loop. *Applied Artificial Intelligence Journal, Special Issue on Socially Intelligent Agents*, 12:12–7, 1998.
- Dautenhahn, K. and I. Werry. Issues of robot-human interaction dynamics in the rehabilitation of children with autism, 2000.
- de Poel, H. J., C. L. E. Peper, and P. J. Beek. Intentional switches between bimanual coordination patterns are primarily effectuated by the nondominant hand. *Motor control*, 10(1):723, January 2006. ISSN 1087-1640. URL <http://europepmc.org/abstract/MED/16571905>.
- de Souza, R., S. El-Khoury, J. Santos-Victor, and A. Billard. Recognizing the grasp intention from human demonstration. *Robotics and Autonomous Systems*, 74, Part A:108 – 121, 2015. ISSN 0921-8890. doi: <http://dx.doi.org/10.1016/j.robot.2015.07.006>.
- Dergachyova, O., D. Bouget, A. Huaulmé, X. Morandi, and P. Jannin. Automatic data-driven real-time segmentation and recognition of surgical workflow. *International Journal of Computer Assisted Radiology and Surgery*, pages 1–9, 2016. ISSN 1861-6429. doi: 10.1007/s11548-016-1371-x.
- Dimitriou, M., D. W. Franklin, and D. M. Wolpert. Task-dependent coordination of rapid bimanual motor responses. *Journal of Neurophysiology*, 2011. ISSN 1522-1598.
- Ding, H., J. Heyn, B. Matthias, and H. Staab. Structured collaborative behavior of industrial robots in mixed human-robot environments. In *2013 IEEE International Conference on Automation Science and Engineering (CASE)*, pages 1101–1106, Aug 2013. doi: 10.1109/CoASE.2013.6653962.
- Dunn, J. L. Using learning preferences to improve coaching and athletic performance. *Journal of Physical Education, Recreation and Dance*, 80(3):30–37, 03 2009. URL <https://search.proquest.com/docview/215757787?accountid=27198>. Copyright - Copyright American Alliance for Health, Physical Education and Recreation Mar 2009; Document feature - Photographs; ; Last updated - 2016-07-23.
- El-Khoury, S., R. de Souza, and A. Billard. On computing task-oriented grasps. *Robot. Auton. Syst.*, 66(C):145–158, April 2015. ISSN 0921-8890. doi: 10.1016/j.robot.2014.11.016. URL <http://dx.doi.org/10.1016/j.robot.2014.11.016>.

- Elissa, W. Using a kinesthetic learning strategy to engage nursing student thinking, enhance retention, and improve critical thinking. *Journal of Nursing Education*, 53(6):348–351, June 2014. doi: doi:10.3928/01484834-20140512-02.
- Erden, M. S. and A. Billard. Hand impedance measurements during interactive manual welding with a robot. *IEEE Transactions on Robotics*, 31(1):168–179, Feb 2015. ISSN 1552-3098. doi: 10.1109/TRO.2014.2385212.
- Evrard, P., E. Gribovskaya, S. Calinon, A. Billard, and A. Kheddar. Teaching physical collaborative tasks: object-lifting case study with a humanoid. In *2009 9th IEEE-RAS International Conference on Humanoid Robots*, pages 399–404, Dec 2009. doi: 10.1109/ICHR.2009.5379513.
- Fasola, J. and M. J. Matarić. *Socially Assistive Robot Exercise Coach: Motivating Older Adults to Engage in Physical Exercise*, pages 463–479. Springer International Publishing, Heidelberg, 2013. ISBN 978-3-319-00065-7. doi: 10.1007/978-3-319-00065-7\_32. URL [http://dx.doi.org/10.1007/978-3-319-00065-7\\_32](http://dx.doi.org/10.1007/978-3-319-00065-7_32).
- Ferrand, L. and S. Jaric. Force coordination in static bimanual manipulation: effect of handedness. *Motor Control*, 10(4):359–370, Oct 2006.
- Ficuciello, F., L. Villani, and B. Siciliano. Variable impedance control of redundant manipulators for intuitive human robot physical interaction. *IEEE Transactions on Robotics*, 31(4):850–863, Aug 2015. ISSN 1552-3098. doi: 10.1109/TRO.2015.2430053.
- Figueroa, N. and A. Billard. On discovering structure in heterogeneous, unstructured and sequential tasks from demonstrations. In *In preparation for JMLR*, 2016.
- Forbes, M., M. J. Chung, M. Cakmak, and R. P. N. Rao. Robot programming by demonstration with crowdsourced action fixes. In *Proceedings of the Second AAAI Conference on Human Computation and Crowdsourcing, HCOMP 2014, November 2-4, 2014, Pittsburgh, Pennsylvania, USA*, 2014. URL <http://www.aaai.org/ocs/index.php/HCOMP/HCOMP14/paper/view/8975>.
- Franz, E. A., H. N. Zelaznik, and G. McCabe. Spatial topological constraints in a bimanual task. *Acta Psychologica*, 77(2):137 – 151, 1991. ISSN 0001-6918. doi: [http://dx.doi.org/10.1016/0001-6918\(91\)90028-X](http://dx.doi.org/10.1016/0001-6918(91)90028-X).
- Gielniak, M. J. and A. L. Thomaz. Spatiotemporal correspondence as a metric for human-like robot motion. In *Proceedings of the 6th international conference on Human-robot interaction*, pages 77–84, 2011.
- Giusti, L. and P. Marti. Interpretative dynamics in human robot interaction. In *Robot and Human Interactive Communication, ROMAN*, pages 111 –116, 2006.
- Gorniak, S. L. and J. L. Alberts. Effects of aging on force coordination in bimanual task performance. *Experimental Brain Research*, 229(2):273–284, 2013. ISSN 1432-1106. doi: 10.1007/s00221-013-3644-8.
- Gregg, M. J., J. O., and C. R. Hall. Examining the relationship between athletes’ achievement goal orientation and ability to employ imagery. *Psychology of Sport and Exercise*, 24:140 – 146, 2016. ISSN 1469-0292. doi: <http://dx.doi.org/10.1016/j.psychsport.2016.01.006>. URL <http://www.sciencedirect.com/science/article/pii/S1469029216300061>.

- Gribovskaya, E. and A. Billard. Combining dynamical systems control and programming by demonstration for teaching discrete bimanual coordination tasks to a humanoid robot. In *Human-Robot Interaction (HRI), 2008 3rd ACM/IEEE International Conference on*, pages 33–40, March 2008.
- Gribovskaya, E., A. Kheddar, and A. Billard. Motion learning and adaptive impedance for robot control during physical interaction with humans. In *Robotics and Automation (ICRA), 2011 IEEE International Conference on*, pages 4326–4332, 2011. doi: 10.1109/ICRA.2011.5980070.
- Grollman, D. H. and O. C. Jenkins. Dogged learning for robots. In *Proceedings 2007 IEEE International Conference on Robotics and Automation*, pages 2483–2488, April 2007. doi: 10.1109/ROBOT.2007.363692.
- Grollman, D. H. and A. G. Billard. Robot learning from failed demonstrations. *International Journal of Social Robotics*, 4(4):331–342, Nov 2012. ISSN 1875-4805. doi: 10.1007/s12369-012-0161-z. URL <http://dx.doi.org/10.1007/s12369-012-0161-z>.
- Grollman, D. H. and O. C. Jenkins. Incremental Learning of Subtasks from Unsegmented Demonstration. In *IEEE/RSJ International Conference on Intelligent Robots and Systems*, October 2010.
- Groten, R., D. Feth, H. Goshy, A. Peer, D. A. Kenny, and M. Buss. Experimental analysis of dominance in haptic collaboration. In *RO-MAN 2009 - The 18th IEEE International Symposium on Robot and Human Interactive Communication*, pages 723–729, Sept 2009. doi: 10.1109/ROMAN.2009.5326315.
- Guiard, Y. Asymmetric division of labor in human skilled bimanual action: the kinematic chain as a model. *J Mot Behav*, 19(4):486–517, Dec 1987.
- Guillot, A., C. Genevois, S. Desliens, S. Saieb, and I. Rogowski. Motor imagery and placebo-racket effects in tennis serve performance. *Psychology of Sport and Exercise*, 13(5):533 – 540, 2012. ISSN 1469-0292. doi: <http://dx.doi.org/10.1016/j.psychsport.2012.03.002>. URL <http://www.sciencedirect.com/science/article/pii/S1469029212000325>. A Sport Psychology Perspective on Olympians and the Olympic Games.
- Hall, E. T. *The Hidden Dimension: Man's Use of Space in Public and Private*. The Bodley Head Ltd, 1966.
- Han, M. J., C. H. Lin, and K. T. Song. Robotic emotional expression generation based on mood transition and personality model. *IEEE Transactions on Cybernetics*, 43(4):1290–1303, Aug 2013. ISSN 2168-2267. doi: 10.1109/TSMCB.2012.2228851.
- Hanson, D. Expanding the aesthetics possibilities for humanlike robots. In *Proc. IEEE "Humanoid Robotics" Conference, special session on the Uncanny Valley*, 2005.
- Hars, M. and C. Calmels. Observation of elite gymnastic performance: Processes and perceived functions of observation. *Psychology of Sport and Exercise*, 8(3):337 – 354, 2007. ISSN 1469-0292. doi: <http://dx.doi.org/10.1016/j.psychsport.2006.06.004>. URL <http://www.sciencedirect.com/science/article/pii/S1469029206000616>.

- Hart, S. G. and L. E. Staveland. Development of nasa-tlx (task load index): Results of empirical and theoretical research. *Advances in Psychology*, 52:139 – 183, 1988a. ISSN 0166-4115. doi: [http://dx.doi.org/10.1016/S0166-4115\(08\)62386-9](http://dx.doi.org/10.1016/S0166-4115(08)62386-9). Human Mental Workload.
- Hart, S. and L. Staveland. Development of nasa-tlx (task load index): Results of empirical and theoretical research. In *Human mental workload*, pages 139–183, 1988b.
- Hassenzahl, M., M. Burmester, and F. Koller. Attrakdiff: Ein fragebogen zur messung wahrgenommener hedonischer und pragmatischer qualität. In *Mensch & Computer 2003: Interaktion in Bewegung*, volume 196, page 187. B. G. Teubner, 2003.
- Hebert, P., N. Hudson, J. Ma, and J. W. Burdick. Dual arm estimation for coordinated bimanual manipulation. In *Robotics and Automation (ICRA), 2013 IEEE International Conference on*, pages 120–125, May 2013. doi: 10.1109/ICRA.2013.6630565.
- Hebesberger, D., T. Koertner, C. Gisinger, J. Pripfl, and C. Dondrup. Lessons learned from the deployment of a long-term autonomous robot as companion in physical therapy for older adults with dementia a mixed methods study. In *2016 11th ACM/IEEE International Conference on Human-Robot Interaction (HRI)*, pages 27–34, March 2016. doi: 10.1109/HRI.2016.7451730.
- Hegel, F., S. Gieselmann, A. Peters, P. Holthaus, and B. Wrede. Towards a Typology of Meaningful Signals and Cues in Social Robotics. In *International Symposium on Robot and Human Interactive Communication*, pages 72–78. IEEE, 2011. doi: 10.1109/ROMAN.2011.6005246.
- Hinds, P. J., T. L. Roberts, and H. Jones. Whose job is it anyway? a study of human-robot interaction in a collaborative task. *Hum.-Comput. Interact.*, 19(1):151–181, 2004.
- Hirose, J., M. Hirokawa, and K. Suzuki. Robotic gaming companion to facilitate social interaction among children. In *The 23rd IEEE International Symposium on Robot and Human Interactive Communication*, pages 63–68, Aug 2014. doi: 10.1109/ROMAN.2014.6926231.
- Ho, C.-C. and K. F. MacDorman. Measuring the uncanny valley effect. *International Journal of Social Robotics*, 9(1):129–139, 2017. ISSN 1875-4805. doi: 10.1007/s12369-016-0380-9. URL <http://dx.doi.org/10.1007/s12369-016-0380-9>.
- Howard, M., S. Klanke, M. Gienger, C. Goerick, and S. Vijayakumar. A novel method for learning policies from variable constraint data. *Autonomous Robots*, 27(2):105–121, 2009. ISSN 0929-5593. doi: 10.1007/s10514-009-9129-8.
- Huang, J. and M. Cakmak. Programming by demonstration with user-specified perceptual landmarks. *CoRR*, abs/1612.00565, 2016.
- Huettenrauch, H., K. S. Eklundh, A. Green, and Elin. Investigating Spatial Relationships in Human-Robot Interaction. In *International Conference on Intelligent Robots and Systems*, pages 5052–5059, 2006.

- Hughes, C. M. L., B. Mueller, H. Tepper, and C. Seegelke. Interlimb coordination during a cooperative bimanual object manipulation task. *Laterality: Asymmetries of Body, Brain and Cognition*, 18(6):693–709, 2013. doi: 10.1080/1357650X.2012.748060. URL <http://dx.doi.org/10.1080/1357650X.2012.748060>.
- Iacono, I., H. Lehmann, P. Marti, B. Robins, and K. Dautenhahn. Robots as social mediators for children with autism - a preliminary analysis comparing two different robotic platforms. In *2011 IEEE International Conference on Development and Learning (ICDL)*, volume 2, pages 1–6, Aug 2011. doi: 10.1109/DEVLRN.2011.6037322.
- Ishiguro, H. Studies on humanlike robots - humanoid, android and geminoid. In *Simulation, Modeling, and Programming for Autonomous Robots, First International Conference, SIMPAR 2008, Venice, Italy, November 3-6, 2008. Proceedings*, page 2, 2008. doi: 10.1007/978-3-540-89076-8\_2. URL [http://dx.doi.org/10.1007/978-3-540-89076-8\\_2](http://dx.doi.org/10.1007/978-3-540-89076-8_2).
- Ivaldi, S., S. Lefort, J. Peters, M. Chetouani, J. Provasi, and E. Zibetti. Towards engagement models that consider individual factors in hri: On the relation of extroversion and negative attitude towards robots to gaze and speech during a human–robot assembly task. *International Journal of Social Robotics*, 9(1):63–86, 2017. ISSN 1875-4805. doi: 10.1007/s12369-016-0357-8. URL <http://dx.doi.org/10.1007/s12369-016-0357-8>.
- Jain, S., K. Barsness, and B. Argall. Automated and objective assessment of surgical training: Detection of procedural steps on videotaped performances. In *Digital Image Computing: Techniques and Applications (DICTA), 2015 International Conference on*, pages 1–6, Nov 2015. doi: 10.1109/DICTA.2015.7371233.
- Jäkel, R., S. R. Schmidt-Rohr, M. Lösch, and R. Dillmann. Representation and constrained planning of manipulation strategies in the context of programming by demonstration. In *ICRA*, pages 162–169, 2010.
- Jaric, S., J. Collins, R. Marwaha, and E. Russell. Interlimb and within limb force coordination in static bimanual manipulation task. *Experimental Brain Research*, 168(1-2):88–97, 2006. ISSN 0014-4819. doi: 10.1007/s00221-005-0070-6. URL <http://dx.doi.org/10.1007/s00221-005-0070-6>.
- Javaid, M., M. efran, and B. D. Eugenio. Communication through physical interaction: A study of human collaborative manipulation of a planar object. In *The 23rd IEEE International Symposium on Robot and Human Interactive Communication*, pages 838–843, Aug 2014. doi: 10.1109/ROMAN.2014.6926357.
- Jkel, R., S. R. Schmidt-Rohr, M. Lsch, and R. Dillmann. Representation and constrained planning of manipulation strategies in the context of programming by demonstration. In *Robotics and Automation (ICRA), 2010 IEEE International Conference on*, pages 162–169, May 2010. doi: 10.1109/ROBOT.2010.5509959.
- Jog, A., B. Itkowitz, M. Liu, S. DiMaio, G. Hager, M. Curet, and R. Kumar. Towards integrating task information in skills assessment for dexterous tasks in surgery and simulation. In *Robotics and Automation (ICRA)*,

- 2011 *IEEE International Conference on*, pages 5273–5278, May 2011. doi: 10.1109/ICRA.2011.5979967.
- Johansson, R. S., A. Theorin, G. Westling, M. Andersson, Y. Ohki, and L. Nyberg. How a lateralized brain supports symmetrical bimanual tasks. *PLoS Biol*, 4(6):e158, 2006. ISSN 1545-7885.
- Kadivar, Z., J. L. Sullivan, D. P. Eng, A. U. Pehlivan, M. K. O’Malley, N. Yozbatiran, and G. E. Francisco. Robotic training and kinematic analysis of arm and hand after incomplete spinal cord injury: A case study. In *2011 IEEE International Conference on Rehabilitation Robotics*, pages 1–6, June 2011. doi: 10.1109/ICORR.2011.5975429.
- Kahn, P. H., Jr., T. Kanda, H. Ishiguro, S. Shen, H. E. Gary, and J. H. Ruckert. Creative collaboration with a social robot. In *Proceedings of the 2014 ACM International Joint Conference on Pervasive and Ubiquitous Computing*, UbiComp ’14, pages 99–103, New York, NY, USA, 2014. ACM. ISBN 978-1-4503-2968-2. doi: 10.1145/2632048.2632058. URL <http://doi.acm.org/10.1145/2632048.2632058>.
- Kaiser, M., H. Friedrich, and R. Dillmann. Obtaining good performance from a bad teacher. In *ICML*, 1995.
- Kanda, T., T. Miyashita, T. Osada, Y. Haikawa, and H. Ishiguro. Analysis of humanoid appearances in human-robot interaction. *IEEE Transactions on Robotics*, 24(3):725–735, June 2008. ISSN 1552-3098. doi: 10.1109/TRO.2008.921566.
- Kannan, B. and L. Parker. Metrics for quantifying system performance in intelligent, fault-tolerant multi-robot teams. In *Intelligent Robots and Systems, 2007. IROS 2007. IEEE/RSJ International Conference on*, pages 951–958, Oct 2007. doi: 10.1109/IROS.2007.4399530.
- Kazennikov, O., S. Perrig, and M. Wiesendanger. Kinematics of a coordinated goal-directed bimanual task. *Behavioural Brain Research*, 134(12):83 – 91, 2002. ISSN 0166-4328. doi: [http://dx.doi.org/10.1016/S0166-4328\(01\)00457-0](http://dx.doi.org/10.1016/S0166-4328(01)00457-0).
- Kennedy, J., P. Baxter, and T. Belpaeme. Nonverbal immediacy as a characterisation of social behaviour for human-robot interaction. *International Journal of Social Robotics*, 9(1):109–128, 2017. ISSN 1875-4805. doi: 10.1007/s12369-016-0378-3. URL <http://dx.doi.org/10.1007/s12369-016-0378-3>.
- Khansari-Zadeh, S. M. and A. Billard. Learning stable nonlinear dynamical systems with gaussian mixture models. *IEEE Transactions on Robotics*, 27(5):943–957, Oct 2011. ISSN 1552-3098. doi: 10.1109/TRO.2011.2159412.
- Khansari-Zadeh, S. M. and A. Billard. A dynamical system approach to realtime obstacle avoidance. *Autonomous Robots*, 32(4):433–454, 2012. ISSN 1573-7527. doi: 10.1007/s10514-012-9287-y.
- Konidaris, G., S. Kuindersma, R. Grupen, and A. Barto. Robot learning from demonstration by constructing skill trees. *Int. J. Rob. Res.*, 31(3):360–375, 2012. ISSN 0278-3649.
- Kormushev, P., S. Calinon, and D. G. Caldwell. Imitation Learning of Positional and Force Skills Demonstrated via Kinesthetic Teaching and Haptic Input. *Advanced Robotics*, 25(5):581–603, 2011.

- Koschate, M., R. Potter, P. Bremner, and M. Levine. Overcoming the uncanny valley: Displays of emotions reduce the uncanniness of humanlike robots. In *2016 11th ACM/IEEE International Conference on Human-Robot Interaction (HRI)*, pages 359–366, March 2016. doi: 10.1109/HRI.2016.7451773.
- Krishnan, V. and S. Jaric. Effects of task complexity on coordination of inter-limb and within-limb forces in static bimanual manipulation. *Motor Control*, 14(4):528–544, Oct 2010.
- Kronander, K. and A. Billard. Learning compliant manipulation through kinesi-  
thetic and tactile human-robot interaction. *IEEE Transactions on Haptics*, 7(3):367–380, July 2014. ISSN 1939-1412. doi: 10.1109/TOH.2013.54.
- Kulic, D. and Y. Nakamura. Scaffolding on-line segmentation of full body human motion patterns. In *IROS*, pages 2860–2866, 2008.
- Kulic, D., W. Takano, and Y. Nakamura. Combining automated on-line segmen-  
tation and incremental clustering for whole body motions. In *ICRA*, pages 2591–2598, 2008.
- Kulic, D., C. Ott, D. Lee, J. Ishikawa, and Y. Nakamura. Incremental learning of full body motion primitives and their sequencing through human motion observation. *I. J. Robotic Res.*, 31(3):330–345, 2012.
- Lee, S. H., H. K. Kim, and I. H. Suh. Incremental learning of primitive skills from demonstration of a task. In *Proceedings of the 6th international conference on Human-robot interaction, HRI '11*, pages 185–186. ACM, 2011. ISBN 978-1-4503-0561-7.
- Levillain, F., E. Zibetti, and S. Lefort. Interacting with non-anthropomorphic robotic artworks and interpreting their behaviour. *International Journal of Social Robotics*, 9(1):141–161, 2017. ISSN 1875-4805. doi: 10.1007/s12369-016-0381-8. URL <http://dx.doi.org/10.1007/s12369-016-0381-8>.
- Leyzberg, D., E. Avrunin, J. Liu, and B. Scassellati. Robots that express emotion elicit better human teaching. In *Proceedings of the 6th international conference on Human-robot interaction, HRI '11*, pages 347–354, 2011.
- Li, M., H. Yin, K. Tahara, and A. Billard. Learning object-level impedance control for robust grasping and dexterous manipulation. In *2014 IEEE International Conference on Robotics and Automation (ICRA)*, pages 6784–6791, May 2014. doi: 10.1109/ICRA.2014.6907861.
- Lieberman, J. and C. Breazeal. Tikl: Development of a wearable vibrotactile feedback suit for improved human motor learning. *IEEE Transactions on Robotics*, 23(5):919–926, Oct 2007. ISSN 1552-3098. doi: 10.1109/TRO.2007.907481.
- Likar, N., B. Nemec, L. Iajpah, S. Ando, and A. Ude. Adaptation of bimanual assembly tasks using iterative learning framework. In *2015 IEEE-RAS 15th International Conference on Humanoid Robots (Humanoids)*, pages 771–776, Nov 2015. doi: 10.1109/HUMANOIDS.2015.7363457.
- Likert, R. A technique for the measurement of attitudes. *Archives of Psychology*, 22(140):1–55, 1932.

- Lin, J. and D. Kulic. Automatic human motion segmentation and identification using feature guided hmm for physical rehabilitation exercises. *Robotics for Neurology and Rehabilitation, Workshop at IEEE/RSJ International Conference on Intelligent Robots and Systems (IROS)*, 2011.
- Liu, T., Y. Lei, L. Han, W. Xu, and H. Zou. Coordinated resolved motion control of dual-arm manipulators with closed chain. *International Journal of Advanced Robotic Systems*, 13(3):80, 2016. doi: 10.5772/63430. URL <http://dx.doi.org/10.5772/63430>.
- Lukic, L., J. Santos-Victor, and A. Billard. Learning robotic eye-arm-hand coordination from human demonstration: a coupled dynamical systems approach. *Biological Cybernetics*, 108(2):223–248, 2014. ISSN 1432-0770. doi: 10.1007/s00422-014-0591-9.
- Madan, C. E., A. Kucukyilmaz, T. M. Sezgin, and C. Basdogan. Recognition of haptic interaction patterns in dyadic joint object manipulation. *IEEE Transactions on Haptics*, 8(1):54–66, Jan 2015. ISSN 1939-1412. doi: 10.1109/TOH.2014.2384049.
- Mangin, O. and P.-Y. Oudeyer. Learning to recognize parallel combinations of human motion primitives with linguistic descriptions using non-negative matrix factorization. In *IROS*, pages 3268–3275. IEEE, 2012. ISBN 978-1-4673-1737-5.
- Matsuo, T., Y. Shirai, and N. Shimada. Automatic generation of hmm topology for sign language recognition. In *Pattern Recognition, 2008. ICPR 2008. 19th International Conference on*, pages 1–4, 2008.
- McMorris, T. *Acquisition and Performance of Sports Skills*. John Wiley & Sons Ltd, 2004. ISBN 9780470849958.
- Milot, M. H., M. Hamel, P. O. Provost, J. Bernier-Ouellet, M. Dupuis, D. Ltourneau, S. Briere, and F. Michaud. Exerciser for rehabilitation of the arm (era): Development and unique features of a 3d end-effector robot. In *2016 38th Annual International Conference of the IEEE Engineering in Medicine and Biology Society (EMBC)*, pages 5833–5836, Aug 2016. doi: 10.1109/EMBC.2016.7592054.
- Mohareri, O., C. Schneider, and S. E. Salcudean. Bimanual telerobotic surgery with asymmetric force feedback: A davinci® surgical system implementation. In *2014 IEEE/RSJ International Conference on Intelligent Robots and Systems, Chicago, IL, USA, September 14-18, 2014*, pages 4272–4277, 2014. doi: 10.1109/IROS.2014.6943165.
- Mori, M. The uncanny valley. *Energy*, 7:33–35, 1970.
- Morone, G., S. Paolucci, A. Cherubini, D. De Angelis, V. Venturiero, P. Coiro, and M. Iosa. Robot-assisted gait training for stroke patients: current state of the art and perspectives of robotics. *Neuropsychiatric Disease and Treatment*, 13:1303–1311, 2017. ISSN 1178-2021. doi: <http://doi.org/10.2147/NDT.S114102>. URL <http://www.ncbi.nlm.nih.gov/pmc/articles/PMC5440028/>.
- Muhlig, M., M. Gienger, J. Steil, and C. Goerick. Automatic selection of task spaces for imitation learning. In *IEEE/RSJ International Conference on Intelligent Robots and Systems, 2009. IROS 2009.*, pages 4996–5002, oct. 2009.

- Murphy, K. and M. Darrah. Haptics-based apps for middle school students with visual impairments. *IEEE Transactions on Haptics*, 8(3):318–326, July 2015. ISSN 1939-1412. doi: 10.1109/TOH.2015.2401832.
- Murphy, R. and D. Schreckenghost. Survey of metrics for human-robot interaction. In *Human-Robot Interaction (HRI), 2013 8th ACM/IEEE International Conference on*, pages 197–198, March 2013. doi: 10.1109/HRI.2013.6483569.
- Mutha, P. K. and R. L. Sainburg. Shared bimanual tasks elicit bimanual reflexes during movement. *J Neurophysiol*, 102(6):3142–55, 2009. ISSN 1522-1598.
- Nakanishi, J., H. Sumioka, M. Shiomi, D. Nakamichi, K. Sakai, and H. Ishiguro. Huggable communication medium encourages listening to others. In *Proceedings of the Second International Conference on Human-agent Interaction*, HAI '14, pages 249–252, New York, NY, USA, 2014. ACM. ISBN 978-1-4503-3035-0. doi: 10.1145/2658861.2658934. URL <http://doi.acm.org/10.1145/2658861.2658934>.
- Nehaniv, C. L., K. Dautenhahn, J. Kubacki, M. Haegele, C. Parlitz, and R. Alami. A methodological approach relating the classification of gesture to identification of human intent in the context of human-robot interaction. In *Proc. IEEE Int. Symp. on Robot and Human Interactive Communication*, pages 371–377, 2005.
- Nicolescu, M. N. and M. J. Mataric. Natural methods for robot task learning: instructive demonstrations, generalization and practice. In *Proceedings of the second international joint conference on Autonomous agents and multiagent systems*, AAMAS '03, pages 241–248. ACM, 2003. ISBN 1-58113-683-8.
- Niekum, S., S. Chitta, A. G. Barto, B. Marthi, and S. Osentoski. Incremental semantically grounded learning from demonstration. In *Robotics: Science and Systems*, 2013.
- Noohi, E. and M. Zefran. Quantitative measures of cooperation for a dyadic physical interaction task. In *2014 IEEE-RAS International Conference on Humanoid Robots*, pages 469–474, Nov 2014. doi: 10.1109/HUMANOIDS.2014.7041403.
- Nyga, D. and M. Beetz. Cloud-based Probabilistic Knowledge Services for Instruction Interpretation. In *International Symposium of Robotics Research (ISR)*, Sestri Levante (Genoa), Italy, 2015.
- Olsen, D. and M. Goodrich. Metrics for evaluating human-robot interactions. In *Proc. NIST Performance Metrics for Intelligent Systems Workshop*, 2003.
- Oriolo, G. and M. Vendittelli. A control-based approach to task-constrained motion planning. In *Intelligent Robots and Systems, 2009. IROS 2009. IEEE/RSJ International Conference on*, pages 297–302, 2009.
- Otero, N., C. L. Nehaniv, D. Syrdal, and K. Dautenhahn. Naturally occurring gestures in a human-robot teaching scenario. In *Proceedings of the 15th IEEE International Symposium on Robot and Human Interactive Communication (IEEE Ro-Man 2006)*, pages 533–540, 2006.
- Pais, A. L. and A. Billard. Learning bimanual coordinated tasks from human demonstrations. In *Proceedings of the 2015 ACM/IEEE International Conference on Human-robot Interaction*, HRI '15. ACM, 2015. doi: 10.1145/2701973.2702007.

- Pais, A. L., B. D. Argall, and A. G. Billard. Assessing interaction dynamics in the context of robot programming by demonstration. *International Journal of Social Robotics*, 5(4):477–490, 2013. ISSN 1875-4805. doi: 10.1007/s12369-013-0204-0. URL <http://dx.doi.org/10.1007/s12369-013-0204-0>.
- Pais Ureche, A. L. and A. Billard. Constraints extraction from asymmetrical bimanual tasks and their use in coordinated behavior. *Submitted*, 2017a.
- Pais Ureche, L. and A. Billard. Automatic skill assessment in learning from demonstration. *Under Submission, IJSR*, 2017b.
- Paperno, N., M. Rupp, E. M. Maboudou-Tchao, J. A.-A. Smither, and A. Behal. A predictive model for use of an assistive robotic manipulator: Human factors versus performance in pick-and-place/retrieval tasks. *IEEE Transactions on Human-Machine Systems*, 46(6):846–858, Dec 2016. ISSN 2168-2291. doi: 10.1109/THMS.2016.2604366.
- Park, H. A. and C. S. G. Lee. Extended cooperative task space for manipulation tasks of humanoid robots. In *2015 IEEE International Conference on Robotics and Automation (ICRA)*, pages 6088–6093, May 2015. doi: 10.1109/ICRA.2015.7140053.
- Park, Y., S. Itakura, A. M. Henderson, T. Kanda, N. Furuhashi, and H. Ishiguro. Do infants consider a robot as a social partner in collaborative activity? In *Proceedings of the 3rd International Conference on Human-Agent Interaction, HAI '15*, pages 91–95, New York, NY, USA, 2015. ACM. ISBN 978-1-4503-3527-0. doi: 10.1145/2814940.2814953. URL <http://doi.acm.org/10.1145/2814940.2814953>.
- Paxton, C., M. Kobilarov, and G. D. Hager. Towards robot task planning from probabilistic models of human skills. *CoRR*, abs/1602.04754, 2016. URL <http://arxiv.org/abs/1602.04754>.
- Peacock, M. Match or mismatch? learning styles and teaching styles in efl. *International Journal of Applied Linguistics*, 11(1):1–20, 2001.
- Perrig, S., O. Kazennikov, and M. Wiesendanger. Time structure of a goal-directed bimanual skill and its dependence on task constraints. *Behavioural Brain Research*, 103(1):95 – 104, 1999. ISSN 0166-4328. doi: [http://dx.doi.org/10.1016/S0166-4328\(99\)00026-1](http://dx.doi.org/10.1016/S0166-4328(99)00026-1).
- Peters, R. A., C. L. Campbell, W. J. Bluethmann, and E. Huber. Robonaut task learning through teleoperation. In *Robotics and Automation, 2003. Proceedings. ICRA '03. IEEE International Conference on*, volume 2, pages 2806–2811 vol.2, Sept 2003. doi: 10.1109/ROBOT.2003.1242017.
- Pinzon, D., R. Vega, Y. P. Sanchez, and B. Zheng. Skill learning from kinesthetic feedback. *The American Journal of Surgery*, 2016. ISSN 0002-9610. doi: <http://dx.doi.org/10.1016/j.amjsurg.2016.10.018>. URL <http://www.sciencedirect.com/science/article/pii/S0002961016309539>.
- Ponce, J., S. Sullivan, A. Sudsang, J. daniel Boissonnat, and J.-P. Merlet. On computing four-finger equilibrium and force-closure grasps of polyhedral objects. *IJRR*, 16:11–35, 1996.

- Robins, B., K. Dautenhahn, C. L. Nehaniv, N. A. Mirza, D. Francois, and L. Olsson. *Sustaining interaction dynamics and engagement in dyadic child-robot interaction kinesics : Lessons learnt from an exploratory study*, pages 716–722. 2005.
- Ros, R., E. Oleari, C. Pozzi, F. Sacchitelli, D. Baranzini, A. Bagherzadhalimi, A. Sanna, and Y. Demiris. A motivational approach to support healthy habits in long-term child–robot interaction. *International Journal of Social Robotics*, 8(5):599–617, 2016. ISSN 1875-4805. doi: 10.1007/s12369-016-0356-9. URL <http://dx.doi.org/10.1007/s12369-016-0356-9>.
- Rozo, L., S. Calinon, D. G. Caldwell, P. Jimnez, and C. Torras. Learning physical collaborative robot behaviors from human demonstrations. *IEEE Transactions on Robotics*, PP(99):1–15, 2016. ISSN 1552-3098. doi: 10.1109/TRO.2016.2540623.
- Russell, J. A circumplex model of affect. *Personality and Social Psychology*, 39, 1980.
- Russell, J. Culture and the Categorization of Emotions. *Psychological Bulletin*, 110(3):426–450, 1991.
- Russell, J. Reading emotions from and into faces: Resurrecting a dimensional-contextual perspective. In Russell, J. A. and J. M. Fernández-Dols, editors, *The Psychology of Facial Expression*, pages 295–320. Cambridge: Cambridge University Press, 1997.
- Saha, D. J. and P. Morasso. Bimanual control of an unstable task: Stiffness vs. intermittent control strategy. In *RO-MAN, 2010 IEEE*, pages 779–784, Sept 2010. doi: 10.1109/ROMAN.2010.5598708.
- Salcudean, S. E., S. Ku, and G. Bell. Performance measurement in scaled teleoperation for microsurgery. In *Proceedings of the First Joint Conference on Computer Vision, Virtual Reality and Robotics in Medicine and Medical Robotics and Computer-Assisted Surgery*, CVRMed-MRCAS ’97, pages 789–798, London, UK, UK, 1997. Springer-Verlag. ISBN 3-540-62734-0.
- Sardar, A., M. Joosse, A. Weiss, and V. Evers. Don’t stand so close to me: users’ attitudinal and behavioral responses to personal space invasion by robots. In *Proceedings of the seventh annual ACM/IEEE international conference on Human-Robot Interaction*, HRI ’12, pages 229–230, 2012.
- Sausser, E. L., B. D. Argall, G. Metta, and A. G. Billard. Iterative learning of grasp adaptation through human corrections. *Robot. Auton. Syst.*, 60:55–71, 2012.
- Schneider, A., B. Baur, W. Frholzer, I. Jasper, C. Marquardt, and J. Hermsdrfer. Writing kinematics and pen forces in writers cramp: Effects of task and clinical subtype. *Clinical Neurophysiology*, 121(11):1898 – 1907, 2010. ISSN 1388-2457. doi: <http://dx.doi.org/10.1016/j.clinph.2010.04.023>. URL <http://www.sciencedirect.com/science/article/pii/S1388245710003767>.
- Schutter, J. D., T. D. Laet, J. Rutgeerts, W. Decré, R. Smits, E. Aertbeliën, K. Claes, and H. Bruyninckx. Constraint-based task specification and estimation for sensor-based robot systems in the presence of geometric uncertainty. *I. J. Robotic Res.*, 26(5):433–455, 2007.

- Seegelke, C. and T. Schack. Cognitive representation of human action: Theory, applications, and perspectives. *Frontiers in Public Health*, 4:24, 2016. ISSN 2296-2565. doi: 10.3389/fpubh.2016.00024. URL <https://www.frontiersin.org/article/10.3389/fpubh.2016.00024>.
- Seth, A. K. A matlab toolbox for granger causal connectivity analysis. *Journal of Neuroscience Methods*, 2010a.
- Seth, A. K. A matlab toolbox for granger causal connectivity analysis. *Journal of Neuroscience Methods*, 186(2):262 – 273, 2010b. ISSN 0165-0270. doi: <http://dx.doi.org/10.1016/j.jneumeth.2009.11.020>. URL <http://www.sciencedirect.com/science/article/pii/S0165027009006189>.
- Seyama, J. and R. S. Nagayama. The uncanny valley: Effect of realism on the impression of artificial human faces. *Presence: Teleoper. Virtual Environ.*, 16(4):337–351, August 2007. ISSN 1054-7460. doi: 10.1162/pres.16.4.337. URL <http://dx.doi.org/10.1162/pres.16.4.337>.
- Shibata, T. Therapeutic seal robot as biofeedback medical device: Qualitative and quantitative evaluations of robot therapy in dementia care. *Proceedings of the IEEE*, 100(8):2527–2538, Aug 2012. ISSN 0018-9219. doi: 10.1109/JPROC.2012.2200559.
- Shim, J. and A. L. Thomaz. Human-like action segmentation for option learning. In *RO-MAN*, pages 455–460, 2011.
- Shiomi, M., K. Nakagawa, K. Shinozawa, R. Matsumura, H. Ishiguro, and N. Hagita. Does a robot’s touch encourage human effort? *International Journal of Social Robotics*, 9(1):5–15, 2017. ISSN 1875-4805. doi: 10.1007/s12369-016-0339-x. URL <http://dx.doi.org/10.1007/s12369-016-0339-x>.
- Shiwa, T., T. Kanda, M. Imai, H. Ishiguro, and N. Hagita. How quickly should a communication robot respond? delaying strategies and habituation effects. *International Journal of Social Robotics*, 1(2):141–155, 2009. ISSN 1875-4805. doi: 10.1007/s12369-009-0012-8. URL <http://dx.doi.org/10.1007/s12369-009-0012-8>.
- Shukla, A. and A. Billard. Coupled dynamical system based arm-hand grasping model for learning fast adaptation strategies. *Robotics and Autonomous Systems*, 60(3):424 – 440, 2012. ISSN 0921-8890.
- Silvrio, J., L. Roza, S. Calinon, and D. G. Caldwell. Learning bimanual end-effector poses from demonstrations using task-parameterized dynamical systems. In *Intelligent Robots and Systems (IROS), 2015 IEEE/RSJ International Conference on*, pages 464–470, Sept 2015. doi: 10.1109/IROS.2015.7353413.
- Smith, A., C. Yang, H. Ma, P. Culverhouse, A. Cangelosi, and E. Burdet. Dual adaptive control of bimanual manipulation with online fuzzy parameter tuning. In *2014 IEEE International Symposium on Intelligent Control (ISIC)*, pages 560–565, Oct 2014. doi: 10.1109/ISIC.2014.6967605.
- Stanton, C. M., P. H. Kahn, R. L. Severson, J. H. Ruckert, and B. T. Gill. Robotic animals might aid in the social development of children with autism. In *2008 3rd ACM/IEEE International Conference on Human-Robot Interaction (HRI)*, pages 271–278, March 2008. doi: 10.1145/1349822.1349858.

- Steffen, J., C. Elbrechter, R. Haschke, and H. Ritter. Bio-inspired motion strategies for a bimanual manipulation task. In *2010 10th IEEE-RAS International Conference on Humanoid Robots*, pages 625–630, Dec 2010. doi: 10.1109/ICHR.2010.5686830.
- Steinfeld, A., T. Fong, D. Kaber, M. Lewis, J. Scholtz, A. Schultz, and M. Goodrich. Common metrics for human-robot interaction. In *Proceedings of the 1st ACM SIGCHI/SIGART Conference on Human-robot Interaction, HRI '06*, pages 33–40, New York, NY, USA, 2006. ACM. ISBN 1-59593-294-1. doi: 10.1145/1121241.1121249.
- Stilman, M. Task constrained motion planning in robot joint space. In *in IROS*, 2007.
- Stirling, B. V. Results of a study assessing teaching methods of faculty after measuring student learning style preference. *Nurse Education Today*, 55:107 – 111, 2017. ISSN 0260-6917. doi: <https://doi.org/10.1016/j.nedt.2017.05.012>. URL <http://www.sciencedirect.com/science/article/pii/S0260691717301156>.
- Sukhoy, V., V. Georgiev, T. Wegter, R. Sweidan, and A. Stoytchev. Learning to slide a magnetic card through a card reader. In *ICRA*, pages 2398–2404, 2012.
- Sung, J. Y., L. Guo, R. E. Grinter, and H. I. Christensen. "My Roomba is Rambo": intimate home appliances. In *UbiComp'07: Proceedings of the 9th international conference on Ubiquitous computing*, pages 145–162, 2007.
- Suzuki, Y., H. Takase, Y. Pan, J. Ishikawa, and K. Furuta. Learning process of bimanual coordination. In *Control, Automation and Systems, 2008. ICCAS 2008. International Conference on*, pages 2830–2835, Oct 2008. doi: 10.1109/ICCAS.2008.4694241.
- Taheri, H., S. A. Goodwin, J. A. Tigue, J. C. Perry, and E. T. Wolbrecht. Design and optimization of partner: A parallel actuated robotic trainer for neurorehabilitation. In *2016 38th Annual International Conference of the IEEE Engineering in Medicine and Biology Society (EMBC)*, pages 2128–2132, Aug 2016. doi: 10.1109/EMBC.2016.7591149.
- Takano, W. and Y. Nakamura. Humanoid robot’s autonomous acquisition of proto-symbols through motion segmentation. In *Humanoids*, pages 425–431, 2006.
- Tao, L., E. Elhamifar, S. Khudanpur, G. Hager, and R. Vidal. Sparse hidden markov models for surgical gesture classification and skill evaluation. In Abolmaesumi, P., L. Joskowicz, N. Navab, and P. Jannin, editors, *Information Processing in Computer-Assisted Interventions*, volume 7330 of *Lecture Notes in Computer Science*, pages 167–177. Springer Berlin / Heidelberg, 2012. ISBN 978-3-642-30617-4.
- Ureche, A. L. P., K. Umezawa, Y. Nakamura, and A. Billard. Task parameterization using continuous constraints extracted from human demonstrations. *IEEE Transactions on Robotics*, 31(6):1458–1471, Dec 2015. ISSN 1552-3098. doi: 10.1109/TRO.2015.2495003.
- Ushida, H. Effect of social robot’s behavior in collaborative learning. In *Proceedings of the 5th ACM/IEEE international conference on Human-robot interaction, HRI '10*, pages 195–196, 2010.

- van den Brule, R., G. Bijlstra, R. Dotsch, P. Haselager, and D. H. J. Wigboldus. Warning signals for poor performance improve human-robot interaction. *Journal of Human Robot Interaction*, 5(2), 2016. doi: 10.5898/JHRI.5.2.Van\_den\_Brule.
- Vijayakumar, S., A. D’Souza, and S. Schaal. Incremental online learning in high dimensions. *Neural Computation*, 17(12):2602–2634, Dec 2005. ISSN 0899-7667. doi: 10.1162/089976605774320557.
- Villani, L. and J. De Schutter. Force control. In Siciliano, B. and O. Khatib, editors, *Springer Handbook of Robotics*, pages 161–185. Springer Berlin Heidelberg, 2008. ISBN 978-3-540-23957-4.
- Wang, L., W. Hu, and T. Tan. Recent developments in human motion analysis. *Pattern Recognition*, 36(3):585–601, 2003.
- Wrgtter, F., C. Geib, M. Tamosiunaite, E. E. Aksoy, J. Piater, H. Xiong, A. Ude, B. Nemec, D. Kraft, N. Krger, M. Wchter, and T. Asfour. Structural bootstrapping: A novel, generative mechanism for faster and more efficient acquisition of action-knowledge. *IEEE Transactions on Autonomous Mental Development*, 7(2):140–154, June 2015. ISSN 1943-0604. doi: 10.1109/TAMD.2015.2427233.
- Xu, W., H. Liu, Y. She, and B. Liang. Singularity-free path planning of dual-arm space robot for keeping the base inertially stabilized during target capturing. In *2012 IEEE International Conference on Robotics and Biomimetics (RO-BIO)*, pages 1536–1541, Dec 2012. doi: 10.1109/ROBIO.2012.6491186.
- Yagoda, R. and D. Gillan. You want me to trust a robot? the development of a humanrobot interaction trust scale. *International Journal of Social Robotics*, pages 1–14, 2012.
- Yamazaki, R., S. Nishio, K. Ogawa, K. Matsumura, T. Minato, H. Ishiguro, T. Fujinami, and M. Nishikawa. Promoting socialization of schoolchildren using a teleoperated android: an interaction study. *I. J. Humanoid Robotics*, 10(1), 2013. doi: 10.1142/S0219843613500072. URL <http://dx.doi.org/10.1142/S0219843613500072>.
- Yang, C., P. Liang, Z. Li, A. Ajoudani, C. Y. Su, and A. Bicchi. Teaching by demonstration on dual-arm robot using variable stiffness transferring. In *2015 IEEE International Conference on Robotics and Biomimetics (ROBIO)*, pages 1202–1208, Dec 2015. doi: 10.1109/ROBIO.2015.7418935.
- Ye, G. and R. Alterovitz. Demonstration-guided motion planning. *International Symposium on Robotics Research (ISRR)*, 2011.
- Yohanan, S. and K. E. MacLean. Design and assessment of the haptic creature’s affect display. In *Proceedings of the 6th international conference on Human-robot interaction*, HRI ’11, pages 473–480, 2011.
- Zacharias, F., D. Leidner, F. Schmidt, C. Borst, and G. Hirzinger. Exploiting structure in two-armed manipulation tasks for humanoid robots. In *Intelligent Robots and Systems (IROS), 2010 IEEE/RSJ International Conference on*, pages 5446–5452, Oct 2010. doi: 10.1109/IROS.2010.5651121.
- Zhu, Q., T. Mirich, S. Huang, W. Snapp-Childs, and G. P. Bingham. When kinesthetic information is neglected in learning a novel bimanual rhythmic

coordination. *Attention, Perception, & Psychophysics*, May 2017. ISSN 1943-393X. doi: 10.3758/s13414-017-1336-3. URL <http://dx.doi.org/10.3758/s13414-017-1336-3>.

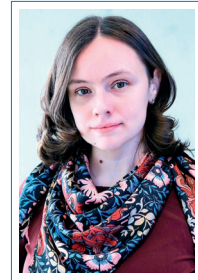
Zollner, R., T. Asfour, and R. Dillmann. Programming by demonstration: dual-arm manipulation tasks for humanoid robots. In *Intelligent Robots and Systems, 2004. (IROS 2004). Proceedings. 2004 IEEE/RSJ International Conference on*, volume 1, pages 479–484 vol.1, Sept 2004. doi: 10.1109/IROS.2004.1389398.

Zollner, R. D. and R. Dillmann. Using multiple probabilistic hypothesis for programming one and two hand manipulation by demonstration. In *Intelligent Robots and Systems, 2003. (IROS 2003). Proceedings. 2003 IEEE/RSJ International Conference on*, volume 3, pages 2926–2931 vol.3, Oct 2003. doi: 10.1109/IROS.2003.1249315.

# Lucia Ureche

## Curriculum Vitae

Rue du Centre 72  
1025 St-Sulpice, Switzerland  
☎ +41 76 236 5035  
✉ [analucia.ureche@gmail.com](mailto:analucia.ureche@gmail.com)



*Robotics Engineer:  
Human-robot interaction, User profiling,  
Machine learning algorithms, Robot motion control*

### Education

- 2011–Present **École Polytechnique Fédérale De Lausanne, EPFL.**  
PhD Student in Robotics, Laboratory of Learning Algorithms and Systems (LASA),  
Graduation – Expected 2017
- 2009–2011 **Polytechnic University of Bucharest, UPB.**  
Master in Intelligent Control Systems
- 2009–2011 **Polytechnic University of Bucharest, UPB.**  
B.S. degree in Automation and Systems Engineering

### Professional and Research Experience

- 2011–Present **PhD Project, LASA, EPFL, ongoing.**  
"Autonomous extraction of task constraints from demonstrated robot motion" - Focuses on applying machine learning algorithms for segmenting human demonstrations into subtasks, and obtaining models to be used for robot control (EU project RoboHow).
  - segmentation of complex tasks demonstrated by the user
  - task constraints extraction and motion modeling
  - user profiling based on tool manipulation and force-torque data
- 2011 **Internship, LASA, EPFL, 6 months.**  
Studied human robot interaction dynamics on the humanoid robot iCub Part of the EU FP 7 project RoboSkin
  - emotion modeling and validation on the iCub robot
  - analyzing user interaction patterns
  - validating feedback modalities for sustained interaction
- 2011 **Master Thesis, UPB.**  
Integrated framework for emotion recognition and expression using robot artists.
- 2009 **Internship, Dacia Groupe Renault, 3 months.**  
Bachelor project "Motion optimization for a carrier robot serving a finishing lathe".

---

## Professional Skills

Robot control	iCub, KUKA LWR, Barrett hand, various sensors (ATI 6 axis FT sensors, Tekscan tactile sensors, OptiTrack motion capture), educational robots
Programming	Matlab, C++
Machine Learning	Regression and Classification algorithms
Graphics	Corel Paint Shop Pro, Painter, Draw, VideoStudio

---

## Research Interests

- Human Robot Interaction
- Robot Collaborative Tasks
- Programming by Demonstration
- User skill-based profiling
- Robot Tactile Sensing
- Machine Learning

---

## Languages

English	<b>Fluent</b>	<i>TOEFL score: 110/max.120</i>
French	<b>Intermediate</b>	<i>B2 - Conversationally fluent</i>
Romanian	<b>Fluent</b>	<i>Mother tongue</i>

---

## Scientific Publications

### Journals:

- [J1]: Pais Ureche A. L., Billard A. (2017) **Automatic skill assessment in learning from demonstration**, [*Under submission*]
- [J2]: Pais Ureche A. L., Billard A. (2017) **Constraints extraction from asymmetrical bimanual tasks and their use in coordinated behavior**, [*Under submission*]
- [J3]: Pais Ureche A. L., Umezawa K, Nakamura Y, Billard A (2015) **Task parameterization using continuous constraints extracted from human demonstrations**, IEEE Transactions on Robotics, 31(6):1458–1471, [TRO 2015]
- [J4]: Pais A. L., Argall B.D. and Billard, A. (2013) **Assessing Interaction Dynamics in the Context of Robot Programming by Demonstration**, International Journal of Social Robotics, November 2013, Volume 5, Issue 4, pp 477-490, [IJSR 2013]

### Conferences and Abstracts:

- [C1]: Figueroa N., Pais Ureche A. L., Billard A. (2016) **Learning complex sequential tasks from demonstration: A pizza dough rolling case study**, In Proceedings of the 2016 ACM/IEEE International Conference on Human-robot Interaction, ACM, [HRI 2016]
- [C2]: Pais, A. L., Billard, A. (2015) **Learning Bimanual Coordinated Tasks From Human Demonstrations**, Proceedings of the 2015 ACM/IEEE International Conference on Human-robot Interaction, [HRI 2015]
- [C3]: Pais, A. L. and Billard, A. (2015) **Metrics for Assessing Human Skill When Demonstrating a Bimanual Task to a Robot**, Proceedings of the 2015 ACM/IEEE International Conference on Human-robot Interaction, [HRI 2015]
- [C4]: Beetz M., Beßler D., Winkler J., Worch J.H., Balint-Benczedi F., Bartels G., Billard A., Bozcuoglu A.K., Fang Z., Figueroa N., Haidu A., Langer H., Maldonado A., Ureche A.L., Tenorth M., Wiedemeyer T. (2016)

**Open Robotics Research Using Web-based Knowledge Services**, IEEE International Conference on Robotics and Automation, [ICRA 2016, *Accepted*]

- [C5]: Pais, A. L. and Billard, A. (2014) **Encoding bi-manual coordination patterns from human demonstrations**, In Proceedings of the 9th ACM/IEEE International Conference on Human-Robot Interaction, [HRI 2014]
- [C6]: Pais, A.L., Billard, A., Robins, B., Dautenhahn, K., **Improving human-robot interaction through facial expressions of emotion and touch detection**, In CogSys, Vienna, Austria, 2012
- [C7]: Dichiou, D., Pais, A.L., Moga, A., Buiu, C., **A Cognitive System for Detecting Emotions in Literary Texts and Transposing them into Drawings**, IEEE Int. Conf. on Systems, Man, and Cybernetics, October 2010, [SMC 2010]

### Workshops and other Publications:

- [W1]: Pais Ureche, A. L. and Billard, A. (2015) **Analyzing Human Behavior and Bootstrapping Task Constraints from Kinesthetic Demonstrations**, HRI Pioneers Workshop, HRI 2015
- [W2]: Pais, A. L., Keisuke Umezawa, Yoshihiko Nakamura and Billard, A. (2013) **Learning Robot Skills through Motion Segmentation and Constraints Extraction**. Workshop on Collaborative Manipulation, HRI 2013
- [W3]: Pais, A.L., Billard, A., **Tactile interface user-friendliness evaluated in the context of robot programming by demonstration**, Workshop on Advances in tactile sensing and touch based HRI, HRI 2012
- [W4]: El-Khoury, S., Li, M., Pais, A.L., Billard, A., **Teaching Robots to Grasp through a User Friendly Interface**, Workshop: Beyond Robot Grasping - Modern Approaches for Dynamic Manipulation, IROS 2012
- [W5]: Pais, A.L., Moga, A., Buiu, C., **An Integrated Framework for Emotion Recognition and Expression using Robot Artists**, ICIC Express Letters, Part B : Applications, Vol. 1, No. 2, Dec. 2010, pp. 169-174, ISSN 2185-2766, 2010
- [W6]: Pais, A.L., Moga, A., Buiu, C., **Emotions and robot artists: state-of-the-art and research challenges**, BMIF - Mathematics, Informatics, Physics Series, ISSN 124-4899, Vol. LXII, No. 1, pp. 26-40, 2010

For a full list of publications please see [DBLP](#) or [Google Scholar](#) profiles.

### Personal Details

Romanian citizen, Swiss B permit, married, 1 child. References available upon request.

[Last updated on July 26, 2017.](#)

